On Capacity Estimation and Capacity-Safety Relationship in an Air Transportation Network

Author:
Hossain, Md Murad

Publication Date:
2016

DOI:
https://doi.org/10.26190/unsworks/19118

On Capacity Estimation and Capacity-Safety Relationship in an Air Transportation Network

Md. Murad Hossain

M.Sc (Computer Sc.) University of New South Wales, Australia

B.Sc (Computer Sc. & Engg.) Rajshahi University of Engg. & Tech., Bangladesh

A thesis submitted in partial fulfillment of the requirements
for the degree of Doctor of Philosophy at the
School of Engineering and Information Technology (SEIT)
University of New South Wales
Australian Defence Force Academy

February, 2016

Abstract

Air transportation is a complex system of interlinked distributed networks in which different components have their own constraints and performance measures. For example, an airport network in which each airport is treated as a node and models the departures/arrivals of flights as links considers capacity as its limiting factor. Whereas, an airspace network that consists of airways (as links) and waypoints (as nodes) providing an orderly flow of air traffic and safe separation between flights considers collision risk as its limiting factor. To accommodate the increasing demand to safely manage air traffic flow, it is imperative to understand the interactions between these two components and the limiting factors that define their characteristics. Understanding this relationship is a major consideration when determining whether and which components should aim to increase safety and capacity. In this thesis, I propose a model for airport network capacity estimation and a model of airspace network risk analysis. I then develop a framework for modelling and integrating airport and airspace networks in an overall air transportation system. Finally, I propose a methodology for determining their complex interactions to analyse the relationship between capacity and safety.

One challenge in analysing the capacity-safety relationship for air transportation is measuring its capacity. In air transportation, capacities have traditionally been measured based on the individual elements of the network, such as links (sector capacity and airspace complexity) and nodes (terminals and runway throughput). These measures obviously do not constitute the overall system-level capacity of a network. This research involves developing a network-level capacity estimation model and method. The proposed model does not require knowledge of an individual airport's capacity and offers an understanding of the relationship between the flow capacity and safety metric of its corresponding airspace.

Experimental and empirical results establish the nature of the relationship between airport network capacity and airspace safety when considered in an interacting air transport system. As the hourly flow increases in the airport network, the overall collision risk increases linearly and, after a certain level, crosses the target level of safety. Such a capacity-safety relationship indicates that the capability of existing air traffic control systems to safely handle projected growth in aircraft operations appears to be artificially limited by the airspace.

Keywords

Air Transportation Network

Airport Network

Airspace Network

Network Capacity

Collision Risk

Complex Network

Dedicated to
my family

Acknowledgements

All praises are due to Allah the almighty God, the most beneficent and the most Merciful. I thank Him for bestowing His Blessings upon me to accomplish this task.

No words of gratitude are enough to thank my supervisors, Dr. Sameer Alam and Professor Hussein A. Abbass, School of Engineering and Information Technology, UNSW, Canberra, who provided endless support, guidance and motivation to fulfill this work. Their technical guidance, moral support and thoughtful approach to study have trained me to complete this work. I give special thanks to Dr. Sameer Alam for the intense concentration he gave to the writing of my publications and this thesis.

I would like to thank the School of Engineering and Information Technology for providing me with a full-fee studentship, and sponsoring my conferences. I am also grateful to the University of New South Wales at the Australian Defence Force Academy for providing me with the TFS with UCPRS, one of the most prestigious scholarships in Australia, to complete this research.

I would like to thank Mr. Fareed Alawai and Mr. Fathi Thawadi of ICAO-MIDRMA for providing the necessary traffic data and aeronautical information.

I would like to thank the Australian National Computational Infrastructure (NCI) and INTERSECT, for providing a massive high-performance computing facility which helped me to execute a large numbers of experiments.

I also express my heartiest gratefulness to my wife, Sharmin Aktar for her endless encouragement, moral support and kindness and also to my adorable daughter Manha Hossain and my other family members.

Appreciations also goes to my friends Dr. Mohammad Nurul Islam and his family, Dr. Bin Zhang and many others for their help support and encouragements.

Originality Statement

I hereby declare that this submission is my own work and, to the best of my knowledge and belief, contains no material previously published or written by another person, nor material that to a substantial extent has been accepted for the award of any other degree or diploma at UNSW or any other educational institution, except where due acknowledgement is made in the thesis. Any contribution made to the research by colleagues, with whom I have worked at UNSW or elsewhere, during my candidature, is fully acknowledged.

I also declare that the intellectual content of this thesis is the product of my own work, except to the extent that assistance from others in the project's design and conception or in style, presentation and linguistic expression is acknowledged.

Md. Murad Hossain
UNSW, Canberra

Authenticity Statement

I certify that the Library deposit digital copy is a direct equivalent of the final officially approved version of my thesis. No emendation of content has occurred and if there are any minor variations of formatting, they are the result of the conversion to digital format.

Md. Murad Hossain
UNSW, Canberra

List of Publications

Journal Publications

1. **Md Murad Hossain**, Sameer Alam, Fergus Symon and Henk Blom, *A Complex Network Approach to Analyze the Effect of Intermediate Waypoints on Collision Risk Assessment*, Journal of Air Traffic Control Quarterly, Vol. 22, Number 2, Page 87-114, 2014.

2. Sameer Alam, **Md Murad Hossain**, Fareed Al-Alawi, and Fathi Al-Thawadi, *Optimizing Lateral Airway Offset for Collision Risk Mitigation Using Differential Evolution*, Journal of Air Traffic Control Quarterly, Vol. 23, Number 4, Page 1-24, 2015.

3. **Md Murad Hossain** and Sameer Alam, *A Complex Network Approach Towards Modeling and Analysis of Australian Airport Network*, Journal of Air Transport Management, Elsevier, *Submitted.*

4. **Murad Hossain** and Sameer Alam, *An Evolutionary Optimization Approach for Capacity-Collision Risk Trade-off Analysis in Air Transportation Network*, Journal of Transportation Research Part C: Emerging Technologies, Elsevier, *Submitted.*

Conference Publications

5. **Md Murad Hossain**, Sameer Alam, Tim Rees and Hussein Abbass, *Australian airport network robustness analysis: a complex network approach.* Proceedings of the 36th Australasian Transport Research Forum (ATRF 2013), Brisbane, Queensland, Australia.

6. Fergus Symon, Sameer Alam, **Md Murad Hossain** and Henk Blom, *Airspace Network Characterization for Effect of Intermediate Waypoints on Collision Risk Assessment*, Proceedings of the 6th International Conference on Research in Air Transportation, ICRAT-2014, Page 1-8, Istanbul, Turkey (**Best paper award**).

7. Sameer Alam, **Md Murad Hossain**, Fareed Al-Alawi, and Fathi Al-Thawadi, *Shift for Safety: A Diffrential Evolution Approcah to Optimize Lateral Airway Offset for Collision Risk Mitigation*, Eleventh USA/Europe Air Traffic Management Research and Development Seminar (ATMRnD 2015),June 23rd - 26th 2015, Lisbon, Portugal (**Best paper award**).

8. Sameer Alam, **Murad Hossain**, C. Lokan, S. Barry, G. Aldis, R. Butcher, and Hussein Abbass, *Real time prediction of worst case air traffic sector collision risk using evolutionary optimization*. Proceedings of the IEEE Symposium on In Computational Intelligence, 2013, (pp. 72-79) (**Nominated for best paper award**).

9. **Murad Hossain**, Sameer Alam and Hussein Abbass, *A Dynamic Multi-Commodity Flow Optimization Algorithm for Estimating Airport Network Capacity*, Proceedings of the 4th ENRI International Workshop on ATM/CNS, (EIWAC 2015), Tokyo, Japan.

Contents

List of Figures

List of Tables

List of Acronyms

ANSP	Air Navigation Service Provider
ASE	Altimetry System Error
ATC	Air Traffic Controller
ATM	Air Traffic Management
ATOMS	Air Traffic Operations and Management Simulator
ATS	Air Transportation System
CNS	Communication, Navigation and Surveillance
DRN	Direct Route Network
FL	Flight Level
GNSS	Global Navigation Satellite System
IATA	International Air Transport Association
ICAO	International Civil Aviation Organization
IFR	Instrument Flight Rules
IMC	Instrument Meteorological Conditions
IWN	Intermediate Waypoints Network
MCF	Multi-Commodity Flow
MIDRMA	Middle East Regional Monitoring Agency
RVSM	Reduced Vertical Separation Minimum
SLOP	Strategic lateral Offset Procedure
TLS	Target Level of Safety
VFR	Visual Flight Rules
VMC	Visual Meteorological Conditions

Chapter 1

Introduction

This chapter contains a brief introduction to the perceived problem and motivation for conducting this research, its specific objectives and major contributions, and organisation of this thesis.

1.1 Overview

The air traffic has grown dramatically worldwide during the last few decades and is projected to continue. According to the International Civil Aviation Organization (ICAO) forecast, worldwide air traffic is expected to continue to increase at a rate of 4.7% per annum until 2025 [50]. There is growing concern among airlines and air navigation service providers (ANSPs) that the air transportation network (ATN) in some regions is experiencing severe capacity-demand imbalances [231]. In the light of unprecedented growth in air traffic worldwide, ANSPs are exploring new paradigms (e.g. SESAR [98] and NextGen [185]) and air traffic procedures such as dynamic sectorisation [215], automated separation assurance [70, 142, 152], and Reduced Vertical Separation Minimum (RVSM) [116] for the efficient and safe management of an ATN. An ATN can be considered a composition of two major networks: (i) an airport network–in which each airport is treated as a node and the flights connecting them create the links; (ii) an airspace networkwhich considers waypoints as nodes and airways as making the links. Although in many cases the airports and airspace system of an ATN act as temporal bottlenecks [165], they are expected to support such growth if managed efficiently and effectively.

It is usually understood that the capacity is dependent mainly on the airports, with the airspaces considered relatively unconstrained [76, 219]. In the air transportation domain, the capacity of an airspace or airport normally represents its ability to safely handle a number of aircraft per unit of time [24]. However, one of the major constraints in air traffic operations is maintaining safe separation among the aircrafts. One key measure for judging the safety of operations in an airspace is the collision risk estimate. According to the ICAO, the unit of collision risk is fatal accidents per aircraft flight hour [113]. Increasing the number of flight operations (arrivals and departures) in an airport network will increase the traffic flow in the upper airspace, which will increase the crossing frequency and possibility of loss of separation. In such a situation, it is vital to understand the relationship between the capacity and safety of an ATN. Despite the interest in increasing both capacity and safety in an ATN, there is no industry- or regulatory-recognised 'standard' to limit the capacity of an ATN based on a ceiling imposed by the regulation authorities on airspace safety. Virtually no research has been accomplished that links the upper limits of capacity to safety.

In current operational concepts, air traffic flow management (ATFM) plays a central role in maintaining capacity-demand balancing by adjusting traffic flows according to the capacity of an airport or air traffic control airspace. Each airport and air traffic control sector declares its maximum capacity. When the declared capacity is exceeded, ATFM approaches are taken to reduce the traffic demand to manage congestion. There are two popular ATFM strategies: holding patterns and ground delay programmes. Of these, the ground delay programme is proven to be very effective as it delays flights before they depart from their origin airports, keeping traffic at an acceptable level for the effected airport or airspace. However, the real challenge is to manage the congestion of an airspace that may lead to an increase in the risk of collision when demand exceeds the capacity limit.

The capacity of an air transportation network has generally been measured at the levels of its individual elements, such as links (sector capacity and airspace complexity) and nodes (terminals and runway throughput), which obviously does not constitute its overall system-level capacity. From the network point of view, the system-level capacity of an ATN can be measured from its underlying airport network. In an airport network the nodes are serving as a source/sink for the traffic flow, which enables us to develop a mathematical model to estimate the capacity upper bound. However, for complex metrics such as the collision risk of an airspace, it is necessary to develop high-fidelity discrete-event simulations. Although significant effort has been expended on developing large-scale, discrete-event simulations of an air transportation network system, a simple macroscopic theoretical model for estimating the system-level capacity of an airport network is lacking. Developing an airport network capacity estimation model and integrating it with a large-scale simulation environment will enable us to gain insights into the relationship between capacity and safety in an ATN. Moreover, the utility of such a framework should allow policy decision-makers to understand the basic relationships between observable metrics and macroscopic investment options in the airport network or the airspace infrastructure.

Traditionally, a network's flow capacity is determined by modelling it as a classical multi-commodity flow (MCF) problem [190], examples being in communication networks, and water distribution and electric power systems. One of the major requirements of existing algorithms for solving an MCF problem is that the resources required by the commodities at a node or link need to be static (not change over time) and must be independent of the mixing/interactions among the commodities. As a result, MCF problem modelling and its algorithms are limited to certain types of network and not precisely applicable to air transportation. MCF modelling and algorithms are not directly applicable to an air transportation network for the following reasons: (a) its movements involve flows of aircraft with different speeds; (b) its flow is heterogeneous given the different wake vortices and categories of aircraft, viz. light, medium and heavy; (c) different types of aircraft require different amounts of resources at arrival and departure airports; (d) there must be a minimum separation distance between two consecutive aircraft, which depends on the type of operation (landing or take-off) and the preceding aircraft's type and operation for managing wake vortices; (e) aircraft departing from an airport are expected to land at destination airports within a time window because they cannot remain in the air indefinitely; (f) slot management; and (g) the flows between different multiple origin-destination (O-D) pairs are not exchangeable or substitutable. In addition, managing safe separation among the aircraft in an airspace and keeping overall collision risk within it below a certain threshold leads to yet another set of constraints. Maintaining the collision risk below a certain threshold and considering the abovementioned flow characteristics make estimating the capacity of an air transportation network a complex, yet interesting, problem to solve, which this thesis addresses.

In this thesis, I develop a model that extends the MCF formulation for estimating the capacity of a given airport network without knowing its individual airports' capacities. The key assumption of the proposed model is that it considers these capacities as fixed time slots per hour that remain constant over time, with the flows between connected airports considered as different commodities. Then, a hill-climbing-based heuristic algorithm is developed to solve the MCF-based formulation for an airport network. Finally, to investigate the capacity-safety relationship due to the interaction(s) between the airport and airspace network in an ATN, I develop a framework that integrates the airport and airspace network. To estimate the collision of the airspace network of a given airport network capacity limit, the capacity of an airport network needs to be translated into traffic scenarios from which airspace collision risk can be estimated. For that purpose, I propose an evolutionary computation-based framework that converts an airport network's capacity into air traffic scenarios. The traffic scenarios are then executed in an air traffic simulator to calculate the airspace network's collision risk. Then, the capacity-safety relationship curves for different scenarios are generated and actual capacity limit due the airspace safety threshold are analysed. The proposed methodology will facilitate a better understanding of the bottlenecks in an ATN and pave the way for discovering where the major bottlenecks that cause system inefficiencies occur.

1.2 Motivation

In an ATN, it has been considered that an airspace network is relatively unconstrained and is the main bottleneckt[76, 219]. An airspace network, which is mainly responsible for an orderly flow and safe separation between flights, considers safety its limiting factor. The interactions between two network, which are created by actual flow between them, plays an important role for an ATN's actual capacity estimation. Figure 1.1 shows a hypothetical representation of an airport and airspace network and the interactions between them. The capacity of an airport network can be increased by adding more runways or by utilising the regional airports around a country's major airports in a hub-spoke manner. However, the question is whether increasing airports capacity will actually increase the overall capacity of the entire ATN. It is obvious that increasing the flow among airports will increase flight densities in the airspace network and, as a result, eventually may increase the risk of collision. In such a situation, it is necessary to determine the relationship between the capacity and airspace collision risk for an ATN. This thesis is motivated to address this issue.

The non-linear, stochastic and time-dependent interdependency among components in the above airport-airspace interactions make classical mathematical assumptions of linearity and homogeneity obsolete. Nature-inspired techniques such as evolutionary computation, genetic algorithms, differential evolution etc. have proven to be highly effective in addressing complex problems of the air transportation domain for which traditional methodologies are ineffective or infeasible [62, 63, 69, 181, 203]. In this thesis, I have developed an evolutionary computation-based framework and techniques for translating the airport network capacity into air traffic scenarios to estimate the collision risk of a given airspace network. The proposed methodology may facilitate a better understanding of the actual bottlenecks in an air transportation network.

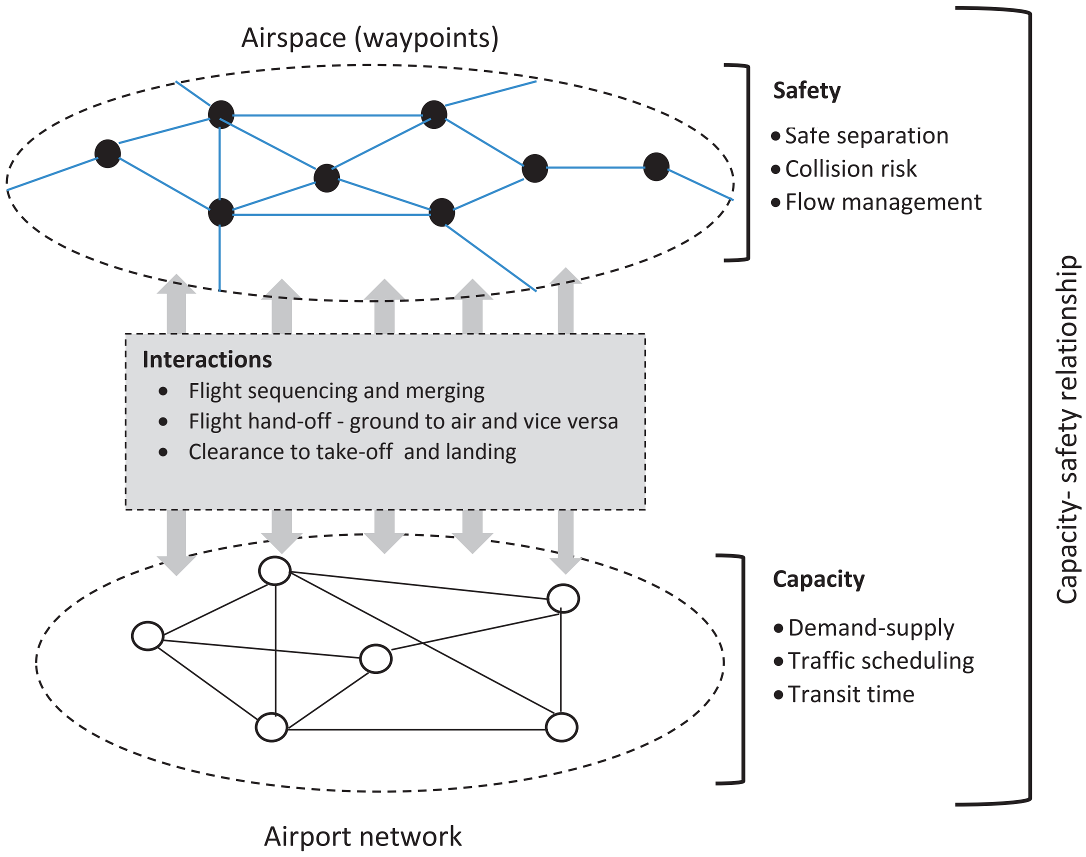

FIGURE 1.1: Conceptual representation of interactions and constraints of airport and airspace network

1.3 Research Questions and Hypothesis

For an ATN, its major components, the airport and airspace network, have their own limitations and performance measures. How these two networks with their own limitation(s) can interact to achieve an overall system objective to balance the two is the focus of my dissertation. This thesis hypothesises that an airspace network contributes significantly to the upper bound of the overall capacity of an ATN due to the safety threshold and, in some cases, could be a bottleneck for the whole system. Also, increasing the flow density in the airport network will increase the risk of collision for en-route airspace. To support this hypothesis, the thesis specifically investigates the following research question.

What is the relationship between the airport network capacity and airspace safety in an air transportation network?

In order to answer this main research question, the following related sub-questions need to be considered.

1. *What is an appropriate model for an airport network for capacity analysis?* An airport network forms the backbone of an air transportation network. In such a network, the links between origins and destinations results in a complex network of routes that can be complemented with associated information about the routes themselves; for instance, traffic loads and distances. Complex network theory provides a theoretical framework that may help to develop models and analyse the topology and characteristics of the resulting network. Based on this, airports are modelled as graphs (networks) consisting of airports as vertices linked by flights connecting them. Complex network metrics can further be correlated with system performance measures such as capacity.

2. *How to estimate the flow capacity of an airport network?*

   The capacity of a network indicates the maximum throughput it can handle without becoming congested. A good network capacity estimation model would enable us to predict how much additional demand could be accommodated by an airport network. Furthermore, it could enable us to determine what measures can be taken to prepare for the time when additional capacity will be required for future growth. Estimating a networks capacity is generally known as one of the most difficult problems in the transportation field [46]. Conventionally, in traffic flow networks, the maximum flow capacity is estimated using an MCF model [46]. However, this model is not directly applicable to an air transportation network, which has non-linear interactions among its different components and heterogeneous flows that make modelling its capacity a complex problem.

3. *What is an appropriate model for an airspace network for collision risk analysis?*

Collision risk is one of the key safety indicators of an air transportation system and is usually compared with a defined threshold value. This threshold value is defined by ANSPs and is known as the Target Level of Safety (TLS). TLS provides a quantitative basis for judging the safety of operations in an airspace network [144]. I hypothesise that the collision risk of an airspace network is correlated to its structure and, to handle the increasing traffic demand, the underlying network structures need to be managed. To answer this research question I used real-world traffic data to estimate the collision risk of different airspaces. I then developed network models to represent an airspace and measure its structural properties and features. Finally, the network features are correlated with the estimated collision to investigate the relationship between collision risk and network structure.

4. *What changes in airspace network be made to manage collision risk?*

   The continued increase in air traffic and the limited airspace resources have resulted in serious congestion and flight delay due to maintaining the collision risk of an airspace below the target level of safety. One of the ways to increase the capacity and safety of an airspace is to optimise its network structure. However, a complete new design or extensive modification of an existing airspace network will make the controllers experience irrelevant in managing the air traffic flow. One of the possible ways to optimise an airspace for collision risk with minimal or virtually no change in its structure is to laterally offset the airways to its right or left. Offsetting an airway will not change the number of waypoints within it or its network structure. I applied this concept and designed an evolutionary algorithm to find the optimal lateral shift for each airway in a given airspace that may reduce the overall collision risk.

5. *How the interaction between the airport and airspace network effect capacity-risk trade-off?*

To address this question, I developed a framework to integrate the airport and airspace network for an air transportation network and proposed a methodology for the interaction of the two networks to analyse the relationship between capacity and safety. The framework comprises user-defined airport system simulation, a network-level capacity model and an airspace network collision risk estimation. The capacity estimation model provides the hourly flow density (flight movements per hour) and a traffic schedule. The traffic schedule consists of scheduled departure and arrival time for each flight. To analyse the collision risk of a given traffic scenario, an evolutionary computation-based scenario generation technique is developed. Finally, the capacity upper bound is determined by simulating different traffic scenarios in the Air Traffic Operations and Management Simulator (ATOMS) [11].

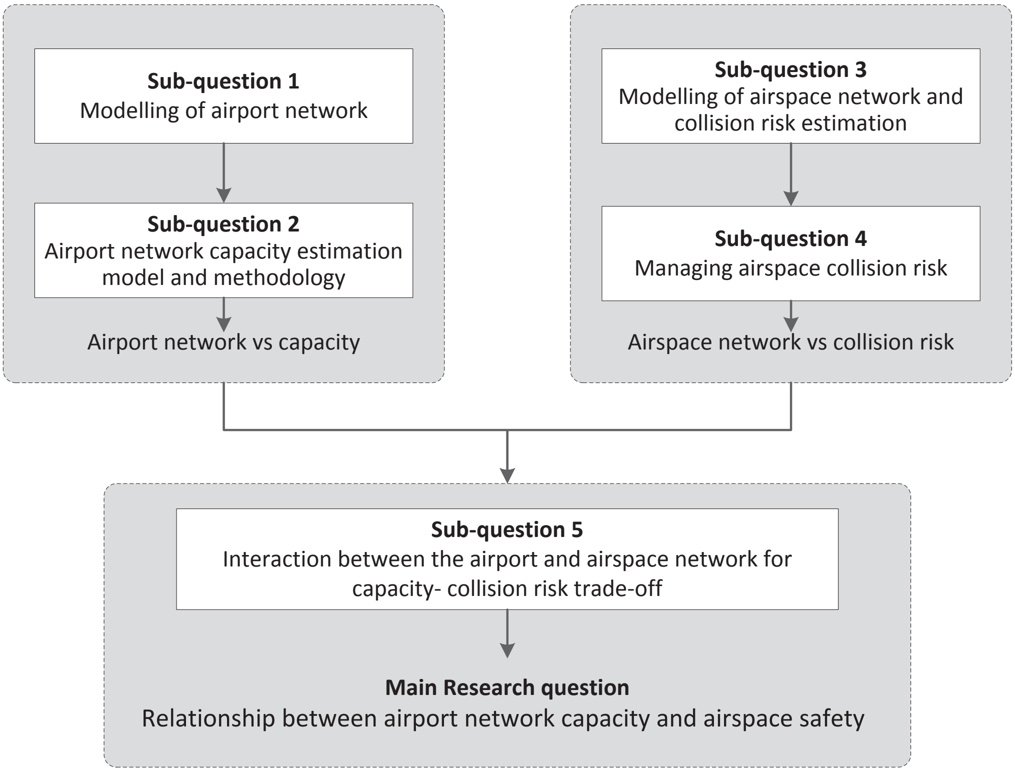

Figure 1.2: Relationships among research questions

To address the main research question, I first need to develop models that estimate the flow capacity limit of an airport network to answer sub-questions 1 and 2. On the other hand, to analyse the safety of an airspace, I need to answer sub-question

3. The answer to sub-question 3 provides models to represent an airspace as a network and find the collision risk of an airspace with its network features. The relationship of airspace collision risk with its network model paves the way for developing a methodology to manage the collision risk, which answers sub-question 4. Then, I combine the outputs of questions 1 and 2 with those of questions 3 and 4 to answer sub-question 5, which investigates the capacity-risk trade-off due to the interaction between the airport and airspace network. Answering all of the sub-questions in an integrated manner will eventually answer the main research question of this thesis. Figure 1.2 illustrates the relationship among the sub-questions and their flow to answer the main research question.

1.3.1 Key Assumptions

To answer the sub-questions of this thesis, I make the following key assumptions:

- The air transportation network is considered a combination of two major sub-networks: (i) airport network and (ii) airspace network.
- The airport and airspace networks are considered to be static. The components of these network nodes (airports and waypoints) and the connections among them (links) do not change.
- To estimate the capacity of an airport network and the collision risk of an airspace, tactical flight management operations are not considered. Once a flight path is set or defined, it remains unchanged in my experimental simulation. In the present day, the modern flight management system integrates with the data link interface, which allows it to transmit its current position, velocity, wind and weather data and to receive update flight plans from the ground. Given the technological advancement, especially with the improvement of communication, navigation and surveillance technologies, it is possible to generate 4D trajectories that will be conflict free in an airspace network.

1.4 Organisation of Thesis

This thesis aims to provide specific insights into the capacity-safety relationship in an air transportation network. It consists of the following seven chapters.

Chapter 1 begins with an overview of the research topic, discusses the motivation behind this study, defines the research question and presents the thesis's organisation.

Chapter 2 provides a background to this thesis. Despite the fact that there are many studies that can be related to this work (from a very wide perspective), this chapter provides a brief but comprehensive survey covering the important aspects and familiarises the reader with the concepts and notations used. It presents some general background information on air transportation systems. Then, the modelling approaches used to analyse an air traffic network, capacity estimation and the constraints for different sub-systems/networks are discussed. Finally, a summary of the collision risk models is provided.

In Chapter 3, I address the first sub-question and develop a complex network model to analyse an airport network. An airport network forms the backbone of an air transportation network. In such a network, the links between origin and destination of flights result in a complex network of routes. In this chapter, I propose a complex network approach to model an airport network for understanding the dynamics of its topology and features. As a case study, an Australian civil domestic airport infrastructure is modelled as a complex network. I then compute complex network measures such as degree distribution, characteristics path length, clustering coefficient and centrality measure as well as the correlation between them to gain an understanding of the topology and the robustness of the Australian airport network.

Chapter 4 presents a model for estimating the flow capacity of an airport network that is an extension of the MCF problem and considers the wake-vortex interactions during landing and take-off. In it, flows between two nodes (airports) are considered as different commodities and the local airport capacity is formulated using a time slot of one hour, with the hourly rate of flow (landings and take-offs) bound by a capacity constraint. Also, a novel heuristic algorithm for solving the capacity estimation problem is proposed. I validate the effectiveness of the proposed model and heuristic algorithm using randomly generated networks of different topologies and the Australian airport network.

Chapter 5 addresses the research question of *What is an appropriate model for an airspace network for collision risk analysis?* In this chapter, two different models – a direct route model and intermediate-waypoints-based model – are proposed for an airspace. Traffic data (more than 200,000 flights) from 12 countries in the Middle East region is analysed to estimate the collision risk. The estimated collision risk is then correlated with the network features from the two proposed models.

Chapter 6 addresses the research sub-question of *What changes in airspace network be made to manage collision risk??* In recent years, the ICAO has introduced SLOP, which allows suitably equipped aircraft to fly with a 1nmi or 2nmi lateral offset to the right of the airway's centreline in oceanic airspace. I utilise the SLOP concept to minimise the collision risk in an airspace. I propose an evolutionary framework using a differential evolution process to identify optimal lateral offsets for each airway in a given airspace in order to reduce the overall collision risk. Airway-specific lateral offsets are then correlated with airway-traffic features using multiple regression models to identify which features can determine the optimal lateral offset, based on which, the proposed approach establishes a generic mapping that can suggest optimal lateral offsets to mitigate the collision risk for a given airspace.

In Chapter 7, the relationship between capacity and mid-air collision risk is investigated. I propose a methodological framework for understanding the relationship between the capacity and safety of an air transportation system. I first present a conceptual approach to the problem and then integrate a collision risk model with an air traffic simulator. Then, I develop an evolutionary method for generating traffic scenarios to estimate the mid-air collision risk and a simulation framework.

Details of the simulation, including air traffic network generation, traffic scenario generation and collision risk estimation, are presented. Finally, the overall experimental framework for testing and evaluating the proposed methodology is presented.

Finally, chapter 8 provides a summary of the research conducted and its key findings, with potential future research directions indicated.

Figure 1.3 shows a graphical organisation of the chapters and their relationship.

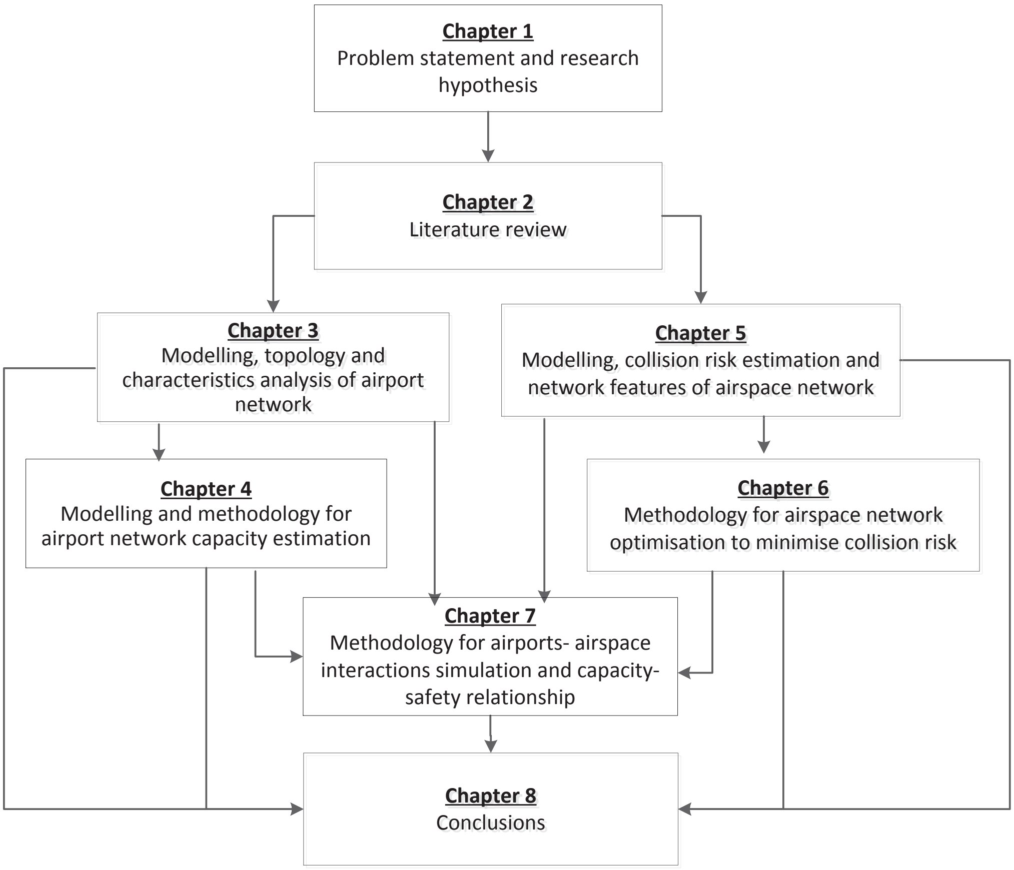

Figure 1.3: Organisation of thesis chapters

1.5 Key Contributions

A list of the scientific contributions arising from this thesis is given bellow:

- a model and methodology for estimating the capacity of an airport network considering different fleet mixes and travel times

- a methodology for investigating the relationship between an airspace networks features and its collision risk
- a differential evolution methodology for identifying the optimal lateral offset of the airways of an airspace network required to minimise the collision risk; and
- an evolutionary framework in which traffic scenarios are generated, capacity estimated and collision risk evaluated in an integrated manner to identify the capacity-safety relationship of a given air transportation network.

Chapter 2

Literature Review

Despite the fact that there are a huge number of studies that can be related to this thesis (from a very wide perspective), this chapter provides a brief but comprehensive survey covering the important aspects, and familiarises the reader with the concepts and notations. It presents a general description of the air transportation system.

2.1 The Air Transportation System

Air transportation is one of the most important components of the world's transportation systems. It is a large-scale (extends worldwide geographically), complex (exhibits structural as well as behavioural complexity), adaptive (changes dynamically in response to continuous and punctual stimuli) and socio-technical (has both social and technical components) system. The key function of this system is to provide domestic and international air transportation services for both passengers and freight.

Air traffic has grown dramatically during the last few decades and is projected to continue. However, there are concerns that, in future, the system, due to its structured and centralised nature, may not scale to meet demand [37, 38, 133]. As a result, I can anticipate a more congested and potentially problematic airspace, particularly in and around major transportation hubs. Higher traffic densities will cause more flights to be rescheduled or rerouted to avoid conflicts, more delays for aircraft arriving and departing from terminals, and increased instances of near misses between aircraft. To help develop a better, more efficient air transportation system, it is important to understand the capacity and safety constraints of the system. Several research analyses, including one conducted by the Office of Technology Assessment, have demonstrated that linear increases in air traffic operations result in a quadratic decrease in airspace safety [53].

Both operationally and structurally, an air transportation system is a complex system with the main components including airlines, airports, airspaces and air traffic controllers. All of these components interacting with each other and constitute a very complicated, highly distributed network of human operators, procedures and technical systems. The topology of the air transportation system is coupled in such a way that changes/disturbances in one sub-system may have significant impact on other sub-systems or the whole. For example, the volcanic ash clouds over Iceland recently effected over 70% of worldwide air traffic [5]. Such disruption due to airspace and traffic constraints or other uncertainties also have significant impact on the systems performance. Therefore, there is an urgent need to explore, investigate and understand the relationship between the interaction and performance of different components of air transportation systems. In this thesis, I am looking to develop a method to analyse the relationship between the airport network capacity and the safety of the airspace/en-route network.

In addition to the key components of an air transportation system a more complex depiction of it must include passengers, the organisations that run and control the systems, communication navigation and surveillance (CNS) and other stakeholders that are affected by its operations. However, because this thesis emphasises in relationship between flow capacity and safety between the sub-components, the focus is on those factors and components. The following sections describe some of the key components.

2.1.1 Airport

The airport is an essential element in the air transport system (ATS) for all payloads – passenger as well as cargo – to gain access to the aircraft for transport from origin to destination. The air traffic flow in an ATS originates and also terminates at the airports. In other words, airports are the sources and sinks of an ATS.

The airport can have a very simple structure, with a small runway for the aircraft for take-off and landing and a type of hangar to prepare for passenger boarding, baggage treatment and formalities such as customs or passenger checks. It should have the infrastructure to allow the preparation of the flight with meteorological information, route planning and aircraft loading. On the other hand, there are the big airports that handle several hundred-thousand passengers per day, have up to six parallel runways and can handle thousands of aircraft per day, with a very sophisticated infrastructure, hotels, conference centres and business areas as an integral part of the airport.

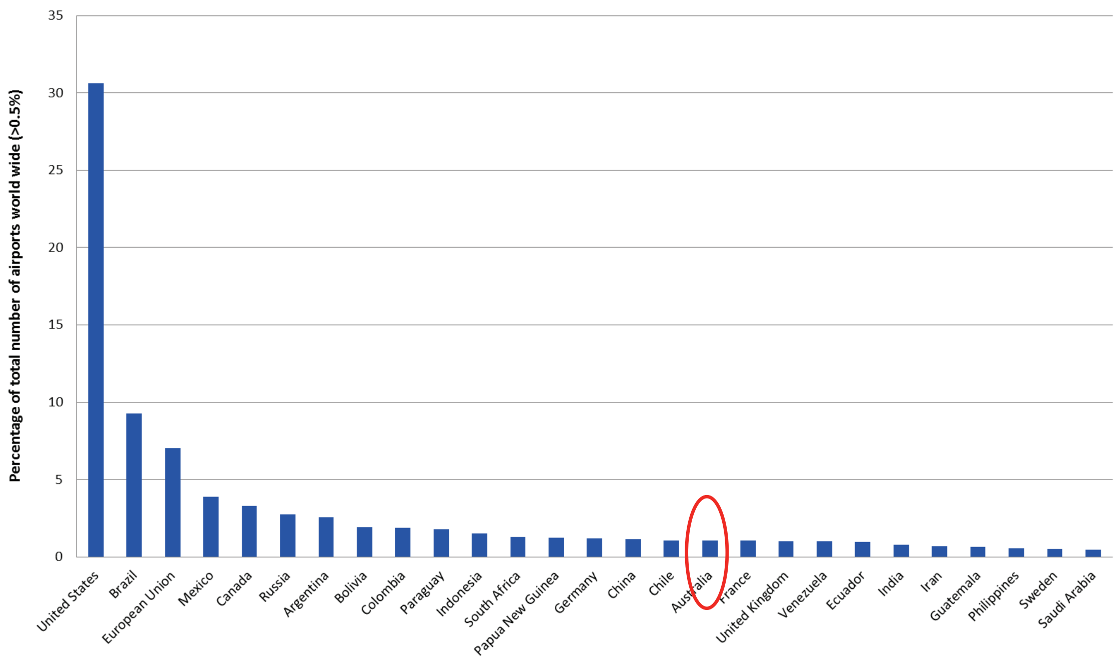

FIGURE 2.1: Ranking of countries according to its number of airport.

There are approximately 50,000 airports around the world, with approximately 32% situated in the United States, whereas, Australia has only 500 airports. Figure 2.1 shows the distribution of the number of airports in the major countries.

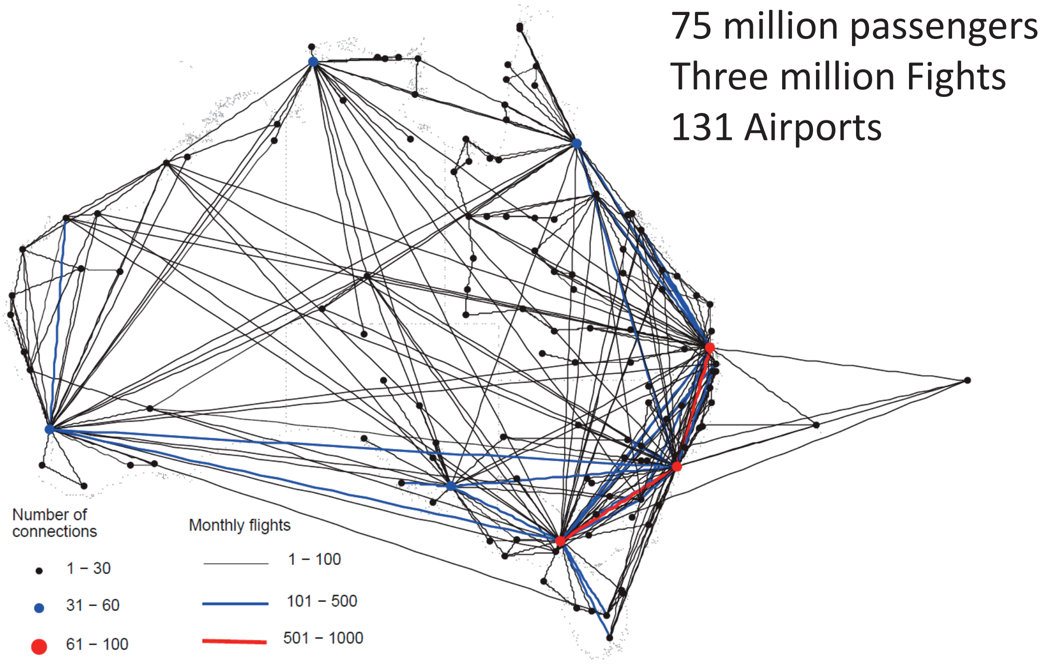

FIGURE 2.2: Geographical distribution of airports in Australia

Figure 2.2 shows the geographical distribution of airports in Australia. Of the 500 airports in Australia, only 131 operate passenger flights regularly [108]. In Australia, there are almost three million flight movements per year, carrying approximately 75 million passengers [6]. From the geographical locations of Australian airports, I have found that higher concentrations of airports are situated in the south coast region that forms a typical 'J'curve. This concentration of airports is generally correlated with the distribution of population. Due to the lack of population in the middle part of the country, there are very few airports in central Australia.

2.1.2 Airspace

Airspace is the portion of the atmosphere controlled by a country above its territory, including its territorial waters or, more generally, any specific three-dimensional portion of the atmosphere. It is not the same as aerospace, which is the general term for Earth's atmosphere and the outer space in its vicinity.

According to general operating rules and procedures, airspace is classified into four different classes. The intention of the classification is to ensure pilot flexibility with acceptable levels of risk appropriate to the type of operation and traffic density within each class of airspace. In general, the classification schema is designed to provide maximum separation and active control in areas of dense or high-speed flight operations. According to the FAA, all airspaces fall into four general categories [169].

- Positive Controlled Airspace (PCA): In this type of airspace, the air traffic controller (ATC) separates all aircraft, whether instrument flight rules (IFR) or visual flight rules (VFR). PCA is reserved for either very-high-altitude flights at or above 18,000 feet from mean sea level or around high-density airports.

- Controlled Airspace: In this airspace, ATC separation services are provided to IFR aircraft. IFR aircraft are authorised to fly into clouds or areas of reduced visibility and are provided ATC assistance to remain separate from other IFR aircraft. IFR aircraft, when operating in areas in which weather conditions and traffic density permit other aircraft to be safely observed and avoided, are still responsible for separating themselves from VFR aircraft. VFR aircraft operating in controlled airspace are also responsible for separating themselves from all other aircraft. VFR flight operations are permitted as long as the weather conditions are sufficient to enable pilots to "see and avoid"other aircraft in this type of airspace.

- Uncontrolled Airspace: In uncontrolled airspace, ATC separation services are not provided by the FAA. Regardless of the weather conditions, all aircraft, IFR or VFR, must ensure their own separation.

- Special Purpose Airspace: Special purpose airspace is an area designated for operations of a nature such that limitations may be imposed on aircraft not participating in those operations. Often, these operations are of a military nature. Special purpose airspace can lie within either controlled or uncontrolled airspace and can potentially affect both IFR and VFR aircraft.

Apart from the general operating rules and procedures, based on the altitude range, all of the airspace above the US has been designated by the FARs into six classes. Table 2.1 reports the general descriptions of these classes.

TABLE 2.1: Features of different airspace class ([169])

Airspace Features	**Class A**	**Class B**	**Class C**	**Class D**	**Class E**	**Class G**
Dimensions	Altitudes at and above 18,000ft from mean sea level	Surrounding high-density airports up to an altitude of above 10,000ft from ground level	Surrounding medium-density airports up to an altitude of 4,000ft above the airport elevation	Surrounding non-radar control towered airports up to an altitude of 2,500 ft. from the airport surface	Airspace floor varies between the surface of the Earth, 700ft or 1,200ft above ground level. Airspace extends up to but not including 18,000ft above mean sea level	Airspace not included in class A, B, C, D or E designations
Level of Control	Positive controlled	Positive controlled	Controlled	Controlled	Controlled	Uncontrolled
Permitted Flight Operation	IFR only	IFR and VFR if weather conditions permit	IFR and VFR if weather conditions permit	IFR and VFR if weather conditions permit	IFR and VFR if weather conditions permit	IFR and VFR if weather conditions permit
Entry Requirements for Aircraft	ATC clearance required for both IFR and VFR	ATC clearance required for both IFR and VFR	ATC clearance required for IFR. VFR aircraft must make radio contract prior to entry	ATC clearance required for IFR. VFR aircraft must make radio contract prior to entry	ATC clearance required for IFR. VFR aircraft are not required to contact ATC	ATC does not provide separation services to either IFR or VFR aircraft

Continued on next page

Table 2.1 – *Features of different airspace class*

Airspace Features	**Class A**	**Class B**	**Class C**	**Class D**	**Class E**	**Class G**
ATC services to IFR aircraft	Standard separation (5nm laterally, 1,000ft vertically) to all aircraft	Standard separation between IFR aircraft. (3nm laterally, 1,000ft vertically) to all aircraft	Standard separation between IFR aircraft. (3nm laterally, 1,000ft vertically) to all aircraft	Standard separation between IFR aircraft. (3nm laterally, 1,000ft vertical radar separation or standard non-radar separation)	Standard separation between IFR aircraft. (3nm laterally, 1,000ft vertical radar separation or standard non-radar separation)	No services required nor will clearances be issued. If traffic conditions permit, IFR aircraft might be provided traffic advisories and flight following
ATC services to VFR aircraft	VFR aircraft not permitted	Aircraft will be separated from large or jet IFR aircraft by either $1\frac{1}{2}$ nm and 500ft separation	Aircraft will be separated from IFR or VFR aircraft by either target resolution, visual, or 500ft vertical separation	Provided traffic information concerning IFR and known VFR aircraft	If traffic conditions permit, VFR aircraft might be provided traffic advisories and following	No services required nor will clearances be issued. If traffic conditions permit, VFR aircraft might be provided traffic advisories and flight following

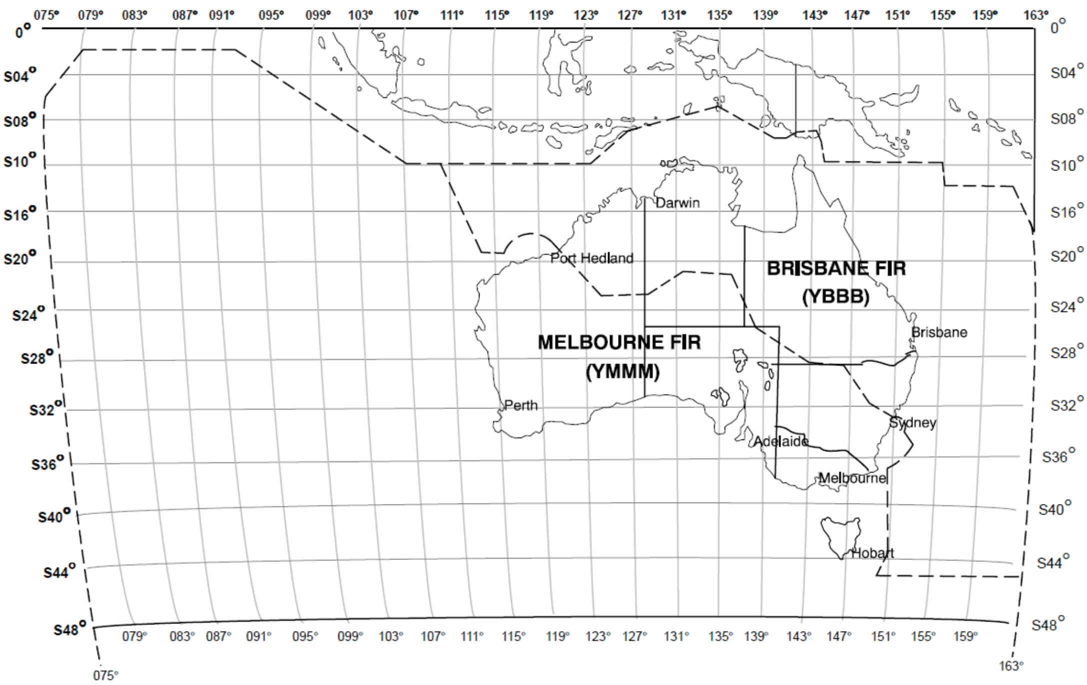

Figure 2.3: Flight information region in Australia

Airspace is a complex system that is partitioned for several reasons, mainly for air traffic control to maintain safe separation among the flight flow within it. Each country has its own National Airspace, which is typically partitioned into air control centres. For example, Australia has two control centres, one in Melbourne and the other in Brisbane. Figure 2.3 shows the location of flight information regions (FIRs) in Australia. Australian airspace includes the nation's sovereign airspace and international airspace over the surrounding oceans including the FIR's of the Solomon Islands and Nauru. Its airspace stretches in latitude from two degrees to 90 degrees south, and in longitude from 75 degrees west to 163 degrees east. The total area is almost 20 million square nautical miles (51.7 million square kms) or approximately 11

From the air traffic control perspective, flights in controlled airspace are managed by ground-based air traffic controller (ATC). An ATC is responsible for managing air traffic flow in a portion of airspace, known as a 'sector', which is the smallest unit of control [215]. However, the human cognitive limitations of an ATC restrict

Figure 2.4: Sector configurations in Australian airspace

the number of aircraft that can be safely managed by an ATC. The typical tasks conducted by an ATC include safe and efficient flow of air traffic, monitoring aircraft movements, conflict detection and resolution and aircraft handover from/to his sector. Hence, the airspace is partitioned into sub-airspace as sectors in which air traffic is distributed to ensure that ATCs can safely and efficiently manage the air traffic without being overloaded. Figure 2.4 shows the current sectors in the Australian FIR. Finally, inside the sectors, the actual routing of aircrafts operates in a network of airways. These airways consist of navigational aid (NAVAIDs) that define a point on the ground, which is also known as a waypoint. The position of a waypoint is given by a latitude and a longitude, but not an altitude. A flight plan is therefore a succession of waypoints, together with time stamps and altitudes that an aircraft is supposed to follow. So, the routing of an aircraft consists of maintaining its assigned set of waypoints and defined altitude, or, equivalently, a set of jet routes that create a path from the origin to the destination airport. Figure 2.5 shows an air route (airway) between Sydney and Melbourne.

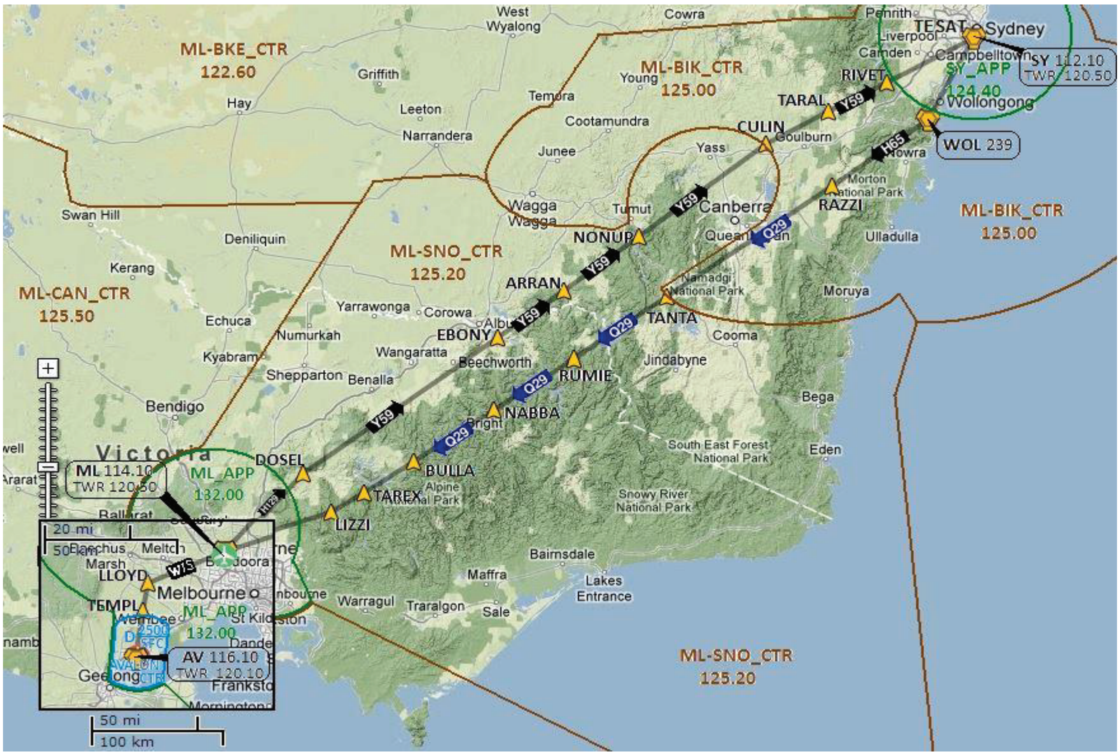

FIGURE 2.5: Flight route (air-route) between Sydney and Melbourne

2.1.3 Air Navigation Service Providers

An air navigation service provider (ANSP) is a body that manages air traffic on behalf of a company, region or country. ANSPs are either government departments, state-owned companies or privatised organisations. The ANSPs provide information designed to ensure the safe and socially efficient provision of air transportation [65] and air traffic management (ATM) [156] services. The key responsibility of ANSPs is to provide communication, navigation and surveillance (CNS) services.

- Communication: Air traffic communication is typically divided into two parts: air-to-ground and ground-to-ground. For ground-to-ground voice communication, telephone lines are commonly used. For ground-to-ground data exchange, the primary means is the Aeronautical Fixed Telecommunication Network (AFTN). The AFTN is used mainly by the control centres and air traffic service provider, but not the airline operation centres. In Europe, alongside AFTNs, the 'Socièt é Internationale de Telecommunications Aronautiques'(SITA) network is also used for ground-to-ground data exchange, mainly by AOCs [51]. In the US, airline operation centres often use AviNet by ARINC Inc., which provides advanced data communications such as message switching and content services. An integrated communication system can greatly benefit both ATSP and AOCs in the form of collaborative decision making. Both air-to-ground and/or ground-to-air voice communication involves HF (high frequency), VHF (very high frequency) and UHF (ultra-high frequency), using both analogue and digital signals [169]. The VHF spectrum is primarily used by civilian air traffic, whereas the HF spectrum is mainly used by long-distance oceanic flights. The UHF spectrum is reserved for military aircraft. As an aircraft flies over different air traffic service providers, it must tune to the appropriate frequency. FMS systems in modern aircraft can automatically select and tune to appropriate frequency. All communications over this frequency can be heard by any pilot who tunes to it. This provides pilots with a major source of situational awareness regarding neighbouring traffic. A standard set of communication procedures is followed between the ATCs and pilots to avoid any misunderstanding or confusion [169]. The only means of data link between the air-to ground and ground-to-ground network is ACARS (Airborne Communication and Addressing System), which uses VHF radio and the satellite communication link [54]. However, it is not yet approved for flight safety critical messages.

- Navigation: Traditionally, aircraft have relied on ground-based radio beacons and inertial navigation systems to navigate. The present navigation system consists of airways and a variety of ground-based navigation systems such as VHF Omnidirectional Range (VOR), Distance Measuring Equipment (DME), LOng RAnge Navigation (LORAN) and Tactical Air Navigation (TACAN), to name a few [169]. The airways depending upon their altitude are named as "victory"airways (up to 18,000ft MSL) and "Jet"airways (18,000ft to 45,000ft MSL). In the US, they are known as Federal Airways and in Europe and Australia they are known as designated airways. At the moment VOR/DME is the ICAOs approved primary means of navigation [117]. For departure control and arrival management, a set of published routes and procedures known as Standard Integrated Departures (SIDs) and Standard Terminal Arrival Rules (STARs) are used. With advances in satellites navigation, in-flight GPS is becoming an important means of navigation in the cockpit and a primary means of navigation in oceanic and remote areas [117]. GPS provides not only higher accuracy but also greater redundancy.

  Due to accuracy and worldwide availability, the Global Navigation Satellite System (GNSS) has been designated by the ICAO as the future navigation system for all civil aviation needs. In addition, required navigation performance (RNP) is introduced, which is a measure of the lateral navigational accuracy of an aircraft in an airspace[117]. An RNP-certified aircraft has the ability to maintain specified navigational accuracy during flight, which improves the en-route and approach accuracy.

- Surveillance: In present day ATM systems, surveillance is performed by an array of radars that consist of primary surveillance radars (PSR) and secondary surveillance radars (SSR) [169]. The PSR provides information about the bearing and distance of the aircraft and the SSR provides information about aircraft identification and its altitude. PSR radars are further subdivided into long-range air-route surveillance radar (ARSR), which scans a wide area (generally a 250-mile radius), and airport surveillance radar (ASR), which uses a shorter range and scans a narrower area (generally a 60-mile radius). SSR radars have a variety of modes called A, C and S. Mode C and S provides pressure-altitude referenced to 29.92in of mercury in 100ft increments from 1,000ft to 126,700ft. SSR Mode S is the current standard for civil aircraft [1]. The PSR and SSR radar data are processed by the radar data processor to assess the quality and integrity of the data. The data are further processed to identify aircraft, calculate their positions, track their movements, transform the data to display coordinates and display the resulting information along with maps on the controllers' plan view displays.

A new system known as automatic dependant surveillance (ADS) is proposed, which will eventually replace ground-based surveillance systems. In ADS, an aircraft transmits its position based on on-board navigational instruments. There are two versions of ADS, ADS-A (addressable), also known as ADS-C (contract), and ADS-B (broadcast). The ADS-A system exchanges information about specific aircraft and ATC on request. The ADS-B system broadcasts information periodically to all aircraft in the immediate vicinity and all ATM facilities in specified areas.

2.2 Network Representation of Air Transportation System

The Air Transportation System (ATS) is a complex network composed of several heterogeneous and mutually interacting sub-systems [17]. The mobility of passengers and goods is just the final result, which is carried by flight movements from airport to airport. Therefore, it is not surprising that most analyses have focused on the mobility of aircraft, disregarding other technical details. With this point of view, the construction of a network is straightforward and an ATS can easily be represented by an interlinked set of networks. It can easily be decomposed in several layers, from the mobility (or demand) to the capacity (or infrastructure) layer. Figure 2.6 illustrates the composite nature of networks in an ATS.

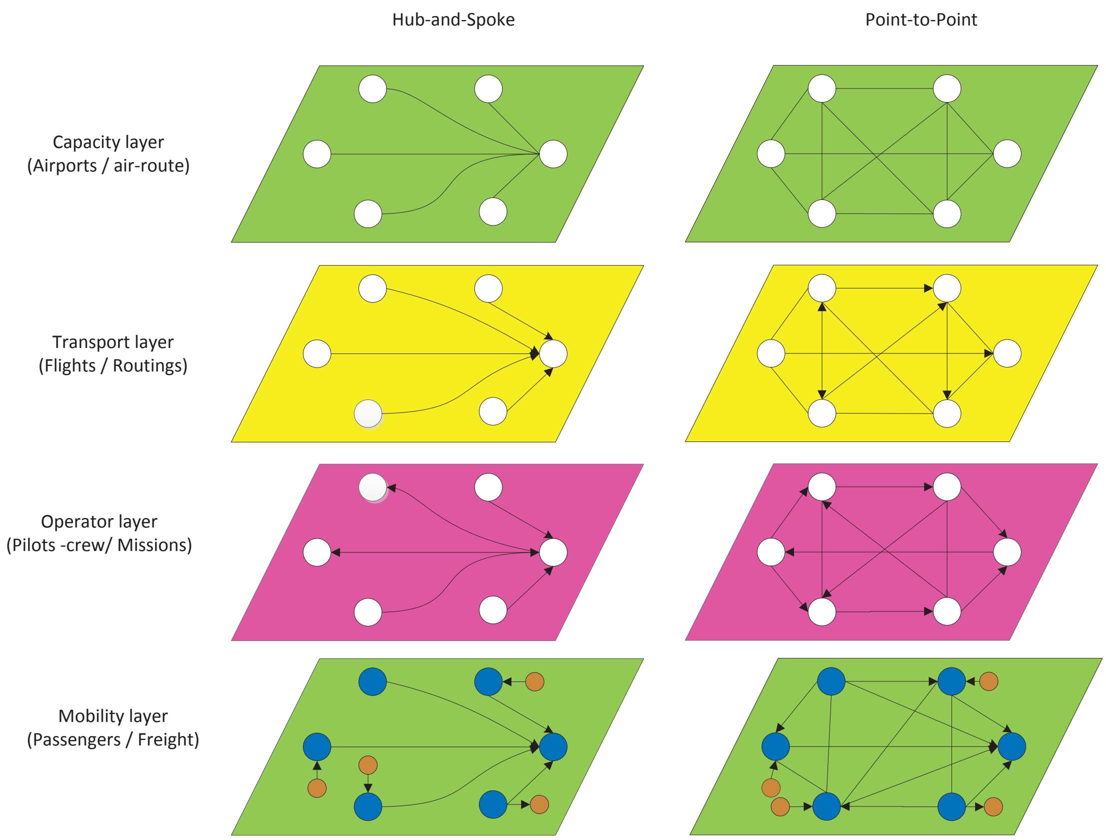

FIGURE 2.6: Multiple network layered composition in air transportation

The multiple-layered representation considers the physical layer as the network of airports (as nodes) linked by airways and departure and approach procedures (see Figure 2.6); the transport layer is the network of aircraft (as nodes) linked by ATC radar; the operations layer is the network of pilots, crew, dispatchers and controllers (as nodes) linked by VHF communications; and the applications layer is the mobility of people, packages and travel planners (as nodes) linked by telephone (or internet) to produce tickets or bills of lading.

The flow capacity of the overall transport system is dependent hugely on the physical layer, which is also known as the capacity or infrastructure layer. This layer is composed of the foundational elements of a National Airspace system (NAS). It is further decomposed into two major sub-layers: (i) airport network and (ii) airspace network. Figure 2.7 shows the decomposition of the infrastructure layer.

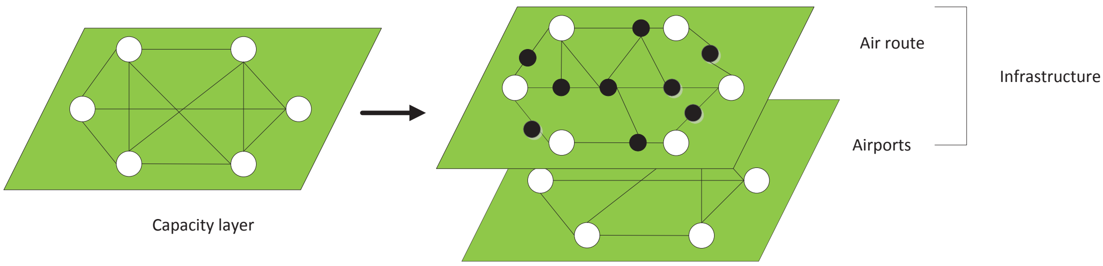

FIGURE 2.7: Infrastructure network layer

The next lower layer network is the operator layer, which is comprised of the schedule flights flown by airlines, regional carriers etc. Below this, the mobility layer is the reflection of the demand layer. The demand layer is defined as the set of true airport-to-airport paths that passengers and cargo go through regardless of constraints on supply.

2.2.1 Air Transportation Network

According to Barthélemy “A transport network, or transportation network, is a realisation of a spatial network, describing a structure that permits either vehicular movement or flow of some commodity ” [30]. Examples are networks of roads and streets, railways, pipes, aqueducts and power lines. Following the definition of a transportation network, I can clearly find that the air transportation network is the infrastructure layer of ATS that facilities the flow of commodities in the form of aircraft from source airport to destination airport. In this thesis, I define the air transportation network (ATN) as a transport network of airports and waypoints that connects the actual path for the aircraft. Mathematically, an ATN is modelled as graph $G(N, L)$, where N is the set of vertices or nodes and L is the set of links. Let,AP and W denote the set of airports and the set of all waypoints, respectively, then $N = AP \cup W$. There are several assumptions related to the characteristics of nodes and links in an ATN, which are given below:

- each of the nodes (AP or W) embedded in a geographical location.
- the nodes in the AP set are treated as both source and destination and the waypoints (W) are treated as intermediate nodes that only deliver flights from one to another.
- there are two sets of links: (i) connection between an Ap to an W or vice versa, and (ii) connection between two W nodes.

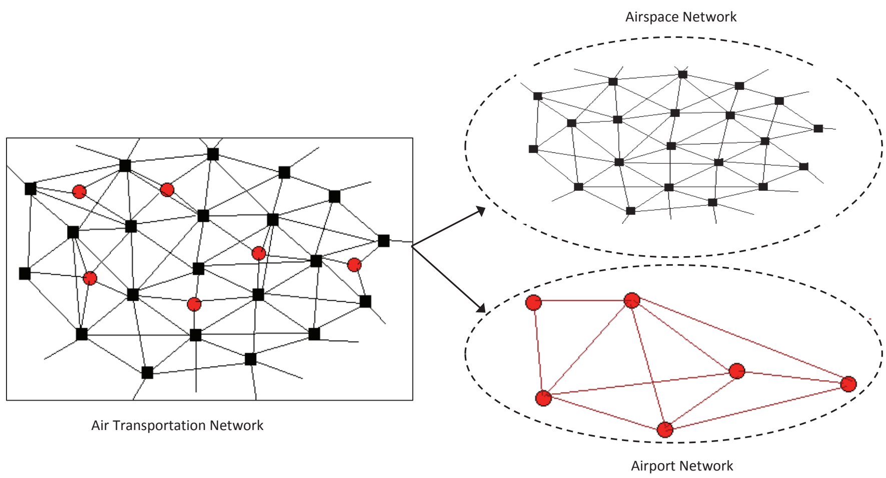

FIGURE 2.8: An Air Transportation Network (ATN) and its sub-networks

Since, in a real-world situation, a flight starts from an airport and goes through airways (a series of connected waypoints), there is no actual direct connection between two airports. However, from the source destinations of the flight links, I can model the direct connection among the airports as a sub-network. As a result, it is possible to decompose an ATN into two different sub-networks: (a) airport network and (a) airspace network. Figure 2.8 shows an ATN and its two sub-networks.

2.2.1.1 Airport Network

The airport network is defined as a graph in which nodes are airports and two nodes are connected if at least one flight per day goes from one node to another in a defined time interval. The topology and the characteristics of airport networks has been analysed by using the tools of complex network theory in recent years [14, 36, 213]. In these studies, the world airport network is in some cases described as a graph formed with the passenger commercial airports as vertices and the direct flights between airports as edges [101, 102]. Each edge also bears a weight corresponding to the number of seats available in the connection. These studies include a network description with an analysis of the degree (number of connections per node) and node strength (sum over the weights of the connections of a node) distributions, degree-degree correlations, density of triangles, etc. In this work, Guimera focuses on the correlations between network topology and fluxes of passengers finding a non-linear relation between them [101, 102]. The world airport network also is analysed later with graph clustering techniques[200] to classify airports according to their connectivity patterns. The airport network structure has also been investigated on domestic levels [21, 108, 217], involving countries with different economic and politic situations, and population/area sizes. Some attempts to model the world airport network (WAN) have been proposed considering geopolitical constraints [101], passenger behaviour [111] and optimisation principles [31]. Table 2.2 compares the topological properties of different airport networks. These studies measure network features that include degree distribution, average path length and clustering coefficient. From these studies, it has been found that most of the airport networks share a common small-word topology and a scale-free degree distribution. The scale-free connectivity is mainly due to the existence of the hub-and-spoke system, where the major big airports serve as the hub and provide connectivity to a large number of small airports. The data presented in Table 2.2 are discussed in detail in Chapter 3.

Table 2.2: Characteristics of airport network of different countries/regions

Author	Country	No. Nodes (n)	No. Edges (m)	Average degree $\langle k \rangle$	Average path length (L)	Clustering coefficient (C)	Network structure
Bagler [21]	India	79	455	11.52	2.26	0.66	Small-world(SW)
Guimera et al. [101]	World	3883	27051	13.93	4.4	0.62	Scale-free (SF) SW
Guida et al. [100]	Italy	50	310	12.4	1.98∼2.14	0.07∼ 0.1	SF SW Fractal
Xu & Harriss [222]	US	272	6566	48.28	1.84∼1.93	0.73∼0.78	SW
Wang et al. [217]	China	144	1018	14.14	2.23	0.69	SW
Hossain al. [108]	Australia	131	596	9.10	2.90	0.50	SW

An airport network is a complex entity by virtue of its topology and traffic dynamics [21, 22], whereby the complex network analysis of the network reveals useful information for travellers. For example, the average degree measures the average number of direct links between two airports (cities), and the average path length reveals the depth of the air transportation, which also measures the convenience of travel [108]. Whereas, the clustering coefficient reflects the intensity of the inter-connectivity of the system. Apart from topological studies, the airport network also has been investigated for the performance measures of air transportation systems [21, 188].

2.2.1.2 Airspace Network

An airspace can be considered as a multi-scale, dynamic network of interconnected entities. It is possible to define different networks describing an airspace. At a microscopic level, the first graph is the network of waypoints or the airways network. In this network, each node is a waypoint and two nodes are connected if at least one flight goes directly from one node to another in the considered time interval.

Similarly, at a macroscopic level, the second graph is the network of sectors. Each sector is a node and two nodes are connected if at least one flight per day goes directly from one to another in the considered time interval. Both of these networks are directed and can be weighted. The weight can be the number of flights between two connected nodes in the given time interval. Usually, the time interval is set by the nature of the analysis. Whereas, in the case of the direction, I have noticed that most of the graphs are almost symmetric. As a result, considering a small error, it can be viewed as a symmetric undirected network.

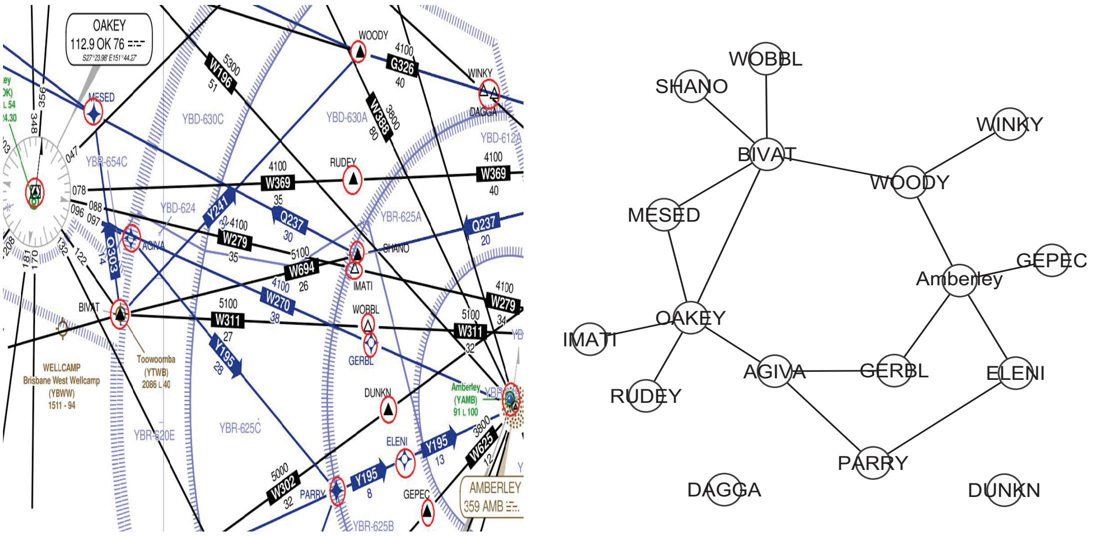

(a) A portion of airspace

(b) Graph based representation of a portion of airspace

FIGURE 2.9: A portion of Australian airspace map and its corresponding network representation (airspace network).

In this thesis, I am mainly concerned about the first representation of the airspace network – the network of waypoints or the airway network. Mathematically, the airway network is defined as a directed graph $G = (V, E)$ with vertices V and edges E. Edges connect one vertex to another, which is to say that an edge e connecting vertex v_i to vertex v_j has $head(e) = v_i$ and $tail(e) = v_j$. In some cases, each edge $e \in E$ may have a minimum transit time. Figure 2.9(a) shows an example of airspace in which the waypoints and navigational aids are circle in red, and these are considered as nodes to model an airspace as a graph/network. In the subsequent part of this thesis, I define the airspace network as a network of waypoints and I use these two terms interchangeably.

In the vertical dimension, airspace is divided into different levels to separate flights vertically from each other. A flight level (FL) is a specific barometric pressure, expressed as a nominal altitude in hundreds of feet. More specifically, a flight level

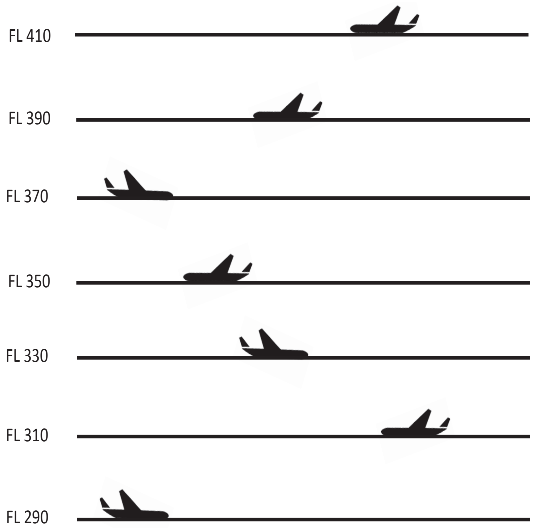

(a) non-RVSM

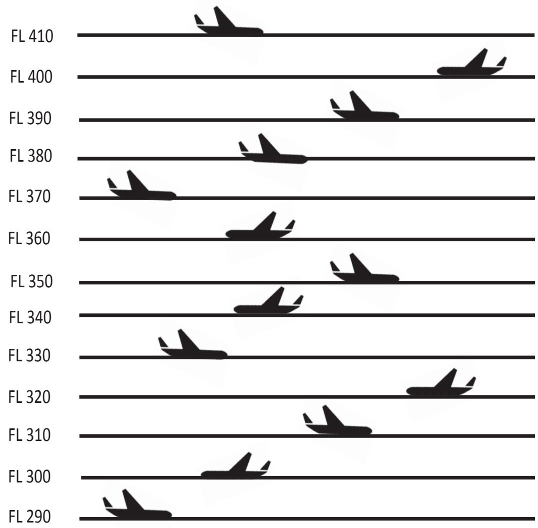

(b) RVSM

FIGURE 2.10: Vertical separation of airspace using flight levels.

is defined as a level of constant atmospheric pressure related to a reference datum of 29.92 inches of mercury [169]. Each flight level is stated using three digits that represent hundreds of feet. For example, FL250 represents a barometric altimeter of 25,000 feet.

Among the flight levels, the standard vertical separation is set to 1,000 feet from the surface to FL290 and 2,000 feet above the flight level FL290. With the technological improvement of altimeter systems and pilots being able to maintain a set flight level, the vertical separation is reduced to 1,000 feet, which is known as reduced vertical separation minima or minimum (RVSM) [64]. Figure 2.10 shows the concept of flight levels in standard and RVSM. RVSM is implemented to reduce the vertical separation above FL290 from 2,000-ft minimum to 1,000-ft minimum. The benefit of RVSM allows aircraft to fly more optimum profiles safely, gain fuel savings and increase airspace capacity.

The inclusion of flight level in the model and representation of the airspace network makes it very complicated. Since an air traffic controller advises the pilot to change flight level to avoid potential conflict, and a pilot also can climb up or descend to another flight level for the aircrafts optimal level to minimise fuel burn and environmental impact, changing a cruise flight level is considered a rare event and I can ignore this information to model an airspace network. Thus, the airway networks at different flight levels eventually remain same. So, I can consider the overall airspace network as single waypoint networks stacked on top of each other, separated by at least 1,000 feet. Figure 2.11 shows such a stack-based visualisation of airspace networks at different flight levels.

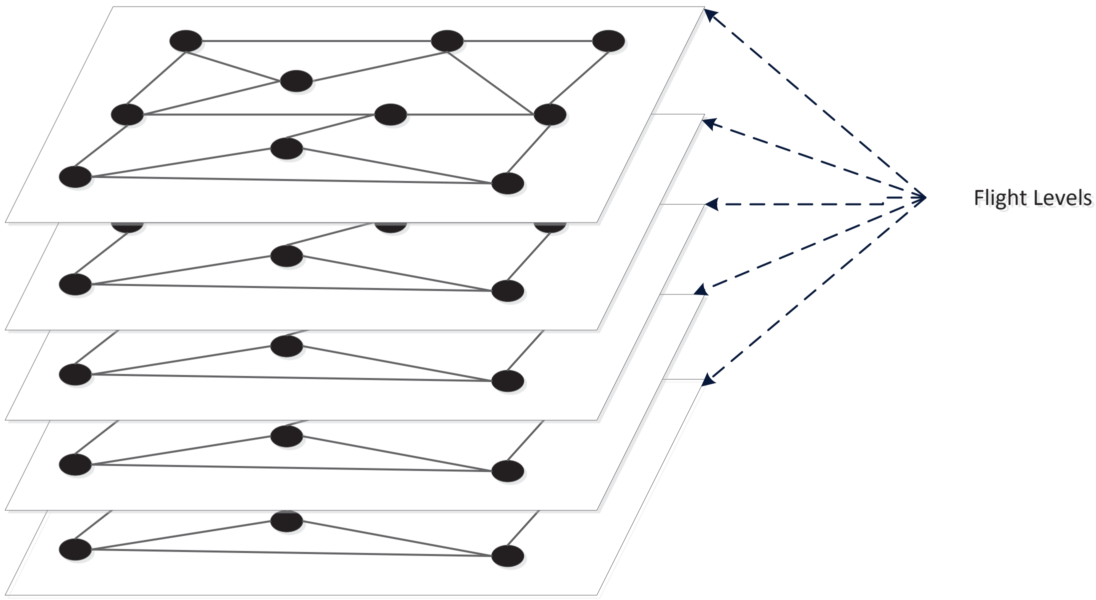

Figure 2.11: Airway network in different flight levels.

Several studies have been investigated to reveal the topological properties of the airspace network [129, 146, 204]. One such example is the Chinese air route network, which is found to be more homogeneous compared to its underlying airport network [129]. The shortest path length and the network diameter of it is much higher than the airport network, with a very low clustering coefficient. Apart from the topological properties, the effect of the waypoints network model with the mid-air collision risk for the 13 countries in the Middle East region has also been investigated in recent years [214].

2.2.2 Interaction Between Networks

The major actors in the air transportation network (ATN) are the air service providers (e.g. airlines, regional carrier operators, freight service operators, etc.), which present the interface between the foundation of the system (the National Airspace system) and the passengers and freight that are transported [38]. In ATS, the majority of the interactions among air traffic actors have relatively localised interaction in space and time, and the complex interactions present among all the actors of this system make it a 'system-of-systems' structured as a layered collection of interacting networks [58]. The sub-networks of the ATN are not independent of each other since they interact through the transport layer. Figure 2.12 shows the interactions between an airport network and an airspace using the actual flow of flights. The main ingredient of the interaction between an airport network and the corresponding airspace is the flow of the traffic. In these two sub-networks, the traffic management procedures and constraints are different. In an airport network, the management of traffic involves the allocation of slots for landing or take-off of different flights and maintaining a time gap between them. A time gap is imposed between two consecutive flight operations to avoid wake turbulence. Whereas, in the case of airspace, flights usually fly at a constant speed and the main constraint is maintaining the safe separation among the flights where there is a spacing between the mutual location of the airways. Aircraft separation generally refers to the horizontal and vertical spacing between aircraft as they transit through an airspace or sector. The air traffic controller is responsible for aircraft separation assurance in controlled airspace. In general, the minimum separation standards are affected by accuracies of navigation and surveillance, by controller/pilot response and communications delays, and by response times of aircraft manoeuvres. As a result, any loss of separation that occurs may result in a probability of collision. So, to ensure the safety of an airspace, the probability of collision always needs to be below a define threshold, which is known as the target level of safety [144].

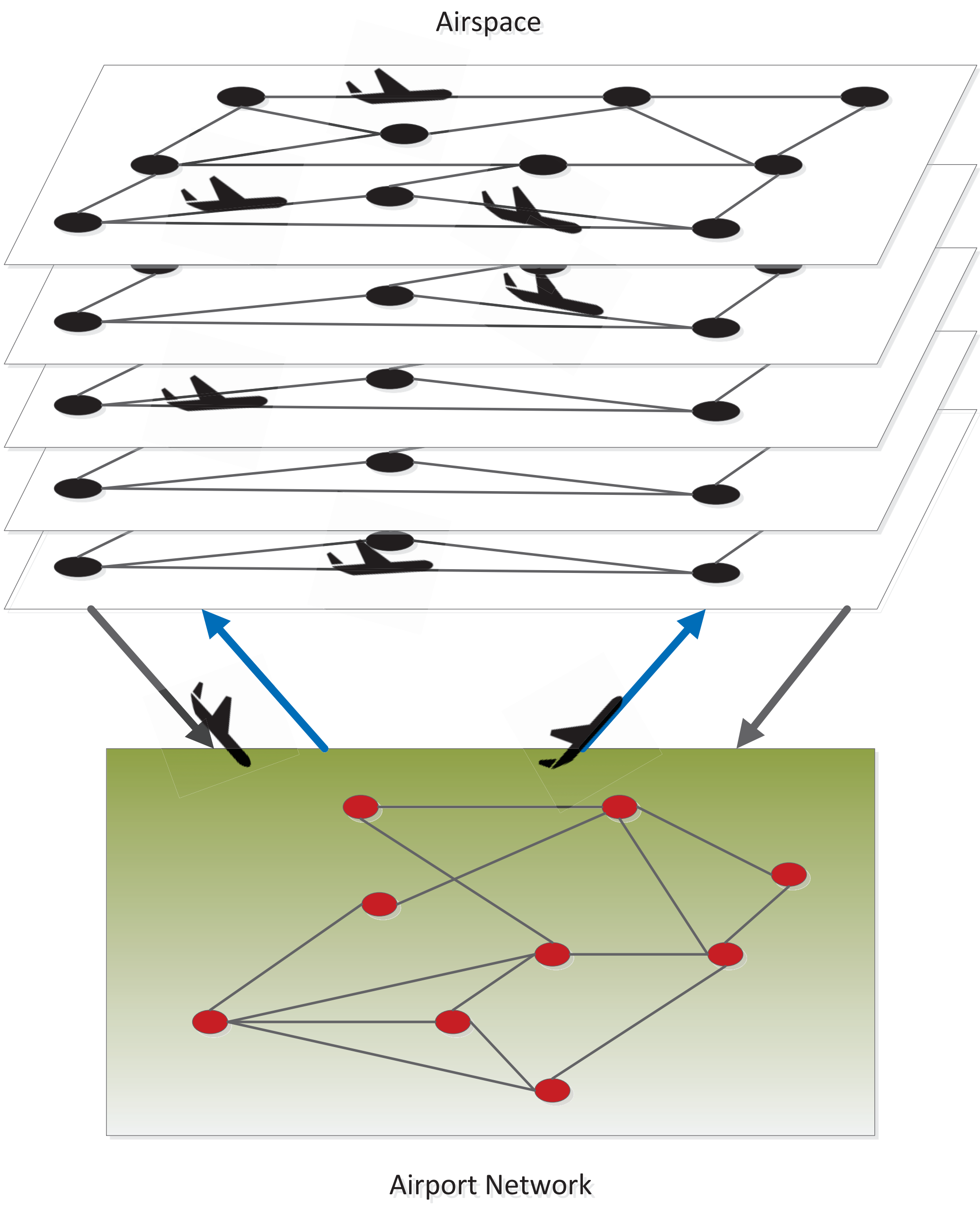

FIGURE 2.12: Interaction between airport network and airspace network in the form of flight path.

Currently, the movements of flights do not follow a smooth and optimised trajectory. Instead, they follow a predefined path from the departure airport through sets of waypoints together with time stamps and altitude to the destination airport. Assigning the flight plan is considered a traffic assignment problem that creates the interaction between the airport network and the airspace network. The traffic assignment problem consists of distributing flow across the air transportation network in order to optimise a certain number of predetermined criteria such as delay, cost, environmental impact and complexity. The problem is inherently multi-objective and each of the sub-networks (for example, airports and airspace networks) has its own set goal and constraints. As I know that the different sub-networks has its own different characteristics and performance measures, solving the traffic assignment in a collective manner (considering all the constraints of different sub-networks) is quite impossible. As a result, it is very important to investigate the relationship of the key performance metrics of different sub-networks, in particular, the safety and capacity and their joint emergent behaviours [52, 78, 83]. Understanding the interactions between the airport network and the airspace is crucial, especially when anticipating growth in traffic on both layers.

2.3 Air Transport Network Constraints

2.3.1 Capacity Constraints

In the air transportation domain, the capacity of an airspace or airport normally represents its ability to safely handle a number of aircraft per unit of time [219]. In an ATN, capacity depends on many factors, such as the configuration of an airspace, the layout of the airport ground infrastructure, ATM operations and procedures, the capability and availability of air traffic control, and the capacity and availability of element resources in the airspace or airport. Some of these factors are inherently dynamic (e.g. disturbance to the availability of an element resource in the airport due to adverse weather), and any change in such factors can influence the overall capacity. Air traffic demand is normally measured by the number of flights per unit of time serving an airspace or airport. It is usually represented by the space and time information of the aircraft fleet mix. Any variation in these factors can affect air traffic demand. When the amount of aircraft allocated to an airspace or airport mismatches the number of aircraft it can safely handle, capacity and demand imbalance occurs. In addition, both airport and sector capacity depend on weather conditions such as visibility, cloud ceiling and the location of thunderstorms, and are therefore prone to uncertainty [182]. There are two major capacity constraints in an ATN: (i) airport capacity and (ii) airspace capacity.

2.3.1.1 Airport Capacity Constraints

Airport capacity constraints limit the flow through an airport at any time. In the case of an airport, if there is a spacing requirement of 2 minutes between successive aircraft, this translates to an airport's throughput of 30 aircraft per hour. However, the situation at an airport is more complex since different types of operations – arrival and departure – can occur at any time simultaneously. It is even more complex since there are different types of aircraft, such as light, medium and heavy, which require different separation minima among them. Different combinations of aircraft and their operations (arrival and/or departure) will result in different throughputs. As a result, the true capacity estimation of an airport network system is considered an NP-hard problem.

Airport capacity is the number of operations, either take-offs or landings that can be performed in a unit of time, usually an hour, without violating aircraft safety regulations. Airport capacity can be discussed from two viewpoints: airside capacity and landside capacity. The airside capacity includes components such as the runway, the taxiway system, and adjacent airspace to the airport. Landside capacity includes the terminal, gate and access roads. Combining these two sides together, the capacity of an airport is determined by its arrival capacity (the number of aircraft landings per hour) and its departure capacity (the number of departures per hour). The arrival or departure capacity is primarily limited due to the temporal separation requirements imposed by predefined guidelines between successive operations. The inter-operational separations are used to avoid potential physical conflicts when using airport resources. Due to the shared nature of ground resources such as runways and taxiways, there is a trade-off between the simultaneous arrival and departure capacity at an airport [93]. The trade-off between an airport's arrival and departure capacity is quantified using the concept of the capacity envelope. An airport capacity envelope is the boundary (generally approximated as a convex polygon on the plane with the arrival and departure rates as axes) that defines the envelope of the maximum capacities that can be achieved under specified operating conditions, and captures the trade-off between the maximum arrival and departure rates [60]. The operating conditions influencing the trade-off encompass factors such as the relative alignment of arrival and departure runways (defined as the runway configuration), meteorological factors such as wind and visibility, the aircraft fleet mix, etc. Each of these factors dictates the required inter-operational separations that, in turn, determine the airport's operational capacities. Figure 2.13 illustrates the representative capacity envelopes of an airport for an arbitrary runway configuration split between two visibility categories typically defined for operations.

2.3.1.1.1 Airport Capacity Estimation: There are two broad categories of airport capacity estimation models: a) Analytic models b) Simulation-based models

Analytic models consist of a series of close-form equations that compute hourly

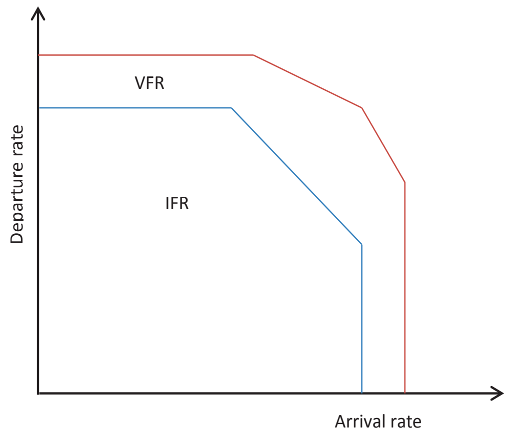

FIGURE 2.13: Capacity envelope for an airport under a particular runway configuration, for different meteorological conditions: Visual Flight Rules (VFR) and Instrument Flight Rules (IFR).

airport capacity with known input parameters. Airport capacity is affected by various external factors such as air traffic controller procedures and pilot behaviour, approach and departure speeds, runway and taxiway occupancy times, weather, etc. [186]. Analytic approaches to capacity estimation have traditionally modelled these factors through simplified models of aircraft behaviour, and derived the capacity using the mandated separation time between successive aircraft operations [35, 106, 167]. These analytic models construct the capacity envelope through linear interpolation between capacity values computed at specific arrival/departure mix ratios. Newell [167] and Odoni et al. [173] provide comprehensive reviews of contemporary analytical and simulation methods that adopt the above approach. In addition, there are systematic statistical approaches based on the principle of quantile regression for estimation of intra- and inter-airport capacity envelopes from observed data [189]. On the statistical estimation methods, quantile regression attempts to determine statistics such as the median or a general percentile of the dependent variable as a function of independent variables from a given sample of observations [125, 136].

Simulation models emulate the movement of aircraft by using discrete-event or fixed-timed techniques [232]. These models use statistical sampling techniques, and then infer the airport capacity with the data generated during the simulation [80, 202]. One of the key limitations of simulation models is that they do not estimate airport capacity directly. Capacity is inferred from values of delay calculated by these models [122]. Lee et al. compared several airport capacity models developed over the past three decades [143]. In this study, the authors comment that simulation-based models emulate detailed manoeuvers of airport operations. However, these models require extensive data and long computing times to generate results. For this reason, simulation models can only be applied to a limited number of airports or airport configurations considering practical resources and data input requirements. In addition, large data inputs and outputs take longer to collect and analyse for simulation models. In contrast, analytical models require fewer parameters and many cases can produce adequate capacity estimations.

2.3.1.2 Airspace Capacity Constraints

Airspace capacity constraints limit the number of aircraft that can be in a sector or airspace at any time, and are driven by the geometry of the sector, the traffic patterns, overall collision risk and controller workload. The capacity of the ATM system is fundamentally bound by the separation standards in effect for both the airspace and successive aircraft at the runway threshold [65]. Airspace throughput is a measure of the realised flow through it in a given time period and is further constrained by the controller's ability to accommodate traffic demand to maintain the target level of safety [144]. Periods when demand exceeds capacity in parts of the system can overload the separation assurance agent and thus increase the collision risk. Thus, it is very important to assess the airspace capacity limit that can be achieved without violating the safety constraints.

2.3.1.2.1 Airspace Capacity Estimation: An airspace capacity can be defined as the maximum number of aircraft going through a given geometrical airspace for a given time period. It is based on the spatial control constraints that govern the internationally specified separation between any two aircraft given their performance characteristics [75]. There are several factors that affect the capacity of an airspace. These are constant demand for service, the aircraft mix, the characteristics of control tasks, the characteristics of avionics, ground navigational aids and equipment being available to the air traffic controller. These factors may influence the separation rules that may be applied between the aircraft [158, 170, 172]. Based on the type of airspace managed, airspace capacity models can be classified as: model of terminal airspace capacity; model of an air route, comprising two sub-models – capacity model of air route segment and capacity model of air route intersection; and capacity model of an en-route ATC sector [126]. None of these models consider the impact of 'human factor' such as air traffic controller workload on the capacity of the airspace [127, 128, 150].

The models of airspace capacity based on the air traffic controller are dependent on the quantification of human workload generated by the air traffic requesting handle, control and service, while in the airspace of his/her administration. These models are based on the assumption that the air traffic controller always performs two kinds of mutually exclusive activity: monitoring the traffic situation and executing the control task to provide safe separation and efficient movement of aircraft in the defined volume of airspace [126].

Methodologies to estimate the capacity of an airspace can be classified into the following three groups:

Analytical modelling and judgmental or subjective methods: These types of method are based on the subjective ratings of subject matter experts, who have an overall idea of the system performance and base their judgments on their knowledge about the system [95, 99]. This method is extremely flexible and quick, although, when lacking an appropriate framework and methodology, they can produce biased outputs. A main concern within this method is associated with the validation issues.

Fast Time Simulations (FTS) techniques: these techniques are usually comprised of a traffic generator and an ATC workload calculator [79, 84, 183]. The key assumption for these kinds of method is that capacity is directly linked to ATC workload and the controller workload remains the main capacity bottleneck of the system. These methods have the potential of accurately capturing short-term implementations, in which insignificant functional variations are held in the system.

Real Time Simulations (RTS) or Human-In-The-Loop (HITL) simulations: these methods have the potential to accurately model the evaluated concept, ensuring higher fidelity levels than an FTS in the system modelling. Most of these methods are focused on workload and some use different human performance metrics [42]. Different studies use different techniques to measure the workload metric, which can be included in one of the following groups: performance-based, subjective and physiological/biochemical [82]. The main drawback of these methods stands in their reduced flexibility to capture different concepts and in their high associated costs along with time-consuming issues. In addition, controller workload can be estimated from the airspace configuration [89].

Additionally, an airspace capacity can also be estimated from the average flight time and human judgment of its complexity [141]. Simplified dynamic density [134], which is a weighted sum of seven traffic components, is used to measure the airspace complexity. Since the flight time only partially accounts for the traffic pattern, it is a partial measure of workload. In such a model, the human judgment is based on past experience. As a result, traffic in sectors is over and under constrained. The sector capacity rule of "5/3 of average flight time" has been used to estimate capacity sector boundaries [40, 223]. The capacity rule is based on the flight time without regard to judgment. As a result, the cognitive aspects of controller workload are not reflected in dynamic density capacity estimation models.

2.3.2 Separation minima

The paramount goal of an ATC/ATM system is to provide safe air traffic flow. In order to fulfil this Goal, ATC services separate aircraft during flight. Separation is very important because it influences airspace capacity and safety. It is recognised as a fundamental capacity constraint for an airspace [196]. Reich [193–195] defined a set of necessary considerations for safe, practical and least-cost aircraft separation standards. Aircraft separation standards are used to safeguard against the uncertainties in aircraft position in the along-track, cross-track and vertical axes. Reich identified an economic optimum separation standard as one that minimises the costs to airlines from route deviations required by the standards and the costs of collisions. Today, it is the international standards that require aircraft to maintain a 5 nautical mile horizontal separation and a vertical separation of 2,000 feet for aircraft above 29,000 feet and 1,000 feet below this altitude [177].

2.3.3 Target Level of Safety

The target level of safety (TLS) provide a quantitative basis for judging safety of operation in an airspace network. The setting and achieving of a target level of safety is a key concept in aviation safety. TLS sets an important upper bound on the aspired level of risk [144]. Historically, the International Civil Aviation Organization (ICAO) has led the development of TLS through sophisticated mathematical models, air traffic movements and accident data, together with many assumptions. For different flight operations and/or flight environments, there are different TLS values. For example, TLS for airspace operation is different from

Table 2.3: Various TLS for airspace operations

TLS	Value
TLS for access North Atlantic parallel routs by NATSPG (1960s)	
Original TLS	2.34×10^{-7} per flight hour (p.f.h)
Improved TLS	4.68×10^{-8} p.f.h
TLS with minimum navigation performance specification by Brooker and Ingham (1977) [43]	6×10^{-8} p.f.h
TLS for reduced vertical separation minima RGCSP (1988) [121]	0.25×10^{-8} p.f.h
TSL for enroute mid-air collision RGCSP (1995) [112]	1.5×10^{-8} p.f.h

TLS for landing and take-off. Table 2.3 reports some of TLS values for different airspace operations. For more details, please see the survey paper of Xunguo Lin et al. [144].

2.3.4 Collision Risk

One of the principal requirements in the daily operation of civil aviation is the prevention of conflicts between aircraft, either while airborne or on the ground, which might escalate to collision. With the improvement of communication, navigation and surveillance (CNS) technologies, flying errors have been reduced significantly, which makes aircraft collision very rare. Although aircraft collisions are very rare events contributing to a very small proportion of the total fatalities, they always cause relatively strong impact, mainly due to the relative large number of fatalities per single event and the complete destruction of the aircraft involved. In air traffic, the term risk is used to represent a numerical index of safety: the unit of collision risk assessment is fatal accident per aircraft flight hour [113].

2.3.4.1 Collision Risk Modelling Approaches

In general, separating aircraft using space and time separation standards (minima) has prevented conflicts and collisions. However, due to the reduction of this separation, in order to increase airspace capacity and thus cope with growing air transport demand, assessment of the risk of conflicts and collisions under such conditions has been investigated using several important methods/models.

The Reich-Marks Model: the Reich-Marks model was developed in the early 1960s by the Royal Aircraft Establishment [193–195]. It was originally developed to estimate collision risk for oceanic traffic over the North Atlantic and to determine the appropriate lateral separation between aircraft. This is the first model to specify the separation standards for flight trajectories [207]. It also has been used to evaluate collision risk and perform numerous safety assessments approved by the ICAO. It also has been used to estimate collision probability for four EUR-SAM corridors in the South Atlantic [130]. A fundamental input of this model is the probability distribution of the deviations. One of the key insights of the Reich model is that it is a distance-based model that assumes that collision risk is a function of navigation position error and speeds from the expected. The main assumptions of the Reich model are: (i) the lateral/vertical deviations of aircraft on adjacent tracks are uncorrelated; (ii) the lateral/vertical speed of an aircraft is not correlated with its lateral/vertical deviation; (iii) the protected zone of an aircraft is a rectangular box; and (iv) there is no corrective action by pilots to avoid collision. According to Reich, the collision rate between aircraft on adjacent tracks is given by the following equation:

$$N_{ay} = P_y(S_y)P_z(0)\frac{\lambda_x}{S_x}\left\{\begin{array}{cc} & E_y(same)\left[\frac{|\triangle\bar{v}|}{2\lambda_x}+\frac{|\bar{\dot{y}}|}{2\lambda_y}+\frac{|\bar{\dot{z}}|}{2\lambda_z}\right] \\ + & E_y(opposite)\left[\frac{|\bar{v}|}{2\lambda_x}+\frac{|\bar{\dot{y}}|}{2\lambda_y}+\frac{|\bar{\dot{z}}|}{2\lambda_z}\right]\end{array}\right\} \tag{2.1}$$

where,

N_{ay} y is the expected number of accidents per flight hour due to the loss of lateral separation between aircraft flying on tracks with nominal spacing S_y

S_y is the lateral separation of the track centrelines

$P_z(S_y)$ is the probability of lateral overlap of aircraft nominally flying on the lateral adjacent paths at the same flight level

$P_z(0)$ is the probability of vertical overlap of aircraft nominally flying at the same flight level

$E_y(same)$ is the same direction lateral occupancy, i.e. the average number of same direction aircraft flying on the laterally adjacent tracks at the same flight level within segments of length $2S_x$, centred on the typical aircraft

$E_y(opposite)$ is the opposite direction lateral occupancy, i.e. the average number of opposite direction aircraft flying on laterally adjacent tracks at the same flight level within segments of length $2S_x$, centred on the typical aircraft

S_x is the length of the longitudinal window used in the calculation of occupancies

λ_x is the average length of an aircraft

λ_y is the average width of an aircraft

λ_z is the average height of an aircraft

$|\triangle\bar{v}|$ is the average relative along-track speed of two aircraft flying at the same flight level in the same direction

$|\bar{v}|$ is the average ground speed of an aircraft

$|\bar{\dot{y}}|$ is the average lateral cross-track speed between aircraft that have lost their lateral separation

$|\bar{\dot{z}}|$ is the average relative vertical speed of aircraft flying at the same flight level

The main limitations of the Reich model are that it does not account for lane change manoeuvers, pilot control loops, or failures of the on-board automated separation assurance system. As a result, the Reich model does not adequately cover situations in which ground controllers monitor the air traffic though radar surveillance and provide tactical instructions to aircraft crews [34].

The Machol- Reich Model: the Machol-Reich is a modified generalised model of the Reich-Marks model. It was developed in 1966 with the aim of increasing airspace capacity after the ICAO had established the NAT SPG (North Atlantic System Planning Group)[148]. To overcome the limitations of the Reich model, which had been used, so far, to deal only with simple cases, [194] was extended to a generalised form in the Machol-Reich model. Some special types of collision scenario, such as overtaking, were accommodated into this generalised model.

Intersection Models: these models belong to the simplest collision risk models. They are based on the assumption that aircraft follow pre-determined crossing trajectories at constant speeds. The probability of a collision at the crossing point is computed using the intensities of traffic flow on each trajectory, aircraft speeds and airway geometry [110, 208]. The Hsu model [110] is a perfect example of this kind of model. The Hsu model is based mainly on the concept of the Reich model [194], which assumes that each aircraft is shaped like a 3D cylinder with a diameter (λ_{xy}) and vertical height (λ_z). Assuming that an aircraft (A) is a double-sized cylinder, i.e. has a radius of λ_{xy} and height of $2\lambda_z$, with another aircraft/point in the space denoted by B, the two aircraft will touch each other when, for example, B moves in any direction in the cylinder of A. It is assumed that two aircraft are at nominal distances of d_1 and d_2 before intersecting at time t_0, with constant speeds of v_1 and v_2, respectivel during a time interval of t_0 to t_1 during which a collision risk is to be estimated. According to Hsu, this risk is:

$$CR(t_0, t_1|v_1, v_2) = P_z(h_z) \times \left(1 + \frac{|\dot{z}|}{2\lambda_z} \times \frac{\pi\lambda_{xy}}{2V_{rel}}\right) \times HOP(t_0, t_1|v_1, v_2) \quad (2.2)$$

where, $HOP(t_0, t_1|v_1, v_2)$ denotes the probability of a horizontal overlap of these two aircraft during a time interval of $[t_0, t_1]$ given their speed v_1 and v_2, $P_z(h_z)$ the probability of their instantaneous vertical overlap at height λ_z, their nominal vertical separation by distance h_z at the time of a horizontal overlap, $|\dot{z}|$ the average vertical speed of an aircraft with a horizontal overlap and V_{rel} the relative difference in speed of the two aircraft.

Geometric Conflict Models: another type of collision risk model are the geometric conflict models. Similar to the intersection model, these models consider the speed of the aircraft as constant but their initial three-dimensional positions are random. Based on extrapolating the position of the aircraft in time, it is possible to geometrically describe the set of initial locations that eventually lead to a conflict. This situation will occur when two aircraft are closer than the separation minima, for example, of 5nm. In such a situation, after integrating the probability density of the initial aircraft locations over the conflicting region, the collision risk can be estimated [23, 124, 177, 178].

Generalized Reich Model the generalised Reich model was developed by removing restrictive assumptions from the Reich model based on the fact that the Reich model does not adequately cover certain real air traffic situations. Such a generalised collision model was developed during the 1990s and has been in use as part of the TOPAZ (Traffic Optimization and Perturbation Analyzer) methodology [33, 34].

The ICAO has developed the Collision Risk Model (CRM) as a mathematical tool used in predicting the risk of mid-air collision. During development of the ICAO CRM [115, 119], they adopted the Reich [193–195] and Hsu [110] formulae and further defined a unified framework for derivation of collision risk models. The ICAO called this the Rice formula [119, 154]. From the Rice formula, it is possible to derive the Reich and the Hsu formulae [154].

The models discussed above are analytical models to estimate collision risk. A central problem with these models is that they apply only to simple scenarios. For example, they generally apply to level flight and do not consider corrective actions by pilots or controllers. In particular, the analytical models do not account for corrective actions by the pilots to avoid a collision. However, the Hsu model can be integrated with an air traffic simulator that can handle these types of situation and successfully be used to estimate the collision of complex traffic scenarios [13]. In this thesis, I used the same integration principle of a collision risk model with an air traffic simulator in order to execute complex traffic scenarios and to evaluate the collision risk of an airspace; for this purpose I have chosen the Hsu model.

2.3.4.2 The Hsu Model

Similar to the intersection-type models, the Hsu model [110] is a slightly more complex model, which is mainly based on the concept of the Reich model [194]. This model assumes that each aircraft is shaped like a 3D cylinder, with diameter

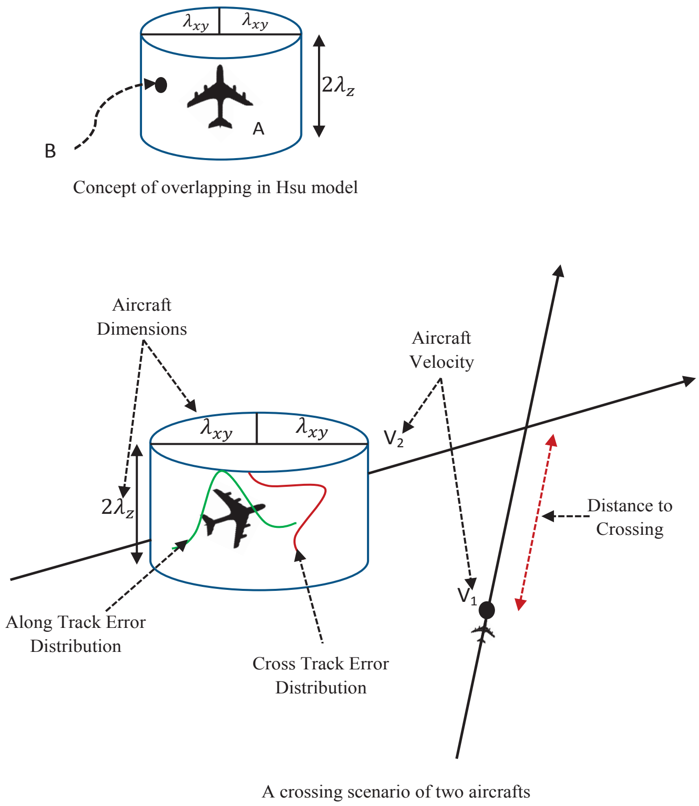

FIGURE 2.14: A geometric representation of the Hsu collision risk model of two aircrafts in a crossing scenario (upper part- the concept of overlapping)

λ_{xy} and vertical height λ_z. Let us consider that an aircraft (A) is represented as a double-sized cylinder, i.e. a cylinder of radius λ_{xy} and height of $2\lambda_z$ and another as a point in the space denoted by B. Under these assumptions, two aircraft are touching each other when, for example, B enters along any direction into the cylinder of A.

As illustrated in Figure 2.14, in a crossing scenario, two aircraft are assumed to be at nominal distance of d_1 and d_2 before the intersection at time t_0, with constant speed v_1 and v_2 during a time interval t_0 to t_1 during which collision risk is to be estimated. According to Hsu, the collision risk between these two aircraft during the interval $[t_0, t_1]$ is

$$CR(t_0, t_1|v_1, v_2) = P_z(h_z) \times \left(1 + \frac{|\dot{z}|}{2\lambda_z} \times \frac{\pi\lambda_{xy}}{2V_{rel}}\right) \times HOP(t_0, t_1|v_1, v_2) \qquad (2.3)$$

where, $HOP(t_0, t_1|v_1, v_2)$ denotes the probability of a horizontal overlap of two aircraft during a time interval of $[t_0, t_1]$ given their speed v_1 and v_2. $P_z(h_z)$ is the instantaneous vertical overlap probability of the two aircraft of height λ_z, nominally separated vertically by distance h_z at the time horizontal overlap occurs. $|\dot{z}|$ is the average vertical speed of an aircraft given that it has a horizontal overlap and V_{rel} is the relative speed between the two aircraft.

2.4 Network Capacity Estimation

The network capacity estimation is generally known as one of the most difficult problems in the transportation field. Pioneering work to solve the network capacity problem traces back to Ford and Fulkerson [85], who developed a labelling algorithm for the network maximum-flow problem on the basis of max-flow min-cut theory. However, the max-flow min-cut algorithm is ideal for solving problems with a single origin-destination [190]. To obtain realistic network capacity, many researchers have made contributions in this area. In 1972, Iida [123] developed an incremental assignment approach in which a certain portion of origin-destination (OD) demand matrix was iteratively added to the network. On the basis of the updated link cost (travel times), a link was eliminated from the network if it reached its capacity threshold. Finally, the network capacity was obtained when a certain OD pair was no longer connected. The main drawback of this approach is the choice of the route. Realising the effects of route choice behaviour and congestion, Asahura and Kashiwadani proposed a bi-level programming approach to address the network capacity problem, in which the traveller route choice behaviours (routing strategies) and congestions effects were explicitly considered [8, 19]. In a recent study by Chen et al. [45], the authors developed a bi-level model to deal with the network turning restriction design problem in which traffic are prohibited from driving into restricted downstream links at a group of intersections. Along with the bi-level model, the importance of developing probabilistic procedures for quantitative evaluation of the capacity [47, 48] and flexibility [45] of transportation network capacity has also been investigated in recent years.

Despite the significant contribution of previous studies to various aspects of network capacity modelling, a comprehensive approach is lacking in the literature to investigate the flow capacity of an air transportation network. A small number of attempts have been made to estimate the total capacity of an entire air transportation system for any region or country [66, 67]. There is growing concern among airlines and a small group of policy analysts are concerned that the air transportation system is running out of capacity [66, 162].

Conventionally, in traffic flow networks, the maximum flow capacity is estimated using a Multi Commodity Flow (MCF) model [46, 86]. The multi-commodity network flow problem is defined over a network in which more than one commodity needs to be shipped from specific origin nodes to destination nodes while not violating the capacity constraints associated with the arcs. In general, there are three major MCNF problems in the literature: the max-MCNF problem, the max-concurrent flow problem and the min-cost MCNF problem. The max-MCNF problem is to maximise the sum of flows for all commodities between their respective origins and destinations. The max-concurrent flow problem is a special variant of the max-MCNF problem, and maximises the fraction (throughput) of the satisfied demands for all commodities. In other words, the max-concurrent flow problem maximises the fraction z for which the min-cost MCNF problem is feasible if all the demands are multiplied by z. The min-cost MCNF problem is to find the flow assignment satisfying the demands of all commodities with minimum cost without violating the capacity constraints on all arcs. The network capacity problem is generally considered a max-MCNF problem. However, the existing models and methods for the max-MCNF problem are not directly applicable to the air transportation network, where capacity modelling characteristics are quite different, for the following reasons: (a) the movement in a transportation network involves flows of aircraft with different speeds; (b) flow is heterogeneous given different wake vortices categories of aircraft, viz. light, medium and heavy; (c) different types of aircraft require different amounts of resources at landing and departure airports; (d) there must be a minimum separation distance between two consecutive aircraft, which depends on the type of operation (landing or take-off) and the preceding aircraft type and operation for managing wake vortices; (e) aircraft departing from an airport are expected to land at destination airports within a time frame, because aircraft cannot hold in the air for a long time, which will increase the amount of delay; (f) multiple OD pairs exist and the flow between different OD pairs is not exchangeable or substitutable in an air transportation network capacity problem. These characteristics make the modelling of air transportation network capacity a complex, yet interesting, problem to solve.

2.5 Evolutionary Computation in Air Transportation Problem

Finding optimal solution(s) for a real-world problem may be computationally expensive or even impossible, as the complexity of the problem prevents exact methods from being applicable. Specifically in the case of air traffic management, for example, generating traffic scenarios for evaluating complex metrics such as collision risk for an airspace, capability assessment of conflict detection and resolution algorithms and evaluating advance ATM concepts are such problems. Traditional optimisation techniques such as gradient descent, linear programming and integer programming are not suitable for the problems associated with the air transportation domain because of the complex interactions among the sub-systems. The large search space (possibilities) and non-linear interactions between different components of an air transportation system make traditional search methods, such as

Monte Carlo, computationally infeasible [13]. Nature-inspired techniques such as evolutionary algorithms (EA) have emerged as an important tool to effectively address complex problems in the air transportation domain [12, 61, 90, 97, 151]. It has been successfully applied in air traffic planning [226], conflict detection and resolution [140, 160, 216], scenario generation [10, 88, 176] and weather avoidance [9].

In this section, I present two major evolutionary algorithms: genetic algorithms (GA) and differential evolution (DE). Both GA and DE output the descriptive representation of solutions as an array of bits, integers, floats or data structures. From these arrays, solutions are usually obtained through simulation.

2.5.1 Genetic Algorithm

Genetic algorithms (GAs) are adaptive search algorithms based on the evolutionary concepts of natural selection and genetics. GA represents an intelligent exploitation of a guided search used to solve optimisation problems. The process of GA starts with a random solution of the problem and then guides towards the optimal solution by some operators inherited from nature. Although it starts with randomised solutions, GAs are by no means stochastic; instead, they exploit historical information to direct the search into the region of better performance within the search space. The basic techniques of the GAs are designed to simulate processes in natural systems necessary for evolution, specifically those that follow the principles first laid down by Charles Darwin of 'survival of the fittest', since, in nature, competition among individuals for scanty resources results in the fittest individuals dominating over the weaker ones.

Genetic algorithms simulate the process of natural selection in a hostile environment linked to the problem under consideration [59]. The basic building blocks of GAs are solution representation, the process of selection and reproduction of better solutions (crossover and mutation). The candidate solution of the problem is encoded into chromosomes, which refers to individuals in a population.

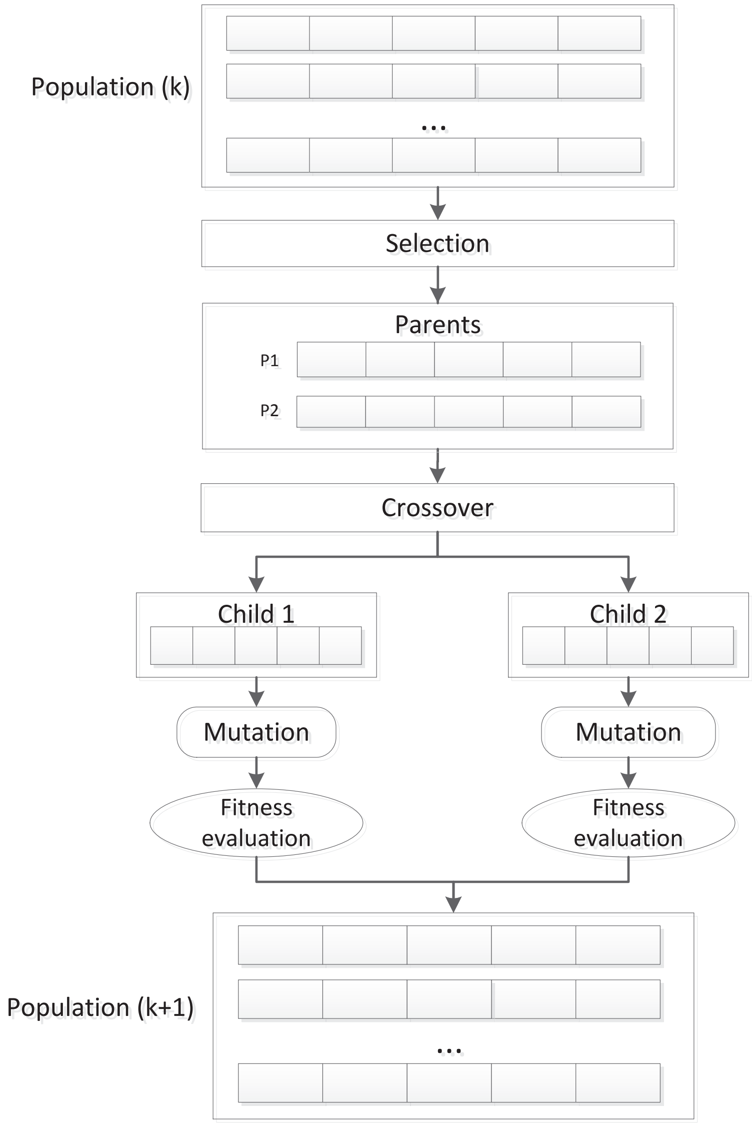

FIGURE 2.15: Principle of genetic algorithms

In the context of optimisation, each individual represents a candidate solution point in the search space, which associates a value of the optimisation problem. The value of a candidate solution is calculated by the fitness function(s), which provide the solution to the optimisation problems given value of each independent variable of the problem. The GAs start with a randomly generated population of individuals, from which it aims to select the best solution while ensuring efficient exploration of the search space. Figure 2.15 shows the steps of operations used in genetic algorithms.

- **Initialization:** the individuals of the initial population are usually generated randomly. The choice of the number of individuals depends on the problem. Typically, the initial population contains several hundred to thousands of individuals. The randomly generated population can help to explore the entire search space. In some cases, instead of random initialisation, the population starts with seed solutions in promising areas of the search space, where the likelihood of optimal solutions existing is high [131, 132].

- **Selection:** in each generation, a pool of individuals is selected from the current population to breed a new generation. Selection is implemented, based on the fitness of individuals. Some selection methods rank the fitness of each solution, and the best solutions are preferentially selected. However, this method may consume a lot of time. Other methods rank only a number of random individuals.

- **Reproduction:** In the reproduction process, a new population is created from the pool of selected individuals by genetic operators (crossover and/or mutation). Biologically inspired, two parent (in our example, Figure 2.15 P1 and P1) solutions are selected from the pool to reproduce a new child until the set of offspring reaches a predefined size. In general, crossover is used to mix the genes of individuals in the population, whereas mutation is used to generate new genes.

  In the reproduction process, the application of crossover is done through a probability p_c, which generates the children, then some of their genes are modified by applying a mutation operator with a probability p_m. The values of p_c and p_m play an important role in determining the degree of solution accuracy, the convergence speed that genetic algorithms can achieve and the divergence of the population. Generally, p_c is set to a high value, while p_m is low (where the role of mutation is to avoid the loss of potential solutions). However, some research uses mutation as the main operator because the crossover operator may not be useful in some cases. For example, when individuals in a population are similar, the crossover operator will create children similar to their parents. Some genetic algorithms with adaptive parameters (AGAs - adaptive genetic algorithms) use the population information to adjust the p_c and p_m to obtain the population diversity and convergence [179].

- **Fitness Evaluation:** GAs simulate the survival of the fittest among individuals over consecutive generations to solve a problem through fitness evaluation. Fitness value is used to show how good an individual is in relative comparison to other individuals in the population.

  In some complex problems, the exact fitness function may require a lot of time to evaluate (such as a number of hours), for example, estimation of the collision risk for a traffic scenario [13]. Furthermore, the fitness evaluation is repeated in every individual of a population through generations. Typical genetic algorithms cannot resolve such types of problem. In this case, an approximated fitness that requires less time to evaluate can be a solution.

- **Termination:** The evolution terminates when a certain condition has been satisfied. Commonly, the terminating conditions are a found solution meeting the minimum criteria, reaching the maximum number of generations, reaching the allocated budget (such as computation time) or successive iterations no longer producing better results.

2.5.2 Differential Evolution

Differential evolution (DE) is a branch of evolution algorithms for optimising problems in continuous spaces to produce multiple solutions in one run [7, 210]. DE uses direction information to guide the search and compare the fitness of an offspring directly with the fitness of the corresponding parent, which results in faster convergence speeds than other EAs [104]. In addition, DE is also easy to use, requires fewer control parameters and can find near optimal solutions regardless of the initial parameter values [71]. In DE, the gene values are real numbers in the chromosome. An individual is selected randomly for replacement and three different individuals are selected randomly as parents, one of which is selected as the main parent. The child is generated by adding to each variable in the main parent a ratio of the difference between the values in the two other parents. In other words, the main parent's vector is perturbed by the other two parent vectors. This process represents the crossover operator in DE. If the child vector generated is better than that chosen for replacement, it replaces it; otherwise, the vector chosen for replacement is retained in the next generation. The steps of a DE algorithm are described bellow:

A DE starts with a population of NP candidate solutions, which is represented as $X_{i,G}, = [X_{1,i,G}, X_{2,i,G}, ..., X_{d,i,G}], i = 1, ..., NP$, where i index denotes the population, and G denotes the generation to which the population belongs.

In the initialisation phase, the upper and lower bounds for each chromosome value $X_j^L \leq X_{j,i,1} \leq X_j^U$ are set for each variable. After that, the initialisation is done by randomly selecting the chromosome values uniformly in the intervals $[X_j^L, X_j^U]$. After the initialisation, the effective evolution of DE depends on the manipulation and efficiency of three main operators, mutation, reproduction and selection, which are described briefly in this section.

Mutation: the mutation operator is the prime operator of DE and it is the implementation of this operation that makes DE different from other evolutionary algorithms. The mutation operation of DE applies the vector differentials between the existing population members for determining both the degree and the direction of perturbation applied to the individual subject of the mutation operation.

The mutation process at each generation begins by randomly selecting three individuals (r_1, r_2, r_3) in the population. There are many mutation strategies in the literature [15]; among them, the following is the most popular.

$$V_{i,G+1} = X_{r_1,G} + F \times (X_{r_2,G} - X_{r_3,G}) \tag{2.4}$$

where, F is the mutation factor, which is set usually between 0 and 2.0, and $v_{i,G+1}$ is the donor vector.

Crossover: once the mutation phase is complete, the crossover process is applied, that perturbed the donor vector , $V_{i,G+1} = V_{1,i,G+1}, ..., V_{d,i,G+1}$, and the current population member, $X_{i,G} = X_{1,i,G}, ..., X_{d,i,G}$, are subject to the crossover operation, which finally generates the population of candidates, or 'trial' vectors,$U_{i,G+1} = U_{1,i,G+1}, ..., U_{d,i,G+1}$ as follows:

$$U_{j,i,G+1} = \begin{cases} V_{j,i,G+1} & \text{if } rand_j \leq cr \vee j = k \\ X_{j,i,G} & otherwise \end{cases} \tag{2.5}$$

where, $j = 1, ..., d, k \in 1, ..., d$ is a random parameter's index, chosen once for each i, $rand_j \in [0, 1]$, and the crossover rate, $cr \in [0, 1]$. The parameter index, k, ensures that $V_{i,G+1} \neq X_{i,G}$.

Selection: the selection scheme of DE also differs from that of other EAs. The population for the next generation is selected from the individual in the current population and its corresponding trial vector according to the following rule:

$$X_{j,G+1} = \begin{cases} U_{i,G+1} & \text{if } f(U_{i,G+1}) \leq f(X_{i,G}) \\ X_{i,G} & otherwise \end{cases} \tag{2.6}$$

Thus, each individual of the temporary (trial) population is compared with its counterpart in the current population. The individual with the better objective function value will survive from the tournament selection to the population of the next generation. As a result, all individuals of the next generation are as good or better than their counterparts in the current generation.

The empirical study shows that the differential evolution algorithm has a greater degree of computational complexity for combinatorial problems than the genetic algorithm [105]. This largely arises from the encoding scheme used to represent the permutations as vectors and from redefining those vector operations inherent to differential evolution. The time required to reach convergence increases greatly as the problem size increases in both problems. The biggest advantage of the differential evolution approach over the genetic algorithm approach is its stability. The greatest setback for the genetic algorithm approach are problems with premature convergence.

2.5.3 Airport Capacity Management Using GA

GA is a large-scale parallel stochastic searching and optimising algorithm, and it is effective for solving a wide range of complex optimisation problems [96]. There have been many studies that have applied GA to resolve the airport capacity estimation problem [92, 155, 206]. The capacity of an airport depends on multiple factors such as the arrival-departure management, the geometric layout of the runway, the number of runways, the number of taxiways, the number of gates, aprons, the efficiency of the ATC and weather conditions [186]. Capacity maximisation by utilising multiple resources is a challenging task. The optimisation of multiple resources makes the airport capacity estimation a NP-hard problem [206]. To address this problem, evolutionary algorithms such as GA have been found to be effective in many cases [92, 155, 206]. In [206], the authors used a self-adaptive mutation-only GA algorithm to optimise the airport capacity curve.

They viewed this problem as a slot assignment problem and encoded the flight information such as the number of arrival and departure flights within a time frame, the time slot of landing and take-off, airborne holding delay, etc., into a chromosome. The chromosomes then went through an evolution process using mutation only to increase the airport capacity while ensuring no conflicts between successive operations (landing or take-off).

2.5.4 Application of EAs in Traffic Scenarios Generation

Many complex ATM problems require searching through a large number of possible solutions. Some problems require complex solutions that are difficult to programme by hand. Air traffic scenario generation is an example of this kind of problem. EA provide a simple way of addressing these problems when the evolutionary process involves searching among a large number of possibilities. In [160], Mondoloni applied GA to generate traffic scenarios to access the capabilities of an airborne conflict resolution algorithm. In [160] the proposed approach, each gene in a chromosome represents a possible flight plan. These traffic scenarios are first perturbed through genetic operators and then boundary constraints are imposed on them. Scenarios in the form of flight trajectories are generated through these flight plans and a conflict detection function is called. The fitness of each trajectory is evaluated based on conflict information for conflicted flight plans. A flight rules function is used to accept conflict information and determine whether the aircraft should move according to the rules of flight. The newly evaluated flight plans are then combined with the best flight plans from the prior iteration and ranked according to fitness. In the selection process, flight plans are selected in proportion to their fitness, where higher fitness flight plans have a higher probability of selection. In a similar problem, Paglione [176] applied GA for generating conflict scenarios by time shifting recorded air traffic data. GAs are utilised to determine the values of time shifts for the recorded air traffic data to obtain the desired conflict properties. The time shift of each flight is a gene on a chromosome that represents a vector of N time shifts for a set of N flights. Therefore, the number of genes in a chromosome is equal to the number of flights in the scenario. The fitness function is based on the number of encounters that fall in the defined primary conflict properties bounds.

Alam [9] used GA for path planning in a weather-constrained free flight air traffic environment. The weather-constrained airspace is discretised into a hyper-rectangular grid and a GA is used to find weather-free routes while incorporating other flight optimisation objectives such as minimising deviation from planned trajectories and reducing excessive climb and descent manoeuvers.

Recently, Alam [13] used a multi-objective GA to generate traffic scenarios to rank traffic flow management (TFM actions) that lead to high collision risk in an airspace. In this problem, a scenario is defined as a set of flight paths and a set of TFM actions with their execution times. The scenarios are encoded into a chromosome and its collision risk is evaluated using an air traffic simulator. Based on the fitness of scenario and applying the GA operators, TFM actions are evaluated over a generation and the scenarios with TFM actions that lead to higher collision risk are survived in the next generation. Finally, after the final generation, the TFMs are classified based on their impact on the increase of collision risk.

2.6 The Emergent Questions

From the literature survey, it is evident that, in the ATM domain, the capacity of an air transportation network has generally been measured at the levels of its individual elements, such as links (sector capacity and airspace complexity) and nodes (terminals and runway throughput), which obviously does not constitute its overall system-level capacity. There is almost no research on estimating the system-level or network-level capacity of an air transport network. Therefore, it is necessary to develop a model for air transportation network capacity estimation.

So, the ultimate question that arises is: how can the capacity of an air transportation network be estimated? From the network point of view, the system-level capacity of an ATN can be measured from its underlying airport network. Network capacity estimation is an optimisation problem with several constraints making up an NP-hard problem. It cannot be solved by any simple formulas. Traditionally, a network's capacity is determined by modelling it as a classical multi-commodity flow (MCF) problem [190], which is being applied successfully in communication networks, and water distribution and electric power systems. The unique characteristics of air traffic flow and the nature of interaction among the different components of an ATN makes the MCF formulation obsolete. However, with some modification, an airport network capacity can be formulated as an MCF problem. It is a challenge to develop such a formulation of the ATN capacity estimation problem. Chapter 3 addresses this challenge by the design and proposes a hill-climbing heuristic algorithm to solve the airport network capacity problem.

An air transport network is a complex combination of several integrated subcomponents. It can be considered a composition of two major networks: (i) the airport network – in which each airport is treated as a node and the flights connecting them create the links; (ii) airspace network considers the waypoint as a node and airways make the links. These two sub-network have their own constraints and goals. For example, an airport network is mainly concerned with increasing the throughput or individual capacity. Whereas, the airspace network, which is mainly responsible for an orderly flow and safe separation between flights, considers safety its limiting factor. The interaction between these two networks, which are created by the actual flow between them, plays an important role in an ATN's actual capacity estimation. Without considering these interactions, it will not be feasible to estimate the actual capacity bound/limit of an air transportation network. Although significant effort has been expended on developing large-scale, discrete-event simulations of an air transportation network system, a simple macroscopic theoretical model for estimating the system-level capacity estimation and integration of it with a simulations is lacking. Such a framework will enable us to gain insights into the relationship between the capacity and safety of an ATN. In Chapter 7, I address this issue and propose the abovementioned framework.

For developing a framework for capacity – safety relationship analysis of an ATN – several questions arise, such as: what is an appropriate collision risk model that can be used in a real simulation environment? Here, an appropriate model means that the model is efficient to handle a large amount of air traffic data (one day, one month or one year) and can accommodate different kinds of aircraft and their performance. Secondly, complex air transportation network modelling with individual airport and airspace network will be required. Finally, the capacity of an airport needs to be translated into an air traffic scenario that can be executed in a simulator from where the collision risk can be estimated. Methodologies of generating/developing air traffic scenarios for collision risk assessment are highly tedious and time consuming. Recorded air traffic data does not contain adequate alternatives, since any possible loss of separation situation is already resolved by the controllers. Thus, an algorithmic approach to generate traffic scenarios with desired properties is highly desirable. All of these challenges are addressed in Chapter 7, where validation and evaluation experiments are conducted with a set of scenarios representing different air transportation networks with different capacity limits.

Chapter 3

Airport Network Modelling and Topological Analysis

Work in this chapter has been published partially in the following papers:

- Md Murad Hossain, Sameer Alam, Tim Rees and Hussein Abbass, *Australian airport network robustness analysis: a complex network approach.* 36th Australasian Transport Research Forum (ATRF 2013), Brisbane, Queensland, Australia.
- Md Murad Hossain and Sameer Alam, *A Complex Network Approach Towards Modeling and Analysis of Australian Airport Network*, Journal of Air Transport Management, Elsevier, *Submitted.*

An airport network forms the backbone of an air transportation network. In such a network, the links between the origins and destinations of flights result in a complex network of routes, which can then be complemented with information associated with the routes themselves, such as frequency, traffic load and distance. In this chapter, I propose a complex network approach to model an airport network for understanding the dynamics of its topology and features. As a case study, the Australian civil domestic airport infrastructure is modelled as a complex network. This chapter address the following research question, which has been the focal point of the ATM community over the years. *What is an appropriate model for an airport network for capacity analysis?* To address this question, I compute complex network measures such as degree distribution, characteristics path length, clustering coefficient and centrality measure as well as the correlation between them to gain an understanding of the topology of an airport network.

3.1 Introduction

In recent years, the transportation domain has witnessed a renewed interest in network and graph theory due to the understating gained that many natural [94, 157, 213, 218], artificial [26, 230] and combinatorial optimisation problems [109, 197, 198] can be explained in terms of complex networks. More recently, the advancement of complex network theory has generated a huge interest in the area of airport networks [16, 21, 102, 217, 222].

To analyse the topology and characteristics of the airport network, at a regional, national or global level, it is best to abstract and integrate the airports in a way that allows us to assess uncertainty and other properties of interest without needing to include too much detail. Complex network theory provides a theoretical framework that may help us to develop such models and to analyse the topology and characteristics of the resulting network. From the complex network point of view, airports are modelled as graphs (networks) comprising airports as vertices that are linked by flights connecting them. exhibit two distinct topological properties:

There have been a few studies applying complex network tools to analyse air transport networks. Notable among them are the Worldwide Airport Network (WAN), which has been studied from a topological as well as an traffic dynamics perspective [101]. Guimerá ei al., observed that the WAN is a scale-free (SW) network and the most connected nodes are not necessarily the "central"-nodes through which most of the shortest paths pass, implying the anomaly of centrality values [102]. In 2004, Guimerá et al. [101] proposed a model incorporating the geo-political constraints to explain this anomaly. Besides the topological features, Barrat et al. [28]

studied the WAN in more detail by considering the traffic dynamics, specifically the strength of interactions between nodes. They also proposed [29] a model for the evolution of weighted evolving networks to understand the statistical properties of real-world systems. Complex network measures are also used for analysing the air transport networks of particular countries and airlines, such as Italy [100], India [21], Brazil [56], China [217] and the Lufthansa airline [192]. Each network was found to have different characteristics and unique connectedness.

In these research works, though the topology and the structure of airport networks have been analysed, one common oversight is the lack of robustness analysis of the air transport networks. There is a research gap in identifying the topological features to asses airport network robustness or vulnerability. To fill this gap, in particular, I am interested in two main questions: (i) which network measures are best suited to assess the damage suffered by airport networks and to characterise the most effective attack (protection) strategies? (ii) how does the network structure influence the system's robustness? My attention is, therefore, focused on the network topology and analysis of the structural vulnerability with respect to various centrality-driven failure (attack) scenarios. In particular, I propose a series of topological and centrality-based features that can be used to identify the key vertices of an airport network. There are two main types of disruption that could happen to an airport network.

- Short time outage of resources such as: closing of special purpose (military use) airspaces for a period; runway or airport unavailable due to weather or congestion; outage of control tower radar; or communication links break down. These types of shortage are usually recovered within a short period of time. As a result, these types of disturbance usually have a small impact on the overall performance of the systems. In the current air transportation system, if an airport is congested, all departure flights are delayed, the arrival traffic (if not departed) is delayed in the origin airports and the airborne flights, approaching the airports under short-term outage, are either put on hold if possible or diverted to another airport until the airport recovers.

- Long-term resources outage can include terror action causing the closing down of air travel in large areas (e.g. 9/11 in 2001); volcanic ash blocking air travel in large areas (e.g. Iceland volcano in 2010); airports affected by floods; runway accidents that damage the runway; or airports damaged by tornados or typhoons. These types of disruption are rare and normal functioning cannot be recovered in a short period of time; each of these rare exceptional events could trigger catastrophic failure of the whole system.

In this chapter, I investigate airport network features and the effect of long-term disruption on the robustness.

3.2 Airport Network Model

An airport network is usually defined as a graph in which nodes are airports and two nodes are connected if at least one flight goes from one node to another in a defined time interval. The topology and the characteristics of airport networks has been analysed by using the tools of complex network theory. Understanding and analysing an airport network can give useful insights into the future development of airports and the redesigning of airspace, and can be an important source of information for policy makers. In this chapter, I have used the AAN as a case study. Though the AAN is used as an example, the results and insights are applicable to transportation or airport networks with similar network features.

The AAN consists of domestic and international airports that conduct regular passenger flights with over 20 airlines (domestic and regional) connecting them. The air movement data among Australian airport-pairs, for 2011, was obtained from the Bureau of Infrastructure, Transport and Regional Economics, Australia (http://www.bitre.gov.au) and the Official Airline Guide OAG (http://www.oag.com) [171].

3.2.1 Unweighted AAN

For the purpose of developing the AAN, links are created between each airport-pair if there is any passenger flight connecting the two airports. From the resulting network, I found that the AAN is a directed network at which all major airports have direct connections. The AAN is represented as a connected network $G = (V, E)$ by V and E, where $V = v_i : i = 1, 2, ..., n, n = |V|$ is the number of nodes, and $E = e_i : i = 1, 2, ..., m, m = |E|$ is the number of edges (links). The network is represented by an adjacency matrix $A_{n \times n}$ such that a_{ij}=1 if a flight link exists between city-pair i and j, otherwise a_{ij}=0. The resulting AAN consists of 131 airports and 596 direct air routes. Most of the links in the AAN are connected in both ways; as a result, I consider it as an undirected network for the subsequent analysis in this chapter.

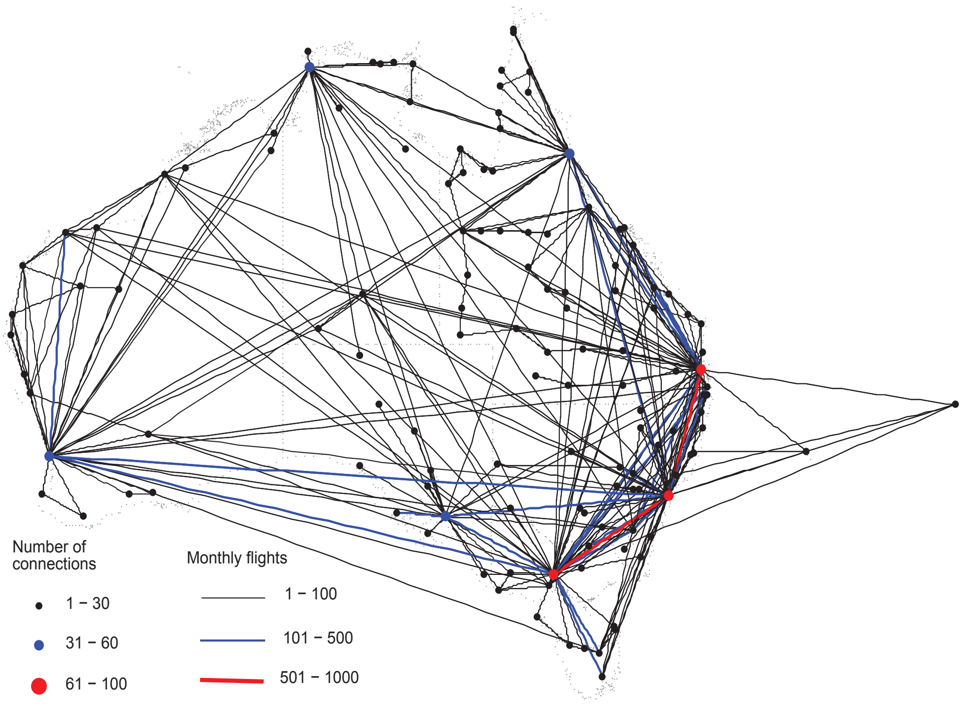

FIGURE 3.1: The Australian Airport Network.

TABLE 3.1: Top 20 cities in Australia by number of passengers.

Rank	City	No. of air routes	Aircraft Movements (thousand)	Passenger volume (million)
1	Sydney	99	158.212	21.878
2	Melbourne	66	149.196	20.492
3	Brisbane	81	110.209	14.315
4	Perth	57	58.352	7.548
5	Adelaide	47	47.584	5.883
6	Gold Coast	25	31.711	4.554
7	Cairns	46	24.829	2.964
8	Canberra	24	31.011	2.688
9	Hobart	10	14.761	1.843
10	Darwin	41	11.321	1.246
11	Townsville	29	13.330	1.316
12	Williamtown	16	8.236	1.078
13	Launceston	16	9.197	1.013
14	Mackay	14	8.346	0.824
15	Sunshine Coast	4	6.237	0.857
16	Karratha	15	6.905	0.690
17	Rockhampton	14	5.791	0.378
18	Alice Springs	19	6.566	0.597
19	Hamilton Island	13	3.423	0.434
20	Broome	21	3.414	0.333

3.2.2 Weighted AAN

Like many other complex networks, the details of the flow of information (traffic load) are a crucial factor for a transportation network. To accommodate the information about the amount of traffic flowing in the network, the AAN is represented as a weighted network by considering the number of flights flying on a route as the weight of that particular link. The weight is defined by a weight matrix A^w, where each element w_{ij} stands for the total number of flights from airport i to airport j. Figure 3.1 shows the AAN, in which proportional circles represent the number of air connections of airports (number of routes) and the width of links represent the monthly average volume of traffic.

Table 3.1 summarises the air traffic volume and air route (number of airports connected) of the top 20 cities of the AAN from January 2011 to December 2011.

The passenger data includes the major domestic airlines (Qantas, Jetstar, Virgin Blue and Tiger Airways) and regional airlines that perform scheduled services. The air route data includes all the airlines (domestic and regional) that provide connectivity between airport pairs. Of all the airports, Sydney has the highest level of air-route connectivity as well as passenger and flight movement.

3.3 Network Characterization and Topological Features

Network structures arise in a wide range of different contexts such as technological and transportation infrastructures, social phenomena and biological systems. Each class of networks presents specific topological features that characterise its connectivity, interaction and the dynamical processes executed by the network [28]. The analysis, discrimination and synthesis of complex networks, therefore, rely on the use of measurements capable of expressing the most relevant topological features, which enable us to characterise the complex statistical properties [55]. Several basic indices are used to measure the topological configuration of the AAN. Table 3.2 summarises the key metrics used to characterise a network. The general implications in Table 3.2 indicate how these various measures imply important roles in a transportation network where the notations and variables have the following meaning:

n = number of nodes

a_{ij} = represent the presence of connection between node i and j

w_{ij} = weight of the link between node i and j

$\langle w_i \rangle$ = average weight incident to node i

k_i = degree of node i

$\langle k \rangle$ = average degree of a network

n_k = number of nodes having degree k

d_{ij} = shortest distance between node i to j

C_i = clustering coefficient of node i

C = clustering coefficient of a network

C_i^w = weighted clustering coefficient of node i

C^w = weighted clustering coefficient of a network

L = average shortest path length

$C_c(i)$ = closeness centrality of node i

$C_c(i)$ = closeness centrality of node i

$C_B(i)$ = betweenness centrality of node i

Table 3.2: Network Metrics

Measure	**Symbol or Equation**	**General Implications**
Node	N/A	Represents an Airport of the Australian Airport Network (AAN)
Non-weighted adjacency matrix	$A = [a_{ij}]_{n \times n}$	Mathematical expression for a network. The matrix size depends on how many nodes compose the network – if there are n nodes in the network, the matrix size will be $n \times n$. Where all the entities are binary, i.e. $a_{ij} = 0$ *or* 1.

Continued on next page

Table 3.2 – *Network Metrics*

Measure	**Symbol or Equation**	**General Implications**
Weighted adjacency matrix	$A^w = [w_{ij}]_{n \times n}$	Similar to non-weighted adjacency matrix but instead of a binary value, each link has a corresponding scalar weight that signifies some distinguishing traffic such as the number of aircraft operating in that link.
Node Degree	$k_i = \sum_{j=1}^{n} a_{ij}$	In network theory, degree refers to the total number of connections node i has with other nodes in the network.
Average Degree	$\langle k \rangle = \frac{1}{n} \sum_{i=1}^{n} k_i$	The average degree of a network refers to the average number of neighbours a node has in the network.
Node weight, or Strength	$s_i = \sum_{j=1}^{n} a_{ij} w_{ij}$	In the transportation network, node weight or strength represents the amount of traffic (operations) associated with the node.
Degree Distribution	$p(k) = \frac{n_k}{n}$	Degree distribution, regarded as a descriptive statistic of the network, is an important characteristic of the nodes in the network. For a network with n nodes, if n_k of them have degree k, the degree distribution $p(k)$ is defined as the fraction of these $k-$degree nodes.

Continued on next page

Table 3.2 – *Network Metrics*

Measure	**Symbol or Equation**	**General Implications**
Cumulative Degree Distribution	$P(> k) = \sum_{k'=k}^{\infty} p(k')$	The degree distribution is very important in studying both real networks, such as the social networks, transportation networks and theoretical random networks. Most real-world networks have degree distributions very different from the random networks.
Cumulative Weight Distribution	$P(> w)$	The cumulative weights distribution $P(> w)$ of a network defines the fraction of links with weight greater than or equal to w. $P(> w)$ also plays an important role for identifying the level of heterogeneity among the traffic flow in a transportation network.
Geodesic Distance	$\ell = d_{ij}$	A shortest path between two nodes is referred to as the geodesic distance. It quantifies how far apart is each pair of nodes in the network. The 'Diameter' has the largest geodesic distance in the (connected) network.

Continued on next page

Table 3.2 – *Network Metrics*

Measure	**Symbol or Equation**	**General Implications**
Average Shortest Path Length	$L = \frac{1}{n(n-1)} \sum_{i \neq j} d_{ij}$	Average shortest path plays an important role in the transport and communication within a network. The smaller the L, the more compact and reachable the network. Thus, L could be used as an indicator of the performance of the airport network [22].
Clustering Coefficient	$C_i = \frac{1}{k_i(k_i-1)} \sum_{j,k} a_{ij} a_{jk} a_{ik}$	Capture the local cohesiveness of a node and also represent the network transitivity.
Average Clustering Coefficient	$C = \frac{1}{n} \sum_i C_i$	Measure of local cohesiveness for a collection of nodes. A node with higher C_i than the network's average clustering coefficient C is more interconnected than the average. This measure has implications on local robustness. Higher C_i indicates greater robustness since alternative connection paths may exist when a neighbouring node fails.

Continued on next page

Table 3.2 – *Network Metrics*

Measure	**Symbol or Equation**	**General Implications**
Weighted Clustering Coefficient	$C_i^w = \frac{1}{k_i(k_i-1)} \times \sum_{j,k} \frac{1}{\langle w_i \rangle} \frac{w_{ij}+w_{jk}}{2} a_{ij} a_{jk} a_{ik}$	Clustering coefficient C and C_i overlook the flow of information on the network and, hence, cannot capture the correct information about the network dynamics [28]. To the overcome this limitation, the weighted clustering coefficient C_i^w measures local cohesiveness by taking into account the interaction intensity present on the local triplets [174, 201]. The weighted clustering coefficient of the network C^w is then given by the average of all individual C_i^w in the network.
Closeness Centrality	$C_c(i) = \frac{n-1}{\sum_{j,i \neq j} d_{ij}}$	The centrality measures the relative importance of a node within a network. Closeness centrality measures the extent to which a node is close to all other nodes along the shortest path and reflects its accessibility in a given network [199].

Continued on next page

Table 3.2 – *Network Metrics*

Measure	**Symbol or Equation**	**General Implications**
Betweenness Centrality	$C_B(i) = \sum_{k \neq i \neq j} \frac{\sigma_{ij}(i)}{\sigma_{kj}}$ where σ_{kj} is the total number of shortest paths from node k to node j, and $\sigma_{kj}(i)$ is the number of those paths that pass through node i	Betweenness centrality is a useful measure of the load placed on a given node in the network as well as its importance to the network other than just connectivity. Betweenness centrality measures the extent to which a particular node lies between other nodes in a network [18, 87].
Degree Correlation	$k_{nn}(k) = \sum_{k'} k' P(k' \mid k)$ where $P(k' \mid k)$ is the conditional probability that a node with degree k is connected to a node of degree k'	Degree correlation demonstrates the extent of a node's degree related to the average degree of its neighbours. This index reflects the node's connection tendency or assortativity of the network.
Weighted Degree Correlation	$k^w_{nn,i} = \frac{1}{s_i} \sum_{j=1}^{N} a_{ij} w_{ij} k_j$	For a network, $k^w_{nn,i}(k)$ is the average weighted nearest neighbour degree over vertices of degree k. $k^w_{nn,i}(k)$ measures the effective affinity to connect with high- or low-degree neighbours according to the magnitude of the actual interactions.

Continued on next page

Table 3.2 – *Network Metrics*

Measure	**Symbol or Equation**	**General Implications**
Clustering Degree Correlation	$C(k) = \frac{1}{N_k} \sum_{v_i \epsilon V, k_i = k} C_i$	Clustering-degree correlation demonstrates the extent of a node's clustering coefficient related to its degree. This property provides insights into how the hub nodes provide connectivity to the peripheral nodes in the network and inter-hub connectivity tendency.
Weighted Clustering Degree Correlation	$C^w(k) = \frac{1}{N_k} \sum_{v_i \epsilon V, k_i = k} C_i^w$	Weighted clustering-degree correlation combines the topological information with the weight distribution of the network. This network feature provides global information on the correlation between weights and topology, specifically by comparing them with its topological analogues $C(k)$.

3.4 Topological Analysis of AAN

Network structures arise in a wide range of different contexts such as technological and transportation infrastructures, social phenomena and biological systems. Each class of networks presents specific topological features that characterise its connectivity, interaction and the dynamical processes executed by the network [28]. The analysis, discrimination and synthesis of complex networks, therefore,

TABLE 3.3: Characteristics of various networks (unweighted).

Network	Characteristics path length (L)	Clustering coefficient (C)	Degree distribution (P(k))
Regular network	Long	Large	point to point
Random network	Short	Small	Poisson or Binomial
Small-world network	Short	Large	Exponential or Power-law
Scale-free network	Short	Large	Power-law
Real network	Short	Large	Similar power-law

rely on the use of measurements capable of expressing the most relevant topological features, which enable us to characterise the complex statistical properties [55]. Several basic indices discussed in Table 3.2 are used to measure the topological configuration of the AAN.

The analysis of the topology of an airport network is important for two main reasons. First, it allows us to identify the most efficient ways to engineer the structure of the network. Specifically, having identified the topology, one can identify which nodes are poorly connected and the way to minimise that problem. Secondly, it provides a systematic way to identify the most central or critical node in the network. The most central nodes play an important role to the entire dynamic and, hence, the risk posed by possible malfunctioning of the airport.

Most network studies rely on measures capable of characterising relevant topological features to identify the unifying principles and statistical properties commonly existing among empirical networks [55]. According to the topological features, the characteristics of different types of network are summarised in Table 3.3. A regular network is a connected graph in which each vertex is connected in the same way exactly as its neighbouring vertices, for example, a *ring* network. A random network consisting of n vertices and m edges is constructed by adding m edges between the nodes at random, avoiding multiple and self-connections. A *small-world* network is a network in between the regular and random network and has a small characteristics path length and high clustering coefficient, i.e. most vertices can be reached from others through a small number of hops or steps. Many empirical graphs are well modelled by *small-world* networks [218]. Many real-life networks such as the road network, electric power grids and gene networks exhibit by *small-world* network characteristics. Another important type of network that is also found in the real-world network is the *Scale-free* network. A scale-free(SF) network is a network whose degree distribution conforms to a power-law [168]. If the connectivity distribution $P(k)$ is the probability that a node is connected to k other nodes, then SF networks are characterised by a power-law behaviour $P(k) \sim k^{-\gamma}$, where γ is a characteristic exponent [55].

3.4.1 Degree and Weight Distribution Analysis

The average degree and the distribution of degree measures provide a holistic view of the structure and organisation of the whole network. The average degree of the AAN is 9.10 with a maximum degree of 99. The AAN's cumulative degree

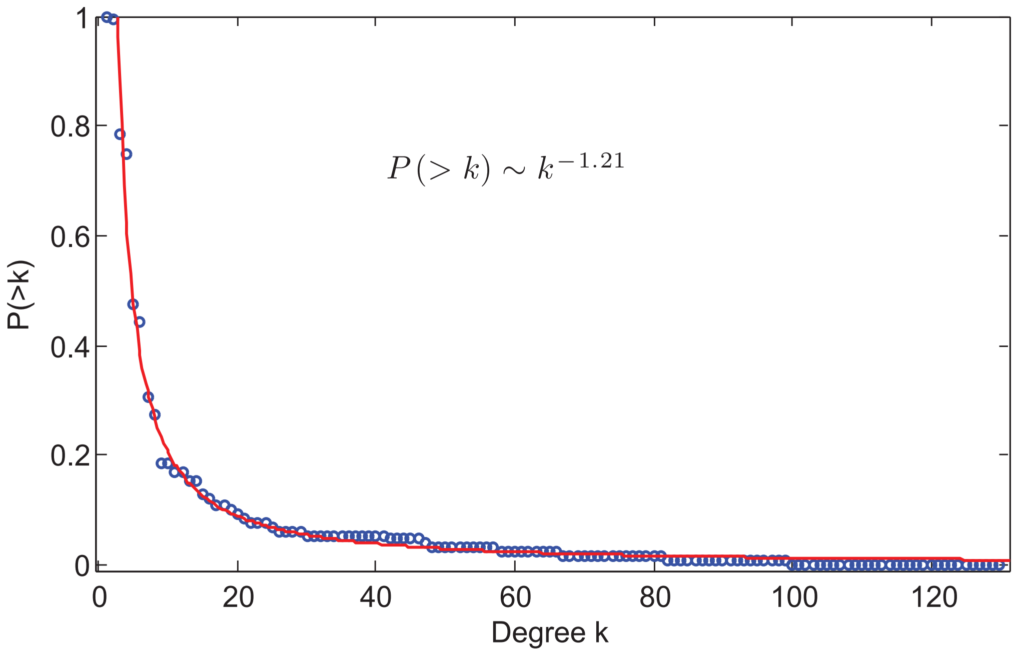

Figure 3.2: Cumulative degree distribution of AAN

distribution follows power-law distribution $P(>k) \sim k^{-1.1211}$ ($R^2 = 0.96$), which is shown in Figure 3.2. It is shown in the figure that a small number of busy airports at the top dominate the system with a large number of air routes. The number of routes to each airport declines quickly, with most of them having only 1-3 air routes at the long tail. For example, the top 20 airports connected with a majority (about 56%) of all air routes, and the bottom half of the airports (67 of the 131 nodes in the network) are only connected with, at most, five other airports. The AAN is, therefore, a clear example of a network with a heterogeneous degree distribution, showing scale-free properties on a moderate range of degree values.

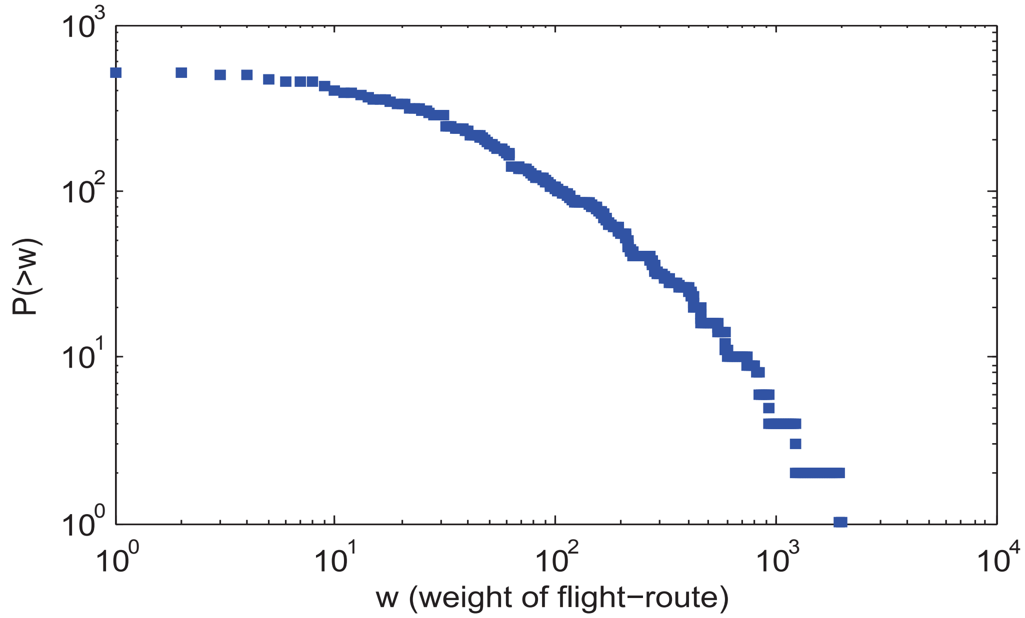

FIGURE 3.3: Cumulative weight distribution of AAN

Similar to the degree distribution, distribution of weights also plays an important role in identifying the level of heterogeneity among the traffic flow in an airport network. The cumulative weight distribution of the AAN is presented in Figure 3.3. The statistical analysis of weights w_{ij} between pairs of airports indicates the presence of right-skewed distributions, which signals a high level of heterogeneity in the system. This phenomena is also found in the case of Airport Network India [21], China [217] and WAN [101].

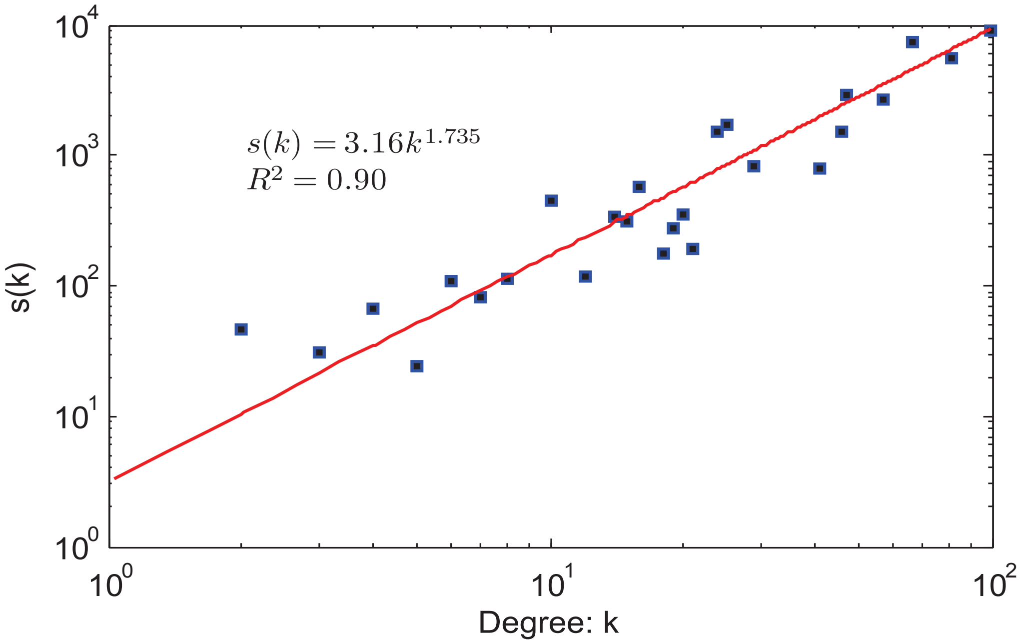

FIGURE 3.4: Average strength $s(k)$ as a function of degree(k).

It has been observed that the individual links weights do not provide a general picture of the network's complexity [227]. A more significant measure of the network complexity considering the flow of information is the node's 'Strength' (s_i). This quantity measures the strength of nodes in terms of the total weight of their connections. It is a natural measure of the importance or complexity of a node i in the network.

To capture the relationship between the node's strength and degree, I investigate the dependence of s_i on k_i. Figure 3.4 shows the relationship between the average strength of nodes with degree k. I have found that the $s(k)$ of vertices with degree k increases with the degree as $s(k) \sim k^{\beta=1.735}$. The value of $\beta = 1.735$ implies that the strengths of nodes are strongly correlated with their degrees in the AAN. This behaviour is expected because it is plausible that the larger the airport in terms of connection, the more traffic it handles. This feature of the AAN is similar to that of the WAN and the airport network of India [21].

3.4.2 Average Shortest Path Length

The average shortest path length analysis provides an indicator of the convenience of traveling in a network. This measurement quantifies the efficiency of the network in sending information (traffic mobility) between vertices [55].

Table 3.4: Distribution of the air routes by number of connection flights.

Hop count	No. of Paths	Percentage of air routes	Cumulative percentage of air routes	No. of flights needed to be change
1	596	3.5	3.5	0
2	5033	29.554	33.053	1
3	7914	46.471	79.524	2
4	2232	13.106	92.631	3
5	816	4.792	97.422	4
6	291	1.709	99.131	5

Table 3.4 summarises the results of the characteristic path length analysis. It provides an overview of the network in terms of the ease of travel and summarises the minimum number of flights needed to be changed (number of stop) for traveling all city-pair. The AAN has 596 unique paths – node-to-node flight routes. Among all possible unique city-pairs ($131(131-1) = 17030$), 596 are reachable by direct flight. However, around 33% of the city-pairs are reachable by changing only one flight, 79.524% and more than 90% are accessible by changing, at best, two and three flights, respectively. The average shortest path length L of the AAN is 2.90, which implies that, on average, it requires almost two flight changes to connect almost all city-pairs. The average path length of the AAN is slightly larger than a random network ($L_r = 2.096$) of the same size and slightly smaller than that of *small-world* network ($L_{SW} = 4.01$). For comparison purposes (comparing the AAN with corresponding small-world networks), a small-world network is generated using the model described in [218], which starts with a ring lattice of 131 nodes. In the ring, every node is connected to its four neighbours (two on either side). After that, each link is rewired with probability $p = 0.15$, with self-connections and duplicate edges excluded. The diameter (defined as the longest of all shortest

paths) of the AAN is 7, which means that one needs to change, at best, six flights to reach from any airport to any other airport in the AAN, including the small airports and isolated island airports (Cocos Island, Rottnest Island, Christmas Island and Norfolk Island). A relatively larger value of D and L implies that, in the AAN, there is much room to improve efficiency in terms of connection and passenger mobility.

Table 3.5: Characteristics of the Australian airport network and other countries/regions.

Author	Country	No. Nodes (n)	No. Edges (m)	Average degree $\langle k \rangle$	Average path length (L)	Clustering coefficient (C)	Network structure
Bagler 2008	India	79	455	11.52	2.26	0.66	SW
Guimera et al. 2004	World	3883	27051	13.93	4.4	0.62	SF SW
Guida et al. 2007	Italy	50	310	12.4	1.98∼2.14	0.07∼ 0.1	SF SW Fractal
Xu & Harriss 2008	US	272	6566	48.28	1.84∼1.93	0.73∼0.78	SW
Wang et al. 2010	China	144	1018	14.14	2.23	0.69	SW
In this chapter	Australia	131	596	9.10	2.90	0.50	SW

Table 3.5 compares the topological properties of the AAN with other similar types of network. From Table 3.5, it is noticeable that the average path length of the AAN (L=2.90) is slightly larger than that of China (2.23) and India (2.26) but much larger than that of the US (ranging from 1.84 to 1.93). From the analysis, it can be inferred that the AAN has evolved the *small-world* topology. According to Watts and Strogatz [218], if L grows almost as $log(n)$ where n is the number of nodes, then the corresponding network can be defined as a *small-world* network. In particular, for the AAN, $L = 2.90$, and $log(n) = 2.12$ for $n = 131$. The average degree of the AAN $\langle k \rangle = 9.10$ is the lowest in the group and has a clustering coefficient of $C = 0.5$. All of these network features of the AAN confirm that it has properties similar to *small-world* characteristics.

3.4.3 Clustering Coefficient Analysis

Clustering coefficient C_i captures the local cohesiveness of a node, which refers to the probability that two airports connected with a third are also directly connected to each other. A large value of C_i means that the node i has a more compact system of connections with its neighbour. Whereas, the average clustering coefficient (C) measures the global density of interconnected nodes in the network. The AAN's clustering coefficient is $C = 0.50$, which is much larger than that of a random network [72] ($C_r = 0.091$,) of the same size and almost similar to that of a *small-world* network ($C_{sw} = 0.635$). A larger clustering coefficient confirms the high degree of concentration and also implies a high probability for traveling with fewer transfers in the network. However, the clustering coefficient (C) does not consider the information provided by the weighted network. To solve this limitation, I introduce the weighted clustering coefficient C_i^w to combine the topological information with the weighted distribution of the network. This coefficient is a measure of the local cohesiveness that takes into account the importance of the clustered structure on the basis of the amount of traffic operating on the local triplets. Weighted clustering coefficient averaged over all nodes(C^w) of the AAN is 0.23, which is much smaller than the non-weighted counterpart $C = 0.50$. In the case of the AAN, $C^w < C$ signals a network in which the topological clustering is generated by links with low weight. The clustering coefficient has a minor effect in the organisation of the network because the largest interactions of traffic frequency are operating on links not belonging to interconnected triplets. This phenomena confirms that most of the network traffic is concentrated in a hub-spoke pattern.

In comparison to the other airport networks, the clustering coefficient of the AAN is slightly smaller than India (0.66) and China (0.69) but much smaller than the US (0.73-0.78) also (See Table 3.5).

3.5 Centrality Analysis

A key issue in the characterisation of networks is the identification of the most important nodes in the system. Centrality is a concept that can identify the important nodes within the system. Centrality can be quantified by various measures. The degree (k_i) is the first intuitive that gives an idea of the importance of a node in terms of connectivity. Whereas, the strength(s_i) quantifies the importance of a node by taking the level of traffic (operating load) into account. However, these local measures do not take into account non-local effects, such as the existence of bottleneck nodes, which may have small degree but act as bridges between different parts of the network. In this context, a well-accepted parameter to investigate node centrality is the betweenness $C_B(i)$, closeness $C_c(i)$ and centrality [87].

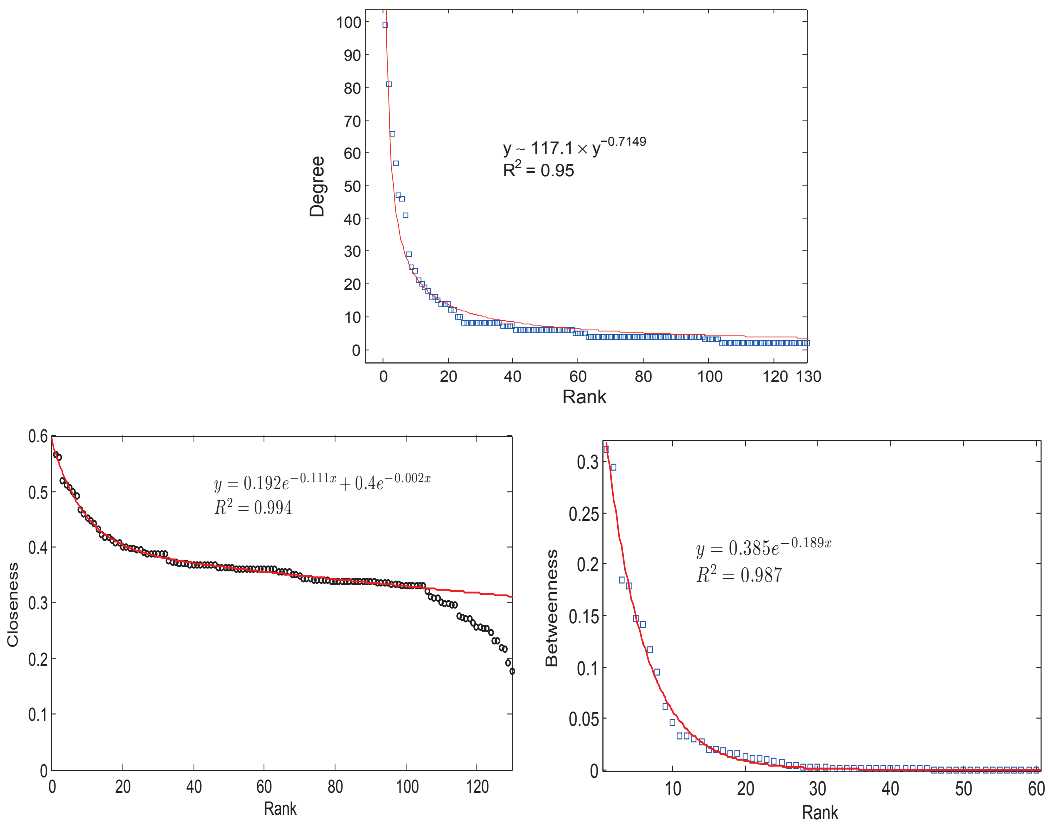

FIGURE 3.5: Statistical distribution of degree, closeness and betweenness centralities.

3.5.1 Statistical Distribution of Centralities

The distribution of all three centrality indices (shown in Figure 3.5) generally confirms either to a power-law or exponential decay function, with R^2 above 0.95. The degree centrality curve confirms that a small number of nodes carry the majority of the routes. Indeed, the top 10 most connected airports account for 43% of air routes. From Figure 3.5, it is observed that the closeness curve has the flattest slope. The steep curve of degree and betweenness indicates that a few hub cities account for most of the transfer capacity. In general, high degree vertices have a large number of topological connections and they usually have high betweenness. But it is not always the case. It is noticed from Figure 3.5 that only two nodes have a high betweenness value compared to a large number of high degree nodes. In the AAN, there are 118 nodes(around 90% of total nodes) have less betweenness value then average betweenness (C_B=0.0145). The sharp decline of

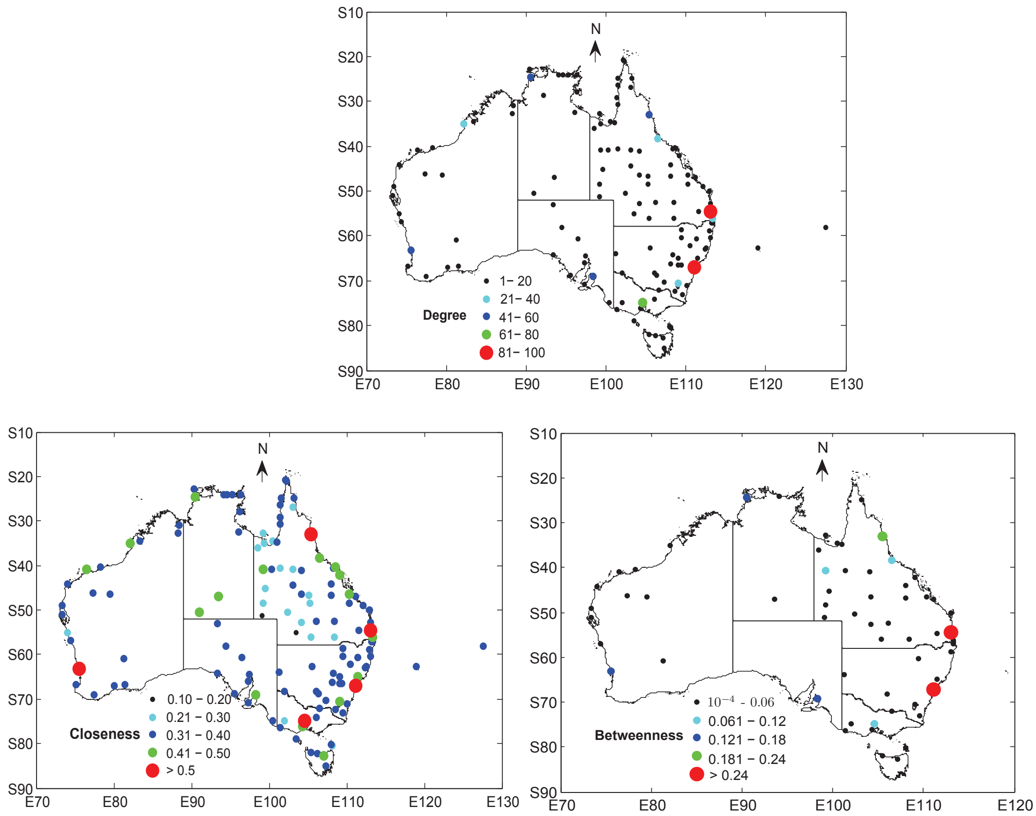

FIGURE 3.6: Spatial distribution of degree, closeness and betweenness.

the betweenness curve and a large number of nodes with low betweenness value suggests the existence of bottlenecks within the AAN, which is confirmed by a low value of clustering coefficient $C = 0.5$ (see table 3.5).

Figure 3.6 shows the spatial distribution of the three centralities. Generally, cities in the east region have better centrality than those in the west. In terms of degree and closeness, the most central cities are mainly clustered around Sydney and Canberra. State capitals such as Brisbane, Melbourne, Perth, Adelaide and Darwin also have high centrality values. In terms of spatial distribution, betweenness has the highest inequality, having high value for only two capital cities (Brisbane and Sydney), whereas closeness has the least inequality. It can be seen from Figure 3.5 that the highest betweenness value for Brisbane (0.31) quickly drops to 0.045 in Toowoomba (10th rank) and 0.0199 in the Gold Coast (15th rank).

3.5.2 Relation Among Centralities

Table 3.6 reports the top 20 cities by degree, closeness and betweenness. Brisbane is ranked at the top by closeness and betweenness, whereas Sydney is at the top by degree index followed by Brisbane. Melbourne is ranked 3rd by degree and closeness indices and placed in 7th position by betweenness, showing a high level of inconsistency in the centrality indices. Perth is ranked in 4th, 5th and 6th by the degree, closenness and betweenness indices, respectively. Adelaide is ranked in 5th, 7th and 5th by the degree, closenness and betweenness indices, respectively. The national capital, Canberra is ranked in 10th and 9th by the degree and closeness, but does not manage to get into top 20 by betweenness. These are the national hubs in the network. However, Broom, Alice Springs, Newcastle, Karratha, Mackay, Rockhampton and Geraldton are in the top 20 by degree but not in the top 20 by betweenness. All of these cities have considerably large numbers of air routes to the peripheral nodes and, thus, have relatively small values of betweenness. Similarly, some cities in peripheral regions such as Toowoomba, Charleville, St. George, Boulia, Quilpie, Doomadgee Mission, Cunnamulla and Bedourie appear in the top 20 cities by betweenness, but do not make it into the top 20 cities by degree.

There are 28 cities with the lowest degree ($C_D = 2$, only one air route to other airports). In terms of closeness, Katherine has the lowest, followed by Thargomindah, Birdsville, Cunnamulla, Windorah and Burketown. All of these airports have very few air routes to their regional hubs. Therefore, it usually takes multiple connection flights for them to reach other nodes in the network. In the case of betweenness, 70 airports have a betweenness value of zero, indicating that there are no shortest paths between other city-pairs passing through them. These airport

Table 3.6: Top 20 Cities by Degree, Closeness and Betweenness

Rank	Degree, C_D	Closeness, C_C	Betweenness, C_B
1	Sydney	Brisbane	Brisbane
2	Brisbane	Sydney	Sydney
3	Melbourne	Melbourne	Cairns
4	Perth	Cairns	Perth
5	Adelaide	Perth	Adelaide
6	Cairns	Darwin	Darwin
7	Darwin	Adelaide	Melbourne
8	Townsville	Alice Springs	Mount Isa
9	Gold Coast	Canberra	Townsville
10	Canberra	Gold Coast	Toowoomba
11	Broome	Broome	Launceston
12	Avalon	Townsville	Charleville
13	Alice Springs	Avalon	St. George
14	Mount Isa	Launceston	Boulia
15	Launceston	Karratha	Gold Coast
16	Newcastle	Mount Isa	Avalon
17	Karratha	Hamilton Island	Quilpie
18	Mackay	Mackay	Doomadgee Mission
19	Rockhampton	Rockhampton	Cunnamulla
20	Geraldton	Newcastle	Bedourie

are the peripheral nodes in the network.

Table 3.6 shows that the rankings by degree, closeness and betweenness are generally consistent. The same 12 cities appear in the top 20 for all three indices, whereas 19 cities appear in the top 20 for degree and closeness. Geraldton is the city that is present in the top 20 by both degree but not in the list of and closeness, and Hamilton island is the opposite. The top 10 cities are highly connected and also play an important role in transferability. Whereas, some cities are less connected but serve as important transfer hubs, such as Toowoomba, Charleville, St. George, Boulia and Bedourie. These are usually located in the peripheral areas and play an important role as connector hubs for regional traffic.

TABLE 3.7: Relationship between centralities.

Correlation coefficient	Degree, C_D	Closeness, C_C	Betweenness, C_B)
Degree, C_D	1	0.6820	0.9276
Closeness, C_C		1	0.5715
Betweenness, C_B			1

Table 3.7 reports the correlation coefficient between the three centrality indices. The correlation coefficient is highest 0.9276 between degree and betweenness, whereas closeness and betweenness have the lowest correlation. Centrality measures indicate a significate level of heterogeneity in connections (links) among the nodes in the AAN.

3.6 Correlation Analysis

3.6.1 Degree Correlation

Degree correlation demonstrates the extent of a node's degree related to the average degree of its neighbours. It is measured by the average degree of the nearest neighbours, $k_{nn}(k)$, for nodes of degree k [180]. In a network without degree correlation, $k_{nn}(k)$ is independent of k. In a correlated network, $k_{nn}(k)$ increases or decreases with k. When $k_{nn}(k)$ increases with k, high-degree nodes tend to link with each other, and this tendency is referred to as 'assortative mixing'. In contrast, high-degree and low-degree nodes tend to connect with each other when $k_{nn}(k)$ has a decreasing behaviour. This property is referred to as 'dissassortative mixing' [168].

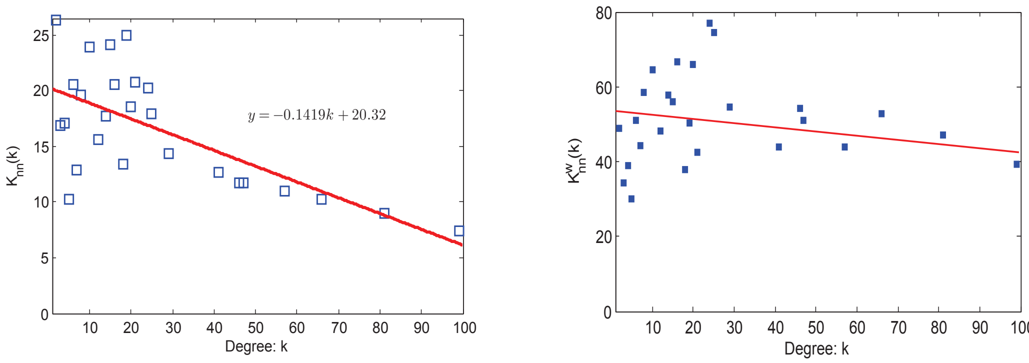

FIGURE 3.7: Degree Correlation of AAN (left-unweighted, right-weighted)

Figure 3.7(left) shows the degree correlation of the AAN. From Figure 3.7, it is found that the AAN shows a disassortative mixing, which means that vertices of high degree tend to connect with vertices of low degree. For example, Sydney and Brisbane have the highest and 2nd-highest degree of 99 and 81, respectively, and a small value of k_{nn} (7.374 and 8.975, respectively). The low-degree vertices are the most correlated. For example, 2-degree airports have the maximum $k_{nn}(k)$ value of 26.315. The consistent disassortativity in the AAN for higher-degree airports could be attributed to the political compulsions on regional and national hubs to provide connectivity to a large number of low-degree airports.

In order to take into account the weights on connection, the weighted degree correlation $k^{w}_{nn}(k)$ has been used to measure the effective affinity to connect with high- or low-degree neighbours according to the magnitude of the traffic interaction. Figure 3.7(right) shows the $k^{w}_{nn}(k)$ as a linear decreasing pattern with the degree.

The topological k_{nn} and the weighted degree correlation $k_{nn}^{w}(k)$ show a clear disassortativity behaviour when $k > 20$. The consistent disassortativity in the AAN (both unweighted and weighted) for higher degree nodes could be attributed to the political compulsions on regional and national hubs to provide connectivity to a large number of low-degree destinations.

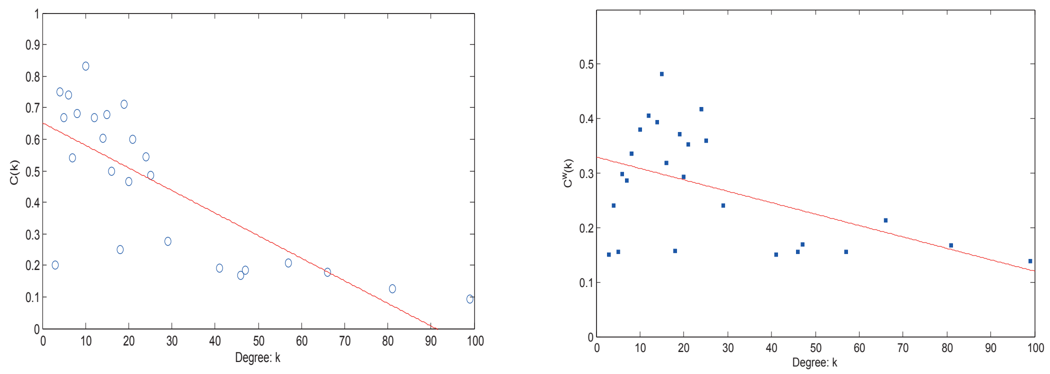

Figure 3.8: Correlation between degree and clustering coefficient (left-unweighted, right-weighted)

3.6.2 Clustering-Degree Correlation

Figure 3.8 shows the relationship between clustering coefficients and degrees that resemble some kind of inverted 'V' shape. The trend can be divided into two parts. When the degree is below the network average degree $\langle k \rangle = 9.10$, the cluster coefficient ($C(k)$ and $C^{w}(k)$) and degree indices are positively correlated. When the degree is above $\langle k \rangle = 9.10$, $C(k)$ and $C^{w}(k)$ are negatively correlated with the degree. As seen in Figure 3.8, after $k > \langle k \rangle$, both the weighted and the unweighted clustering coefficients fall rapidly. This implies that, with increasing degree, airports tend to be surrounded by lower-degree cities (groups of cities), which are less connected themselves. This decaying behaviour of $C(k)$ and $C^{w}(k)$ in the AAN is observed because of the role of national hubs that provide connectivity to a large number of peripheral airports. Therefore, higher-degree cities are associated with lower clustering coefficients in this group of cities.

3.7 Robustness Analysis

Robustness analysis provides an efficient way to analyse the stability of various complex systems [107]. This analysis is obviously practical, as it affects directly the efficiency of any process running on top of the network, and it is one of the important issue to explore in the literature on complex networks [36, 149]. Although robustness is well studied in the literature, it is a rather unknown area in air transportation, both in practical application as well as in research. It is not clear how robust an airport network is to tolerate failures or attacks. The use of complex network-based metrics and simulation provides a promising approach for addressing the complexity of robustness. This chapter addresses the measurement of airport network robustness through the evaluation of its topological and reachability metrics.

3.7.1 Failure Scenario

For the study of failure (attack) vulnerability of the transportation network, the selection procedure of the order in which nodes or links could be removed is an open choice. I study the behaviour of damage measures in the presence of a progressive random damage and of several attack strategies. Transportation networks are inherently resilient to random nodes or edge failure. Even after a large number of node or link failure, all of the metric measures decrease moderately and do not seem to have a sharp threshold after the network is virtually destroyed [57]. Since one of the objectives is to identify the nodes or edges that maximise the disruption in the network, one of the approaches is to select the most central nodes in the network. A straightforward choice is to select the vertices in descending order of degrees of the initial network and then remove vertices one by one starting from the vertex with the highest degree [25]. In addition, I have used various studies based on the different definitions of the centrality ranking of the most important node. Nodes can be removed according to their strength (s_i) and topological betweenness $C_B(i)$.

Apart from node failure, edge or link failure play a very important role in analysing the robustness of an airport network. In the airport network, edge failure corresponds to, for instance, disturbances such as weather or airspace closure preventing travel between a pair of airports. In addition to weather-related disturbances, a link could be failed itself if all the fights operating in it are cancelled. The selection of the edge can be on a random basis or in descending order of weight (traffic) and bottleneck edge (high betweenness link) in the original network.

3.7.2 Measures for Robustness

To analyse the sensitivity of various failure strategies on the AAN, I primarily used two types of measures here: topological sensitivity and reachability.

There are several ways of measuring the topological sensitivity of networks. One key metric is the average geodesic path length L. As the number of removed nodes or edges is increased, the network will eventually break into disconnected sub-networks (sub-graphs). The average geodesic length (L), by definition, becomes infinity for such a disconnected graph, and it is wise instead to study the average inverse geodesic length,

$$l^{-1} = \frac{1}{n(n-1)} \sum_{i \epsilon V} \sum_{i \neq j} d_{ij}$$

which is a finite quantity even for a disconnected graph since $\frac{1}{d_{ij}} = 0$ when there is no path connecting i and j.

Since subsequent node or link failures might fragment the network, the number of non-overlapping sub-graphs and the size of the largest connected sub-graph (giant component) are two important quantities for measuring the sensitivity of the network. In this chapter, the number of sub-graphs and size of the giant component are represented as N_c and S, respectively. In order to quantify the effect of any node or link failures, the values of average inverse geodesic length, number of sub-graphs and giant component are normalised by the corresponding values of initial or original network and are represented as $\widetilde{l^{-1}}$, $\widetilde{N_c}$ and $\widetilde{S}$, respectively.

If a node or a link fails in a directed network, it raises the question of whether the network is fully reachable or not. That is to say, starting from any node, is it possible to reach any other node in the network or not? In order to assess the reachability of the AAN, I calculate the probability of the connectivity between any pair of nodes (i, j) in the network, which is represented as R. The reachability of a node R_i is calculated using the following equation:

$$R_i = \frac{\textit{number of nodes reachable from node } i}{n - 1} \tag{3.1}$$

Where n is the total number of nodes in the network. The reachability R of the overall network is defined as the average of all R_i. A fully reachable network R achieves 1 and a case of an isolated network with no physical connection (links) between the nodes R is always 0.

3.7.3 Tolerance to Vertex Failure

Tolerance to errors (or random failures) is understood as the ability of the system to its structural properties after random deletion of a fraction of its nodes or links. At first, I simulated the failure vulnerability of the AAN under a fraction of node failure f_v randomly and according to the rank of degree k_i, node betweenness $B_v(i)$ and strength s_i.

Figure 3.9(a) illustrates the effect of the removal of nodes on the fragmentation of the network. Within the range of 50% node failure (remove), the number of sub-graphs (N_c) increases more rapidly in the case of centrality-based failure. In this measure, the degree- and betweenness-based failure strategies bring the most significant fragmentation effect to the network. Whereas, the random node failure N_c/n increases almost linearly.

As illustrated in Figure 3.9(b), the removal of only 10% of highly connected or high-betweenness nodes the size of the gain component (largest sub-graph) reduces abruptly to 20% of the original AAN. Similar behaviour also is found in

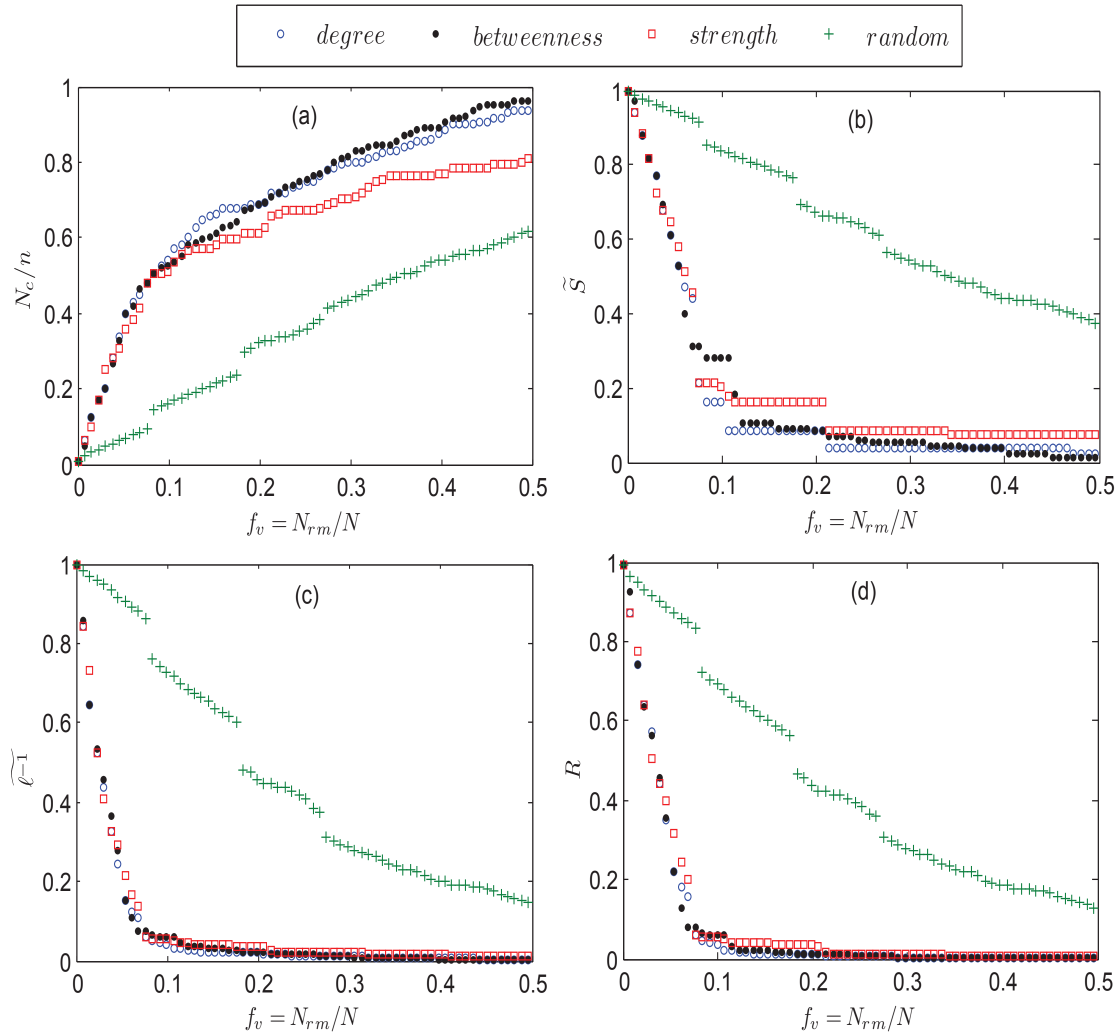

FIGURE 3.9: Comparison of AAN robustness against centrality based node failure and random node failure. The vulnerability is measured by: (a)the number of sub-graphs(N_c), and normalised by the initial size of the network; (b) the average inverse geodesic distance $\widetilde{\ell^{-1}}$; (c) the relative size of the largest connected sub-graph (giant component) $\widetilde{S}$ and; (d) the network reachability R.

the strength-based failure. After removing 50% of nodes, the network almost becomes fragmented at that point, hence the size of the largest sub-graph becomes too small and, as a consequence, the network loses its functionality. However, for random node failure, the relative number of sub-graphs N_c/n and the size of the giant component $\widetilde{S}$ changes linearly with f_v, which means that random node failure has almost no effect on the network fragmentation.

Whereas, if I look at the network efficiency measured by the average inverse geodesic distance l^{-1} as well as the network reachability R, all of these metrics have almost identical behaviour against any method of node failure. For the centrality-based failures (degree and betweenness), the network efficiency drops abruptly at the beginning of the process. The values of $\widetilde{l^{-1}}$ and R drop to almost zero just after 10% of highly central node breakdown. This means that, after removing a small number of hubs or central nodes from the network, the probability of connecting a pair of nodes becomes very low, hence increasing the geodesic distance between them. At this point, the network loses its functionality in terms of passenger mobility.

On the other hand, in the case of random failure, the network seems highly robust, and the network is considerably resilient in terms of connectivity, as the graphs shows in Figures 3.9(c) and 3.9(d). Figure 3.9 demonstrates that the removal of a small proportion of highly connected nodes or highly central nodes produces catastrophic changes in the network. This shows that the AAN is very vulnerable under the targeted failure of its central nodes compared to random unintentional node malfunctioning.

3.7.4 Critical Node Identification

As in many complex systems, it is important to identify which is the most critical node in terms of the network functionality. Using comparison of the vulnerability

Table 3.8: Node importance in terms of robustness measures.

Airport	Network Features			robustness Measures				
	k_i	s_i	$C_B(i)$	N_c	$\Delta L\%$	$\Delta \widetilde{l^{-1}}\%$	$\Delta \widetilde{D}\%$	$\Delta \widetilde{R}\%$
Sydney	**99**	**114052**	0.294	8	7.13	**15.90**	14.29	11.92
Brisbane	81	72199	**0.3118**	4	**17.18**	14.12	**100**	6.79
Melbourne	66	85033	0.1172	3	1.33	4.77	0	3.05
Perth	57	33345	0.1785	5	6	10.81	14.29	9
Adelaide	47	35242	0.1475	9	11.54	11.77	0	11.93
Cairns	46	18289	0.1846	6	10.02	13.28	28.57	**12.62**
Darwin	41	9585	0.141	7	11.86	11.4	0	11.89
Townsville	29	10450	0.0621	2	0.05	2.68	0	1.53
Gold Coast	25	16513	0.0199	2	1.13	2.03	0	1.53
Canberra	24	21681	0.0087	2	1.16	2	0	1.53
Broome	21	2824	0.0116	2	1.18	1.96	0	1.53
Avalon	20	3463	0.0196	2	0.86	2.13	0	1.53
Alice Springs	19	3159	0.0029	2	1.14	2	0	1.53
Mount Isa	18	2530	0.0949	2	3.69	3.55	42.86	1.53
Launceston	16	5535	0.0333	3	2.54	3.33	0	3.05
Newcastle	16	7588	0.0013	2	1.32	1.76	0	1.53
Karratha	15	3912	0.0044	2	1.27	1.82	0	1.53
Mackay	14	6684	0.0016	2	1.29	1.78	0	1.53
Rockhampton	14	5759	0.0016	2	1.29	1.78	0	1.53
Geraldton	14	1563	0.0008	2	1.54	1.52	0	1.53
Port Hedland	12	2424	0.0018	2	1.33	1.73	0	1.53
Learmonth	12	629	0.0003	2	1.55	1.5	0	1.53
Kalgoorlie-Boulder	10	1447	0.0018	2	1.38	1.7	0	1.53
Hobart	10	7100	0	2	1.33	1.72	0	1.53

approaches by progressive node failure, it is difficult to determine which node, if failed, would be most damaging both in terms of topological sensitivity and re-routing cost. That said, alternative methods, particularly a node-by-node failure approach and the sensitivity of the topological and the reachability measure, do provide a better summary measure of node criticality or importance. To measure the sensitivity of a node, I measure the topological properties by removing the node from the network then comparing the measures of the metrics with their corresponding values of the original AAN.

Table 3.8 shows the importance of a particular airport failure and its impact on the topological features and robustness metrics. For each of the measures, the bold text represents the highest value in the corresponding metric. From Table 3.8, I have found that Sydney is the most connected airport in the network and also handles the highest amount of traffic as it has highest value of strength. In terms of the sensitivity, if it is removed from the network, it will increase 7.13% and 14.29% of the characteristics path length and the network diameter, respectively. However, the failure of Sydney will drop the efficiency of the network by almost 16% efficiency, which is measured by the average inverse path length.

In the case of Brisbane, it is the second highest in terms of connectivity and is the most central node in the network (highest betweenness value). It serves as an important bridge in the network, with the result that, if it breaks down, it will increase the diameter to twice ($\Delta\widetilde{D} = 100\%$) its original size. In particular, it requires 14 hops to reach Birdsville from Taree or vice versa, which requires only seven hops if Brisbane is connected. So removing Brisbane from the network will significantly slow down the physical movement of passengers and goods across the AAN. From the high betweenness value and the effect of an increase in the diameter of Brisbane, it is clear that, if I want of protect or break down the flow of any material or disease, Brisbane would be the first place to stop it. If I look at the sensitivity of Melbourne, it is found to be in the less sensitive group and has an impact on the diameter of the network. If I look at the reachability measure, only the top seven connected airports have a significant impact on this and Cairns is found to be the most sensitive in this case.

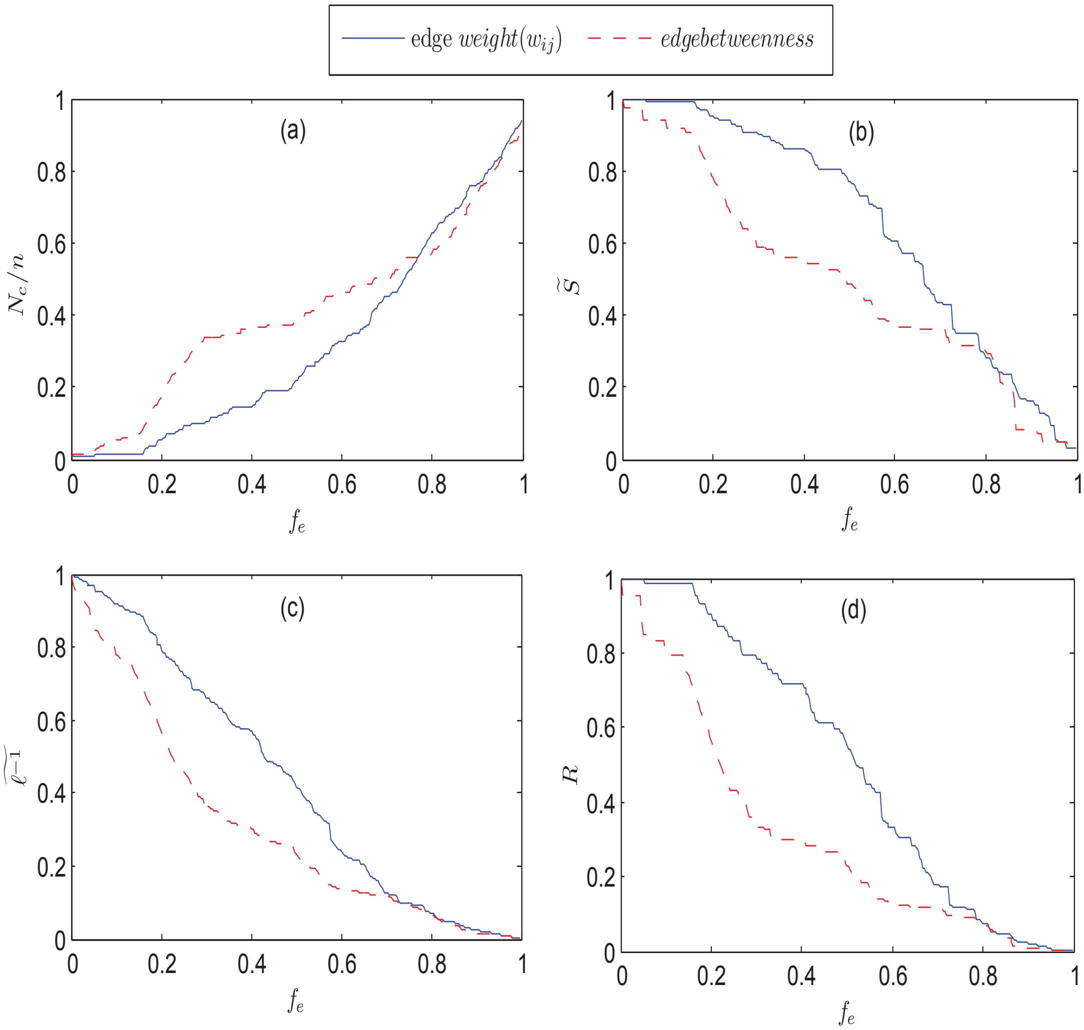

FIGURE 3.10: Comparison of AAN robustness against the most weighted link closure and the bottleneck link closure. The vulnerability measure is the same as in Figure 3.9

3.7.5 Tolerance to Link Failure

Apart from the node failure (airport shutdown), I examined the vulnerability of the AAN, subject to various types of edge failure strategy. Figure 3.10 displays the results for the robustness or the vulnerability to edge failure according to the descending order of weights (number of traffic) and edge betweenness (edge-bottleneck). When the edges are removed, the total number of nodes n does not change, making $\widetilde{\ell^{-1}}$ a monotonically decreasing function with the fraction of removed edges f_e.

From Figure 3.10(a) and (b), it is observable that the network remains connected until 20% of its highly weighted links have been removed. But this is not true in the case of the removed bottleneck edge. However, the number of sub-graphs increases monotonically with the number of edge failures. It can be inferred from Figures 3.10(a) and (b) that the most traffic carried links are not the most bottlenecked in the network. However, for all of the measures (topological sensitivity and reachability), the removed bottleneck link has much more effect compared to the high weight link, which suggests that the edge betweenness is a more suitable quantity than the weight to measure the importance of an edge (link). The highest difference in all four measures between the two edge failure strategies has been observed in the range from $f_e = 0.25$ to $f_e = 0.5$. After 80% of edges are removed, the measure becomes identical for both edge failure strategies. In the case of the removed bottleneck edge, the reachability R drops sharply to almost 30% of its original network after a fraction of $f_e = 0.25$ edges are removed.

In a summary of the analysis presented in this section, it is noticeable from Figures 3.9 and 3.10 that, in the case of vertex failure (both degree-based and betweenness-based) $\widetilde{S}$, $\widetilde{\ell^{-1}}$ and R decrease sharply in contrast to edge failure. Due to the hub and spoke nature of the network, the high-connected node failure is the most destructive in all of the robustness measures. However, because of the heterogeneity of the weights associated with its edges, the network is fairly robust to edge failure though vulnerable to high-degree nodes failure.

3.8 Chapter Summary

In this chapter, the topological features and robustness of the Australian airport network have been analysed from the complex network theory point of view. The AAN has been constructed by associating a node to each airport and a link to each direct connecting passenger flight operating between different airports using real air traffic data for a period of one year (2011). The topological properties of the AAN confirmed the small-world characteristics such as the airport network of the world and other countries such as the US, India and Italy. Its degree distribution is best described by a power-law function, which indicates the presence of nodes of high degree (called hubs), particularly the big three airports (Sydney, Brisbane and Melbourne). The traffic of the AAN is found to be accumulated on an interconnected group of high-degree nodes. It has a disassortative mixing similar to the US and China, i.e. hubs of the network are surrounded by low-degree neighbours. It reveals that the most central nodes are not always the most critical.

The analysis also provides valuable information about the characteristics of the network and the level of vulnerability that it can be exposed to given a random, most central node and a link failure. The study on the response of the AAN subject to different node and edge failure scenarios shows that the network is comparatively robust on edge or air route shutdown but very sensitive (less robust) to central node failure, especially high-degree and high-betweenness nodes. However, due to the limitation of actual passenger movements, the effect on passenger movement due to a node or link failure is omitted.

Overall, this study offers significant insights that can help planners in their task to design the systems of tomorrow, and similar undertakings can easily be imagined in other urban infrastructure systems (e.g. electricity grids, water/ wastewater systems, etc.) to develop more sustainable networks.

Chapter 4

Airport Network Flow Capacity Estimation

This chapter is partially based on the following publication:

- Murad Hossain, Sameer Alam and Hussein Abbass, *A Dynamic Multi-Commodity Flow Optimization Algorithm for Estimating Airport Network Capacity.* Proceedings of 4th ENRI International Workshop on ATM/CNS, (EIWAC 2015), Tokyo, Japan.

In the previous chapter, I modelled and analysed an airport network using complex network tools. In this chapter, I propose a model and methodology to estimate the capacity of an airport network. More specifically, this chapter addresses the following research question: *How can the flow capacity of an airport network be estimated?*

The model proposed in this chapter is based on the multi-commodity flow problem and considers the wake vortex separations during landing and take-off. The underlying premise is that flow in an airport network can be modelled as a multi-path, steady-state network of queues, the maximum capacity of which is the sum of maximum airport operational rates. In my formulation, flow between two nodes (airports) is considered as different commodities and the local airport capacity is formulated using a time slot of one hour where the hourly rate of flow (landings and take-offs) is bound by a capacity constraint.

4.1 Introduction

There is growing concern among airlines and policy analysts that the air transportation system is running out of capacity [66, 162]. A few attempts have been made to estimate the total capacity of an entire air transportation system for a given region or country [66, 67]. The capacity of flow networks indicates the maximum attainable throughput without jamming or congestion. A good network capacity estimation model would enable us to predict how much additional demand can be accommodated by a network and, hence, establish an efficient policy for traffic restraint and growth. Furthermore, it can enable us to determine what educative steps should be taken to prepare for the time when additional capacity will be required to accommodate future growth.

Capacity estimation of an airport network is generally known as one of the most difficult problems in air transportation. In an airport network, capacity has traditionally been measured at individual elements of the network, such as links (city-pairs) and nodes (terminals and runway throughput). These measures obviously do not constitute the overall system-level airport network capacity. Conventionally, in traffic flow networks, the maximum flow capacity is estimated using a multi-commodity flow (MCF) model [46, 49]. This method is not directly applicable to an airport network, where capacity modelling characteristics are quite different for the following reasons: (a) the movement in a transportation network involves flows of aircraft with different speeds; (b) flow is heterogeneous given different wake vortices categories of aircraft, viz. light, medium and heavy; (c) different types of aircraft require different amounts of resources at landing and departure airports; (d) there must be a minimum separation distance between two consecutive aircraft, which depends on the type of operation (landing or take-off) and the preceding aircraft type and operation for managing wake vortices; (e) aircraft departing from an airport are expected to land at destination airports within a time frame, because aircraft cannot hold in the air for long time, which will increase the amount of delay; (f) multiple origin-destination (OD) pairs exist and the flow between different OD pairs is not exchangeable or substitutable in an airport network capacity problem. These characteristics make the modelling of airport network capacity a complex, yet interesting, problem to solve.

4.2 Problem Formulation

The primary objective of an airport network capacity problem is to determine the maximum attainable flow (upper bound) that it can carry. The graph-based model developed in the previous chapter (Chapter 3) is applied to describe an airport network for its capacity problem formulation. The airport network ($G(V, E)$) is encoded using an adjacency matrix ($A_{n \times n}$) such that $a_{ij} = 1$ if a flight link exists between the airport-pair i and j, otherwise $a_{ij} = 0$. In such a network, an OD pair is defined as a pair of nodes that are directly connected by an edge. So, in an airport network, there are $m = |E|$ directly connected OD pairs. For each of the OD pairs, traffic in the form of aircraft enters the network through the origin node and travels along the link to the destination. In such a scenario, the problem is known as a multi-commodity flow problem, in which the traffic of individual OD pairs is considered as commodities and each of the commodities shares common node capacities at the end nodes. Conventionally, in communication and transportation networks, the maximum flow capacity is estimated using a multi-commodity flow model. This method is not directly applicable to an airport network, where the interaction among the different types of aircraft and the wake vortex separation among them bring extra non-linear constraints to the problem formulation.

To model an airport network capacity problem, it is necessary to know the individual airport (node) capacity. In air transportation, airport capacity is defined as the maximum hourly aircraft movements in the network per hour [27]. So, the question is, how can I define an individual airport capacity? One may argue that, from the historical traffic data, it is possible to estimate the true capacity of an airport or runway. However, the true capacity of a runway depends on many factor such as the operating conditions, the weather and, more importantly, the mixing of different wake vortices of aircraft classes. The specific characteristics of aircraft operating in an airport is an important factor to determine its capacity. Under stable conditions (either IMC or VMC), an airport capacity heavily depends on the traffic mix. Traffic mixes consisting of the aircraft possessing different weights and speeds require different rules (minima) to separate specific aircraft while landing and taking-off, which is usually known as the wake vortex separation minimum. In early 2000, EUROCONTROL started researching time-based separation (TBS), a new operating procedure for separating aircraft by time during strong headwind conditions to avoid wake vortex, instead of distance. TBS addresses headwind disruptions by reducing the spacing between pairs of aircraft [163]. In this study, I have used a time-based separation minimum to avoid the wake-vortex turbulence, which is given in the following tables 4.1 (Table 4.1 is just an example extracted from the report (P 070/2010) published by NATS Ltd., UK Aeronautical Information Service [164]).

A runway with identical operating conditions may result in different capacity/throughput only for the difference in sequencing them. Thus, it is better to consider the local capacity of an airport as the total available slots for landing and take-off. In my formulation, I assume the airport capacity upper bound as a total number of slots, where each slot has equal time duration. In other words, I define a node capacity upper bound as the total available time. Since, my intention is to measure the hourly flow capacity of an airport network, I define the node capacity

TABLE 4.1: Separation minima (in minutes) between aircraft considered in this chapter

Separation minima (arrival - departure)			
Leading Aircraft	Trailing aircraft		
	L	M	H
L	2	2	2
M	2	2	2
H	2	2	3
Separation minima (departure - arrival)			
Leading Aircraft	Trailing aircraft		
	L	M	H
L	2	2	2
M	2	2	2
H	2	2	3
Separation minima (arrival - arrival or departure-departure)			
Leading Aircraft	Trailing aircraft		
	L	M	H
L	2	2	2
M	3	2	3
H	3	2	3

$C(i) = 60$ slots for all the nodes in the network where each slot has a one-minute duration and one of the key assumptions of the proposed model is that all of the airports have single runways.

Before going to mode the capacity problem of an airport network, let us define a commodity. A commodity in an airport network is the flow from a node to one of its neighbour nodes. Since in a network there are $m = |E|$ directly connected OD pairs, so the total number of commodities will be $K = 2 \times m$. Let $\phi(F_i^+(t), F_i^-(t), S)$ define a slot assignment function that returns the minimum time required to accommodate the inflow $F_i^+(t)$ and outflow $F_i^-(t)$ at a node i during an hourly interval t given the separation matrix S. The separation matrix S has four dimensions: leading aircraft type, trailing aircraft type, leading aircraft operation and trailing aircraft operation. For example, $S[L][M][A][D]$ define the separation distance in minutes between a light aircraft landing at a node followed by a departure of medium aircraft. With the help of the function $\phi()$ and separation matrix S, I can define the departure-arrival constraints as $\phi\left(F_i^+(t), F_i^-(t), S\right) \leq C(i), \forall i$. In an airport network, an aircraft departing from an airport is expected to land at a destination airport within a time frame, which I have called travel time. This travel time introduces a time dimension into the problem formulation. I have called this constrain the timing constraint. Let t_{ij} denote the required travel time for a flight from airport i to j. I also assume that the travel times for all types of aircraft are equal. Let $TD(f)$ and $TA(f)$ denote the time of departure (take-off) and time of arrival (landing) of a flight $f \in F_i^{k-}(t)$ from node i to j, where $k \in K$ denotes the commodity from node i to j and the minus symbol '$-$'means an outflow from node i. Then, the timing constraints are defined as $TA(f) = TD(f) + t_{ij}, \forall f \in F_i^{k-}(t)$. This timing constraint make the problem very hard to solve. In a real traffic scenario, there is a common practice to associate some delay to a flight to land at the destination airport for capacity improvement and to maintain separation safety. I can modify the timing constraint as $TA(f) = TD(f) + t_{ij} + d_f, \forall f \in F_i^{k-}(t)$, where d_f represents the delay of flight f and its value is bound by $0 \leq d_f \leq 15\ minutes$. The delay variable d_f brings some flexibility to the timing constraints and helps to find a better feasible solution for an optimisation method.

Key assumption: The key assumptions of the proposed model of the airport network capacity problem are as follows:

All the airports have only single runways that share both the departure and arrival operations

The maximum arrival delay $\leq d_f$ is bound by $0 \leq d_f \leq 15\ minutes$

The local capacity ($C(i)$ of an airport (node) is considered as the hourly available slots, more specifically considered as $C(i) = 60$ slots

In the model formulation, the connection flight constraints are not taken into account

Notation: The formulation of an airport network capacity problem requires definition of the following notations.

t = a positive integer that represents the hour of operation

K = set of commodity

For each $k \in K$

s^k = source/origin node of commodity k

d^k = destination node of commodity k

$F_i^{k+}(t)$ = inflow of commodity k of node i during operation hour t, which is a set of arrival flights

$F_i^{k-}(t)$ = outflow of commodity k of node i during operation hour t, which is a set of departure flights

$F_i^{+}(t) = \sum_k F_i^{k+}(t)$, total inflow of node i operation hour t

$F_i^{-}(t) = \sum_k F_i^{k-}(t)$, total outflow of node i operation hour t

Let f denote a flight that is schedule to operate during a day. Then

$D(f)$ = departure/source airport of f

$A(f)$ = arrival/destination airport of f

$TD(f)$ = schedule time of departure of f from $D(f)$

$TA(f)$ = schedule time of arrival of f at $A(f)$

$wv_f \in \{L, M, H\}$ = wake vortex class of f, where L, M and H represent the light, medium and heavy aircraft, respectively

$Op(f) \in \{A, D\}$ = arrival (landing) and departure (take-off) operation of f

$S(a, b, c, d)$ = separation distance in time between the leading and trailing aircraft, where a and b represent the type of leading and trailing aircraft and c and d represent the take-off or landing of the respective flight

d_f = delay of f at $A(f)$

t_{ij} = required travel time for a flight from airport i to j

The airport network capacity model can be formulated as follows:

$$maximize : \sum_k \sum_i F_i^{k-}(t) \tag{4.1}$$

Subject to,

$$TA(f) = TD(f) + t_{ij} + d_f, \quad \forall(i, j, k) \tag{4.2}$$

$$\phi(F_i^+(t), F_i^-(t), S) \leq C(i), \quad \forall i \tag{4.3}$$

$$F_i^{k+}(t) \geq 0 \forall(i, k) \tag{4.4}$$

$$F_i^{k-}(t) \geq 0 \forall(i, k) \tag{4.5}$$

$$\sum_t \sum_k \sum_i F_i^{k-}(t) = \sum_t \sum_k \sum_i F_i^{k+}(t), \quad \forall(i, k, t) \tag{4.6}$$

where, $TD(f), TA(f)$ denote the departure and arrival time of a flight $f \in F_i^(k-)(t)$ from node i to j, $F_i^+(t) = \sum_k F_i^{k+}(t), \quad \forall i$, and $F_i^-(t) = \sum_k F_i^{k-}(t), \quad \forall i$.

4.3 Proposed Heuristic Solution Approach

To solve the proposed airport network capacity model, a heuristic approach is developed in which a certain amount of flow is incrementally added to an initial feasible solution until the network reaches its capacity. The heuristic solution approach consists of two key modules: (i) an initial feasible solution generation; and (ii) an iterative solution improvement method to increase the traffic flow in the network subject to node capacity and departure-arrival timing constraints.

Algorithm 1 Initial Feasible Solution Generation

```
procedure FEASIBLE SOLUTION(r_i(k), KG(V, E))
    K set of commodities
    G(V, E) is an airport network having n nodes
    r_i(k) amount of shared resources of node i assigned to commodity k.
    set ur_i(k) := 0 ∀i, ∀k)
    while (all K commodities have not being initialized) do
        k ← randomly selected un-initialize commodity
        i = s^k
        j = d^k
        while ur_i(k) < r_i(k) & ur_j(k) < r_j(k) do
            Let f represent a flight, then wv_f ← rand(L, M, H)
            for all (available slots in SB(i, t)) do
                randomly select a slot l from SB(i, t)
                find out preceding flight f_p and succeeding flight f_s of slot l at node i
                l_p ←slot index of f_p
                l_s ←slot index of f_s
                if (l_p−l) ≥ S[f_p, f, op(f_p), op(f)] & (l−l_s) ≥ S[f, f_s, op(f), op(f_s)] then
                    TD(f) := t × 60 + l
                    if ( slot q available for landing at j & d_f ≤ 15) then
                        TD(f) := t × 60 + l
                        TA(f) := TD(f) + t_{i,j} + d_f
                        update SB(i, t′), SB(j, t′) for all operational hours t′ ≥ t
                        update ur_i(k)
                        update ur_j(k)
                        break loop for all

                    end if
                else
                    changed l to next available one and continue
                end if


            end loop

        end while
        marked commodity k as initialized

    end while
    return initial feasible solution
```

4.3.1 Initial Feasible Solution Generation

In an airport network capacity estimation problem, the departure-arrival timing constraint eq.(4.2) (all departure flights from a node must land at the destination at a specific time within a maximum delay of 15 minutes) and the separation minima between two aircraft at a node makes it very difficult for a random initial solution to be feasible. In order to generate an initial feasible solution, I divide a one-hour time window into 60 equal slots. I call these 60 slots together 'Slot box'and represent this as SB. Each SB has a unique identification number for each airport to represent an hour of operation. For example, a *SB(i,5)* represents the flow (both departure and arrival) of node i during the operational hour of 5:00 am. To simulate a full day of operation in a network, I need 24 SBs for each node. The flow of a commodity consisting of light, medium and heavy aircraft is placed in the slots of the source and destination node such that the separation between two consecutive flights is maintained and all of the departed aircraft can land at the corresponding destinations within a maximum delay of 15 minutes. Once an aircraft is inserted into an SB of the departure and the landing node, it is copied to all succeeding slot-boxes of those nodes. For example, if a light aircraft is placed in the fifth slot of SB(i,1) for departure and the fifth slot of SB(j,2) as an arrival flight, then all operation hours $t \geq 1$ at node i must have a departure flight at the fifth slot, and node j for all operation hours $t \geq 2$ must also have an arrival at the fifth slot. This means that I consider a continuous deterministic flow, which is a common practice to determine the capacity upper bound of a network [147, 190].

I also assume that the resources of a node are shared equally by its commodities. That is, the hourly resources of 60 slots of a node are shared equally by the commodities associated with its links. If $r_i(k)$ represents the amount of shared resources of node i assigned to commodity k, then the following condition holds for all nodes.

$$C(i) = \sum_k r_i(k), \forall i \tag{4.7}$$

The initial feasible solution is generated using the algorithm 1, which required a random initialisation of the resource sharing variables $r_i(k), \forall i, k$, and the network $G(V, E)$ (a flow chart of the initial feasible solution generation algorithm 1 is also presented in Appendix A, Figure 9.11).

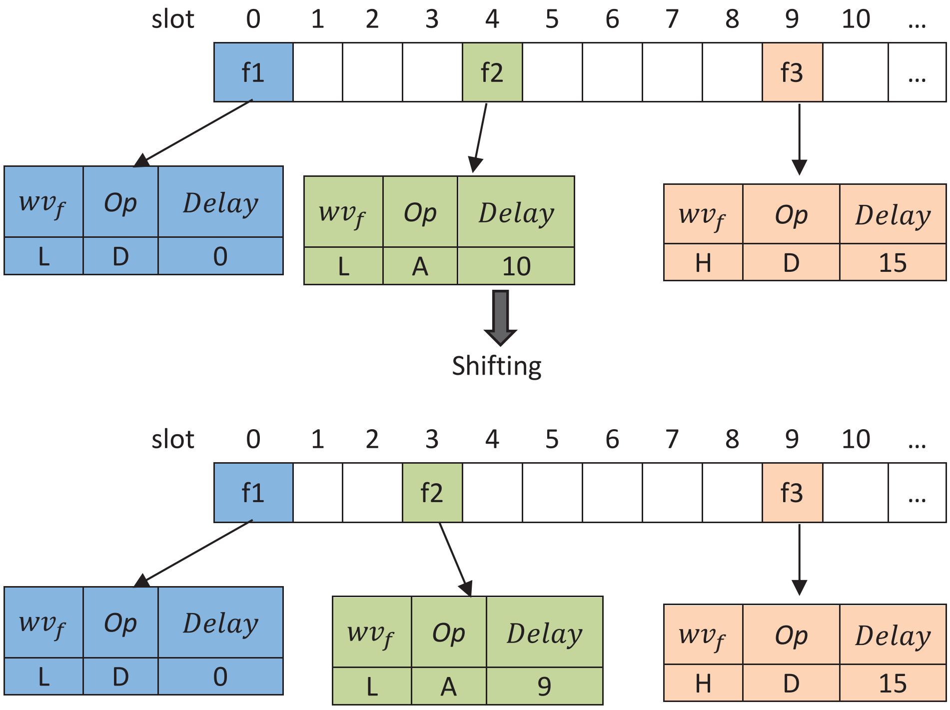

FIGURE 4.1: An illustration of shifting operation in a SB.

4.3.2 Iterative Solution Improvement

After generating an initial feasible solution, the network capacity can be obtained using an iterative solution improvement process, which consists of the following key modules that increase the number of hourly aircraft movements.

4.3.2.1 Shifting

Shifting is an operation to move a flight from its current slot to an earlier slot such that (i) the separation minima between its adjacent flights are maintained and (ii) the delay of the flight remains within the bounds of 0 to 15 minutes. Figure 4.1 shows an example of the shifting operation of a slot-box. In the illustration of a shifting operation in Figure 4.1, the flight $f2$ is shifted to slot 3, which decreases its delay to 9 minutes and the separation distance between f1 and f2 satisfy the minimum requirement of 2 minutes for a light-light departure-arrival. Whereas, flight f3, which is a departing from slot 9, cannot shift to an earlier slot because it will increase its delay beyond the maximum limit of 15 minutes.

4.3.2.2 Swapping

Swapping is an operation to change the sequence of the flights in an SB. Swapping is considered as a hill-climbing operation to improve the quality of the solution, which basically changes the slot of two flights at a time and continues the process until no further improvement is possible, maintaining separation minima and the travel time constraint. Figure 4.2 shows an example of the swapping operation

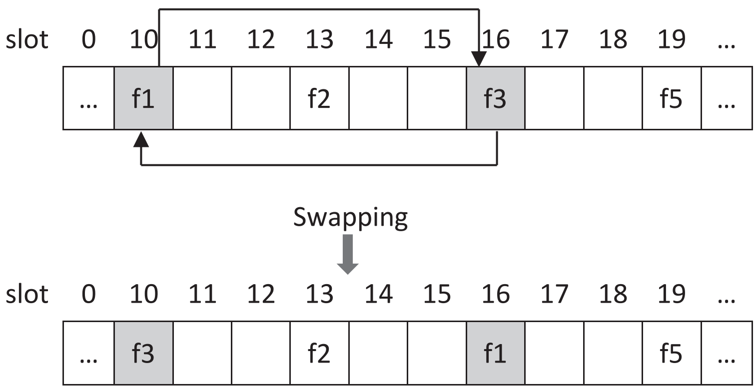

Figure 4.2: An example of swapping operation.

between flights f1 and f3. The purpose of the swapping operation is to make some free slot(s) so that one or more flights can be shifted to an earlier slot. In some cases, a swapping can increase delay and so I maintain all the constraints and allow swapping between two flights if, and only if, the new sequence does not violate any constraint.

4.3.2.3 Inserting

In an initial feasible solution, the operations of swapping and shifting may create free slots where I can insert new flight(s). A new flight is inserted into SBs of source and destination nodes that fulfil the following conditions: (a) at the source node there is enough room between two flights or at the end or beginning of it such that it maintains the separation minima with the adjacent flights; (b) for any neighbours ($j \in Ng(i)$) of the source, if there is also a slot q available for landing that meets the separation minima and satisfies the timing constraint eq.(4.2). The type of the newly inserted aircraft is selected randomly. If the new flight cannot be added to the network due to separation minima and because its type is not a light aircraft then in such a scenario we try to insert a light aircraft. If no light aircraft can be added at a node i as source, then it confirms that there is no room at the slot-box of node i to accommodate extra flow.

After applying the swapping, shifting and inserting operations when no further improvement is possible for a given sequence (solution), the value of the function $\phi()$ (4.3) can be determined by simply calculating the time of the operation of the last flight in the sequence at a given node. Based on the swapping, shifting and inserting operations, the quality of an initial feasible solution can be improved. The algorithm 2 illustrates the procedure to improve a feasible initial solution for the network capacity estimation problem.

Once the initial feasible solution is improved by the solution improvement algorithm 2, the hourly capacity of the network is calculated by counting the total

Algorithm 2 Solution Improvement (FS)

```
procedure SOLUTION IMPROVEMENT(FS, G(V, E), t)
    FS is an initial feasible solution for the network capacity problem
    G(V, E) is an airport network with n nodes and K commodities
    t is the earliest operation hours where the flow of G(V, E) reaches a steady state
    Ng(i) neighbour of node i
    isImprove = true
    while isImprove do
        isImprove = false
        i = 1
        while i < n do
            Repeat for all
            f_a ∈ SB(i, t) & f_b ∈ SB(i, t) | f_a ≠ f_b,
            if swap(f_a, f_b ) in SB(i, t) then
                perform shifting at node i
                for all j ∈ Ng(i)  do
                    if insert(f_new, i → j) of SB(i, t) then
                        isImprove = true
                    end if
                end loop
            end if
            i = i + 1
        end while
    end while
    return solution
```

number of flight movements in the solution, which is the capacity upper bound of the steady-state flow.

4.4 Experimental Setup

The overall experiments are divided into two major parts; in the first part, I illustrate the effectiveness and applicability of the proposed method on two different networks. In these test network, all of the nodes have a single runway. In my experiments, the operating conditions of the nodes do not change over time, i.e. the separation minima remain unchanged. In the second part, I demonstrate how the maximum hourly flow changes with the network size for different network topologies. Each of the network experiments is carried out 30 times with different seeds.

4.4.1 Test Networks

In order to assess the effectiveness of the proposed airport network capacity estimation model, I perform experiments for two different types of network. First, I apply the proposed procedure to a simple network given in Figure 4.3. Our first experimental network consists of three nodes and six directed links, which are shown in Figure 4.3. I named this network 'network-I'. Network-I is a weighted directed graph. The weight of a link represents the travel time between its start and end nodes.

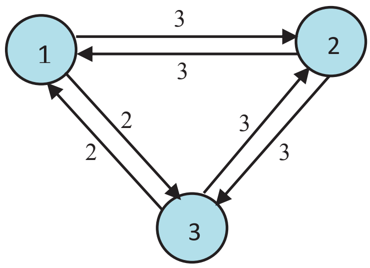

FIGURE 4.3: Example network-I, a fully connected network of three identical nodes.

Apart from the simple network shown in Figure 4.3, I also test the proposed model with a complicated network. Our second network is extracted from the AAN, which I have called 'network-II'. The AAN is a very large network and has many peripheral airports that carry out only a small amount of flights. These peripheral airports have almost no significant contribution to the overall network capacity, whereas the capacity bottleneck mainly lies on the big hub airports. For more detail about the AAN, readers are referred to the following paper [108]. Figure 4.4 shows the test Network-II is the network of Australian airports that operate more than five flights on a daily basis. In Figure 4.4, the size of a node is proportional to the number of its direct connections with other nodes in the network, which is known as the degree [36]. In this network, nodes 8 and 11 have a degree of 20 (10 in-degree and 10 out-degree), which is the highest in the network. Whereas, node

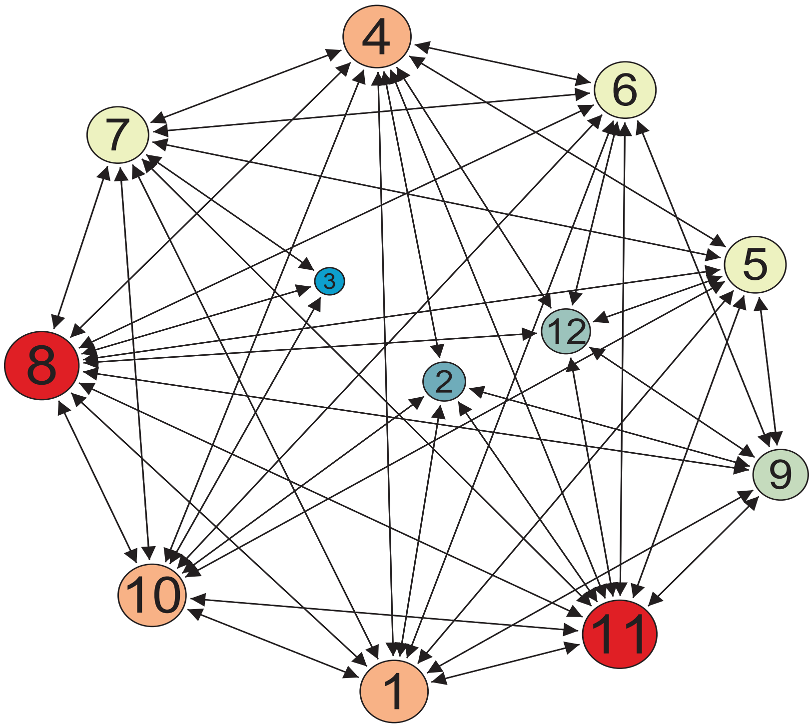

FIGURE 4.4: Example network-II, network of hub nodes of Australian airport network.

3 has the lowest degree of 6. In this network, the travel times of the links are set randomly between 1 hour and 4 hours.

4.5 Results and Analysis

I first present the hourly flow in Network-I over a period of 24 hours. As the objective of the capacity estimation is to find out the maximum attainable flow in an airport network, I find the departure sequences at the nodes that remain unchanged and achieve maximum steady-state flow.

At first, to get an insight into the efficiency of the proposed model, I measure the number of unused slots for every node in the network. The number of unused slots is calculated from the flight sequences in the SBs. It is the difference between the slot positions of consecutive flights and the minimum separation required between

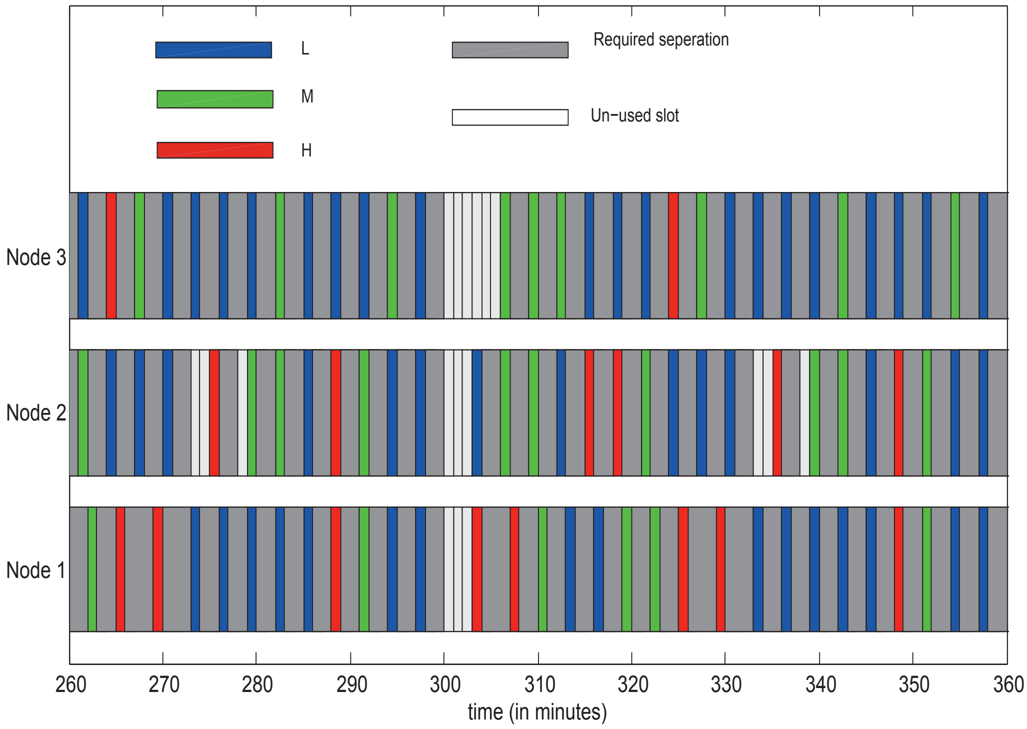

FIGURE 4.5: Status of the nodes in network-I during steady state.

them. For example, if two light aircraft are departing from slots 5 and 9, respectively, then the distance used by these two flights is four slots and the minimum separation required between them is two slots (since each slot is equivalent to one minute). So the number of unused slots in this case is two (four minus two). Figure 4.5 shows the status of the nodes in Network-I during a portion of steady state. Figure 4.5 shows that it is noticeable that there is not enough room between any two nodes to accommodate more flights.

Figure 4.6 shows the hourly departures and arrivals at Network-I. At the very first hour, there is no arrival in the network and as the time goes on the departed flights in the early hours start to arrive. After a certain number of hours, the number of arrivals reaches that of the departures and the flow become steady afterwards. If one can find the right departure sequence, then it is possible to get a maximum steady-state flow that is the capacity of the network. Flow in Network-I reaches a steady state from the 5th hour of operation.

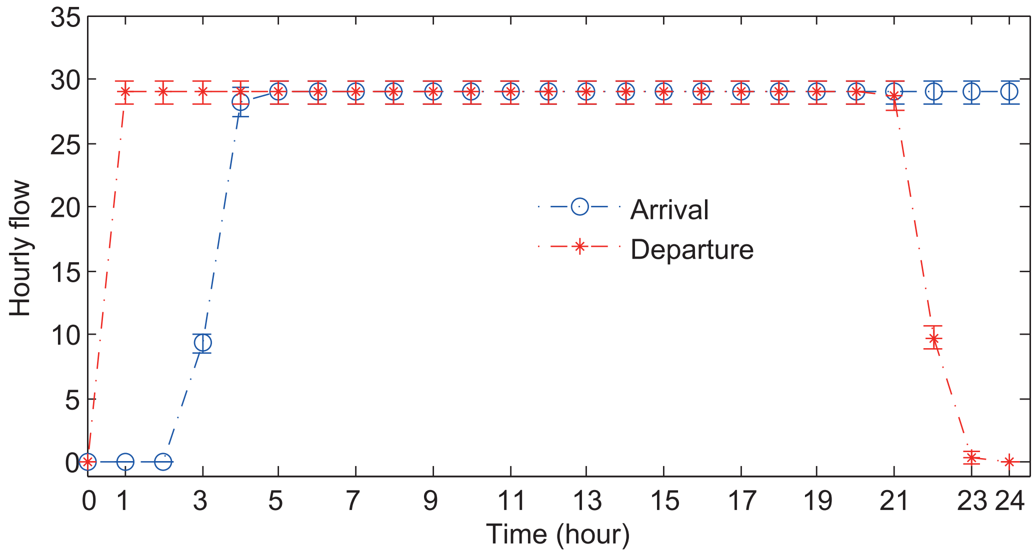

FIGURE 4.6: Hourly traffic flow for Network-I over a period of 24 hours.

TABLE 4.2: Hourly capacity of test networks (average of 30 different runs)

Network	Capacity	$\#L$	$\#M$	$\#H$
I	57.7 ± 1.34	38.7 ± 7.60	10.6 ± 4.01	8.4 ± 3.87
II	222.2 ± 21.04	111.7 ± 33.01	57.5 ± 20.22	53.0 ± 20.21

In a network, the total flow consists of a number of light, medium and heavy aircraft. To better investigate the capacity of a network, I calculate the actual number of light, medium and heavy aircraft. Table 4.2 summarises the capacity of the example networks and Figures 4.7 and 4.8 show the total flight movements thoughout a day of Network-I and Network-II, respectively. In Figures 4.7 and 4.8, it is noticeable that a number of light aircraft dominate in the hourly flow. This is because, during the insertion operation, in the situation in which heavy or medium cannot be inserted in the slot boxes (SBs) of the nodes then the chance is given to a light aircraft.

Tables 4.3 and 4.4 summarise the hourly uses of the nodes of Network-II and Network-I, respectively, during the steady state. From Tables 4.3 and 4.4, I can see that the airport's (nodes) slots are fully utilised, which is confirm by the number of un-used slots except from node-3 in network-II. This is because this

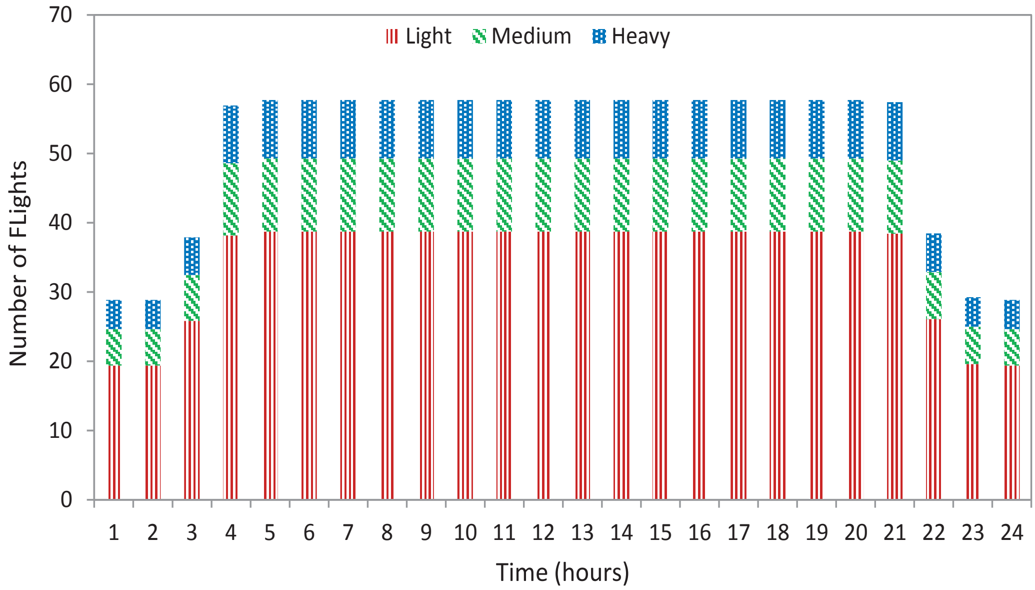

FIGURE 4.7: Hourly traffic of Network-I.

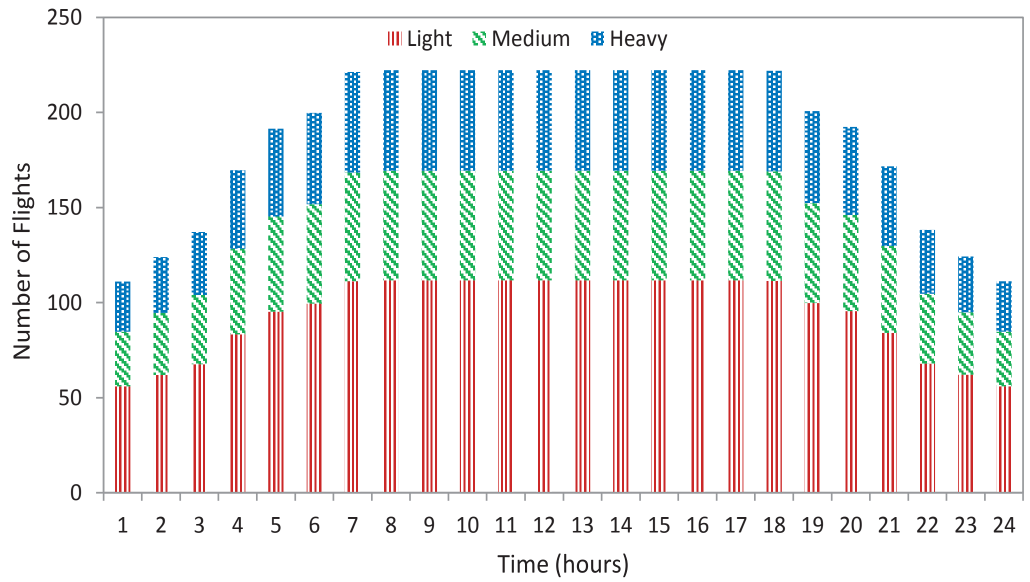

FIGURE 4.8: Hourly traffic of Network-II.

node has a very limited number of connections compared to the others in the network. Though it has some unused slots for departures, its neighbours have enough space for arrivals. As a result, some slots remain unused.

Apart from the details of flow, I also analyse the delay of the solution provided by the proposed method. Table 4.5 reports the delay associated with the flights in Network-I and Network-II over the simulation period of 12 hours. The average

Table 4.3: Summary of the node's hourly utilisation of Network-II at steady state

Node	Total Flow	#L	#M	#H	# un-used slots
1	19.25 ± 2.34	8.70 ± 3.28	5.60 ± 1.82	4.95 ± 1.67	1.15 ± 0.88
2	17.65 ± 1.69	11.35 ± 2.46	3.50 ± 1.67	2.80 ± 1.01	6.55 ± 3.70
3	14.8 ± 1.85	8.30 ± 1.90	3.50 ± 1.28	3.00 ± 1.30	14.15 ± 5.88
4	19.4 ± 3.20	8.40 ± 3.66	5.50 ± 2.48	5.50 ± 2.46	2.50 ± 1.80
5	18.95 ± 0.69	9.30 ± 2.18	5.45 ± 1.36	4.20 ± 1.91	2.05 ± 1.54
6	18.65 ± 0.99	9.15 ± 2.50	4.80 ± 1.32	4.70 ± 1.75	3.05 ± 2.50
7	18.8 ± 0.62	8.00 ± 2.13	6.00 ± 1.69	4.80 ± 1.61	2.15 ± 1.31
8	20.05 ± 3.20	9.20 ± 4.01	5.30 ± 1.69	5.55 ± 2.14	1.85 ± 1.39
9	19.65 ± 2.80	11.80 ± 3.37	3.90 ± 1.53	3.95 ± 1.28	3.05 ± 2.09
10	18.85 ± 1.04	7.90 ± 2.29	5.65 ± 2.23	5.30 ± 1.63	2.65 ± 1.90
11	18.9 ± 1.41	8.65 ± 2.60	5.00 ± 1.56	5.25 ± 1.86	2.60 ± 1.64
12	17.25 ± 1.21	10.95 ± 2.63	3.30 ± 1.59	3.00 ± 1.59	7.25 ± 3.54

Table 4.4: Summary of the node uses of Network-I

Node	Total Flow	#L	#M	#H	# un-used slots
1	19.35 ± 0.99	12.90 ± 2.89	3.50 ± 2.01	2.95 ± 1.19	2.35 ± 1.76
2	19.35 ± 0.87	12.60 ± 3.25	3.85 ± 1.53	2.90 ± 1.94	2.00 ± 1.65
3	19.00 ± 0.56	13.20 ± 2.48	3.25 ± 1.45	2.55 ± 1.54	2.65 ± 1.50

Table 4.5: Summary of delay

Network	Total Flight Movement	Delay(D) Per flight (minutes)	Number of flights delayed ($0 \leq D \leq 10$)	Number of flights delayed ($10 < D \leq 15$)
Network-I	615.55 ± 13.88	4.72 ± 1.13	271.6 ± 53.67	118.9 ± 56.31
Network-II	2271.15 ± 40.91	5.13 ± 0.44	912.1 ± 124.3	516.8 ± 99.87

delay per flight is found to be around 5 minutes for both networks, 4.72 and 5.13, to be exact, for example networks I and II, respectively, which is well accepted in a usual air transportation system. Of the total flights, only about 20% are delayed more than 10 minutes, whereas most have delays less than or equal to 10 minutes.

To investigate the flow capacity of different networks, I consider networks with

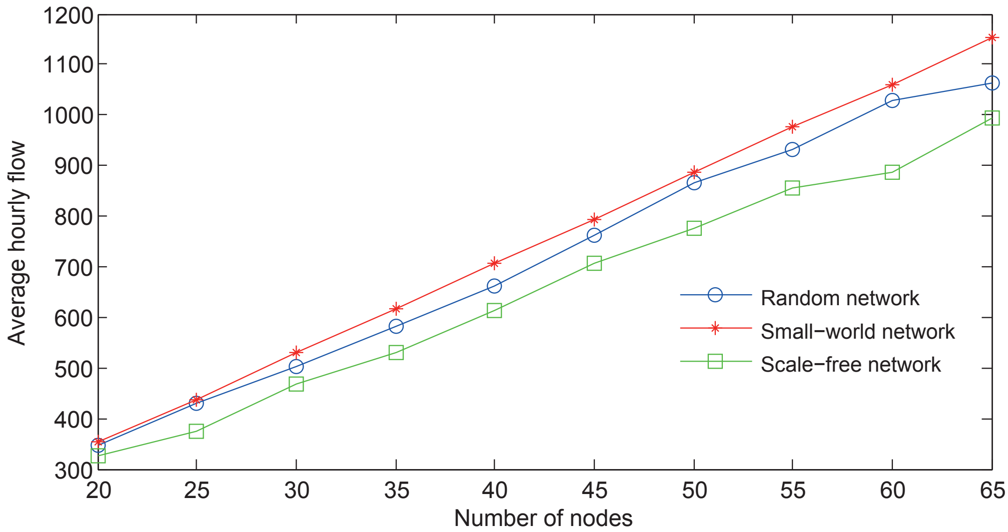

FIGURE 4.9: Estimated network capacity as a function of network size (number of nodes) with constant average degree.

(i) random, (ii) scale-free and (iii) small-world topologies. For each type of network topology, instances are generated using the methods described previously in Chapter 2. For this experiment, network instances are generated by varying the network size, starting from $N = 20$ to 65 nodes with increments of 5. To see how the network capacity varies with different topologies, I first keep the average degree constant and vary the number of nodes. Figure 4.9 shows that the average hourly flow capacity changes with the network size. From Figure 4.9, I can see that the network capacity increases linearly with the number of nodes in the network for all network topologies. Of the three network topologies, small-world (SW) has the highest flow capacity, whereas scale-free has the lowest when the average degree is kept constant at $\langle k \rangle = 6.0$. In the next analysis, I keep the number of nodes constant but change the average degree. Figure 4.10 shows the hourly flow changes with the network average degree for different network topologies with 50 nodes.

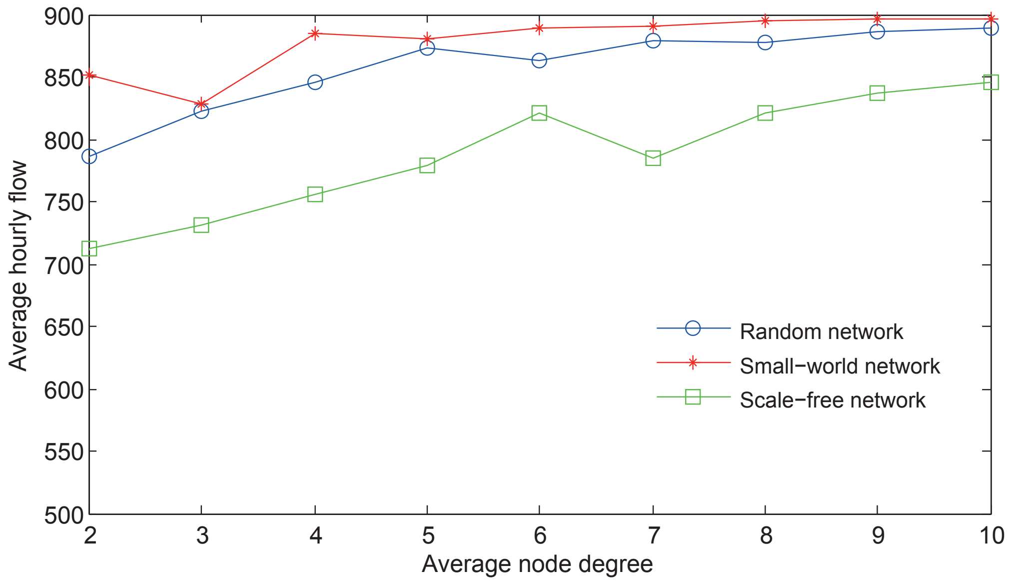

FIGURE 4.10: Estimated network capacity as a function of network average degree with constant network size.

4.6 Chapter Summary

In this chapter, I proposed a methodology to estimate the airport network capacity by modelling the problem as a multi-commodity flow problem. In my formulation, flows between two nodes (airports) were considered as different commodities and the local airport capacity was formulated using a time slot of one hour where the hourly rate of flow (landings and take-offs) was bound by a capacity constraint. A heuristic algorithm was designed to solve the network capacity model in which all flow constraints of air traffic were maintained. The proposed model and algorithm were applied to different test networks; the numerical results reveal that the proposed model is capable not only of estimating the network capacity under different levels of aircraft mix but also of identifying individual flows at different links and the amount of delay for each and every aircraft. In addition, the proposed model provides details of the flow (the actual number and mix of aircraft: light, medium and heavy) and a flight schedule (the departure and arrival of each flight). The experimental results show that an airport network with a small-world topology can accommodate the largest number of traffic compared to random and scale-free topologies with equal numbers of nodes and links.

Chapter 5

Airspace Network Modelling and Topological Analysis

This chapter is partially based on the following publications:

- Md Murad Hossain, Sameer Alam, Fergus Symon and Henk Blom, *A Complex Network Approach to Analyze the Effect of Intermediate Waypoints on Collision Risk Assessment*, International Journal of Engineering and Operations, Air Traffic Control Quarterly, Vol. 22, Number 2, pages 87-114, 2014.
- Fergus Symon, Sameer Alam, **Md Murad Hossain** and Henk Blom, *Airspace Network Characterization for Effect of Intermediate Waypoints on Collision Risk Assessment*, Proceedings of the 6th International Conference on Research in Air Transportation, ICRAT-2014, pages 1-8, Istanbul, Turkey (**Best paper award**).

In the previous two chapters, I have analysed the airport network and developed a model and methods to estimate its capacity. To analyse the relationship between airport network capacity and airspace safety, now I shift to analyse an airspace network. In this chapter, I propose two different models to analyse airspace as a network and relate its network features to estimate collision risk. The proposed airspace network models are characterised using several complex network indicators, which are then correlated with its collision risk.

5.1 Introduction

One of the key challenges faced by the Air Navigation Service Providers (ANSPs) is how to accommodate continued growth in air traffic while meeting the safety targets. ANSPs are exploring new paradigms (e.g. SESAR [4] and NextGen [3]) and procedures (e.g. reduced vertical separation minima [113]) for efficient and safe management of airspace. In the light of predicted traffic growth, maintaining safe separation among the aircraft in an airspace is considered its key limitation factor. One of the vital indicators for estimating air traffic safety is the airspace collision risk [74].

Although mid-air collision is a rare event, the impact is significant due to the large number of fatalities involved. The International Civil Aviation Organization (ICAO) standards separating aircraft in time and space have well served the purpose, until the surge in air traffic during the last decade. ANSPs are now compelled to relax these standards and adopt new procedures to accommodate increasing traffic [166]. There is also a compelling need for safety risk assessment of these new procedures [212].

Most of the collision risk estimation models are based on the Reich Model [193–195], which was developed in the early 1960s to estimate the collision risk for flights over the North Atlantic and to specify appropriate separation rules for the flight trajectories. However, there is no universal model for collision risk assessment due to the different communication, navigation and surveillance capabilities of ANSPs in different regions of the world.

EUROCONTROL uses a sophisticated collision risk model developed by Mathematical Drafting Group, which uses precision 4D radar data/ADS-B data to account for flights vectoring frequently in European airspace [73]. Whereas the African region (ARMA) and the Middle East region (MIDRMA) use the ICAO

Collision Risk Model [193–195] based on entry and exit flight plan data due to the presence of large volumes of procedural airspace and limited communication, navigation and surveillance (CNS) capabilities.

Measuring collision risk based on only the entry and exit flight plan data may lead to reasonable variations from the actual collision risk value. In particular, when an airway network structure is more complex, this may lead to significant variations in collision risk estimates between different Flight Information Regions (FIRs) of the world. One of the motivations of this chapter is how to model an airspace as a network and identify the features that can improve the collision risk estimates given the limited amount of flight data available in regions with limited CNS capabilities. Another research question that I attempt to address is how the collision risk estimate varies with network measures for airspace network complexity. This chapter addresses the abovementioned research questions.

The approach of this chapter is to adopt a complex network approach to model an airspace that can be related to its collision risk. I believe that modelling an airspace as a complex network is important for two reasons. It obviously helps us to characterise the networks based on the measurement of standard metrics of network topology (degree distribution, betweenness centrality, closeness centrality, clustering coefficient, etc.). Secondly, I believe that characterisation of airspace network features and their impact on collision risk estimates may guide the design or modification of airspaces in order to better control air traffic to reduce collision risk.

5.2 Modelling of an Airspace

An airspace is a complex system that is partitioned for a series of reasons, mainly to safely manage/control air traffic. The national airspace of a country is typically partitioned into air traffic control centres. Each of the traffic control centres is also partitioned into sectors, which is the smallest unit of control, being under the direct supervision of air traffic controllers. Finally, inside the sector, a set of navigational waypoints constitutes a grid-like structure where the flight move. The position of a waypoint is defined by a latitude and a longitude, but not an altitude.

There are several airspace analysis models and tools that provide some capability to quantify airspace complexity such as traffic density [139], conflict potential [205] and collision risk [135]. Airspace complexity depends on both structural and flow characteristics of the airspace. The structural characteristics are fixed for a sector/centre and they depend on the spatial and physical attributes of the sector such as terrain, number of airways, airway crossings and navigation aids. On the other hand, the flow characteristics vary as a function of time and depend on features such as the number of aircraft, mix of aircraft, weather, separation between aircraft, closing rates, aircraft speeds and flow restrictions. These characteristics (both structural and flow) of an airspace make it very challenging to model an airspace or NAS operations for collision risk. In general, the collision risk of an airspace depends on the nature of conflict paths, sector density and intervention rules used by ATCs to separate air traffic. It has been proved that the collision risk of an airspace depends on the underlying airspace structure and the traffic scenarios [13]. So it is clear that there is a relation between the airspace structure and the overall collision risk. The modelling of an airspace should include details of its elements that help to estimate the collision risk properly [135].

5.2.1 Airspace Network

In recent years, complex network science has been largely applied to air transportation network analysis [21, 22, 100, 108, 129]. From a complex network point of view, an airspace can be considered a multi-scale, dynamic network of interconnected entities. In an airspace, flights do not always follow a smooth and optimised trajectory. Instead, they follow a path on a predefined grid. The actual flight path is, therefore, a succession of waypoints together with timestamps and altitudes. Based on the flight path information and the location of waypoints in the airspace, I can model it as a graph (network), comprising the waypoints as vertices or nodes linked by the airways connecting them. Figure 5.1 shows an example of an airspace that can easily be modelled as a graph. [13].

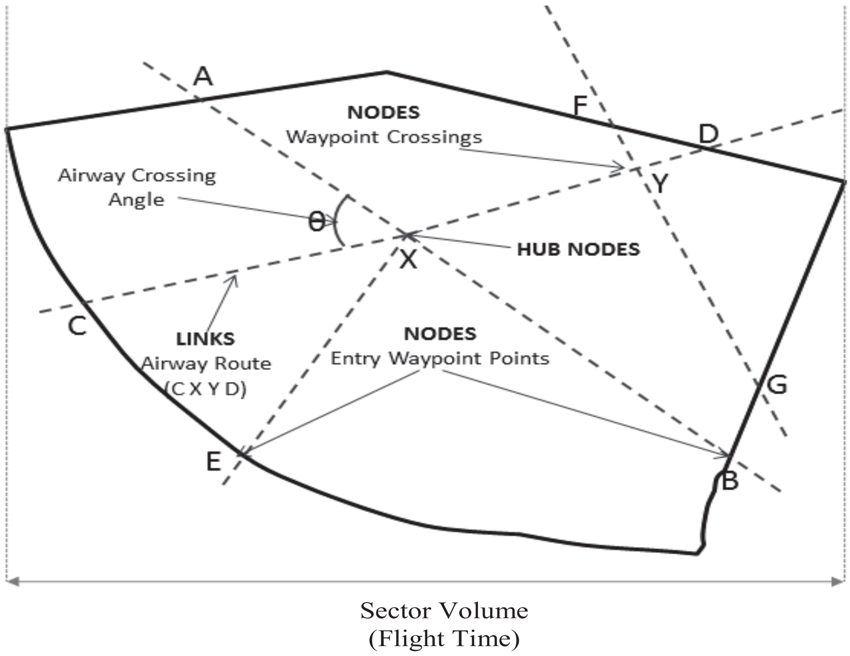

FIGURE 5.1: Airspace network modelled as a graph (network), comprising waypoints as vertices or nodes linked by the airways (links) connecting them.

Beside the entry/exit points and the navigation waypoints, two line segments may also intersect each other, which might virtually create a crossing. As illustrated in Figure 5.1, if there is a direct flight between C to D and A to B, the crossing of the two line segments at X is considered a crossing point. As a result, in addition to the entry/exit points A, B, C, D, E, F and G, the crossing of the two line segments at Y and X are also considered node in an airspace network. So, to model the

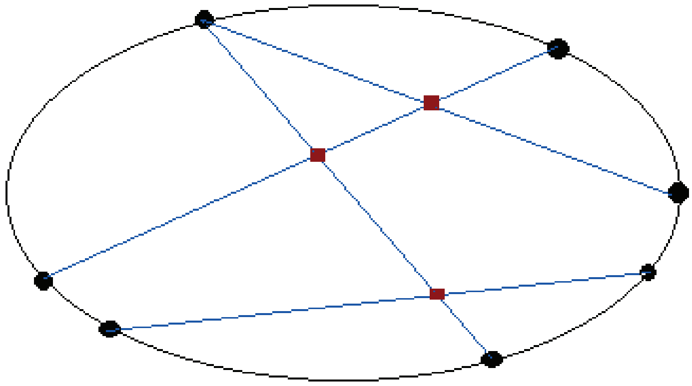

FIGURE 5.2: An example of DRN. The entry/exit nodes are represented as a filled circle and the square represents a crossing node.

airspace network, I consider two different network models: (i) direct route network (DRN) and (ii) intermediate waypoints network (IWN).

5.2.1.1 Direct Route Network (DRN) Model

There are airspaces that are not covered by radar and without any ATC monitoring or separation support. Aircraft are expected to fly direct routes between entry and exit points along the rhumb line of the entry to exit point, confirming the agreed plan with air traffic flow management (ATFM) in such airspaces [81]. Moreover, within a non-radar airspace, although there is a well-defined airway structure, flights generally consider a direct route from entry to exit point (rhumb line of the entry to exit point) for collision risk estimation [159]. To accommodate this concept, I define a direct route network as a graph where the entry/exit points and crossing of the straight lines among them are also considered nodes. In this model, links are created among the nodes by the direct lines among them. Figure 5.2 shows an example of airspace network created by a DRN model.

The direct route model assumes that there is a great circle route between entry and exit waypoints for estimating the crossing frequency. However, in any given airspace/sector, a flight may go through several intermediate waypoints before it

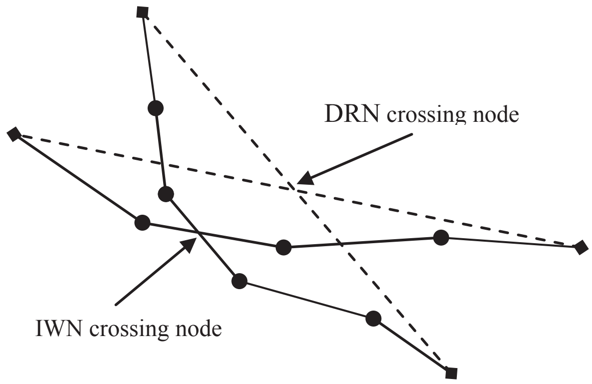

FIGURE 5.3: Difference between a DRN and IWN generation process.

reaches the exit point. As a result, the actual flight path may not be a straight line between entry and exit waypoints but a segment of chords that join the intermediate waypoints. Assumption of a great circle route between entry and exit waypoints results in a simplified airspace network structure and, therefore, an incorrect number of crossings computed as well as an incorrect crossing frequency, which in turn affects the collision risk estimates.

5.2.1.2 Intermediate Waypoints Network (IWN) Model

In the direct route network model, only the entry/exit points are considered nodes and the crossings of the straight line routes from entry to exit points. However, the in-flight route actually consists of a collection of waypoints. A waypoint is a navigation marker the longitude and latitude coordinate of which is determined by the ground navaids and keeping the pilots informed about the desired track and heading direction of the aircraft. To quantify the effect of the waypoints on the topology and the collision risk of an airspace network, I also propose a model that considers all of the waypoints. Figure 5.3 illustrates the difference to calculate the crossing points between the DRN and the IWN models. In Figure 5.3, the intermediate waypoints air route is denoted by the solid line and the direct route is shown by the dotted straight line.

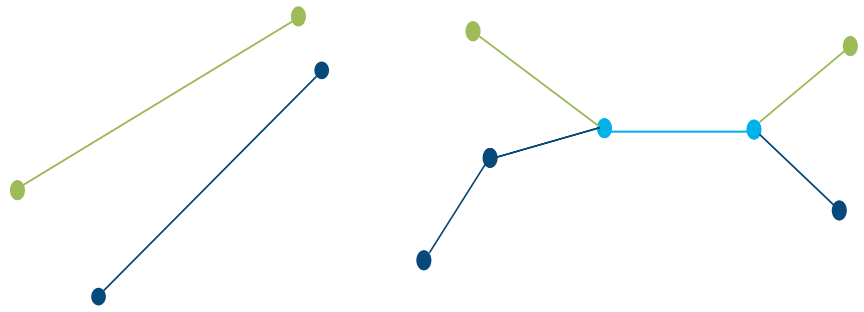

Figure 5.4: Direct flight paths (without intermediate waypoints) (left) and flight paths with intermediate waypoints (right).

In the IWN model, the intermediate waypoint for a given entry-and exit point in the airspace in considered. This may lead to fairly complex routes. The introduction of an intermediate waypoint model has several effects. A higher number of intermediate waypoints will increase the likelihood of an aircraft crossing to occur. This is because it is not uncommon for two flight paths, if represented by the naive flight path (Figure 5.4, left), not to have any possible intersection. However, often, the airway structure is such that these two flights will meet along a common path and then split and deviate, as seen in Figure 5.4 (right).

5.2.2 ICAOs Form 4 Data

To construct an airspace network and estimate it collision risk, I have used the ICAO Form 4 Data (a sample of ICAO Form 4 data can be found in Appendix K in [116]). The ICAO has stipulated the use of Form 4 Air Traffic Flow data [116] for collecting RVSM traffic data from ANSPs. The ICAO Form 4 data provides sufficient detail, but often to quite low resolution for collision risk models to give an estimate of technical vertical collision risk.

ICAO Form 4 records following flight data:

Flight date, Aircraft call sign, Aircraft type, Departure aerodrome, Arrival aerodrome, Entry Waypoint, Entry level, Entry time, Exit Waypoint, Exit level and

Exit time. The ICAO Form 4 data is then processed to compute:

- Total flight time for each region
- Average ground speed for each region
- Number of flight crossings in each region
- Flight time proportions for each aircraft, which is used to calculate:
  - Average aircraft dimensions: The type of aircraft flown in the region is used to determine its dimensions from the BADA (Base of Aircraft Data) database to calculate the average aircraft dimensions
  - Altimetry system error (ASE) probability

The airspace in consideration for this chapter is reduced vertical separation minimum (RVSM) airspace. Within RVSM airspace, air traffic control (ATC) separates aircraft by a minimum of 1,000 feet vertically between flight levels (FL) 290 and 410 inclusive [113]. In my experiment, the flight data was collected for the month of October 2011 for all 12 member countries of the MIDRMA region using ICAO Form 4. In total, there were 203,764 flights flying in the region (FL290 to FL420 inclusive).

5.3 Topological Properties of Airspace Network

In the above DRN and IWN models, the edge set E represents all line segments of air routes between nodes (waypoints, crossing and entry/exit points). However, after generating the initial network, a crossing node can be very close to an existing waypoint; in such a case, the crossing node is merged with the closest node if the distance between them is less than 1 nautical mile. Finally, the network is represented by an adjacency matrix $A_{n\times n}$ such that $a_{ij} = 1$ if a link exists between the city-pair i and j, otherwise $a_{ij} = 0$. From the resulting network, I have found that the networks always remain connected and the IWN is more highly structured than the DRN. Figure 5.5 shows the DRN and IWN of the airspace network of Oman.

Different networks have different topological features that characterise its connectivity, interaction and the dynamical processes executed by the network [28]. The analysis, discrimination and synthesis of airspace networks, therefore, rely on the use of measurements capable of expressing the most relevant topological features, which enable us to characterise the airspace properties. Several network indices – network degree distribution, average degree, clustering coefficient, betweenness centrality, closeness centrality, degree centrality and characteristics path length (discussed in Chapter 3) – are used in this chapter to measure the topological configuration of the airspace network.

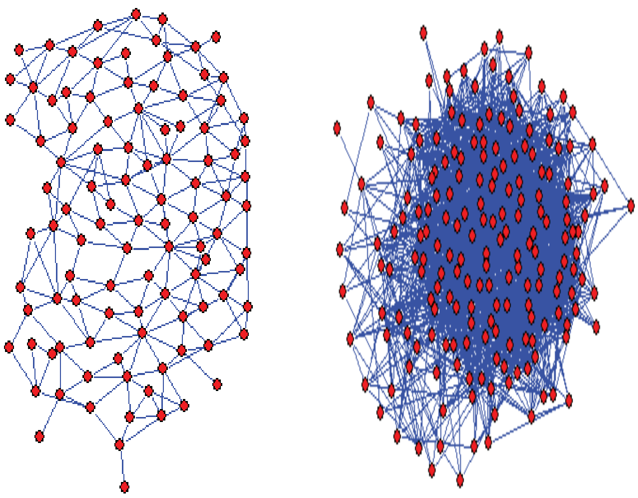

FIGURE 5.5: The DRN (left) and IWN (right) of Oman, one of the countries in the Middle East (MIDRMA) region.

5.3.1 Comparison Between DRN and IWN

Interestingly, many real networks, including airspace networks, share a certain number of topological properties; for example, most are small worlds [102], that is, the average topological distances between nodes increase very slowly (logarithmical or even more slowly) with increases in the number of nodes. Additionally, hubs (nodes with very large degrees (k)) compared with the mean of the degree distribution (k) are often encountered. More precisely, in many cases, the degree distributions exhibit heavy tails, which are often well approximated for a significant range of values of k by a power-law behaviour [14].

Figure 5.6 shows some key topological properties of Oman's DRN and IWN. First, I focus on the degree distribution of the networks. In Figures 5.6(a) and 5.6(b), it is noticeable that the degree distribution of DRN follows normal distribution. It gives strong evidence that the DRN is a kind of random network. Whereas that of IWN is right skewed. In the case of centrality-based measures, both of the networks betweenness and closeness centrality follow exponential function. That is to say, the centrality value declines exponentially with the nodes ranking.

The steep curve of betweenness indicates that a few hub nodes account for most of the traffic transfer capacity. Next, I investigate the clustering coefficient that captures the local cohesiveness of a node. It measure the how the neighbours of a node are connected themselves. A network with a high clustering coefficient is always beneficial to find an alternative if some of its nodes (waypoints) have failed due to bad weather.

The distribution of the clustering coefficient of DRN and IWN are found to be significantly different, as DRN clustering coefficient exhibits a linear decay, while IWN is an exponential decay. Besides the centrality measures, I also investigate the degree-degree correlation of the networks. Figure 5.6(i) and Figure 5.6(j) show the degree-degree correlation of DRN and IWN, respectively. For DRN, there is no significant correlation among the nodes in the network, whereas, for IWN there is apparent positive degree-degree correlation. That is, the high-degree nodes tend to be connected with high-degree nodes.

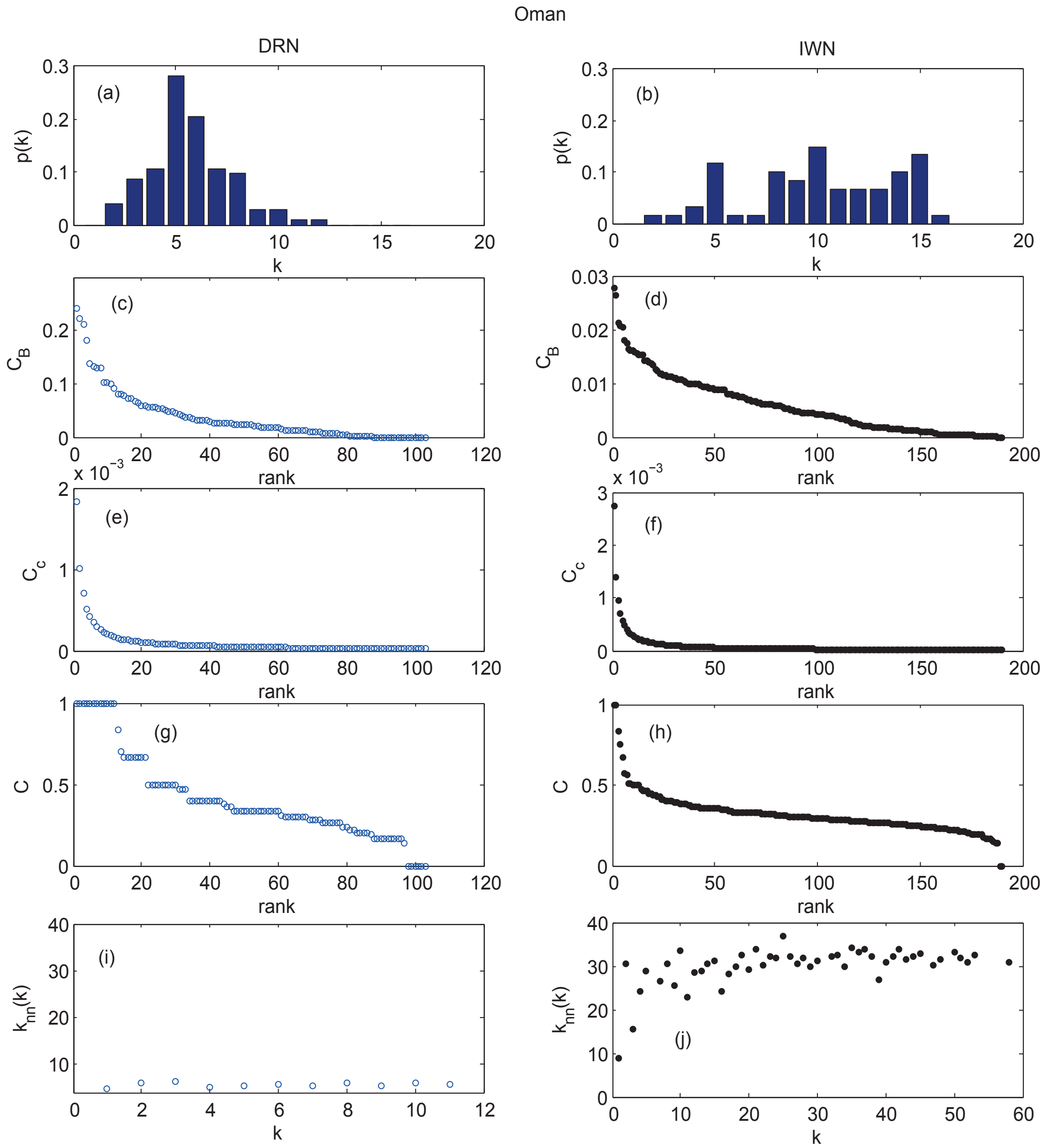

FIGURE 5.6: A one-to-one comparison of topological properties of Omans DRN and IWN (a) and (b) the degree distribution of DRN and IWN respectively, (c) and (d) betweenness centrality, (e) and (f) closeness centrality, (g) and (h) clustering coefficient, ((i) and (j) degree-degree correlation of DRN and IWN.

Thus, it confirms that the IWN is more highly structured than the DRN. Similar behaviour is also observed for the other airspace networks (DRN and IWN) of the countries in the MIDRMA region. The topological properties of the rest of the countries in the MIDRMA region are presented in Appendix **A**.

5.4 Collision Risk Analysis

Collision risk is defined by the ICAO [119] as "the expected number of mid-air aircraft accidents in a prescribed volume of airspace for a specific number of flight hours due to loss of planned separation". The collision risk assessment methodology consists of two elements: first, risk estimation, which concerns the development and use of methods and techniques with which the actual level of risk of an activity can be estimated; and second, risk evaluation, which concerns the level of risk considered to be the maximum tolerable value for a safe system. The level of risk that is deemed acceptable is termed the target level of safety (TLS) [114]. The risk evaluation process consists of comparing the estimated risk against a TLS to provide a quantitative basis for judging the safety of air traffic operations in a given volume of airspace.

The challenge in modelling collision risk for an airspace operation is the nature of conflict paths, sector structure and the intervention of rules used by air traffic controllers to separate traffic. Several collision risk estimation models have been developed in the past [110, 148, 193–195, 208]. Almost all collision risk assessment models are intrinsically based on estimating the expected number of conflicts due to separation violation in the airspace over time. Many of the well-known models for collision risk estimation have used procedural uncontrolled airspace assumptions [41, 194]. Some studies have concentrated on the development of suitable mathematical functions and models to estimate the probabilities of lateral and vertical overlaps [110, 161] (detail of the collision risk models are discussed in Chapter 2). To consider both the DRN and IWN models, I have used the following collision risk stigmatisation model developed by the ICAO [119, 159].

5.4.1 Vertical Collision Risk Model

Technical vertical risk represents the risk of a collision between aircraft on adjacent flight levels due to normal or typical height deviations of RVSM-approved aircraft. The technical vertical collision risk is assessed against a technical TLS of 2.5×10^{-9} fatal accidents per flight hour using a suitable collision risk model [121].

Following [4] the vertical collision risk model for aircraft on adjacent flight levels of the same route, flying in either the same or the opposite direction satisfies:

$$N_{az} = 2P_z(S_z)P_y(0)n_z(equiv)\left[1 + \frac{|\bar{\dot{y}}|}{2\overline{V}} + \frac{\theta_{xy}|\bar{\dot{z}}|}{\lambda_z 2\overline{V}}\right] \tag{5.1}$$

where

$$\begin{aligned} n_z(equiv) = n_z(opp) + n_z(same)&\frac{\frac{\overline{|\dot{y}|}}{\overline{\nabla V}} + \frac{\lambda_{xy}\overline{|\dot{z}|}}{\lambda_z 2\overline{V}}}{1 + \frac{|\bar{\dot{y}}|}{2\overline{V}} + \frac{\lambda_{xy}|\bar{\dot{z}}|}{\lambda_z 2\overline{V}}} + \\ &\frac{1}{P_y(0)} \frac{1}{1 + \frac{|\bar{\dot{y}}|}{2\overline{V}} + \frac{\lambda_{xy}|\bar{\dot{z}}|}{\lambda_z 2\overline{V}}} \sum_{i=1}^{n} n_z(\theta_i)\left[1 + \frac{\frac{\pi}{2}\lambda_{xy}}{V_{ral}(\theta_i)} \frac{\overline{|z|}}{2\lambda_z}\right] \end{aligned} \tag{5.2}$$

with the various symbols in (5.1)-(5.1) explained below.

The left-hand side variable N_{az} represents the expected number of aircraft accidents due to normal technical height deviations of RVSM-approved aircraft for the given traffic geometry. The longitudinal overlap frequency parameters $n_z(same)$ and $n_z(opp)$, together with the kinematics factors in brackets (as functions of the relative speeds and aircraft dimensions), represent a major part of the different levels of exposure to the risk of the loss of vertical separation for the two traffic geometries covered by the collision risk model of equation (5.1). (The subscript z in $n_z(same)$ and $n_z(opp)$ refers to aircraft on adjacent flight levels.)

There are two aircraft dimensions used by the technical vertical risk: the average diameter (λ_{xy}) and the average height (λ_z). The probability of vertical overlap

$P_z(S_z)$ is the probability that two aircraft will overlap vertically, separated by 1,000ft (S_z). This indicates the probability that they will overlap while correctly flying at adjacent flight levels. The probability of lateral overlap ($P_y(0)$) is the probability of two aircraft being in lateral overlap, if they are both correctly flying at adjacent flight levels. This is calculated by taking the proportion of time that an aircraft in the region is flying using satellite navigation (GNSS) versus radio navigation (VOR/DME).

There are five relative speed parameters that appear in the technical vertical risk:

- $\overline{\nabla V}$ is the relative along-track airspeed between two aircraft flying at adjacent flight levels and flying in the same direction.
- $\overline{V}$ is the average ground speed of the aircraft.
- $\overline{|\dot{y}|}$ is the average relative cross-track speed between two aircraft flying at adjacent flight levels.
- $\overline{|\dot{z}|}$ is the average relative cross-track vertical speed between two aircraft that have lost feet of vertical separation.
- $V_{rel}(\theta)$ is the average relative horizontal speed between aircraft flying at adjacent flight levels and intersecting at an angle given by the equation (5.3):

$$V_{rel}(\theta) = \overline{V}\sqrt{2(1 - cos(\theta)} \tag{5.3}$$

5.5 Methodology

This section explains the methodology used for comparing the collision risk and network characteristics of the direct route model (great circle route between airspace entry and exit point) and the intermediate waypoint model (waypoints between entry and exit points). The airspace network features for both models were characterised for each country and analysed given the collision risk estimates. As illustrated in Figure 5.7, the ICAO Form 4 data is the basis for the flight data input to the two models. Both models use the same collision risk model and databases for aircraft positional error distribution and kinematic factors (speed and dimension).

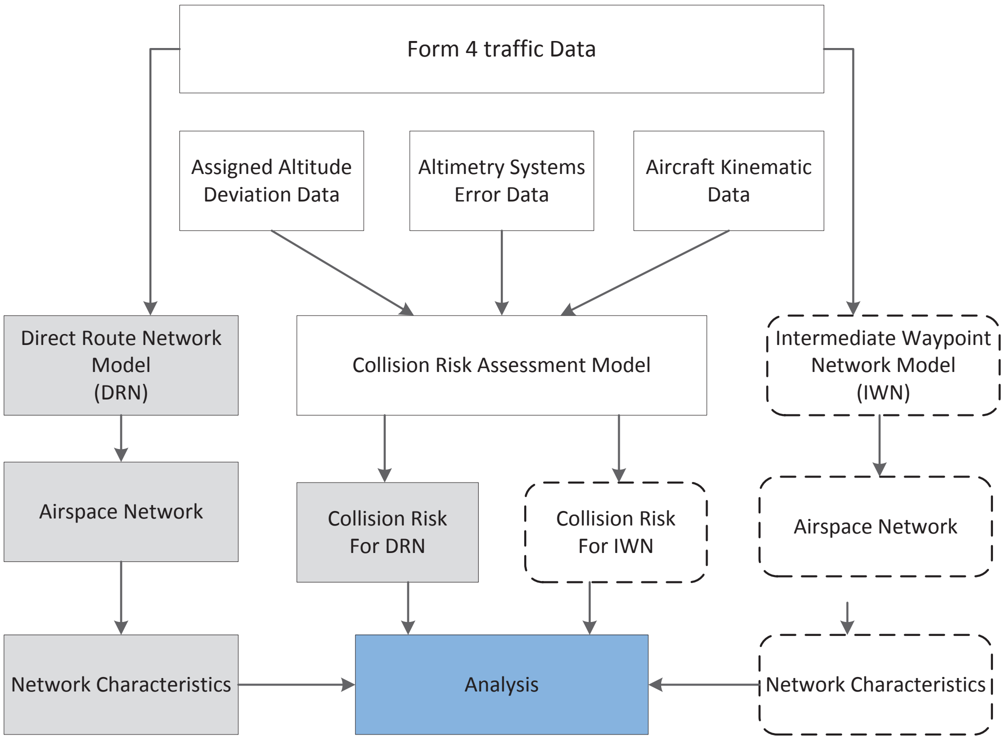

FIGURE 5.7: Proposed methodology for network characteristics analysis of direct route model and intermediate waypoints model for technical vertical risk.

Collision Risk with Direct Route Network Model: In the direct route model, technical vertical risk is computed using the direct route model. In this stage, an airspace network is generated using the entry and exit point data extracted from the Form 4 data. Network analysis is performed and network characteristics are identified.

Collision Risk with Intermediate Waypoint Network Model: In the intermediate waypoint model, technical vertical risk is computed. Again, the airspace network is generated incorporating the intermediate waypoints between entry and exit points using the ICAO Form 4 data.

Processing ICAO Form 4 Data: The two pieces of required information for calculating the number of crossings for an FIR/UIR are the completed ICAO Form 4 data for the time period and a list of waypoints and their coordinates corresponding to the names used in the ICAO Form 4 data. The first step in the process is to read in the list of waypoints and their coordinates. These are stored for use in the later calculations.

The second step in the process is to read in the ICAO Form 4 data, filtering out any data that is either incomplete or suspected to be incorrect. From the first pass of the data, the number of flights (N), total flying time (T, in hours) and average ground speed ($\overline{V}$ in knots) can be calculated. Additionally taken is a list of entry-exit point pairs flown within the FIR/UIR.

The third step is to determine the crossing pairs within the data. This is done by taking the list of entry-exit points from the ICAO Form 4 data scan and computing whether the great circle arc formed by that flight path intersects with any of the other entry-exit great circle arcs.

Finally, each flight in the ICAO Form 4 data is processed to count the number of flights with which it intersects. This is done by picking a flight and checking it against all other flights. For each flight that it is adjacent to, the entry and exit points are compared; if they are both the same, then we check whether they intersect in the same or opposite directions. If the flight has a different entry and exit pair, then then we check whether the two entry-exit pairs intersect; if they do, then we check whether the two flights intersect in a crossing path.

Estimating Crossing Frequency: The passing frequencies are the frequency at which two aircraft at adjacent flight levels pass each other. They can be in the same direction ($n_z(same)$), opposite directions ($n_z(opp)$) or pass each other on crossing tracks $n_z(\theta)$.

The same and opposite direction crossing frequencies can be calculated by taking the number of plane passings divided by the total hours of flight and multiplying by the probability of lateral overlap, as shown in equations eq(5.4) and eq(5.5)

$$n_z(same) = \frac{number\ of\ crossing \times P_y(0)}{total\ flight\ time\ in\ FIR/UIR} \tag{5.4}$$

$$n_z(same) = \frac{number\ of\ crossing \times P_y(0)}{total\ flight\ time\ in\ FIR/UIR} \tag{5.5}$$

The crossing traffic frequency is calculated in a similar manner to the same and opposite directions (with a value calculated for each crossing angle). However, it is not multiplied by the probability of lateral overlap, and a larger crossing diameter is taken when the crossings are counted. This is because, if the crossings were counted on the average aircraft diameter (λ_{xy}), this would result in a very small number of crossings. Therefore, a larger, proximity distance (S_x) is taken in order to better estimate the frequency. The number of crossings is then scaled down by a factor of the aircraft diameter on the proximity distance, as shown in eq(5.6).

$$n_z(\theta) = \frac{number\ of\ crossing \times \frac{\lambda_{xy}}{S_x}}{total\ flight\ time\ in\ FIR/UIR} \tag{5.6}$$

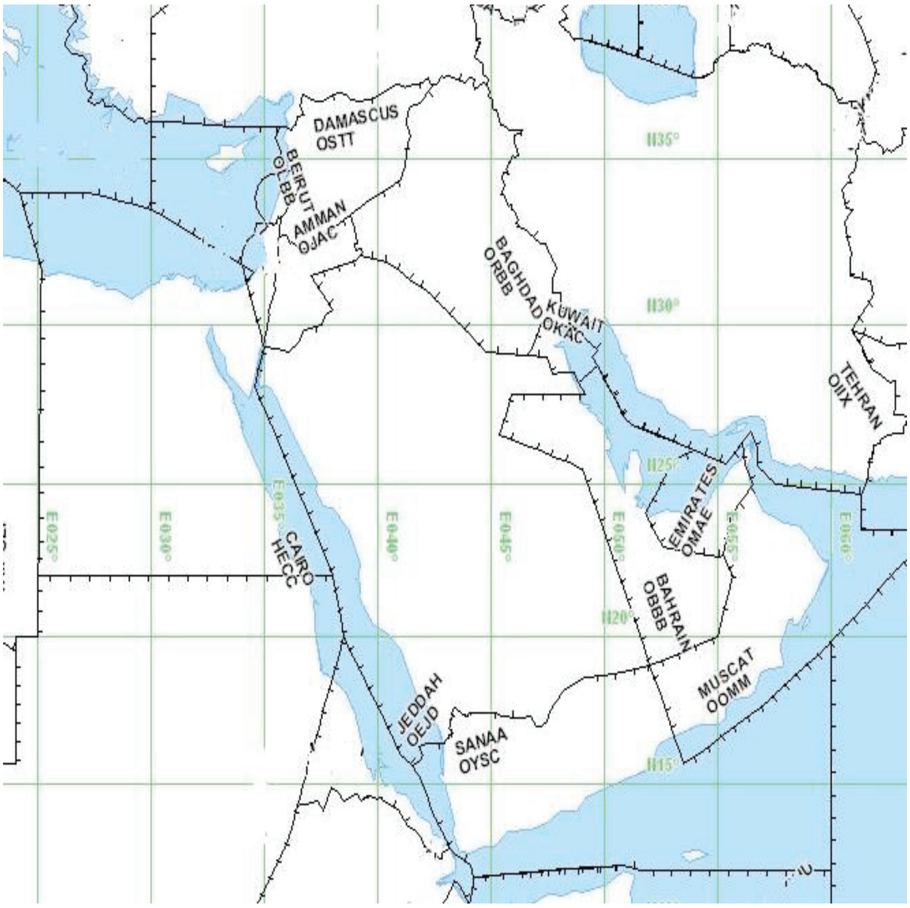

FIGURE 5.8: Map of MIDRMA region comprising of 12 ARTCC/FIR/UIRs.

5.6 Experiments

5.6.1 Region and Traffic Data

The traffic data used in this chapter is provided by the ICAOs Middle East Regional Monitoring Agency (MIDRMA). MIDRMA is the administrator of the RVSM airspace in the Middle East region. The MIDRMA region consists of the following countries: Bahrain, Egypt, Iran, Iraq, Jordan, Kuwait, Lebanon, Oman, Qatar, Saudi Arabia, Syria, the UAE and Yemen. A map of the MIDRMA region is shown in Figure 5.8.

MIDRMA provided Air Traffic data, waypoint data and aeronautical information data for all 12 member states. Data was collected for the month of October 2011

Table 5.1: Number of flights in each region/country for the month of October 2012 and the total number of flight hours flown

Country	Flight Data (Oct 2011) RVSM Airspace	
	Number of Flights	Flight Duration (hours)
Bahrain	39206	23624
Egypt	26322	18160
Iran	17030	20165
Iraq	2810	2795
Jordan	6277	1513
Kuwait	12122	3395
Lebanon	1151	190
Oman	30000	18846
Saudi Arabia	7716	2049
Syria	7716	5398
UAE	20725	3445
Yemen	5025	23624

for all member countries using ICAO Form 4. In total, there were 203,764 flights flying in the RVSM airspace (FL290 to FL420, inclusive) in the region.

In order to collect information about intermediate waypoints for given entry and exit points in an FIR/UIR, MIDRMA issued a circular to all member states to develop a database for all entry and exit points and the most commonly flown routes in the respective regions. The data collection and verification exercise was undertaken over a period of two months. All twelve member states collected and reported data on intermediate waypoints for all entry and exit points in their respective FIR/UIRs. Table 5.1 reports the summary of one months traffic data used to model the national airspace system (NAS) of the constituent countries in the MIDRMA region.

5.6.2 Experimental Parameters and Supplementary data

Table 5.2 reports the parameters of the collision risk model used in the experiments.

Table 5.2: Collision Risk Model's parameters

Parameter	Value
Relative along-track airspeed $\overline{\nabla V}$	15 kn/s
average relative cross-track speed $\lvert\dot{y}\rvert$	20 kn/s
average relative cross-track vertical speed $\lvert\bar{\dot{y}}\rvert$	1.5 kn/s
σ_{GNSS} standard deviations for satellite nav	0.0612 NM
$\sigma_{VOR/DME}$standard deviations for radio nav	0.3 NM
α proportion of flights flying with satellite navigation	75%
Length (λ_x)	173.51 ft
Wingspan (λ_y)	163.35 ft
Diameter (λ_{xy})	159.91 ft
Height (λ_z)	45.451 ft

Aircraft dimension parameters (representing the average dimension of aircraft that fly in the region) are calculated and weighted as per the flight time proportion of each aircraft group.

Based on the navigation data provided by the member states, the proportion of flights flying with satellite navigation in the MIDRMA region was set to 75%. Airspeed parameters were used as recommended by the ICAO [113]. Aircraft performance was modelled using Eurocontrol's Base of Aircraft Data (BADA). For computing the probability of vertical overlap, Eurocontrol's altimetry system error (ASE) parameter database and aircraft aerodynamic parameters (AAD) were used.

The collision risk computation process is illustrated in Figure 5.9. First, the countries for which the collision risk is to be done are selected. Various supplementary data files such as waypoint/airport names and coordinates, BADA database, ASE and AAD parameters and aircraft dimension files are then read and processed. After that, the flight data for the selected countries is read and processed to compute flight time proportion and crossing frequencies. The probability of lateral overlap and the probability of vertical overlap are then computed. These intermediate results are then inputted into equation (5.1) and technical vertical risk is

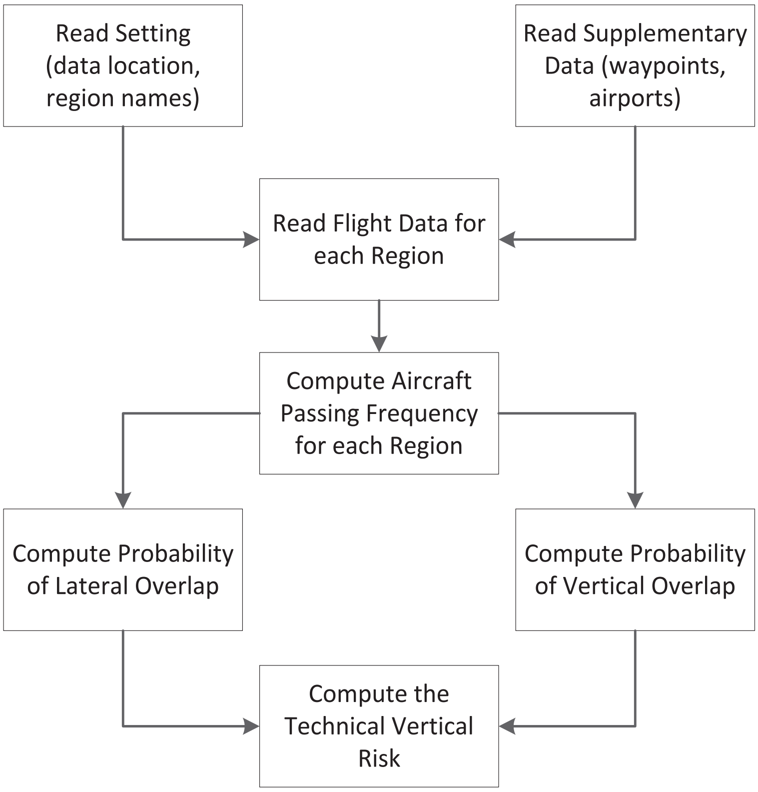

FIGURE 5.9: Technical Vertical Risk Computation Process.

computed.

5.7 Results and Analysis

5.7.1 Network Features

In this section, I compare each of the complex network metrics of the DRN and IWN among the constituent nations of MIDRMA.

Average Degree: Figure 5.10 compares the average degree between the DRN and IWN of the MIDRMA nations. For the intermediate waypoint model, the average degree for almost all of the countries (except Lebanon) increased significantly. This mainly occurred due to the presence of major crossings (especially in large airspaces), which were not captured in the direct route

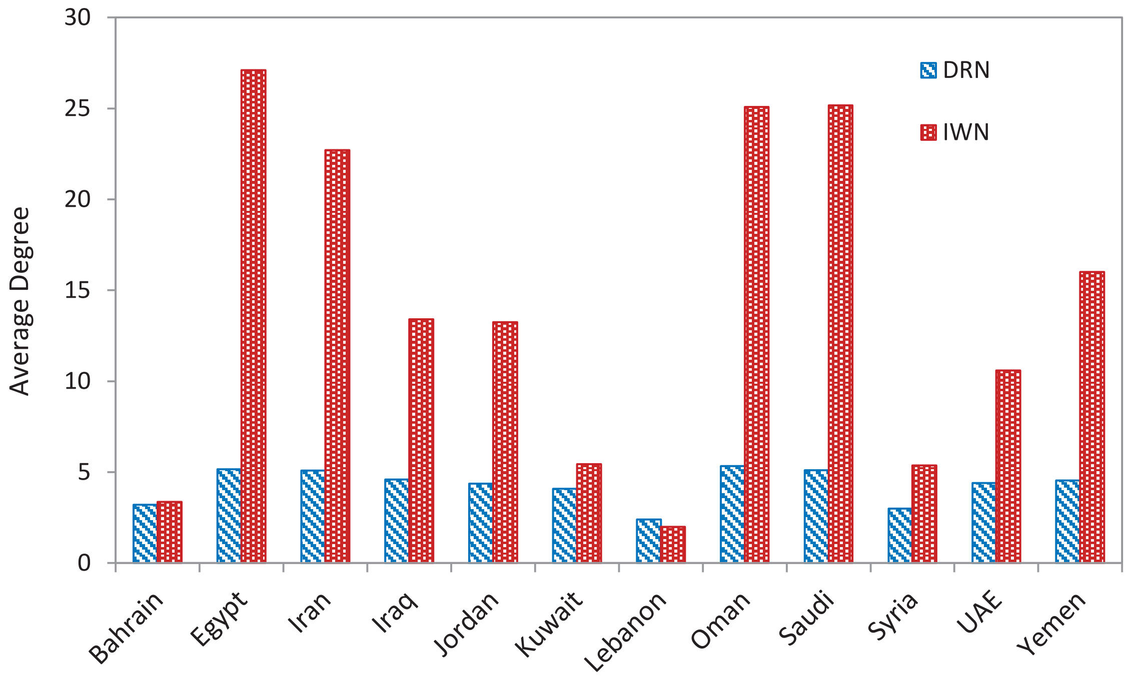

FIGURE 5.10: Average Degree of DRN and IWN for MIDRMA countries.

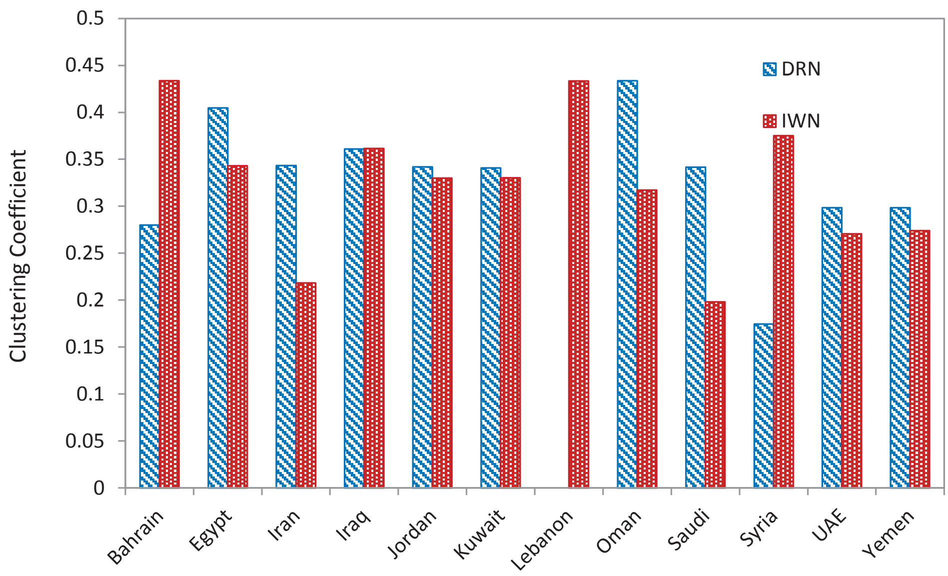

FIGURE 5.11: Clustering Coefficient measure of DRN and IWN for MIDRMA countries.

model, affecting the collision risk computation. Lebanon is a small FIR with a semi-circular design. The airspace structure is simple, with all airways from the boundary of the FIR merging at the Beirut VOR.

Clustering Coefficient: The cluster coefficients are show in Figure 5.11. The

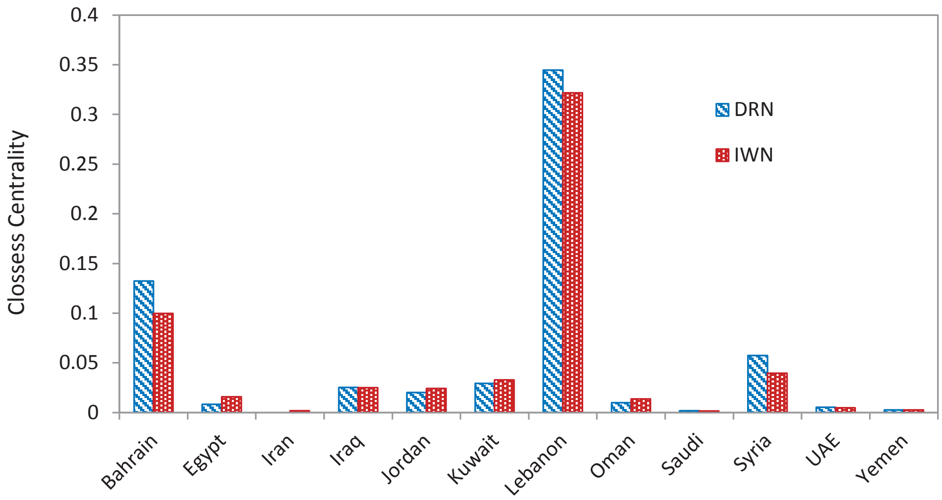

FIGURE 5.12: Closeness Centrality measure of DRN and IWN for MIDRMA countries.

nodes in the Bahrain, Lebanon and Syrian airspace networks appear to have higher tendency to form clusters in the intermediate waypoint model. In Egypt, Iran and Saudi Arabia, a lower clustering coefficient indicates a low collision risk.

Closeness Centrality: From the closeness centrality measures (Figure 5.12), it is noticeable that Iran and Saudi Arabia have the lowest closeness centrality, which is because of their large airspaces. For Lebanon, this measure is high (in both models) due to its very small airspace and very few airways merging at VOR. In Bahrain and Syria, closeness centrality is reduced for the intermediate waypoint model due to their structured airspaces, leading to minimal or no change in collision risk estimates.

Betweenness Centrality: The betweenness centrality is presented in Figure 5.13. As expected, this measure has gone down for all FIRs in MIDRMA, except Lebanon. The intermediate waypoint model reduces the possibility of a particular node lying between other nodes, as opposed to the direct route model, in a network. This indicates that a more unstructured network will lead to a higher collision risk.

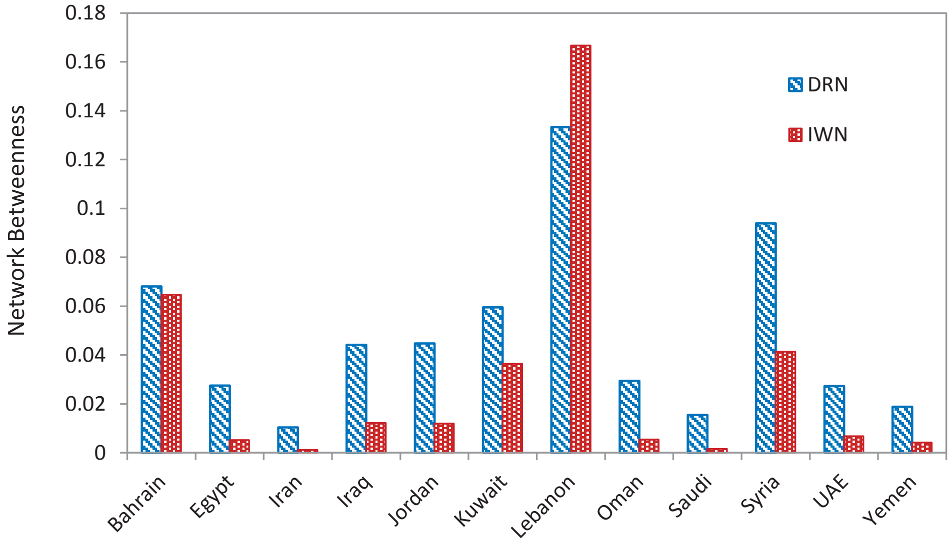

FIGURE 5.13: Betweenness Centrality measure of DRN and IWN for MIDRMA countries.

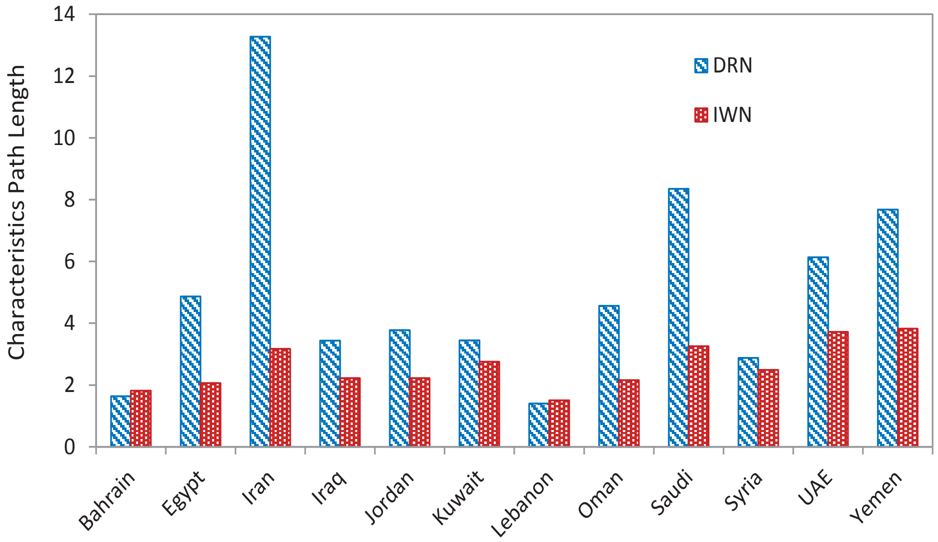

FIGURE 5.14: Characteristics Path Length in DRN and IWN for MIDRMA countries.

Characteristic Path Length: From the characteristic path length (Figure 5.13), the airspace networks of Iran and Saudi Arabia appear to be denser (lower characteristic path length) with the intermediate waypoint network. This is possibly due to the presence of large areas of procedural airspace.

5.7.2 Collision Risk and Passing Frequency

To compare the DRN and IWN in terms of collision risk, I first present the results of crossing frequency per flight hour and the technical vertical risk with the direct route model and the intermediate waypoint model. As can be seen from Table 5.3 and Figure 5.15, with the intermediate waypoint model, Egypt, Iraq, Lebanon and Oman show a significant increase in crossing frequency as well as technical vertical risk.

From Figure 5.15, it is noticeable that, in both models, Bahrain, Iran and Saudi Arabia do not have any significant change in their crossing frequency and technical

Table 5.3: Vertical collision risk assessment (passing frequency and technical vertical risk) For MIDRMA region

Country	Collision Risk Assessment			
	Passing Frequency		Technical Vertical Risk	
	Direct Route	Inter. Waypoint	Direct Route	Inter. Waypoint
Bahrain	0.020211	0.02019	3.63×10^{-11}	3.62×10^{-11}
Egypt	0.019650	0.02843	3.53×10^{-11}	5.10×10^{-11}
Iran	0.023403	0.02348	4.20×10^{-11}	4.21×10^{-11}
Iraq	0.009957	0.05476	1.79×10^{-11}	9.82×10^{-11}
Jordan	0.012597	0.01288	2.26×10^{-11}	2.31×10^{-11}
Kuwait	0.000297	0.00117	5.34×10^{-13}	2.10×10^{-12}
Lebanon	0.003515	0.00872	6.31×10^{-12}	1.56×10^{-11}
Oman	0.027840	0.04504	5.00×10^{-11}	8.07×10^{-11}
Saudi Arabia	0.020981	0.02096	3.77×10^{-11}	3.76×10^{-11}
Syria	0.028031	0.02904	5.03×10^{-11}	5.21×10^{-11}
UAE	0.009877	0.00640	1.77×10^{-11}	1.15×10^{-11}
Yemen	0.006218	0.00720	1.12×10^{-11}	1.29×10^{-11}

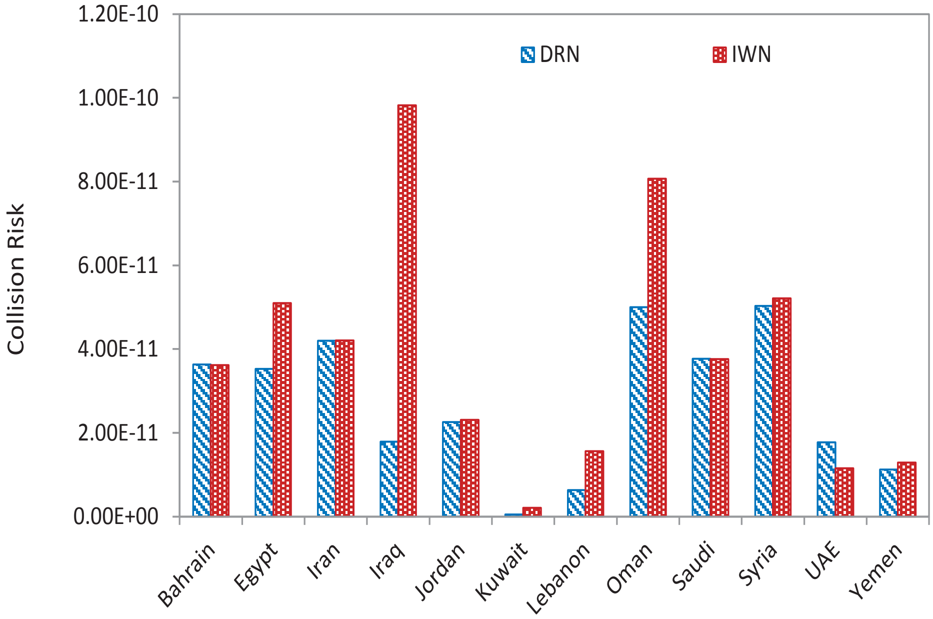

Figure 5.15: Technical Vertical Risk with DRN and IWN for MIDRMA countries.

vertical risk. Most surprisingly, the UAE shows a decrease in its crossing frequency as well as technical vertical risk in the IWN model compare to the DRN model.

The highest variability can be seen in Iraq and Oman, where the collision risk increases significantly with the intermediate waypoint model.

The collision risk for Saudi Arabia and Iran, in both models, remains the same due to large airspaces where the intermediate route has less variability and is more or less similar to the direct route model. As illustrated in Figure 5.16, Bahrain and the UAE have highly structured airways. However, UAE airspace is smaller and more structured when compared to Bahrain airspace. The southern airspace of Bahrain, which adjoins Saudi Arabia, has an unstructured pattern. This might have led to the decrease in collision risk for the UAE in the intermediate waypoint model.

Similarly, the increase in the collision risk estimate of Iraq, for the intermediate waypoint model, can be attributed to the significant increase in crossings (five-fold increase) due to crossing traffic from Iran and Saudi Arabia. So, it can be

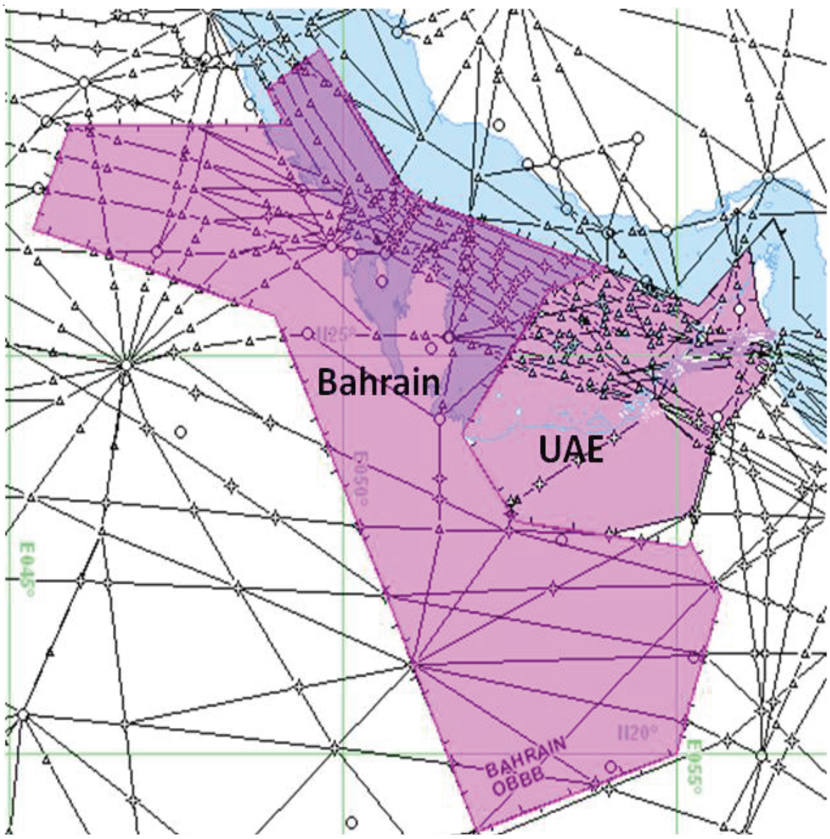

Figure 5.16: Highly structured airway route in UAE and in northern part of Bahrain.

concluded that a denser network results in higher collision risk estimates.

5.8 Chapter Summary

In this chapter, I proposed two different models to represent an airspace, a direct route network model and an intermediate waypoints network model. The degree of distribution of the DRN follows normal distribution, whereas that of the IWN is right skewed. In the case of centrality-based measures, both of the networks show similar exponential distribution. In the IWN, the high-degree nodes tend to be connected with high-degree nodes. For the DRN, there is no significant correlation among the nodes in the network. The network measures confirm that the IWN is more highly structured than the DRN.

Complex network measures were also employed to gain an insight into how the collision risk estimates vary with network measures for airspace network complexity. To estimate the collision risk, one months traffic data from 12 countries in the Middle East region was used. The experimental results indicate that the intermediate waypoints led to a significant increase in collision risk estimates specifically for airspace networks with higher average degree and higher closeness centrality measures. This demonstrates that it is possible to improve the collision risk estimates given the limited amount of flight data available in regions with limited CNS capabilities by using intermediate waypoint data available with ANSPs. The results also indicate that collision risk decreases in networks with lower betweenness centrality. It was also found that a highly dense network results in higher collision risk estimates. From an operational point of view, this indicates that countries that have highly structured airspaces are actually overestimating the collision risk with the direct route model.

Chapter 6

Airspace Network Optimization for Collision Risk

This chapter is partially based on the following publications:

- Sameer Alam, Md Murad Hossain, Fareed Al-Alawi, and Fathi Al-Thawadi, *Optimizing Lateral Airway Offset for Collision Risk Mitigation Using Differential Evolution*, International Journal of Engineering and Operations, Air Traffic Control Quarterly, Vol. 23, Number 3, 2016.
- Sameer Alam, Md Murad Hossain, Fareed Al-Alawi, and Fathi Al-Thawadi, *Shift for Safety: A Differential Evolution Approcah to Optimize Lateral Airway Offset for Collision Risk Mitigation*, Eleventh USA/Europe Air Traffic Management Research and Development Seminar (ATMRnD 2015), June 23rd - 26th 2015, Lisbon, Portugal (**Best paper award**).

In the previous chapter, I developed models to analyse airspace and its safety. The airspace network structure is modelled as a graph, including the entry/exit points and waypoints as nodes and segments as edges. In an airspace network, the location and configuration of the nodes have significant relation to its structure, which eventually impacts its safety. One of the important measures to judge the safety of an airspace is the collision risk estimate. To improve the safety of an airspace, its network needs to be optimised. The optimisation of a national airspace network structure becomes imperative for the increase of air traffic. In this chapter, I develop a methodology using differential evolution to optimise an airspace network structure in order to minimise its collision risk.

6.1 Introduction

The continued increase in air traffic and the limited airspace resources have resulted in more and more serious congestion and flight delay [145]. In the meantime, heavy congestion challenges airspace safety and flight delay costs the airline industry heavily every year [175]. Hence, how to safely accommodate high levels of demand and maximise the use of capacity-limited airspace and airport resources has become a major concern for both researchers and ANSPs.

A key component of air transportation is the national airspace system (NAS). At the highest level, the NAS is partitioned into traffic control centres, each of which is partitioned into sectors. Each sector is managed by one air traffic controller or a small team of two to three controllers at any given time of day. Traditionally, the traffic increase has been accommodated by subdividing highly loaded sectors, which is known as the sectorisation problem. The sectorisation problem has been studied extensively in the ATM literature [32, 63, 228] as a global optimisation problem. The concept of sectorisation has partially fulfilled its objective. Nowadays, many sectors have become too small to be divided. Duong et al. [68] point out that sectors are, therefore, a constraint to the increase of air traffic and that there obviously is a need to explore new practices that could break away from this major constraint. Eurocontrol [77] also points out that it is time to redesign or optimise the airspaces to accommodate the future traffic demand.

Apart from the sectorisation, another alternative to increase the capacity and safety of an airspace is to optimise the airspace network structure itself. A reasonable design of an airspace network can improve the flight efficiency and relieve airspace congestion [44, 113]. In the design or optimisation of an airspace network structure, the most important problem is how to determine the positions and connection of WPs, which is usually referred to as an airspace network optimisation problem (ANOP).

A few studies have been carried out to address the ANOP to increase its capacity or safety. For both en-route and terminal airspace, the design of the airspace is an iterative process that places significant reliance on qualitative assessment and the operational judgement of controllers and procedure designers involved from the outset in the design [77]. During the past decades, several methods for the design of airspace networks have been proposed. The pioneering work was done by Siddiquee, who modelled an airspace network with various attributes, including number and duration of potential conflicts etc., which can be used as optimisation goals and evaluation criteria of different network design alternatives [209]. Although this work did not provide a method for designing an airspace network, it established the basis for further study of the ANOP. Later, subjected to air traffic control constraints, Mehadhebi et al. presented a gradient descent algorithm to minimise the total airline cost by merging and moving the WPs [153], which may result in the scenario shown in Figure 6.1. The merging of multiple WPs may increase the controller workload as well as increase the likelihood of flight crossings. For example, as shown in Figure 6.1, merging P, Q and R into a single waypoint X will definitely increase the number of flight crossings. However, a completely new design or extensive modification of an airspace network is impractical in terms of the controllers convenience. Controllers are trained for several years to manage air traffic flow in an airspace. Radical changes in an airspace network will make controller experience irrelevant in managing the air traffic flow and will eventually increase their workload. In addition, it might disrupt the interaction with the adjacent sectors due to handover timing or location mismatch of the entry/exit waypoints. Thus, it is necessary to keep the changes in an airspace network as low as possible while optimising them for either capacity or safety.

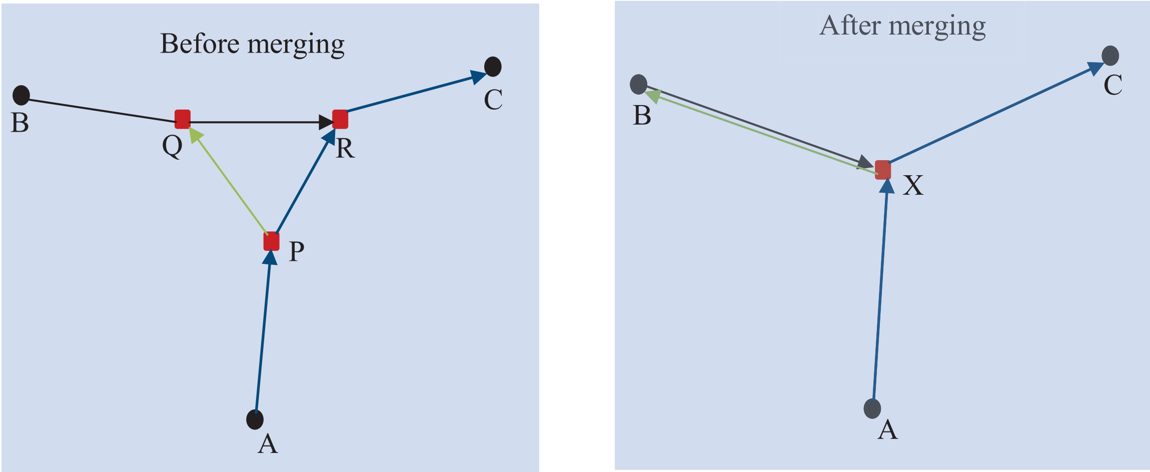

FIGURE 6.1: Merging of waypoints in an airspace network

6.2 Proposed Approach

In this chapter, I consider the optimisation of an airspace network structure to enhance its safety. One of the possible ways to increase the safety of traffic within an airspace with minimal or virtually no changes to its structure is to shift the airways to its right or left. Shifting an airway will not change the number of WPs or the network structure. However, shifting all of the airways in an airspace network structure might not increase its safety. But allowing different amounts of shifting for different airways and splitting some of its WPs may result in a network structure in which the likelihood of flight crossings can be reduced. Such an example is shown in Figure 6.2. In such a configuration (figure 6.2-left), flights in opposite directions in the same airway or segment may offset each other, which will reduce significantly the probability of separation violation. This concept of shift is similar to the ICAO SLOP. The ICAO has introduced Strategic Lateral Offset Procedures (SLOP) that allow suitably equipped aircraft to fly within 1nm (nautical mile) or 2nm lateral offset to the right of the airway centreline. I hypothesise that with the identification of the right offset for airways in an airspace network can minimise the overall collision risk. In other words, the airspace network optimisation problem (ANOP) can be translated into a problem of offset identification for SLOP.

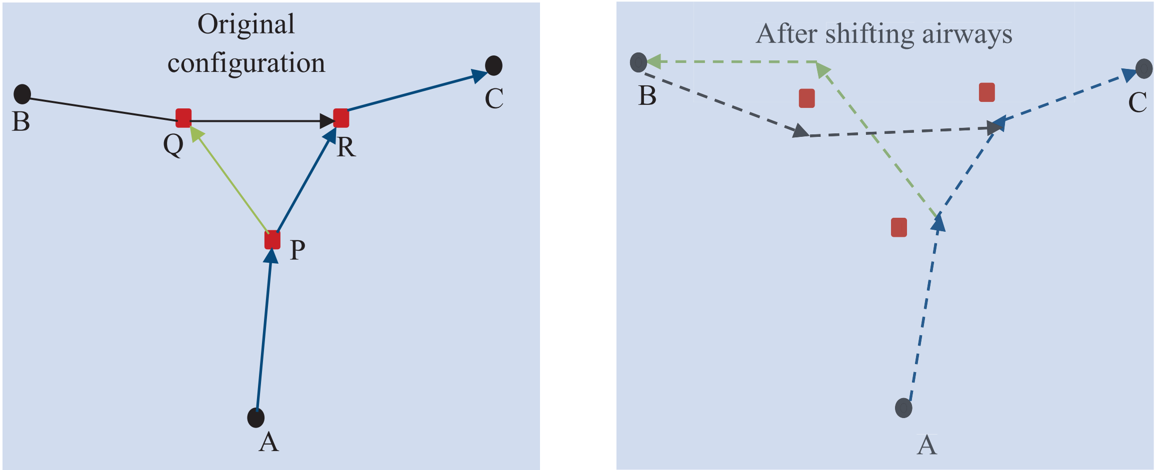

FIGURE 6.2: Example of shifting waypoints in an airspace network

ICAO in PANS ATM Doc 4444 [118] has proposed SLOP in oceanic and remote airspace, which allow aircraft to fly with 1nm or 2nm lateral offset to the right of airway centrelines on a suitably equipped aircraft (automatic offset tracking by flight management system – FMS). SLOP provides an additional safety margin and mitigates the risk of traffic conflict when non-nominal events (normal or large height deviations) occur [2]. SLOP, however, has not resulted in the desired reduction in airspace collision risk for two main reasons:

- Limited implementation: SLOP is implemented in oceanic airspace only and few aircraft use this procedure. The North Atlantic Planning Group has recently expressed concern that not enough aircraft appear to be flying the offset procedure in the North Atlantic, thus negating, in part, the safety benefits [2]. Data collected by the UKs National Air Traffic Services (NATS), which provide ATC services in the eastern part of the North Atlantic, show that less than 10% of aircraft are using SLOP due to a lack of understanding of its safety benefits [220].

- Use of fixed offset in SLOP: The underlying idea behind SLOP was that a random application of the procedure would dramatically reduce the risk of loss of separation events. The key to this dramatic reduction in risk is the randomness of offset application. To create this randomness, aircraft operator procedures must not specify any one of the three offset options (centreline, 1nm and 2nm). Most of the aircraft that fly SLOP elect to use a fixed offset of 1nm, thereby defeating the underlying idea.

Further, no review has been undertaken of the implications of such offsets, and there is minimal advice to pilots and guidelines to safety planners/ATC supervisors on such offset procedures and safety benefits [191]. Since the use of offsets could influence system safety, there is a need to develop criteria enabling the identification of where and how offsets can be safely used, including any limitations that need to be applied. Also, defining operational procedures and requirements for their application is needed to ensure that such offsets can be safely used. Thus, the key research questions are as follows. Instead of having a fixed lateral offset, can I achieve an airway-specific lateral offset that can reduce the overall airspace collision risk? Secondly, which airway and traffic features affect the optimal lateral offset value? This understanding may provide valuable insight into lateral airway offset decisions by safety planners and airline operators to mitigate collision risk in continental airspaces.

The large search space (possible solutions, i.e. lateral offset values for each airway in a continuous range) and interaction of the collision risk model with airway and traffic features make traditional search methods unsuitable for this kind of problem [13]. Nature-inspired techniques such as evolutionary computation [20] have emerged as an important tool to address this kind of problem. In this chapter, I propose an evolutionary framework in which I use: differential evolution [211], a population-based search approach, as a lateral offset optimiser; air traffic simulator ATOMS [11] as a simulator for a given traffic scenario; ICAO collision risk model [119] as an evaluator of collision risk; and a multiple regression model as an identifier of correlation between airway-traffic features and optimal lateral offset.

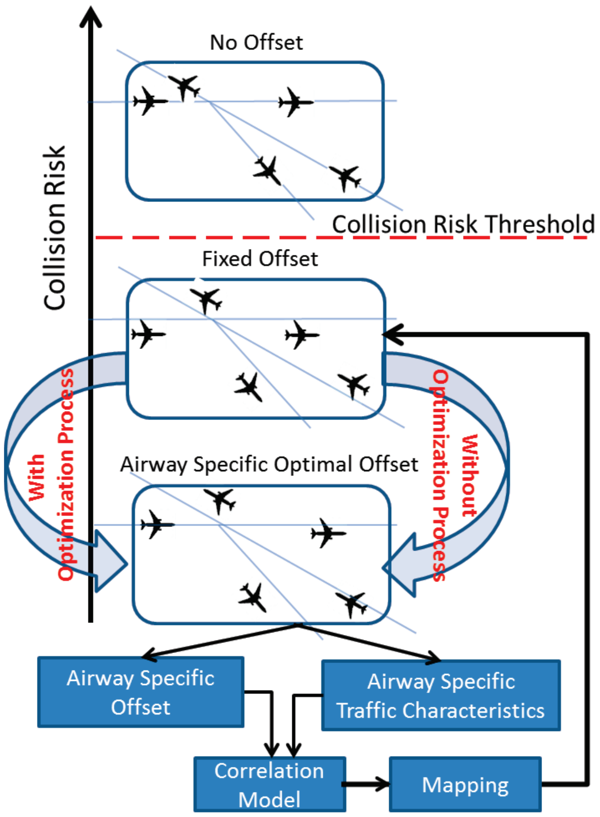

FIGURE 6.3: Proposed approach for airspace collision risk management

Figure 6.3 illustrates, in an abstract manner, the proposed approach. As shown, let us assume that, for a given set of traffic data, airspace and time period, its collision risk is assessed to be above a certain threshold (no offset scenario). Applying a fixed lateral offset of 1nm or 2nm to the right of the airway centreline may reduce collision risk (fixed offset scenario). Our approach is to design a framework that not only estimates the optimal lateral offset for each airway in the given airspace such that the overall collision is reduced, but also identifies the airway and traffic features that affect the offset value to predict the optimal lateral offset values without the need for an optimisation process. This approach is important because any optimisation process for such a large number of possibilities is inherently an expensive process (computation time and resources) and would be impractical to run frequently.

6.3 Navigation Precession and Collision Risk

The RVSM safety assessment shows that the precision of lateral navigation is an important factor with regard to vertical collision risk [120]. A general assumption is that 50% of the flying time is being made with GNSS navigation and the remaining 50% with VOR/DME navigation, while extended use of GNSS navigation should have a risk-increasing effect. For example, an increase of the GNSS flight time proportional to 75% would cause the estimate of the technical vertical risk to increase by a factor of approximately 1.5nm [120]. Therefore, the risk mitigating effects of lateral offset are significant. Further, there is no practical difference between two aircraft colliding on a 'fixed'airway and two aircraft colliding that are coincidentally flying the same random route. Also, there is no difference between two aircraft colliding on a fixed airway or two aircraft colliding over the same random waypoint contained in each of their random routes. In each instance, the collision might be avoided if one, or both, aircraft is flying an offset.

6.3.1 Vertical Collision Risk

A mid-air collision between two aircraft nominally separated by 1,000ft could occur only if either one or both aircraft were to deviate vertically from their assigned flight level such that the vertical separation between the aircraft is lost. There are two main reasons why an aircraft may not be at its assigned flight level: normal height deviations and large height deviations. Normal height deviations arise because of typical assigned altitude deviation (AAD) and altimetry system errors (ASE), whereas large height deviations occur because of operational issues such as a level burst or a TCAS alert. The focus of this paper is on normal height deviations that happen for purely technical reasons. Technical vertical risk is computed, with the use of a mathematical model, using historic flight data and takes into account, among several factors, the accuracy of navigation, the airway structure, the aircraft population and the total flying time within the region.

6.3.2 Strategic Lateral Offset Procedure (SLOP)

SLOP are ICAO-approved procedures [118] that allow aircraft to fly on a parallel track to the right of the centreline relative to the direction of flight to mitigate the vertical overlap probability due to navigational accuracy and wake turbulence encounters in oceanic and remote airspace. As illustrated in Figure 6.4, SLOP allows crews the discretion to fly either on the airway centreline or, conversely, offset to the right by a maximum of 1nm or 2nm depending upon the spacing between route centrelines (30nm or more) in oceanic or remote airspace. The decision to apply a strategic lateral offset shall be the responsibility of the flight crew. The flight crew shall apply strategic lateral offsets only in airspace where such offsets have been authorised by the appropriate ATS authority and when the aircraft flight management system (FMS) is equipped with automatic offset tracking capability.

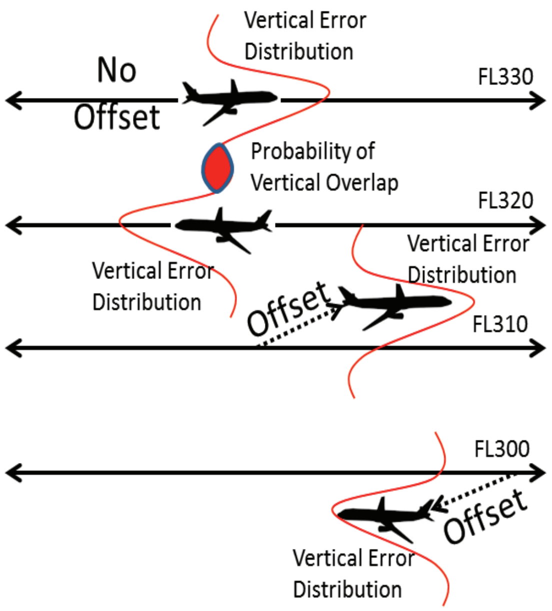

Figure 6.4: Vertical collision risk due to vertical error distribution, with and without lateral offset on adjacent flight levels

6.4 Problem definition

The problem formulation consists of two stages. First is the optimisation stage, in which the optimal lateral offset for each airway is determined such that overall airspace collision risk is minimised; the second is the correlation stage, in which, for a given optimal lateral offset of an airway, correlation, if any, with that airway and traffic features is identified such that the optimal lateral offset can be estimated. This is formulated as follows:

6.4.1 Optimization Stage

Differential evolution [211] is a stochastic, population-based optimisation algorithm belonging to the class of evolutionary computation algorithms. Differential evolution algorithms are highly effective in optimising real valued parameter (lateral offset values in our case) and real valued function (minimising collision risk in our case). They are also highly effective in finding approximate solutions to global optimisation problems (airspace collision risk in our case) [187].

Given an airspace Z with J airways and traffic data D_i where $i = 1$ to m where m is the number of aircraft flying through airspace Z, determine the lateral offset in the direction of traffic (right of the airway centreline) to a maximum of Knm in decimal latitude interval for each airway N' such that it minimises the overall collision risk of the airspace Z. The optimisation function is expressed as follows:

$$minf(CR)_Z s.t.(N_z \rightarrow N_z{}'), whereN_z{}' \in [0, K] \tag{6.1}$$

$$\begin{aligned} \text{minimize} \quad & f(CR)_Z \\ \text{subject to} \quad & (N_z \rightarrow N_z{}') \\ & N_z{}' \in [0, K] \\ & N_z{}' \succeq 0. \end{aligned} \tag{6.2}$$

6.4.2 Correlation Stage

Our primary goal in this stage is to determine the best set of parameters (airway and traffic features), such that the model predicts experimental value y^* (lateral offset) of the dependent variable y as accurately as possible. I also determine whether the model itself is adequate to fit the observed experimental data and check whether all terms in our model are significant. The function is expressed as follows:

$$\begin{aligned} & y^* = b_0 + b_1 x_1 + b_2 x_2 + ... + b_n x_n \\ & \text{subject to} \\ & minimize f(r_j) = y_j^* - y_j \end{aligned} \tag{6.3}$$

Where y is the dependent variable (predicted by a regression model), y^* is the dependent variable (experimental value), b_0 is the intercept (constant), $x_(i)$ $(i = 1, 2, n)$ is the ith independent variable from the total set of p variables, $b_i (i = 1, 2, ..., n)$ is the ith coefficient corresponding to $j = 1, 2, ..., n$ are data points.

6.5 Methodology

6.5.1 Evolutionary Framework

The proposed methodology intends to evolve the optimal lateral offsets for each airway in a given airspace such that it minimises the overall collision risk, as illustrated in Figure 6.5. There are two set of processes in the methodology, illustrated with two different shaded schemes. The process components depicted in white are of air traffic simulation, which evaluates a given set of traffic data for collision risk in an airspace with lateral offset applied. The process components depicted in blue are of evolutionary computation, which involves differential evolution to evolve optimal lateral offset values using evolutionary operators.

In the evolutionary computation process part, I first establish upper and lower bounds for airway offset (in nm). I then randomly initialise (within these bounds) a population of solutions representing a set of vectors in which the size of each vector is equal to the number of airways, i.e. each vector comprises offset values for each airway in a given airspace. These vectors undergo mutation and recombination to generate two vectors, which I call the target vector and the trial vector. These two vectors compete with each other with their set of offset values in the air traffic simulator. The vector that minimises the collision risk for a given set of traffic data is admitted to the next generation and the process continues until maximum generation is reached. At this stage, the best performing solutions (vectors) are selected from the final population.

6.5.2 Chromosome Representation

The solution vectors are encoded into a genetic data structure (chromosome) to facilitate the exchange and crossover of information in the evolutionary process

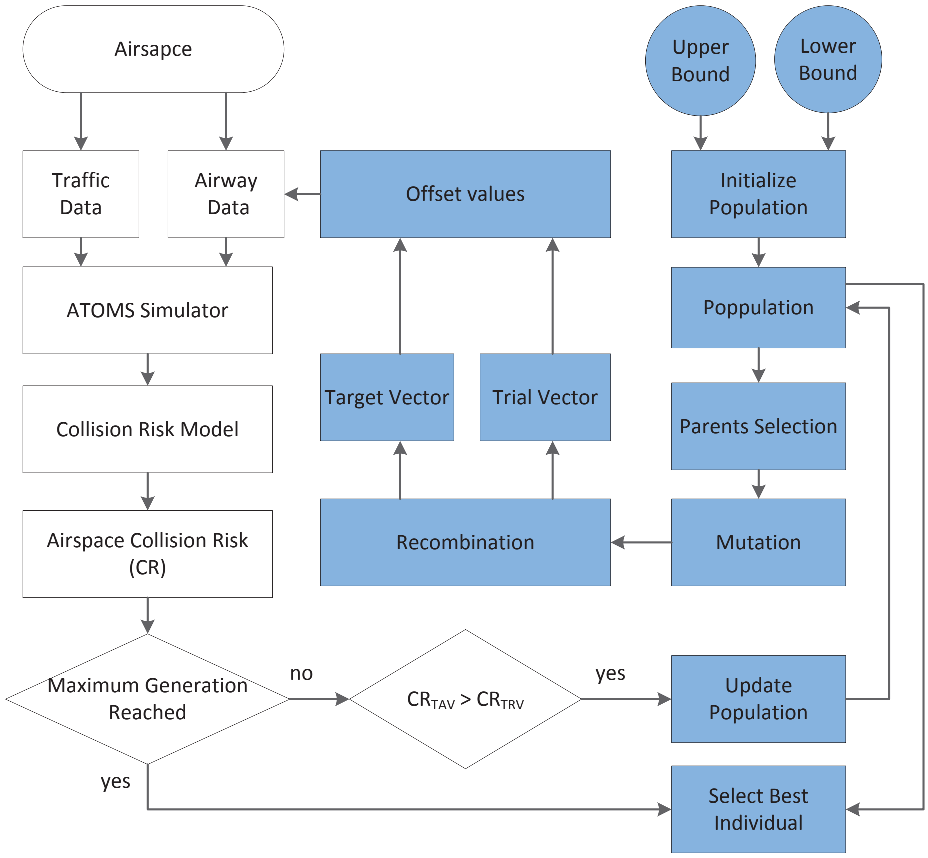

FIGURE 6.5: Airspace network optimisation methodology by airway's offset evolution

of optimisation. Each population of solutions consists of several chromosomes, depending upon the population size, as illustrated in Figure 6.6. Each chromosome represents a set of lateral offset values that would be applied to each airway. For example, if there are n airways, then there will be n offset values in a given chromosome, one for each airway.

6.5.3 The Airway Structure and Lateral Offset

I have chosen the maximum lateral offset as 4nm to the right of the airway centreline. This value is based on the continental airspace airway structure in a radar control environment. As illustrated in Figure 6.7, this offset may be widened if the midpoint between two NAVAIDS is more than 51nm.

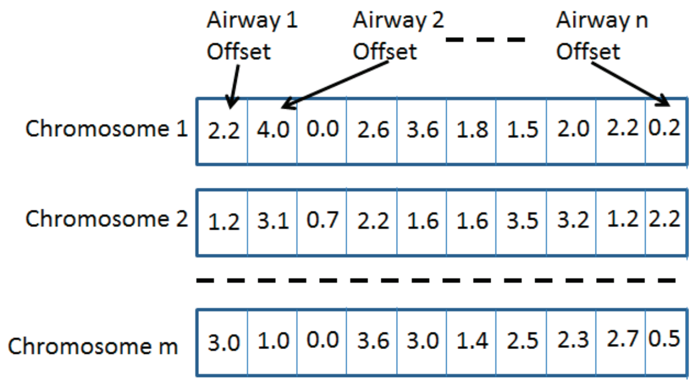

FIGURE 6.6: Chromosome design with offset values for each airway for a traffic scenario

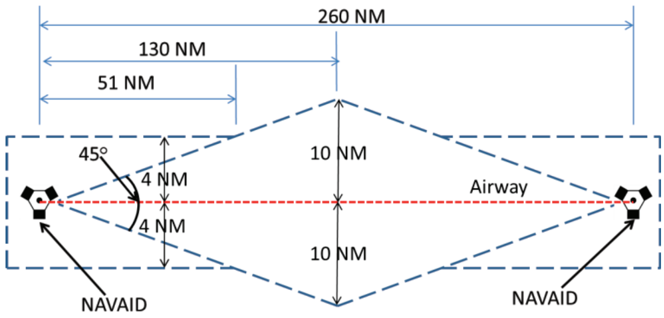

FIGURE 6.7: Airway structure with 4nm spacing from airway centreline if distance between two VOR is less than 51nm

6.5.4 Evolution Process

Given function F to optimise with D real parameters. First select the size of the population N (it must be at least 4). The parameter vectors have the form:

$$x_i, G = [x_{1,i,G}, x_{2,i,G}; ...x_{D,i,G}], i = 1, 2, ..., N \tag{6.4}$$

where G is the generation number.

In the initialisation phase, I define the upper and lower bounds for each parameter such that:

$$x_i^L \leq x_{j,i,1} \leq x_j^U \tag{6.5}$$

The lower bound is 0.0nm, i.e. the centreline, and the upper bound is 4.0nm, the maximum proposed offset value in continental airspace. I then randomly select the initial parameter values uniformly on the intervals: $[x_j^L, x_j^U]$.

After initialisation, each of the N parameter vectors undergoes mutation, recombination and selection. In the mutation phase, which expands the search space, for a given parameter vector $x_{i,G}$ I randomly select three vectors $x_{r_1,G}, x_{r_2,G}$ and $x_{r_3,G}$ such that the indices i, r_1, r_2 and r_3 are distinct. I then add the weighted difference of two of the vectors to the third:

$$v_{i,G+1} = x_{r_1,G} + F\,(x_{r_2,G} - x_{r_3,G}) \tag{6.6}$$

The mutation factor F is a constant from $[0, 2]$ $v_{i,G+1}$ and is called the donor vector.

Recombination incorporates successful solutions from the previous generation. The trial vector $u_{i,G+1}$ is developed from the elements of the target vector, $x_{i,G}$ and the elements of the donor vector, $v_{i,G+1}$. Elements of the donor vector enter the trial vector with probability CR.

$$u_{j,i,G+1} = \begin{cases} v_{j,i,G+1} & \text{if } rand_{j,i} \leq CRorj = I_{rand} \\ v_{j,i,G} & \text{if } rand_{j,i} > CRandj \neq I_{rand} \end{cases} \tag{6.7}$$

$rand_{j,i} \sim U[0, 1]$, I_{rand} is a random integer from $[1, 2, ..., D]$ and I_{rand} ensures that $v_{i,G+1} \neq x_{i,G}$.

In selection, the target vector $x_{i,G}$ is compared with the trial vector $u_{i,G+1}$ and the one with the lowest function value is admitted to the next generation.

$$x_{i,G+1} = \begin{cases} u_{i,G+1} & \text{if } f(u_{i,G+1}) \leq f(x_{i,G}) \\ x_{i,G} & \text{otherwise} \end{cases} \tag{6.8}$$

Mutation, recombination and selection continue until any one of the stopping criteria is reached. The best individual is selected from the final population. This represents the optimal offset values for the airways that minimise the overall collision risk.

6.5.5 Airway Traffic Features

In this chapter, I have focused on the upper airspace region, also known as the reduced vertical separation minima (RVSM) airspace, for its significance in airspace collision risk assessment. Each flight level vertically separated by 1000ft is treated as a unique airway. Even bi-directional routes are treated as unique (one of each side). Based on our previous research on collision risk assessment [11, 13], I have identified the following airway and traffic features of interest in establishing correlation between them and the optimal lateral offset:

- Airway distance (nm): This is the great circle distance from entry waypoint to exit waypoint, including intermediate waypoints for a given airway.
- Number of Aircraft: This is the number of flights that fly on a given airway (each way independent).
- Intermediate Waypoints: This is the number of waypoints on a given airway between its entry and exit waypoints.
- Average Flying Time (min): This is the average flying time of aircraft on a given airway.
- Airway Crossings: This is the number of other airways that cross a given airway.

6.5.6 Regression Analysis

The objective of regression analysis is to predict some criterion variable better. The multiple regression model determines the best set of parameters $(b_0, b_1, b_2, ...b_p)$ in the model $y_j = b_0 + b_1x_1j + b_2x_2j + ... + b_px_{pj}$ by minimising the error sum of squares. These coefficients allow us to calculate the predicted value of the dependent variable y (optimal offset).

To make specific predictions using the model, I would need to substitute all five airways and traffic features scores into the equation and then come up with the predicted offset value. The difference in the predicted offset and the actual offset is known as residual error r_j, which is the difference between the observed value y^* of the dependent variable for the jth experimental data point and corresponding value y^* given by the above regression model. If there is an obvious correlation between the residuals and the independent variable x (say, residuals systematically increase with increasing x), this means that the chosen model may not be adequate to fit the experiment. A plot of residuals is very helpful in detecting such a correlation.

6.6 Experimental Setup

I first estimate the baseline collision risk for the given air traffic data. I then estimate collision risk with 1nm offset and 2nm to the right of airways for the given traffic data. The evolutionary framework is then employed with differential evolution to find the optimal offset values for each airway along with associated airway-traffic features. The multiple regression model is applied to come up with an equation that can predict the optimal offset value for the given airway-traffic features.

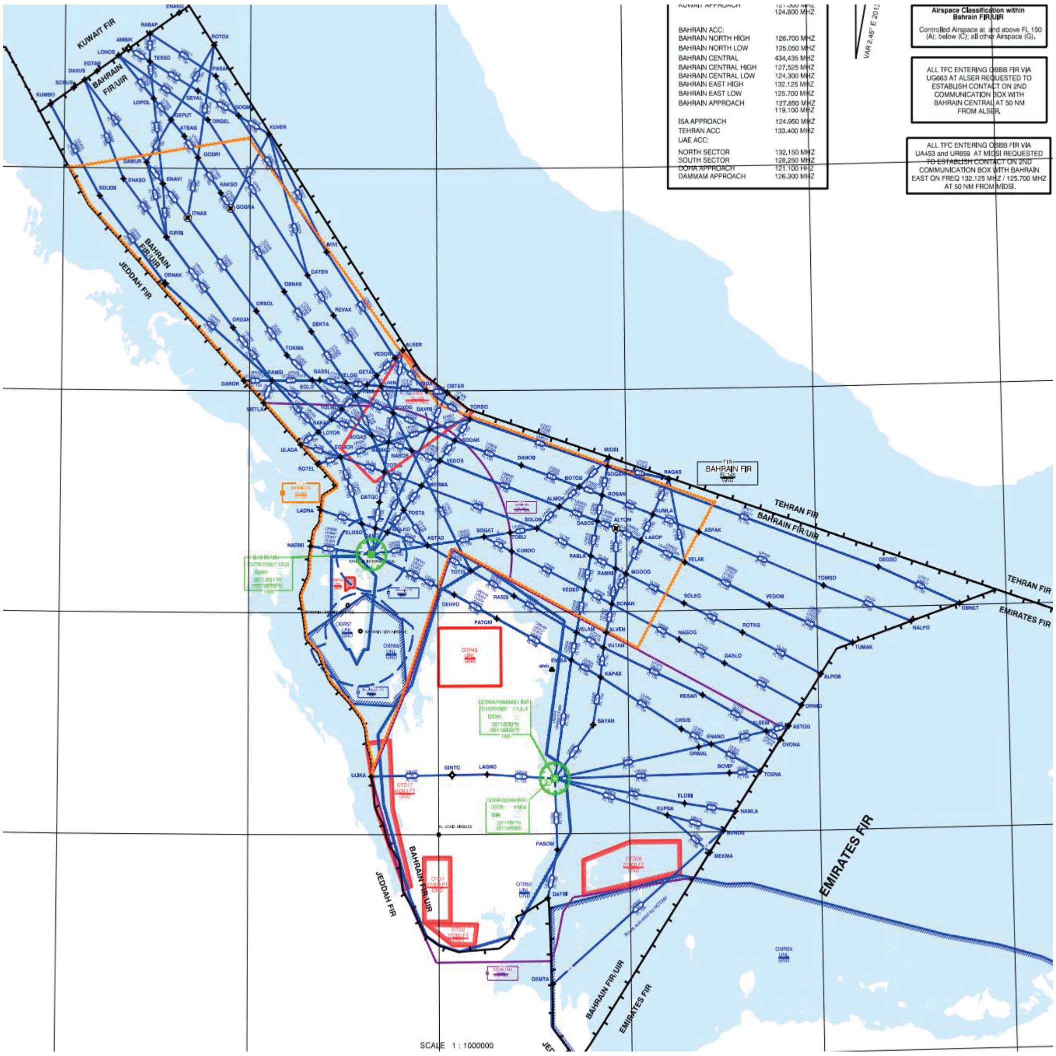

FIGURE 6.8: Bahrain RVSM airspace and airway structure

6.6.1 Test Network

For the experiments, I used the Bahrain airspace network structure and one-day traffic data (710 flights). The traffic data used was of Bahrain upper airspace network, i.e. RVSM with FL290 to FL4190, inclusive. Thus, there were 13 flight levels and I treated each airway uniquely, even bi-directional airways. In total, there were 94 airways in the Bahrain airspace. Figure 6.8 illustrates the Bahrain airspace, which is characterised by three well-identified crossing meshes.

For the Bahrain region, it is assumed that 75% of flights use GNSS and 25% use VOR/DME for navigation. Following the RVSM global system performance specification, the standard deviation for VOR/DME navigation is taken as 0.3nm and a standard deviation of 0.06123nm will be used for the GNSS, i.e. $\sigma_{VOR/DME} =$ 0.3nm and $\sigma_{GNSS} = 0.06123$nm.

6.6.2 Collision Risk model

The ICAO collision risk model [119] is used to compute vertical collision risk. The ICAO collision risk model is different to the basic Reich collision risk model because of the complexity and variability of the traffic patterns in most of the continental radar-controlled airspace for which it accounts. The model has three main parameters: the probability of vertical overlap, the frequency of horizontal overlap events per flight hour and the weighted average of kinematic factors. The latter is the combined parameters dependent on the geometry of the proximate pairs.

6.6.3 Evolution Parameters

For the DE process, the number of generations is set to 100, and the population size (individual solutions) is set to 30. This implies that, for the traffic scenario, there are 30 independent sets of airways offset (in nautical miles) with the bound of 0nm to 4nm with 0.1nm for 710 flights, and the evaluation is repeated 100 times.

For the evolutionary process, the DE mutation parameter F is set to 0.25. To find a proper crossover rate, I have performed experiments with different crossover rates. Figure 6.9 shows the best fitness value after the final generation for different crossover rates ranging from 0.05 to 1.0. From Figure 6.9, I found that the best fitness value is lowest for a crossover rate of 0.65. As a result, the crossover rate for the DE is set to 0.65 for subsequent analysis.

All experiments were run independently on the National Super Computing Facility with a cluster based on Intel Sandy Bridge 8-core processors (2.6 GHz) and 160TB of main memory.

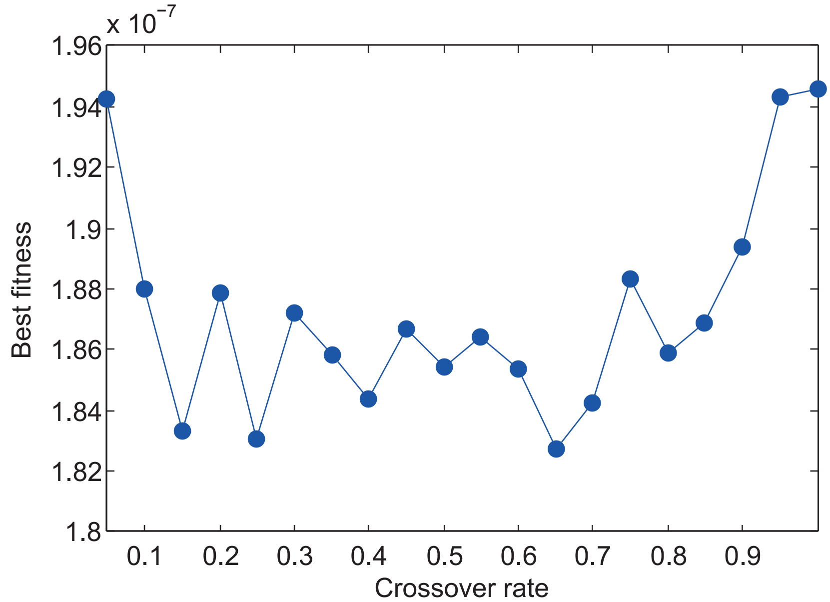

Figure 6.9: Fitness value after the final generation with different crossover rates

6.6.4 Air Traffic Simulator

For air traffic scenario simulation, I have used the Air Traffic Operations and Management Simulator (ATOMS). ATOMS is a high-fidelity, 4D, point-mass model-based, five degrees of freedom air traffic simulator developed by the lead author. The collision risk model is integrated into ATOMS such that every flight pair is evaluated, in each discrete time interval, for collision risk. Thus, ATOMS is used as the evaluation objective function for traffic scenarios: every time it is called with a scenario, it computes the collision risk and other parameters.

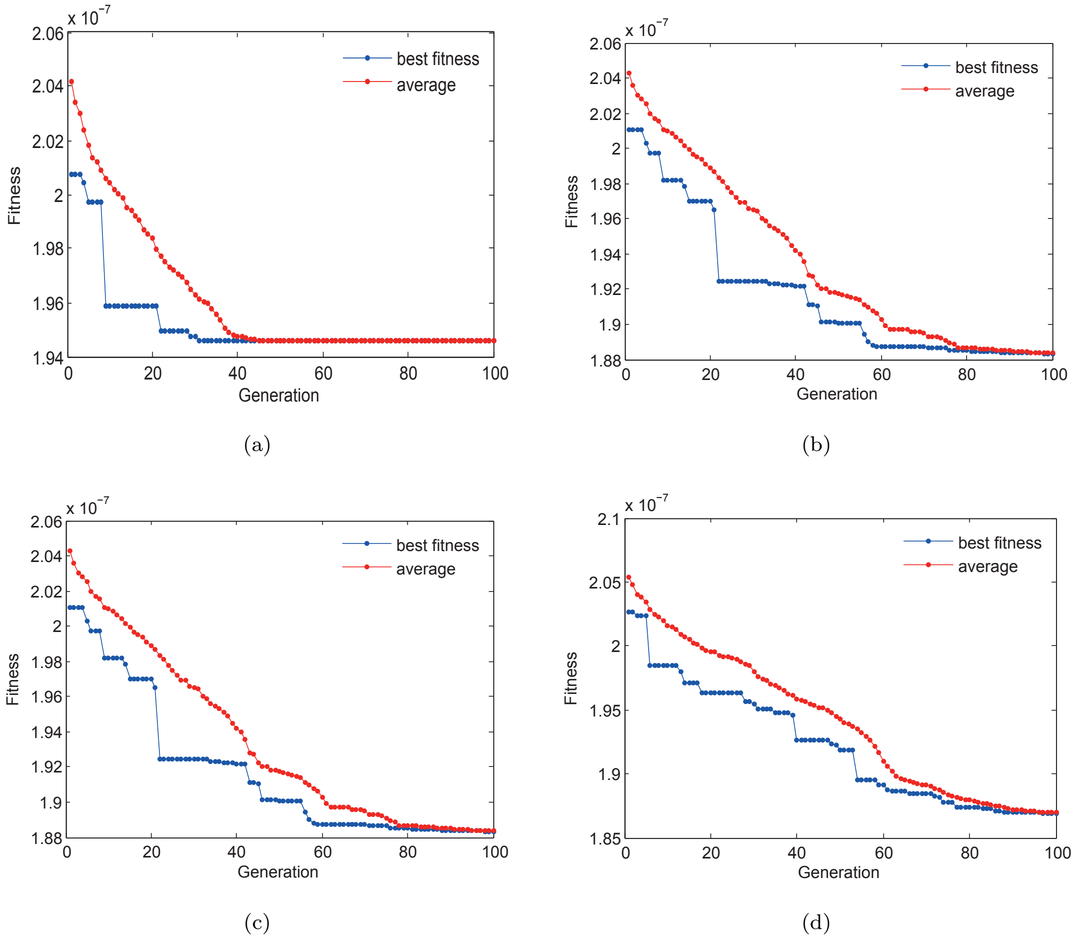

FIGURE 6.10: Convergence of DE process over 100 generations

6.7 Results and Analysis

The collision risk per flight hour for baseline traffic without any offset is 2.951×10^{-7}, 1nm offset to the right is 3.01×10^{-7}, and 2nm offset to the right is 2.94×10^{-7}. I then present how the evolution progressed over 100 generations. As shown in Figure 6.10, the evolutionary process manages to drive the population of initial solutions towards the optimal solution (to minimise the overall collision risk). Initially, the average collision risk, with randomly initialised lateral offset values in the interval of [0.0-4.0]nm for each airway, was 2.06×10^{-7} collisions per flight hour and the best solution in that population had the fitness value of 2.02×10^{-7} collisions per flight hour. By the 100th generation, the upper limit on number of generation, the DE process appears to have converged, and the best solution for the average fitness for different runs are reported in Table 6.1. Table 6.1 illustrates the effectiveness of the DE process in evolving solutions (lateral offsets) for individual airways such that the overall collision risk of a given airspace and traffic data is minimised.

Table 6.1: Best Fitness Value after 100 Generations

Run ID	Best fitness	Run ID	Best fitness
1	1.94×10^{-07}	11	1.86×10^{-07}
2	1.88×10^{-07}	12	1.85×10^{-07}
3	1.83×10^{-07}	13	1.83×10^{-07}
4	1.88×10^{-07}	14	1.84×10^{-07}
5	1.83×10^{-07}	15	1.88×10^{-07}
6	1.87×10^{-07}	16	1.86×10^{-07}
7	1.86×10^{-07}	17	1.87×10^{-07}
8	1.84×10^{-07}	18	1.89×10^{-07}
9	1.87×10^{-07}	19	1.94×10^{-07}
10	1.85×10^{-07}	20	1.95×10^{-07}

Table 6.2 tabulates the evolved lateral offset values, in the best individual of the final population, for 94 airways in the Bahrain airspace. The table also shows the airway and traffic features (distance, intermediate waypoints, number of crossings, number of flights and average flying time). I then present the frequency chart for the offset values in the range of [0.0, 4.0] for the best individual of the evolved population after 100 generations. Figure 9 shows the number of occurrences of offset values for each value on the range discretised by 0.1nm.

Table 6.2: Evolved optimal lateral offset value for each airway and features of the best individual in the final population

Airway ID	Distance (NM)	Number of turns	Number of crossing	Number of Flight	Average Fly Time	Evolved offset (NM)
0	93.74	2	10	9	13.67	3.00
1	275.15	3	19	98	41.60	1.10

Continued on next page

Table 6.2 – *Evolved Optimal Lateral Offset Value for Each Airway and Features of the Best Individual in the Final Population*

Airway ID	Distance (NM)	Number of turns	Number of crossing	Number of Flight	Average Fly Time	Evolved offset (NM)
2	279.52	5	21	39	46.03	1.40
3	160.00	1	14	100	25.33	0.10
4	133.80	1	14	0	0.00	2.40
5	154.83	2	16	1	29.00	1.40
6	149.11	2	15	0	0.00	3.20
7	151.26	2	17	14	26.14	1.40
8	104.59	1	5	0	0.00	2.90
9	102.16	1	7	0	0.00	2.90
10	104.59	1	5	0	0.00	0.80
11	102.16	1	6	4	11.50	2.50
12	143.06	2	11	18	15.78	3.30
13	88.19	2	12	0	0.00	0.90
14	133.38	3	17	2	17.00	2.80
15	145.49	1	15	6	17.33	1.70
16	23.59	1	8	0	0.00	1.40
17	44.62	1	12	0	0.00	1.80
18	38.69	1	12	0	0.00	3.30
19	86.16	1	13	1	9.00	2.70
20	193.46	1	16	3	22.33	2.10
21	180.10	1	19	0	0.00	0.80
22	98.15	1	8	0	0.00	1.90
23	37.84	0	13	0	0.00	1.90
24	215.06	3	19	6	23.17	3.10
25	202.47	1	23	83	21.87	1.30
26	158.64	4	23	0	0.00	0.20
27	179.67	4	25	0	0.00	3.00
28	173.95	5	24	0	0.00	0.60
29	133.94	2	18	0	0.00	1.20
30	248.42	5	27	45	35.13	0.10
31	261.41	6	30	2	36.00	0.90
32	46.31	0	4	0	0.00	3.00
33	289.37	4	16	114	30.91	0.90
34	281.21	4	23	6	30.17	1.40
35	46.31	0	4	0	0.00	2.50
36	55.82	1	14	0	0.00	1.10

Continued on next page

Table 6.2 – *Evolved Optimal Lateral Offset Value for Each Airway and Features of the Best Individual in the Final Population*

Airway ID	Distance (NM)	Number of turns	Number of crossing	Number of Flight	Average Fly Time	Evolved offset (NM)
37	77.01	0	18	0	0.00	3.30
38	71.29	1	17	0	0.00	2.10
39	37.84	0	13	5	5.80	1.20
40	73.44	1	19	0	0.00	0.60
41	88.18	0	14	0	0.00	4.00
42	101.17	1	17	0	0.00	3.90
43	76.69	1	18	0	0.00	2.90
44	96.93	2	18	0	0.00	1.10
45	91.21	2	17	0	0.00	0.90
46	98.13	1	17	7	13.71	2.20
47	93.36	2	19	0	0.00	1.30
48	92.48	5	17	0	0.00	3.70
49	250.42	5	27	28	67.79	1.10
50	251.24	6	25	0	0.00	1.60
51	113.46	2	10	8	37.75	1.30
52	108.39	5	22	0	0.00	1.70
53	263.42	5	30	2	64.00	3.10
54	264.24	6	28	1	44.00	1.20
55	126.45	2	13	0	0.00	1.30
56	133.28	2	15	13	19.92	2.80
57	194.80	2	19	8	25.25	3.50
58	178.25	2	21	0	0.00	3.60
59	87.50	2	16	0	0.00	2.70
60	55.82	1	14	0	0.00	0.20
61	153.84	3	16	6	26.50	1.80
62	154.66	4	14	0	0.00	0.90
63	16.58	0	4	0	0.00	1.20
64	154.02	3	17	1	14.00	1.80
65	215.55	2	21	0	0.00	3.40
66	199.00	2	23	0	0.00	0.90
67	108.25	2	18	0	0.00	1.20
68	77.01	0	18	0	0.00	2.50
69	175.44	4	22	0	0.00	1.60
70	176.26	5	20	0	0.00	0.80
71	38.49	1	6	0	0.00	2.60

Continued on next page

Table 6.2 – *Evolved Optimal Lateral Offset Value for Each Airway and Features of the Best Individual in the Final Population*

Airway ID	Distance (NM)	Number of turns	Number of crossing	Number of Flight	Average Fly Time	Evolved offset (NM)
72	148.30	3	17	0	0.00	2.50
73	209.83	2	21	0	0.00	1.20
74	193.28	2	23	0	0.00	3.70
75	102.53	2	18	0	0.00	3.40
76	71.29	1	18	0	0.00	0.70
77	169.72	4	22	0	0.00	3.50
78	170.54	5	20	0	0.00	3.90
79	32.77	1	6	0	0.00	2.50
80	146.78	0	9	6	15.83	3.70
81	101.30	0	8	1	15.00	3.20
82	46.00	0	11	5	5.00	0.00
83	106.17	0	19	11	11.45	2.90
84	264.41	0	16	23	30.04	4.00
85	94.47	0	4	2	10.50	0.10
86	281.96	0	4	2	31.00	0.10
87	162.61	0	8	1	19.00	0.00
88	152.48	0	14	1	29.00	0.00
89	96.62	0	11	20	22.45	0.00
90	230.64	0	29	1	42.00	3.10
91	52.62	0	3	1	19.00	3.80
92	143.80	0	10	4	21.75	0.30
93	172.41	0	18	1	19.00	4.00
94	181.31	0	19	1	18.00	3.80

Figure 6.11 shows that, for 94 airways, the DE process has come up to an even distribution of offset values in the given intervals. This implies that evenly distributed lateral offset values result in minimising collision risk in an airspace.

I then present the results from the multiple regression analysis. Table 6.3 presents the analysis of variance (ANOVA) analysis, which provides the breakdown of the total variation of the dependent variable (lateral offset) into the explained and unexplained portions. SS regression is the variation explained by the regression

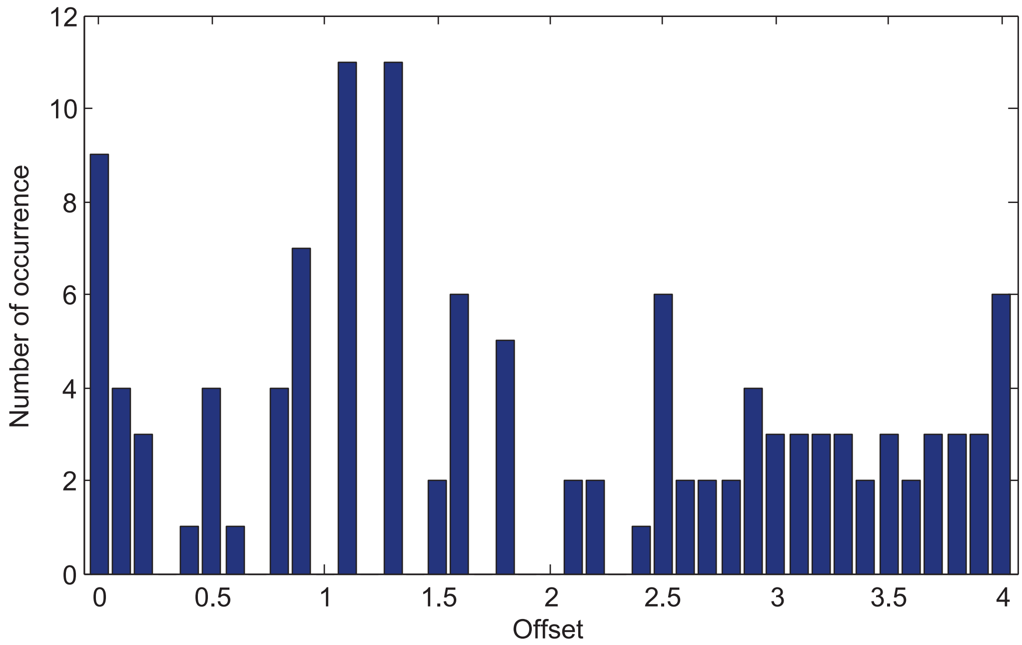

FIGURE 6.11: Offset frequency in each discrete lateral offset interval

TABLE 6.3: Analysis of Variance

Source	Degree of freedom	Adjusted Mean Square	F-Value
Regression	5	1.9729	1.40
Distance (nm)	1	0.4141	0.29
Intermediate waypoints	1	2.6341	1.86
Crossing	1	0.8990	0.64
Number of Flights	1	4.9425	3.50
Average Flying Time	1	0.421	0.30
Error	89	1.4135	
Lack-of-fit	85	1.441	1.89
Pure Error	4	0.7637	
Total	94		

line, which in our case is 9.8%, of which the number of flights (6.04%) and number of crossings (1.8%) are the main contributors. Of the 94 airways, the model was able to predict only five cases. The F-statistic is calculated using the ratio of the mean square (MS) regression; the positive F value in Table 6.2 indicates a positive correlation with the lateral offset value.

Table 6.4 presents the summary of regression statistics; the multiple correlation

Table 6.4: Summary of Regression Statistics

Multiple R	0.269646557
R Square	0.072709266
Standard Error	1.188921049
Observations	94

Table 6.5: Regression Coefficients

Term	Coefficient	Standard Error	95% Confidence Interval	T-Value	P-Value
Constant	1.809	0.355	(1.103, 2.515)	5.09	0
Distance (NM)	0.00161	0.00297	(-0.00430, 0.00751)	0.54	0.59
Intermediate Waypoints	-0.1331	0.0975	(-0.3268, 0.0606)	-1.37	0.176
Crossing	0.0222	0.0278	(-0.0331, 0.0774)	0.80	0.427
Number of Flights	-0.01259	0.00673	(-0.02597, 0.00079)	-1.87	0.065
Average Flying Time	-0.0059	0.0108	(-0.0273, 0.0155)	-0.55	0.587

coefficient is 0.269646557. This indicates that the correlation among the independent and dependent variables is positive. This statistic, which ranges from -1 to $+1$, does not indicate the statistical significance of this correlation. The coefficient of determination, R^2, is 0.072709266. This means that close to 7.2% of the variation in the dependent variable (optimal lateral offset) is explained by the independent variables (airway-traffic features).

The standard error of the regression is 1.188nm, which is an estimate of the variation of the observed optimal lateral offset, in nm, above the regression line. The results of the estimated regression line include the estimated coefficients, the standard error of the coefficients, the calculated t-statistic, the corresponding p-value and the bounds of 95% confidence intervals.

As shown in Table 6.5, the independent variables that are statistically significant in explaining the optimal lateral offset values are the number of crossings and number of flights, as indicated by (a) calculated t-statistics that exceed the critical values, and (b) the calculated p-values that are less than the significance level of 5%. Thus, the regression equation is given by (equation 6.9):

$$\begin{aligned} \textit{Evolved Offset (nm)} &= 1.809 + 0.00161 \times \textit{Distance (NM)} \\ &- 0.1331 \times \textit{Intermediate Waypoints} + 0.0222 \times \textit{Crossings} \\ &- 0.01259 \times \textit{Number of Flights} - 0.0059 \times \textit{Average Flying Time} \end{aligned} \tag{6.9}$$

I then plotted the residual plots for the number of crossings and number of flights, as shown in Figures 6.12 (6.12(a) and 6.12(b)), respectively. As there is no obvious correlation between the residuals and the independent variable lateral offset (residuals do not systematically increase with increasing crossings and number of flights), this indicates that the chosen model may be adequate to fit the experiment.

6.8 Chapter Summary

In this chapter, I proposed a differential evolutionary method to optimise an airspace network structure that assigns an optimal SLOP value to its airways such that the overall collision risk is minimised. The evolutionary process convergence and the evolved lateral offsets are evenly distributed in the respective lateral latitude bands. There is a weak correlation between airway and traffic features with only 7.2% of the variation in the dependent variable (optimal lateral offset) explained by the independent variables. The number of flights and airway crossings are two features that correlate with the optimal lateral offset, with their error residual plots indicating usefulness of the model. Applying airway-specific optimal lateral offset in an airspace may achieve the desired reduction in collision risk. Further, identifying airway and traffic features that affect the lateral offset

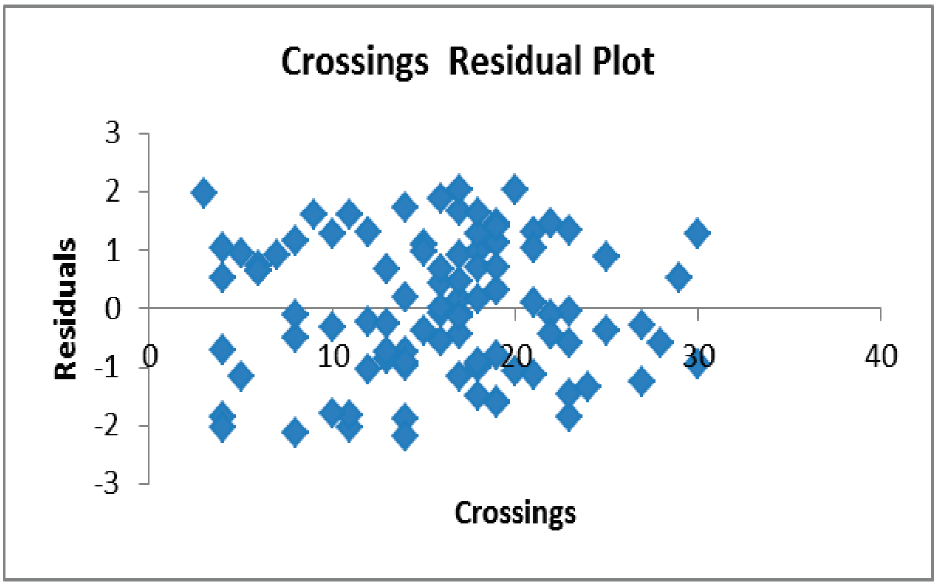

(a) Number of airway crossings

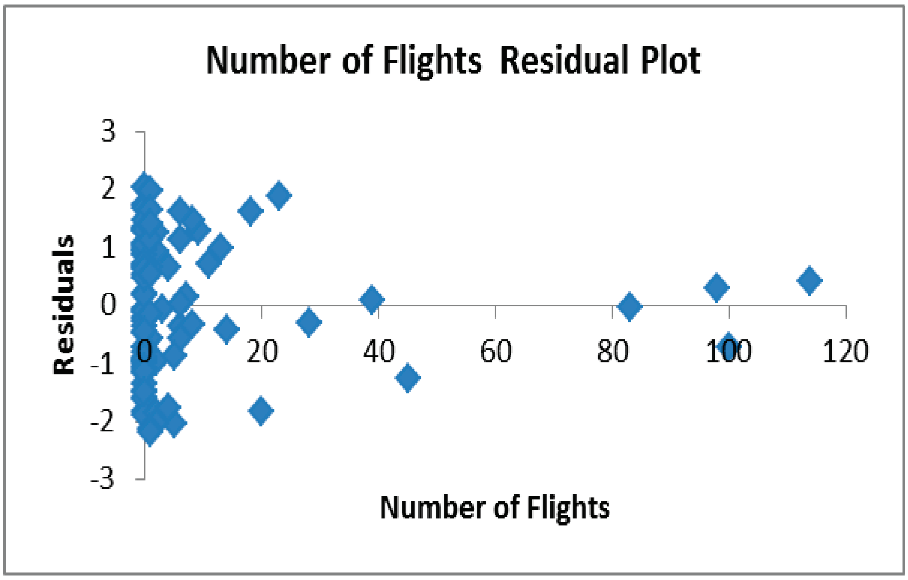

(b) Number of Flights

FIGURE 6.12: Error residual plot

may give airline safety and ATC managers an insight into how to manage traffic flow in their respective airspaces.

Chapter 7

An Integrated Air Transportation Network for Capacity-Collision Risk Relationship

This chapter is partially based on the following publication:

- Murad Hossain and Sameer Alam, *An Evolutionary Optimization Approach for Capacity-Collision Risk Trade-off Analysis in Air Transportation Network*, Journal of Transportation Research Part C: Emerging Technologies, Elsevier, *Submitted*.

In this chapter, I focus on the final research question: *how do the interactions between airport and airspace networks affect the capacity-risk trade-off?* To address this question, I develop a framework that integrates the airport network capacity estimation model (developed in Chapter 4) and the collision risk assessment method (developed in Chapters 5 and 6) for an ATN to analyse the relationship between capacity and collision. The chapter starts with a general approach to address the above research question, then a brief description of the ATN generation process followed by an evolutionary method for generating traffic scenarios for airspace collision risk estimation. Finally, the experimental setup for testing and evaluating the proposed methodology is presented.

7.1 Introduction

An air transportation network (ATN) is one of the most important components of the world transportation systems. In the near future, the ATN is expected to handle the increasingly heavy demand on air traffic. Significant research efforts are continuing to increase the capacity and safety of an ATN. Ongoing efforts to increase capacity in various ways are numerous and include SESAR [98], NextGen [184]) and procedures (dynamic sectorisation [215] and automated separation [152])).

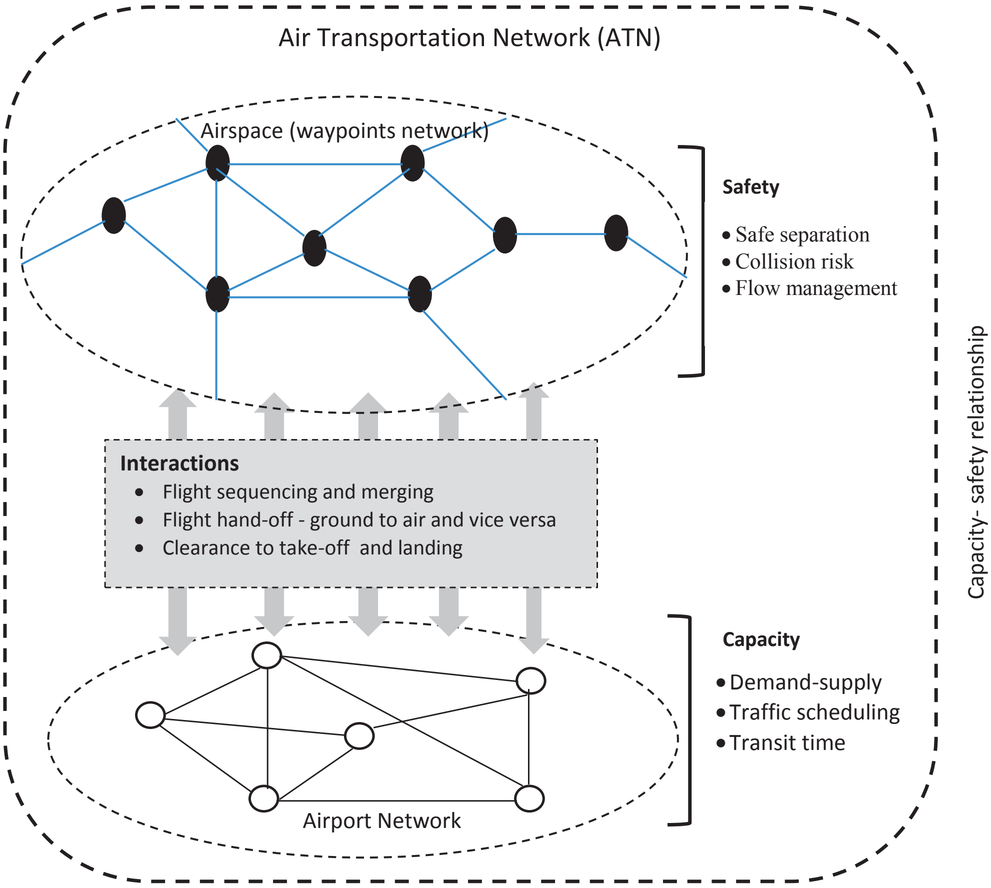

FIGURE 7.1: Interactions and constraints of airport and an airspace network in an ATN

In an ATN, it has been considered that the airspace network is relatively unconstrained and the airport network is the main bottleneck t[76, 219]. The capacity of the airport network can be increased by adding more runways or by utilising the regional airports around a countrys major airports in a hub-spoke manner. While the airspace capacity can be increased through the AAC [137] and AFM [221], the relationship between airport network capacity and airspace safety in an ATN is not fully understood [103, 229]. The interactions between these two networks, which are created by actual flow between them, plays an important role for an ATN's actual capacity estimation. Figure 7.1 shows a hypothetical representation of an airport and an airspace network and the interactions between them. Intuitively, as the aircraft density in a given volume of airspace, or even in a whole ATN, increases, without a change in control procedures, system safety will degrade as a result of more closely spaced operations [225, 229]. Therefore, it is imperative to understand the relationship between capacity and safety in an ATN. So far, the relationship between the airport network capacity and the airspace safety of an air transportation network has not been determined. A very limited body of literature exists on the safety-capacity relationship in an ATN, most of which analyse the relationship between individual elements or components of an ATN [103, 138, 225, 229]. Among the relevant literature, Bojis et al. [225] investigated the trade-off between the collision-risk capacity of an en-route corridor, Haynie [103] studied the relationship between capacity and safety in near-terminal airspace for guiding the adoption of information technology and Kopardekar et al. investigated the sector capacity and complexity.

One way of expressing this relationship is by safety-capacity curves [229], with different possible relationships shown in Figure 7.2. Identifying and understanding such a relationship between capacity and safety is vital when trying to improve the ATN so that capacity can be increased at the best cost, while maintaining or improving airspace safety. In this chapter, I propose a framework for integrating airport and airspace networks for an ATN and develop a methodology for their interactions to analyse the relationship between airport network capacity and

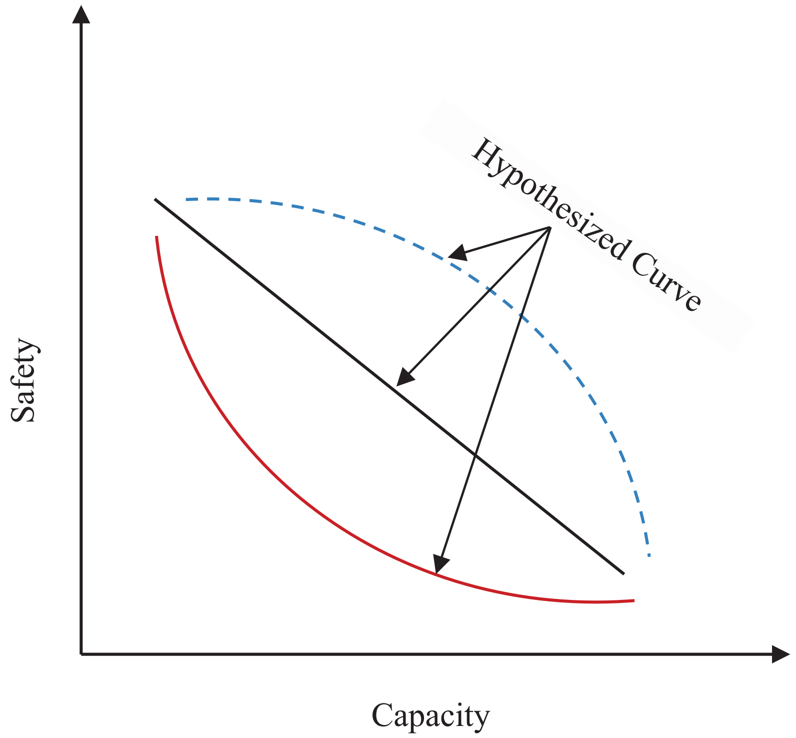

FIGURE 7.2: Hypothetical safety-capacity relationship curves

airspace collision risk.

7.2 Approach

The proposed approach for analysing the capacity-collision risk relationship for an ATN is radically different from systemic safety assessment [212] and capacity estimation [66, 91] methods, which, traditionally, have been investigated separately. In this thesis, I combine these methods to understand their interactions. For the given ATN, I define its underlying airport and airspace networks. Its capacity's upper bound is estimated from the airport network using the capacity estimation model described in Chapter 4, which I have called the flow capacity estimation module in Figure 7.3, in which I have considered the airlines preference and the environmental impact. The output of the flow capacity estimation provides hourly flow densities (flight movements per hour) and a traffic schedule consisting of scheduled departure and arrival times for each flight. The output of

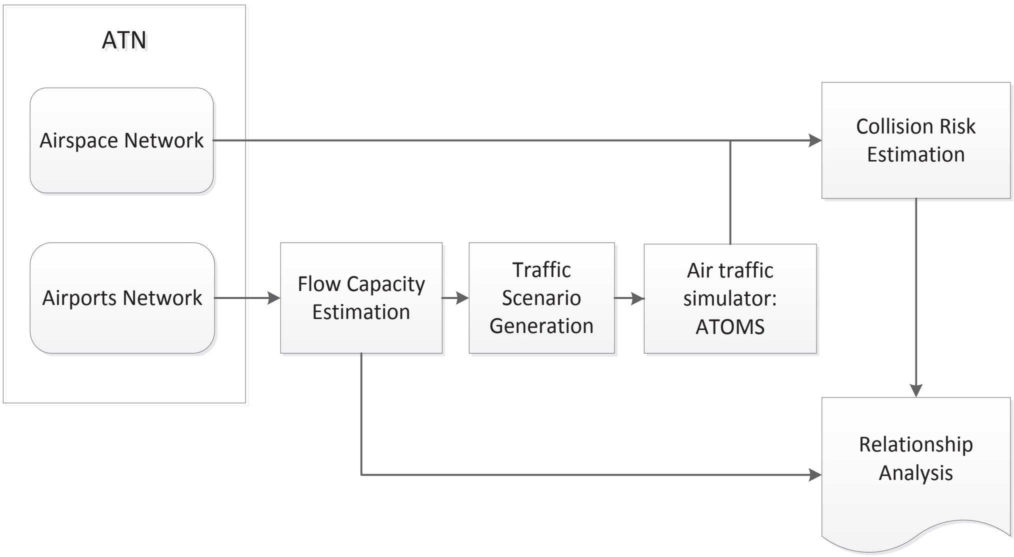

FIGURE 7.3: Conceptual approach for analysing capacity-collision risk relationship in an ATN

the flow capacity estimation module is then converted into traffic scenarios by the traffic scenario generation module. To estimate the collision risk, systematic planning is required to ensure that the given traffic scenarios are feasible and conflict free.

To generate traffic scenario(s) from a given traffic schedule is highly challenging. The large search space (possibilities) of traffic characteristics and non-linear interactions among collision risk parameters make traditional search methods such as Monte Carlo unsuitable for this kind of problem. Nature-inspired global optimisation techniques such as evolutionary computation (EC) [224] have emerged as key approaches for understanding and solving air transportation problems. I apply a differential evolution (DE) optimisation technique [187] to convert the output of the flow capacity estimation module to a traffic scenario, which I simulate in the high-fidelity air traffic simulator ATOMS [11]. The collision risk model is integrated in ATOMS to estimate the overall collision risk for a given traffic scenario and then the capacity-safety relationship curves for different traffic densities are generated and analysed. Figure 7.3 illustrates the formulation of the conceptual

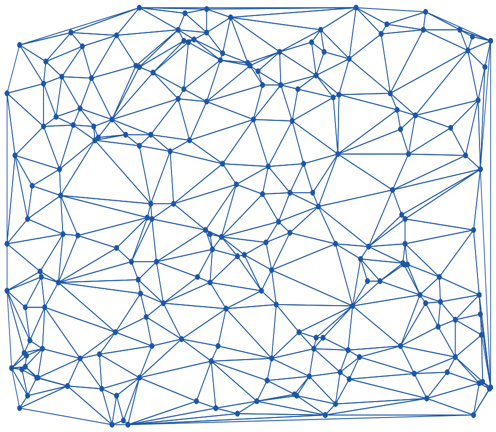

Figure 7.4: Example of Delaunay triangulation network

problem, in which the objective is to integrate and interact the two networks to gain an understanding of the relationship between capacity and collision risk.

7.3 Air Transportation Network Model

An ATN is a composite network of airports and waypoints, which links airports in different areas through a series of crossing waypoints and transmits air traffic flow, and is modelled as a time space network [108, 129, 214]. In the space domain, the height is ignored and the ATN is embedded in a two-dimensional Euclidean space, i.e. the nodes (airports and waypoints) are associated with a stationary geographical location [129]. Since the objective of this thesis is to investigate the relationship between two major sub-networks of an ATN, I model it accordingly.

7.3.1 Network Generation

An ATN can be generated in two different ways: (i) generate a network with two different types of node, airports and waypoints; and (ii) generate the airport network and airspace network separately and then combine them. Both of the approaches will result in a similar ATN. As a result, I have considered the first

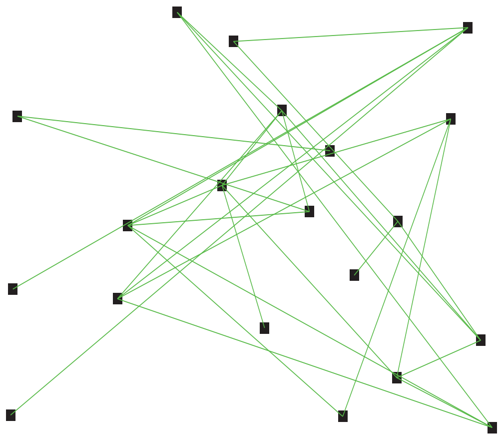

FIGURE 7.5: Random airport network configuration generated from Delaunay triangulation point set (Q)

approach only. To generate this approach, I extend the technique developed by Mehadhebi [153], which consists of the following steps.

- Firstly, a Delaunay triangulation network of Q points is created in a given area. In mathematics and computational geometry, a Delaunay triangulation for a set (Q) of points in a plane is a triangulation ($DT(Q)$) such that no point in Q is inside the circumference of any triangle in $DT(Q)$. I apply the Paul Bourke Delaunay triangulation algorithm [39] to create Q in a two-dimensional plane with no overlapping connections among the points, each of which is an associated value of its latitude and longitude, to define its geographical location. Figure 7.5 shows a Delaunay triangulation network of $Q = 500$ points in an area of 200 square nautical miles.

- As in a Delaunay triangulation network, some of the points tend to be very close to each other, I merge all the intersecting points that are too close. Although this will, in some way, increase the overall route distances, its benefit is reduced complexity of the ATN.

- As I define an ATN as a combination of an airport network and airspace network (network of waypoints), the next step is to create the underlying airport network. Let V be a set of airports chosen randomly from Q ($V \subset Q$)

with the rest of the points (QV) defined as waypoints. The connections among the airports (V) are developed using complex network generation models (random graphs [72] and small-world networks [218]) to create the topology of the airport network. In it, the connected airports are separated by at least 100 nautical miles so that a flight spends at least 70% of its travel time in the cruise phase. Figure 7.5 presents an example of an airport network with 20 airports.

- Finally, the ATN is constructed by combining the shortest paths among the directly connected airports along the Delaunay triangulation network. Letting P be the set of shortest paths for all the connected airports in the airport network, the ATN is defined as:

$$ATN = \bigcup_{p_i \in P} p_i \tag{7.1}$$

Figure 7.6 shows an ATN created from the Delaunay triangulation and airport network described in the above steps.

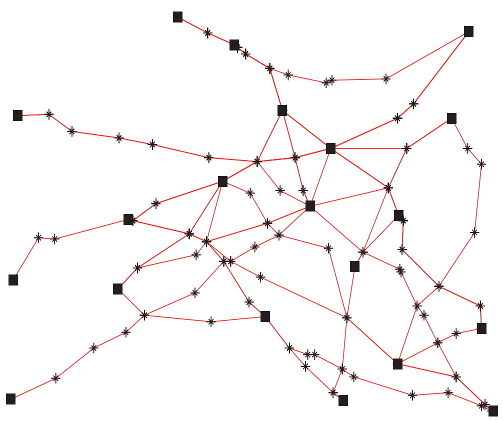

FIGURE 7.6: ATN of 20 airports (filled squares (■) represents present airports and stearics (∗) waypoints)

7.4 Methodology

Having generated the ATN, the methodology for analysing the relationship between the airport network capacity and airspace collision risk involves the following three key stages.

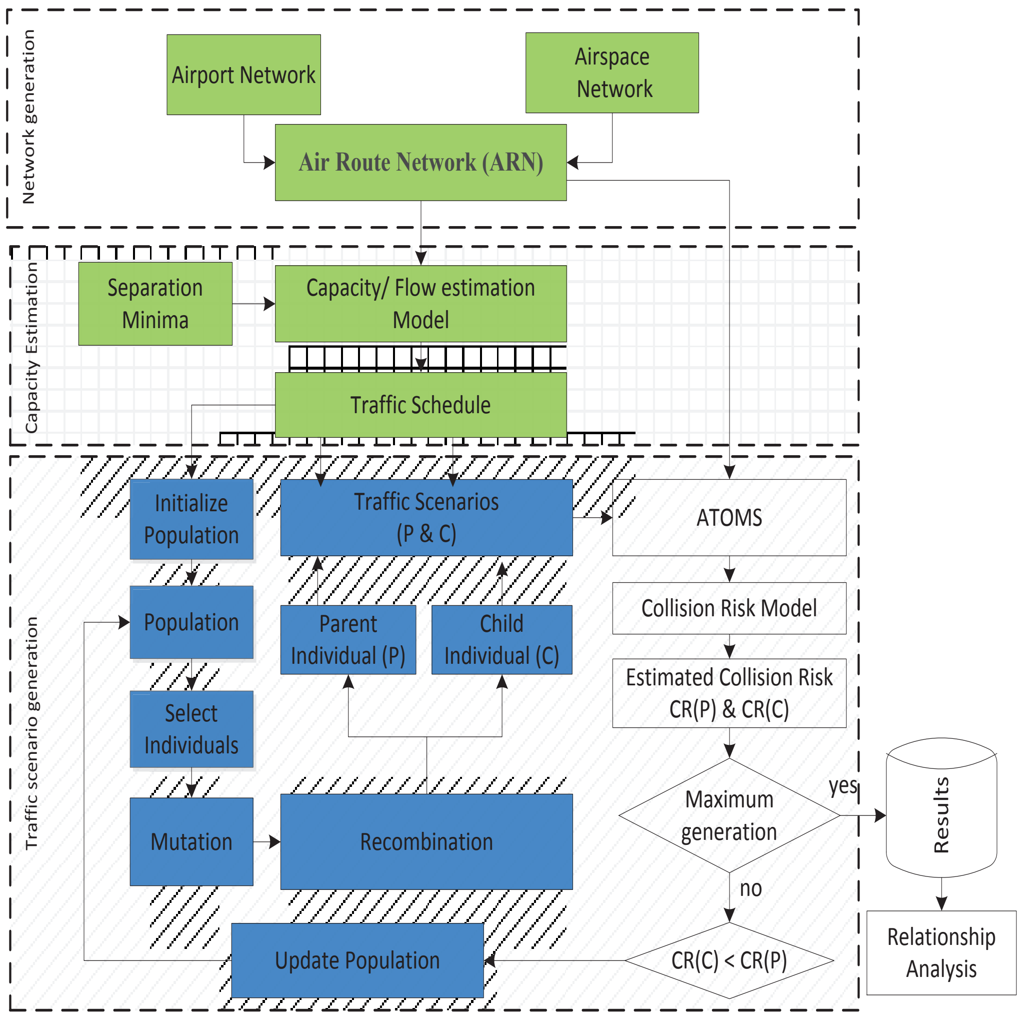

FIGURE 7.7: Evolutionary framework for analysing capacity-collision risk relationship in ATN

1. **Network Capacity Estimation:** The capacity of an ATN is defined as the maximum traffic that can be accommodated by its airport network subject to resource constraints, such as fleet mix and node/link capacity, which determines the limit of feasible flow density an air transportation network can

accommodate. The density level is controlled by the wake-vortex separation minima, with an increase in the wake-vortex separation among aircraft during landing and take-off resulting in a decrease in the hourly flow in the ATN.

2. **Traffic Scenario Generation with Defined Flow Density:** In this stage, given the flow density, a complete traffic scenario is generated in a way that minimises the overall collision risk using evolutionary optimisation. In this chapter, I have used the terms flow density and capacity interchangeably.

3. **Collision Risk Estimation**: The given traffic scenario is simulated in ATOMS to calculate the total number of flight hours and the probability of collision for each proximate pair of aircraft and, integrated with the Hsu model [110], the overall collision risk is estimated.

Figure 7.7 illustrates the process for analysing the trade-off between the flow capacity and collision risk of a given ATN. It begins with a very low flow density and, once a traffic scenario is generated, the overall collision risk for that scenario is estimated. Then, the flow density is increased and the process continues until the flow level reaches the maximum capacity bound. Once all the possible scenarios for different flow levels are evaluated, the repository data is subsequently analysed to reveal the trade-off.

7.4.1 Network Capacity Estimation

Estimating the capacity of an airport network system, I use the mathematical formulation and heuristic solution for estimating the capacity of a given airport considering different fleet mixes and travel times proposed in Chapter 4 and the time-based separation minima given in Table 4.1 to avoid wake-vortex turbulence. I also introduce some extra separation (es) between two consecutive aircraft, the value of which will serve as a control parameter for either decreasing or increasing the maximum hourly flow in the network and, when $es = 0$, the output from the capacity estimation module will provide the upper bound of the capacity (maximum attainable flow). The solution of the capacity estimation module will provide a list of flights and their scheduled departure and arrival times that I call a traffic schedule, which is then converted into a traffic scenario by assigning appropriate flight levels, speeds in different phases using a DE optimisation method and other parameters for the aircraft using ATOMS.

7.4.2 Traffic Scenario Generation

Generating traffic scenarios using simple rules or hand scripting results in a few alternatives from which to derive conclusions. In this chapter, I design a method that combines an airport network capacity estimation model (developed in Chapter 4) and an evolutionary framework to generate traffic scenarios. For a given traffic schedule, a complete traffic scenario must contain the tracks or air routes, feasible flight levels and velocities and rates of climb and descent of different flight phases for all flights. Also, since the ATN is simultaneously shared by many aircraft, the path of each and every aircraft needs to be conflict free. Therefore, converting the output from the airport networks capacity module (traffic schedule) to a traffic scenario is a complex task, to handle which I develop the following evolutionary optimisation framework.

7.4.2.1 Evolutionary Framework Design

Given an ATN and the schedule of departures and arrivals of N flights and their routes, the problem of generating a traffic scenario involves determining the flight path levels of N flights that minimise the overall mid-air collision risk. In this work, I assign the shortest path from the origin to the destination in the ATN as the flight path for each flight. If there is more than one shortest path, one is chosen randomly and the flight levels are evolved using a DE algorithm. The proposed evolutionary methodology for evolving an optimal flight level for each flight is illustrated in Figure 7.7 in which light green depicts the airport networks capacity estimations, which generate a traffic schedule; white denotes the air traffic simulation, which evaluates a given set of traffic data for collision risk in an airspace; and blue depicts the EC, which applies a DE [187] process to evolve optimal flight levels.

The DE process begins by defining the upper and lower bounds of the flight levels for each flight. It then undergoes a random initialisation (within the bounds) of a population of solutions representing a set of vectors, where the size of each vector is equal to the number of aircraft defined by the traffic schedule. Each vector is considered a traffic scenario, which is then simulated in ATOMS for its collision risk estimation, where the speeds of the flights in different stages are determined. After an initial evaluation, these vectors undergo mutation and recombination to generate two vectors, the target and trial vectors, which compete with each other. The vector that minimises the collision risk for the given traffic data is admitted to the next generation and the process continues until the maximum number of generations is reached. Then, the best-performing solutions (vectors) are selected from the final population.

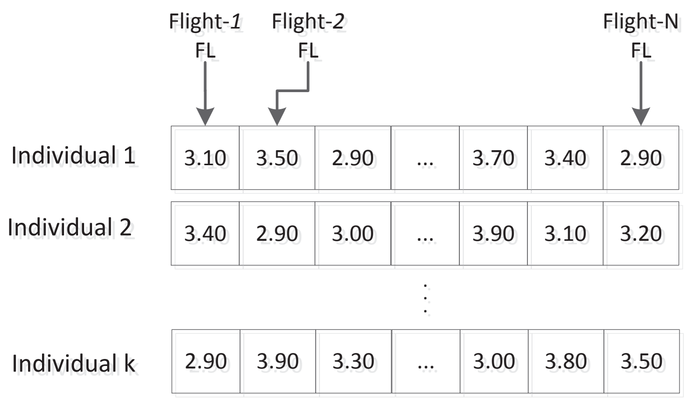

FIGURE 7.8: Chromosome design with encoded flight level (FL) for each flight in a given traffic scenario

Chromosome Representation: Since the objective of generating a traffic scenario is to evolve the right flight level for each and every flight for a given flight schedule, the flight level is encoded in a chromosome. Figure 7.8 illustrates a set of chromosomes that constitute the evolutionary population in which each chromosome represents a set of flight levels to be applied to its corresponding flight; for example, if there are N flights, there will be N flight levels in a given chromosome. In this research, I do not consider semi-circular rules of flying and I choose only flight levels FL290 (29000ft) to FL-390 (39000ft), which are encoded as real values from 2.9 to 3.9 with a precession of 1, from which the actual flight levels are calculated using the equation $FL = (encoded\ value) \times 10000ft$.

Fitness Function: The role of a fitness function in an evolutionary algorithm (EA) is to guide the search process by providing feedback on the quality of a solution represented by a chromosome in the population. Since this quality in our case depends on the estimated collision risk, I define the fitness as:

$$Fitness = min(collision\ risk) \tag{7.2}$$

Differential Evolution: To minimise the collision risk in a traffic scenario, I use a DE optimisation process, which begins with a population of M candidate solutions represented as $\vec{x}^i_{G=k} = \left[x^i_{1,k}, x^i_{2,k}, ..., X^i_{N,k}\right], i = 1, ..., M$, where the N index denotes the dimensions of an individual and G the generation to which the population belongs.

In the initialisation phase, I define the upper and lower bounds for each chromosome value $L \leq x^i_{j,G=k} \leq U, \forall j$, and set them to 2.90 and 3.90, respectively. I then randomly select the initial chromosome values uniformly in/from the intervals $[L, U]$. After initialisation, the effective evolution of DE depends on the manipulation and efficiency of three main operators, mutation, reproduction and selection. The DE algorithm applied in this research is illustrated in Algorithm 3.

Algorithm 3 Traffic Scenario Generation

Let G denote a generation, P a population of size M and $\vec{x}^{j}_{G=k}$ the j^{th} individual of dimension N in population P in generation k. cr is the crossover probability.
Input: $N, M > 4, F \in (0,1), cr \in (0,1)$
Initialize the population P
Each chromosome is a real valued vector
k=1
while (the stopping criterion is not satisfied or until maximum generation is reached) **do**
    j=0
    for all $j \leq M$ **do**
        Randomly select $r_1, r_2, r_3 \in (1, ..., M), j \neq r_1 \neq r_2 \neq r_3$
        for all $l \leq N$ **do**
            if $(random[0,1] < cr)$ **then**
                $x'_l = x^{r_3}_{l,G=k-1} + F \times (x^{r_1}_{l,G=k-1} - x^{r_2}_{l,G=k-1})$
            else
                $x'_l = x^{j}_{l,G=k-1}$
        $f(\vec{x}')$=evaluate $(\vec{x}')$
        $f(\vec{x}^{j}_{G=k-1})$=evaluate$(\vec{x}^{j}_{G=k-1})$
        if $f(\vec{x}') \leq f(\vec{x}^{j}_{G=k-1})$ **then**
            $\vec{x}^{j}_{G=k} = \vec{x}'$
        else
            $\vec{x}^{j}_{G=k} = \vec{x}^{j}_{G=k-1}$
    k=k+1

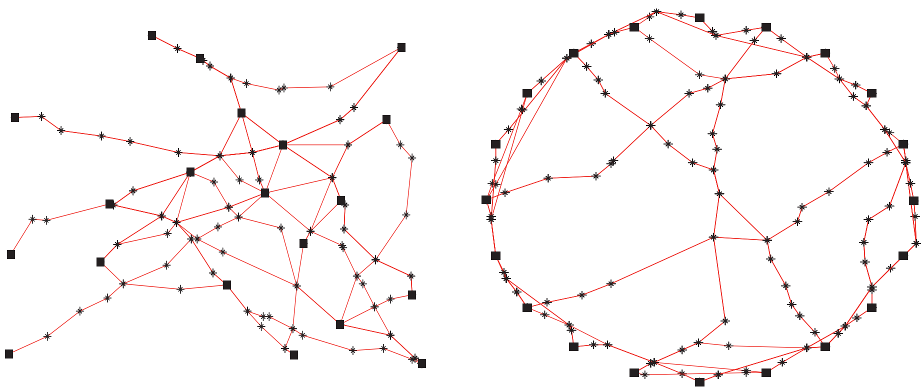

(a) Test ATN-I

(b) Test ATN-II

FIGURE 7.9: Layout of test ATNs

7.5 Experimental Setup

In the experiments, I control the flow density in the network by changing the extra separation parameter (es), starting with a low flow density of es=20 and

Table 7.1: Diameters of cylinder (in metres) for different proximity pairs

Leading Aircraft	Trailing aircraft		
	L	M	H
L	140m	150m	180m
M	150m	192m	192m
H	180m	192m	220m

then gradually decreasing it by 1. For each *es* value, I generate 20 different traffic scenarios, each with the following parameter settings, using the evolutionary framework with different seeds and then estimate the collision risk.

- Test Network: In order to assess the effectiveness of the proposed airport network capacity estimation model, I perform experiments on two different types of test network: (i) ATN-I, in which the airports and their connectivities are chosen randomly; and (ii) ATN-II, in which the locations of the airports are placed on the circumference of a circle and their connectivities are created using the small-world model [218]. Both of these networks consist of 20 airports, as shown in Figure 7.9, with the difference between them as their airport network topologies, as ATN-I is considered a random network and ATN-II a small-world network.

- Collision Risk Parameters: The Hsu collision risk models parameters are set as follows: vertical overlap probability $P_z(0) = 0.55$, vertical speed when in horizontal flight $|\dot{z}| = 1.5m/s$ and aircraft position update time $T_{min} = 0.16$ minutes. The diameter of the aircraft cylinder is set based on the aircraft type of the proximity pair, as shown in Table 7.1, whereas, the height of the cylinder is set to$\lambda_z = 55m$ for all cases.

- Evolution Parameters: In our experiments, I use a population of 50 individuals and a DE mutation factor (F) of 0.40. I conduct a series of experiments to determine the maximum number of generations for stopping and the proper

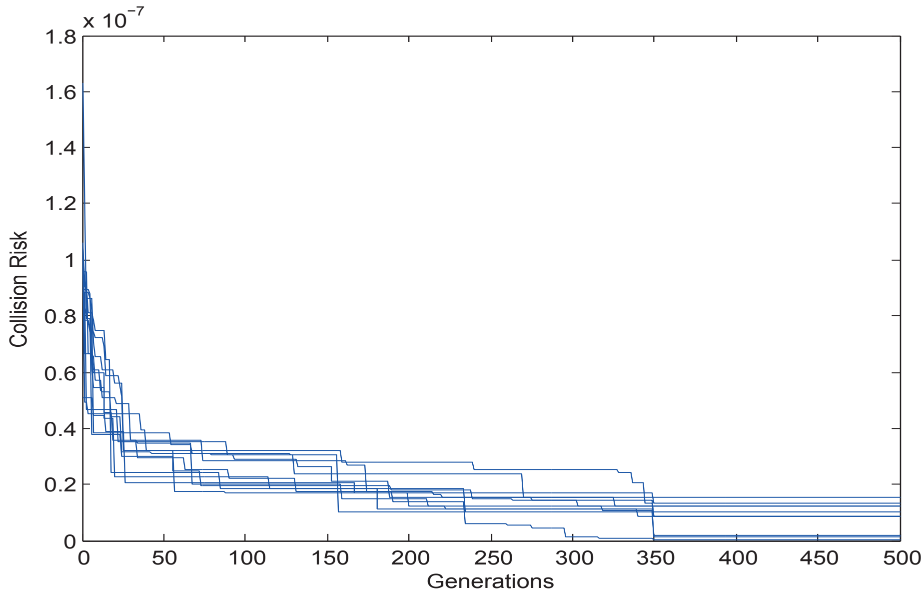

(a) Convergence of collision risk

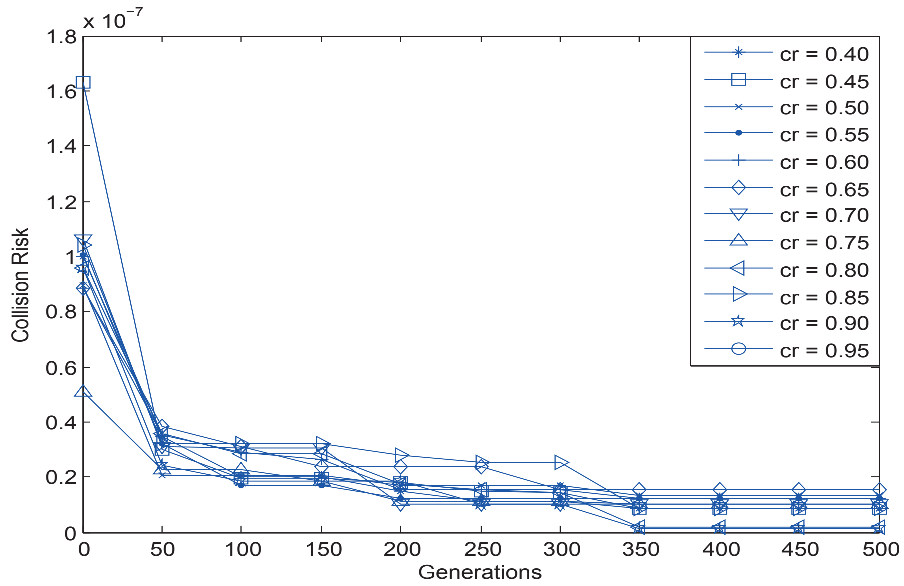

(b) Convergence of collision risk (discretisation after every 50 generations)

FIGURE 7.10: Selection of evolution parameter (maximum generation and crossover rate)

crossover rate by running the evolution for up to 500 generations using different crossover rates. Figure 7.10 shows the best fitness values (minimum collision risks) of the population over generations, from which it is clear that, after 350 generations, the best individual value does not improve in all cases.

Therefore, as I can say that 400 generations is sufficient to converge the evolution process, this is set as the stopping criterion for the DE process in the subsequent analysis.

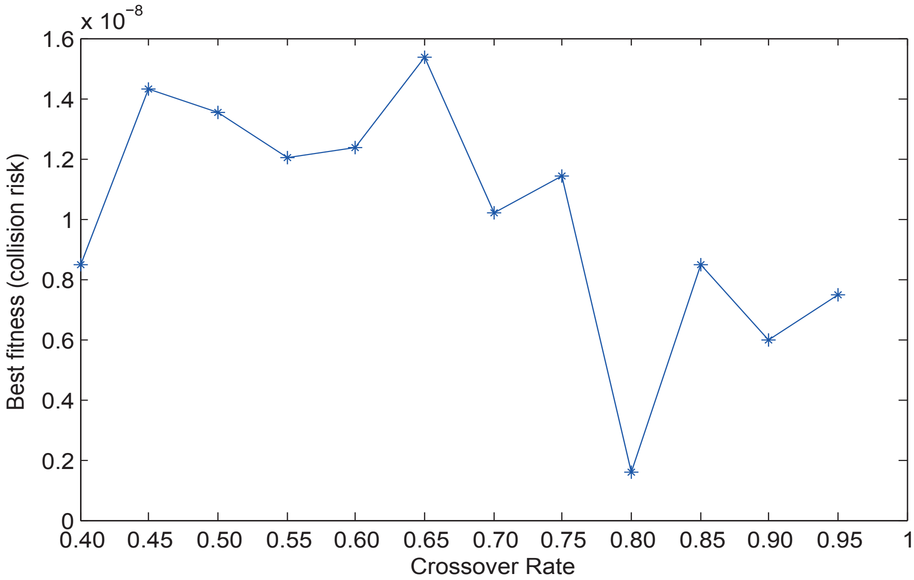

FIGURE 7.11: Best fitness values after final generation with different crossover rates (*cr*)

In order to determine a proper crossover rate, I perform experiments with different rates. Figure 7.11 shows the best fitness values after the final generation for different crossover rates (cr) ranging from 0.40 to 0.95 with an increment of 0.05 after 500 generations, which indicates that the best fitness value is the lowest for a crossover rate of 0.80. Therefore, I set the crossover rate for DE to 0.80 for the subsequent analysis.

7.6 Results and Analysis

I first present the characteristics of the test ARNs. In the test ATN-I, the underlying airport network has a uniform degree distribution, which is shown in Table 7.2. In ATN-II, the small-world topology of the airport network is created with a

Table 7.2: Connectively of the airports in ATN-I.

Node	Degree In	Degree Out	Degree Total	Node	Degree In	Degree Out	Degree Total
0	2	2	4	10	2	4	6
1	1	3	4	11	5	6	11
2	3	4	7	12	2	5	7
3	4	2	6	13	2	3	5
4	7	4	11	14	4	0	4
5	5	2	7	15	1	2	3
6	1	3	4	16	2	5	7
7	4	3	7	17	2	0	2
8	3	1	4	18	4	5	9
9	5	4	9	19	1	2	3

staring ring lattice in which every node is connected to its first $K = 4$ ($K/2$ on either side), then it undergoes a random rewiring with a probability of 0.05.

Apart from the connectivity pattern, I also present the distance in nautical miles among the connected airports and number of waypoints along the shortest path between them for ATN-I and ATN-II in Table 7.3 and Table 7.4, respectively. From Tables 7.3 and 7.4, it is clear that the minimum distances among the airport's links are $100.51nm$ and 101.59 for ATN-I and ATN-II, respectively.

Table 7.3: ATN-I link's distance and number of way points

Links	Distance (nm)	Waypoints	Links	Distance (nm)	Waypoints	Links	Distance (nm)	Waypoints	Links	Distance (nm)	Waypoints
0 , 14	341.43	6	5 , 2	154.92	3	10 , 7	537.71	8	13 , 11	176.72	3
0 , 16	225.46	3	5 , 11	565.58	7	10 , 8	417.47	4	15 , 4	100.51	2
1 , 0	628.55	6	6 , 7	333.96	5	11 , 0	323.68	4	15 , 9	219.56	5
1 , 4	547.41	7	6 , 11	503.38	6	11 , 4	405.45	5	16 , 3	694.39	10
1 , 18	702.30	8	6 , 18	552.33	7	11 , 5	565.58	7	16 , 4	367.65	4
2 , 7	334.18	6	7 , 5	198.86	4	11 , 10	325.18	3	16 , 6	439.81	6
2 , 8	583.37	9	7 , 12	203.75	3	11 , 14	255.60	5	16 , 14	360.83	5
2 , 9	518.58	9	7 , 14	184.96	3	11 , 18	103.41	2	16 , 17	587.00	8
2 , 13	511.75	8	8 , 15	257.21	4	12 , 1	297.97	4	18 , 4	457.41	5
3 , 5	285.63	4	9 , 2	518.58	9	12 , 3	298.52	4	18 , 5	617.53	7
3 , 13	415.10	7	9 , 3	646.48	7	12 , 9	462.20	5	18 , 7	483.68	6
4 , 8	344.00	4	9 , 4	240.89	5	12 , 16	434.96	5	18 , 11	103.41	2
4 , 11	405.45	5	9 , 10	167.77	4	12 , 19	534.46	7	18 , 12	404.86	6
4 , 17	293.52	6	10 , 2	660.91	10	13 , 4	286.76	3	19 , 3	687.93	10
4 , 18	457.41	5	10 , 5	622.44	12	13 , 9	300.27	4	19 , 9	140.89	3

Table 7.4: ATN-II link's distance and number of way points

Links	Distance (nm)	Waypoints	Links	Distance (nm)	Waypoints	Links	Distance (nm)	Waypoints	Links	Distance (nm)	Waypoints
0 , 3	293.89	7	5 , 8	299.67	4	11 , 14	289.68	5	17 , 0	308.87	8
0 , 11	658.06	10	6 , 8	197.95	2	12 , 14	202.78	4	17 , 19	213.04	4
0 , 16	399.68	9	6 , 9	290.31	2	12 , 15	294.82	4	18 , 0	205.66	4
0 , 18	205.66	4	6 , 16	660.93	14	13 , 3	706.53	13	18 , 1	313.29	5
1 , 3	198.50	4	7 , 9	197.65	2	13 , 15	197.52	2	19 , 1	208.00	4
1 , 4	297.23	5	7 , 10	294.85	3	13 , 16	301.20	6	19 , 2	296.00	7
2 , 4	208.28	3	8 , 10	198.63	3	14 , 16	199.54	2			
2 , 5	327.82	5	8 , 11	299.57	5	14 , 17	293.17	4			
2 , 9	595.49	11	9 , 2	595.49	11	15 , 17	197.73	4			
3 , 5	216.73	4	9 , 11	202.15	5	15 , 18	296.33	5			
3 , 6	317.29	5	9 , 12	307.30	6	16 , 0	399.68	9			
3 , 13	706.53	13	10 , 11	101.59	3	16 , 6	660.93	14			
4 , 6	209.94	4	10 , 12	206.74	4	16 , 14	199.54	2			
4 , 7	308.81	5	11 , 0	658.06	10	16 , 18	198.25	4			
5 , 7	200.74	4	11 , 10	101.59	3	16 , 19	303.84	5			

In each ATN, the traffic schedule consists of light, medium and heavy aircraft generated using the capacity estimation module and then converted into a traffic scenario by the evolutionary optimisation method. Figure 7.12 presents the maximum attainable flows in the test ARNs over a period of 24 hours.

As, for a given flow density, there will be many solutions because of the combination of light, medium and heavy aircraft, I generate 20 traffic scenarios in every case. In our experiments, I control the flow density by the extra separation parameter (es). Tables 7.5 and 7.6 summarise the average hourly traffic densities (hourly flight movements) for test ATN-I and ATN-II, respectively. Their maximum hourly traffic flows (capacity) are found to be identical, while the small-world configuration (ATN-II) can accommodate more traffic than its random counterpart (ATN-I).

For a given flow density, the output from the capacity estimation module is converted to a traffic scenario by a DE process, with the purpose of assigning flight levels for each that minimise the overall collision risk, while the speed and other parameters are set by ATOMS. Figure 7.13 shows the percentages of usage of each flight level averaged over 20 scenarios determined by calculating the total number

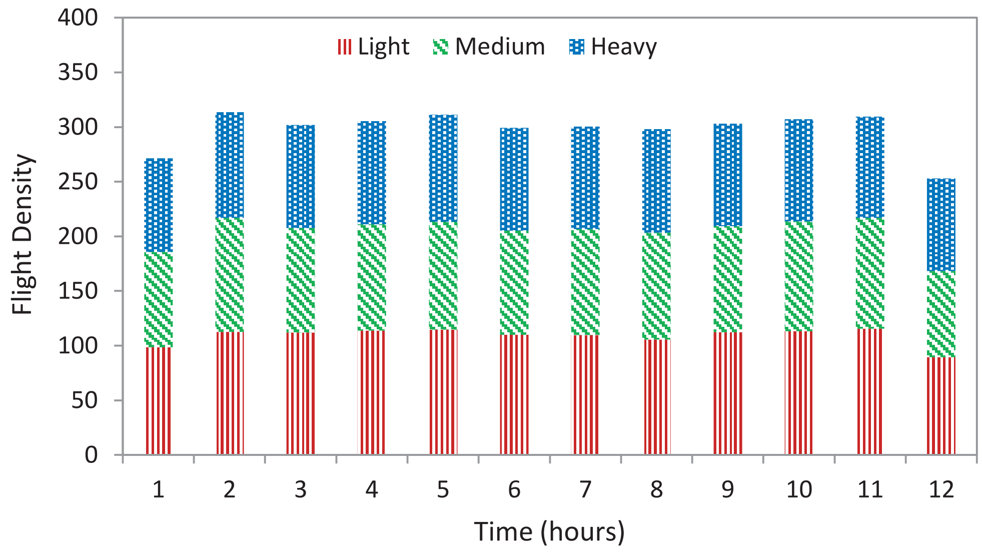

(a) Test ATN-I

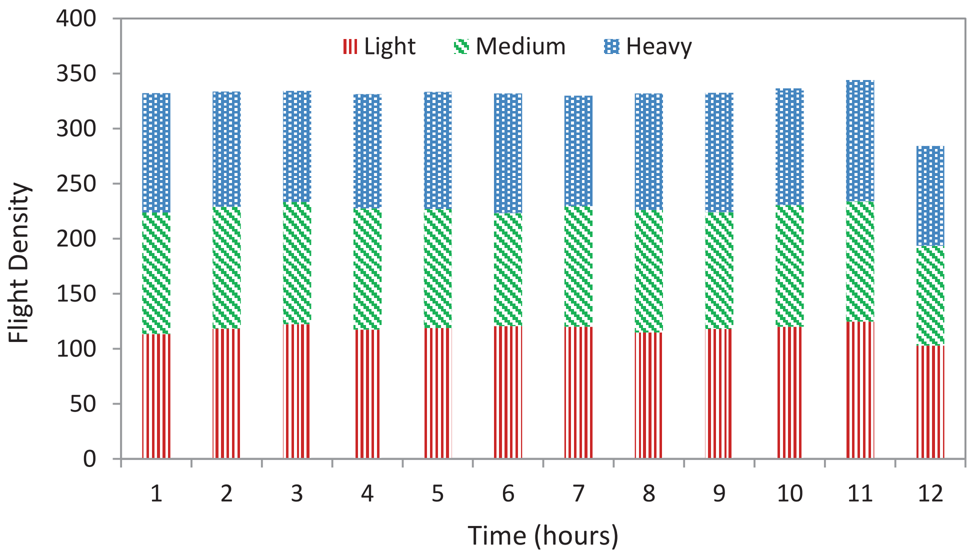

(b) Test ATN-II

FIGURE 7.12: Hourly flow of test ATNs for $es = 0$)

of flight flows through a scenario divided by the total number of flights in it. It is clear that all of the flight levels are almost equally utilised except for some traffic scenarios with es = 18 in which flight levels FL290 and FL390 are the most used in ATN-I and ATN-II, respectively.

Figure 7.14 shows the collision risk of each test ATN as a function of the hourly flow density. As the number of hourly flight movements increases, all collision risks increase almost linearly for both cases, with the average collision risk always

Table 7.5: Hourly flight movements in test ATN I

es	Density	L	M	H
1	325.10 ± 6.04	131.00 ± 7.25	115.80 ± 6.79	109.55 ± 6.45
2	246.50 ± 3.99	95.00 ± 5.24	88.15 ± 5.91	87.10 ± 7.19
4	166.65 ± 3.13	64.80 ± 4.44	62.90 ± 4.81	61.55 ± 3.85
6	125.10 ± 3.18	50.60 ± 3.22	47.55 ± 3.83	46.85 ± 2.70
8	100.20 ± 3.09	40.80 ± 3.64	38.00 ± 3.31	38.05 ± 3.12
10	83.70 ± 2.30	34.00 ± 2.75	32.30 ± 2.99	32.95 ± 3.33
12	71.65 ± 2.81	30.30 ± 2.54	28.00 ± 3.21	27.05 ± 1.79
14	62.70 ± 2.72	26.95 ± 2.31	23.65 ± 3.00	25.40 ± 2.54
16	54.60 ± 2.16	24.25 ± 2.73	21.50 ± 2.26	21.00 ± 2.66
18	50.05 ± 1.85	22.50 ± 1.99	20.20 ± 2.88	19.65 ± 2.50
20	44.90 ± 1.68	20.40 ± 2.56	18.10 ± 2.13	16.90 ± 2.05

Table 7.6: Hourly flight movements in test ATN II

es	Density	L	M	H
1	348.00 ± 3.67	135.70 ± 7.43	125.00 ± 6.62	121.80 ± 6.09
2	265.45 ± 3.99	102.45 ± 6.00	99.65 ± 5.43	93.55 ± 3.73
4	177.50 ± 2.96	70.05 ± 3.32	67.70 ± 4.24	65.35 ± 3.92
6	134.90 ± 2.95	53.50 ± 3.55	53.05 ± 5.41	50.85 ± 4.06
8	108.65 ± 2.37	47.90 ± 4.47	43.10 ± 4.12	42.80 ± 3.78
10	90.30 ± 1.89	38.70 ± 4.35	34.80 ± 2.44	36.15 ± 4.26
12	78.70 ± 2.03	34.30 ± 3.80	31.70 ± 3.63	31.50 ± 3.07
14	69.10 ± 1.45	31.35 ± 3.48	28.30 ± 3.16	29.35 ± 2.92
16	61.20 ± 1.15	27.60 ± 3.17	24.80 ± 2.12	25.85 ± 2.32
18	54.90 ± 1.80	25.55 ± 3.35	22.75 ± 3.11	22.15 ± 2.35
20	50.45 ± 1.54	24.05 ± 2.74	20.75 ± 2.88	20.45 ± 2.28

more for ATN-I than for ATN-II. In both cases, the collision risk hits the TLS (1.5×10^{-8}) [112] as the hourly flight movements among the airports increase, which I call the critical flow density, with those of ATN-I and ATN-II 140 and 120 (hourly flight movements), respectively.

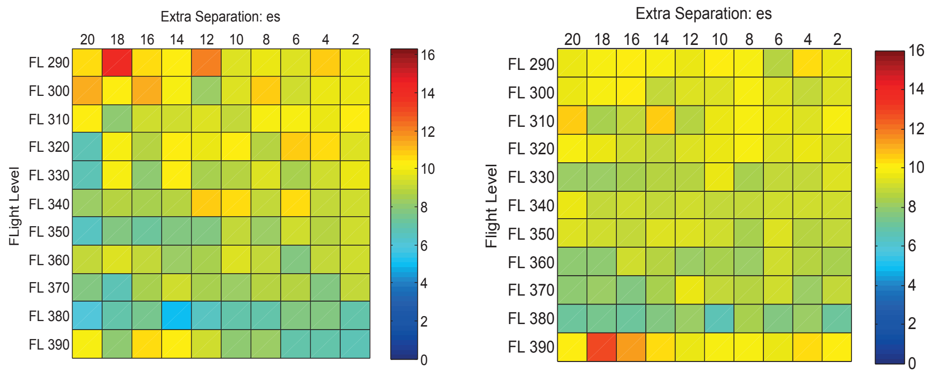

(a) Test ATN-I (b) Test ATN-II

Figure 7.13: Percentages of usage of different flight levels

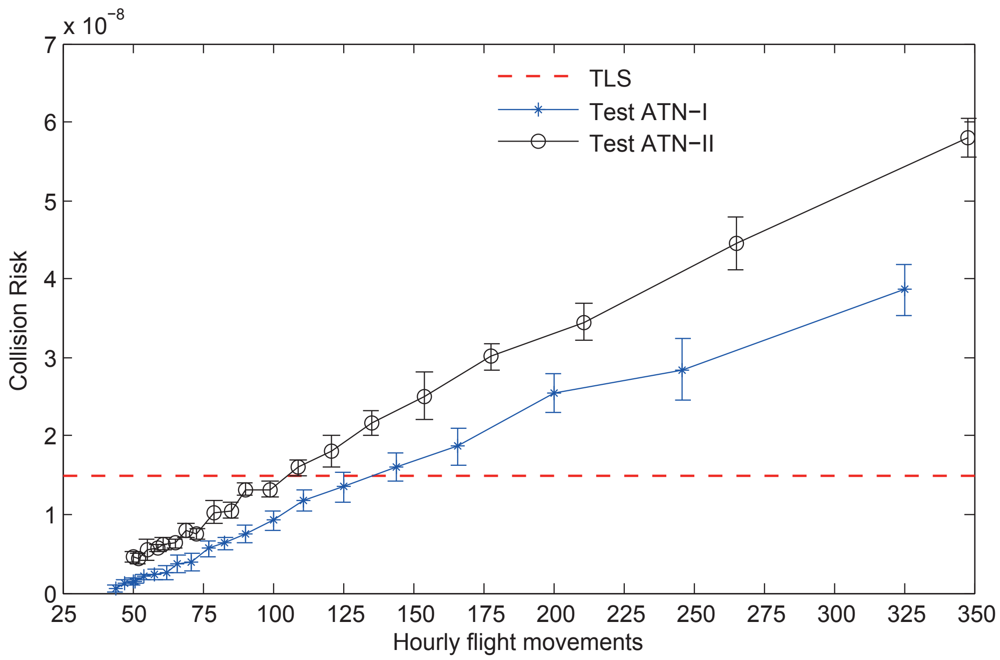

Figure 7.14: Capacity-Collision risk relationship

7.7 Chapter Summary

With the aim of increasing the capacity and enhancing the safety of air transportation, this chapter proposed a framework for integrating an airport and an airspace network to analyse the trade-off between capacity and safety. The proposed methodology was tested on two different ATN topologies random (ATN-I) and small-world (ATN-II) with the same number of airports.

The experimental results indicate that, if the upper airspace TLS is relaxed, the maximum hourly flow (capacity) of the small-world configuration (ATN-II) can accommodate more traffic than the random one (ATN-I). In both cases, as the flow density increased in the airport network, the overall airspaces collision risk increased linearly and crossed the TLS because, although the airport network system could handle more traffic, the safety barrier of the upper airspace served as a bottleneck in terms of the overall capacity of the air traffic network. Therefore, estimating the true capacity of an air transportation network system without considering safety is unrealistic as its maximum capacity depends on the interactions of its underlying airport network and upper airspace waypoints network.

It was found that, in general, the capacitys upper bound depends not only on the connectivity among airports and their individual performances but also on the configuration of waypoints and mid-air interactions among flights. I demonstrated that, as the hourly flow in the network increased after a certain level, the overall collision risk crossed the TLS, which I defined as the critical flow density for the given ATN. However, as the location of the critical point depends on the particular network configuration, it may vary from network to network. The critical flow density of the random topology (ATN-I) was found to be larger than its small-world counterpart, while, in terms of airspace safety, its collision risk was smaller. These results may facilitate decision makers in gaining insights into how capacity and safety interact with each other, discovering system bottlenecks and using such knowledge to improve an ATNs performance and sustainability.

Chapter 8

Conclusion

This chapter summarises the research carried out in the thesis, discusses the findings and conclusions and, finally, indicates possible future research work.

8.1 Summary of Results

Estimating the capacity of an air transportation network is generally known to be NP-hard and one of the most difficult problems in the air transportation domain. The capacity of an air transportation network has generally been measured at the levels of its individual elements, such as links (sector capacity and airspace complexity) and nodes (terminals and runway throughput), which obviously do not constitute its overall system-level capacity. In this thesis, I developed a model and methodology for solving the ATN's capacity estimation problem. **One of the major application of the proposed methodology for transportation planning and management because it addresses the question of whether or not the system has adequate capacity to handle continuing economic surge and traffic congestion. Apart from that, the airport network capacity estimation will definitely help to investigate the reliability and**

resilience of the network, especially when it undergoes some disturbances.

I introduced a multi-commodity-based flow estimation model for estimating the capacity of an airport network, in which I modelled an airport network as a graph with links created based on flight connectivity and introduced heterogeneous travel entities (different aircraft types) and travel times for each link. One of the important features of the proposed model is that it does not require advanced knowledge of the local capacities of the nodes or links, which is a major requirement for most of the existing capacity estimation models. Also, I developed a heuristic algorithm for solving the airport network capacity model in which all of the flow constraints of air traffic are maintained. The proposed model and algorithm were applied to different test networks, with the numerical results revealing that the model is not only capable of realistically estimating the network's capacity with different levels of aircraft mix but also of identifying individual flows at different links and delays for each aircraft. In addition, the proposed model provides details of the flow (the actual number of each type of aircraft, that is, light, medium and heavy) and a flight schedule (the departure and arrival times of each flight). The experimental results demonstrate that the flow capacity of a small-world airport network is greater than that of its random and scale-free counterparts and, surprisingly, it was found that most of the real-world airport networks are small-world.

Apart from the airport network, I also analysed airspace as a network and related its network features to estimate collision risk. For that purpose, I modelled an airspace using two different techniques – a direct route model (which assumes a great circle route between entry and exit waypoints) and an intermediate waypoint model (which uses airway-waypoint routes between entry and exit waypoints). The experimental results demonstrated that the intermediate waypoint model leads to a significant increase in the accuracy of collision risk estimates. The results also showed significant correlations between the estimated collision risk and specific network complexity measures. From an operational perspective, this means that, in a highly structured airspace, the collision risk may be underestimated when using the widely accepted direct route model.

With the increasing traffic demand, managing the collision risk of an airspace network bellow the target level of safety (TLS) involves key changes for air service providers. To manage the collision risk of a given airspace network, I applied the ICAO's strategic lateral offset procedures (SLOP) in such a way as to minimise its overall collision risk. I proposed an evolutionary method for finding the optimal strategic lateral offset for the airways of an airspace network to minimise the collision risk. The experimental results obtained from real-traffic data of Bahrain's upper airspace (FL290-FL410) showed that, by assigning the right offset to the airways, the overall collision risk can be significantly reduced. In addition, the airway's specific lateral offsets were correlated with airway-traffic features using multiple regression models and it was found that the numbers of flights and crossings in an airway are the key features affecting the optimal lateral offset. This approach establishes a generic mapping that can suggest the optimal lateral offsets that mitigate the collision risk for a given airspace based on airway-traffic features.

In this thesis, I developed a methodology for identifying the relationship between the flow density and mid-air collision risk for a given ATN. To estimate the collision risk of an airspace network, given a demand or flow density, I applied evolutionary scenario-generation techniques that can be executed in an air traffic simulator. A high-fidelity collision risk model (Hsu) integrated with the simulator (ATOMS) enabled me to include details of flight dimensions and operational status, such as speed, in the collision risk estimation. From the experimental study, it was found that the capacity upper bound depends not only on the connectivity among airports and their individual performances but also on the configuration of waypoints and mid-air interactions among flights. I demonstrated that, as the hourly flow in the airport network increases, after a certain level, the overall collision risk crosses the TLS, which I defined as the critical flow density for the given ATN. However, as the location of the critical point may depend on the network's configuration, it may vary from network to network. In future work, I will examine the relationship between an ATN configuration and critical flow density.

8.1.1 Key Findings

- A complex network-based analysis reveals that the Australian airport network consisted of small-world characteristics like the world airport network and the airport networks of other countries/regions.
- In an airport network, the flow capacity depends on the configuration of the network. A network with small-world topology can accommodate the largest amount of traffic compared to random and scale-free networks with the same number of nodes.
- Modelling and analysis of an airspace using complex network tools reveal that the collision risk of an airspace network depends on the underlying network modelling and its network structure. An intermediate-waypoints-based model leads to a significant increase in collision risk estimates, specifically for airspace networks with higher average degree and higher closeness centrality measures.
- An airspace collision risk can be managed by applying airway-specific optimal lateral offset. The experimental results of Bahrain airspace show that assigning an optimal offset within a range of 0 to 4 nautical miles can reduce the collision risk from 2.952×10^{-7} to 1.83×10^{-7}, which is almost a 44% improvement.

- In an ATN, the capacity's upper bound depends not only on the airport network and individual performances but also on the airspace network due to safety limits. From the simulation results, it was found that, in an ATN, the overall collision risk of an airspace increase almost linearly with the increase of traffic density in the airport network. If tactical flight management operations are ignored, after a certain, critical traffic density collision risk crossed the TLS. The value of the critical traffic density depends on the ATN configuration. The critical flow density of a random topology is found to be larger than its small-world counterparts.

8.2 Future Work

One of the limitations, as mentioned in Chapter 4, is that the proposed model for airport network capacity estimation is limited to airports with only one runway. However, I believe that a local optimisation or runway slot assignment module could be easily integrated into the proposed model to extend it for multiple runways.

In Chapter 4, a method for estimating the flow capacity of an air traffic network using a hill-climbing optimisation technique was proposed. However, a more versatile optimisation technique, such as an evolutionary algorithm, could be used to solve the problem. Furthermore, adding another dimension to the capacity problem, such as minimising the overall delay, would be a challenge to investigate. The solution of such a multi-objective problem would provide a set of Pareto optimal solutions, the beauty of which would be that different solutions could be employed at different operational times; for example, during the night when demand is usually lower than during the day, the priority could shift from maximising the flow, which is required during peak hours, to minimising the delay. In addition, the proposed airport network capacity estimation methodology in Chapter 4 can also be extended to estimate the capacity of the airspace network and I consider this to be a potential future work.

The evolutionary methodology for evolving the lateral offset could be extended in an advanced air traffic management concept, whereby starting a turn to avoid a bad-weather region would also minimise the collision risk. Airborne weather avoidance, weather patterns and an airways configuration could be encoded into the chromosome-based data structure and evolved using an evolutionary algorithm to determine the optimal solution that would reduce the collision risk. This process could also be used to generate 4D trajectories in a given airways network to minimise the collision risk or other performance metrics such as delay.

In the final technical chapter (Chapter 7), a methodology for identifying the relationship between the airport network capacity and mid-air collision risk was proposed. Although this study does not consider different tactical flight management operations, such as increasing or decreasing speed, climbing or descending, etc., how they may impact differently on the collision risk and capacity-safety relationship is an interesting question, the answering of which would definitely improve the relationship between the flow capacity and collision risk and help to identify safe operations for airspaces with different traffic densities.

Appendix A

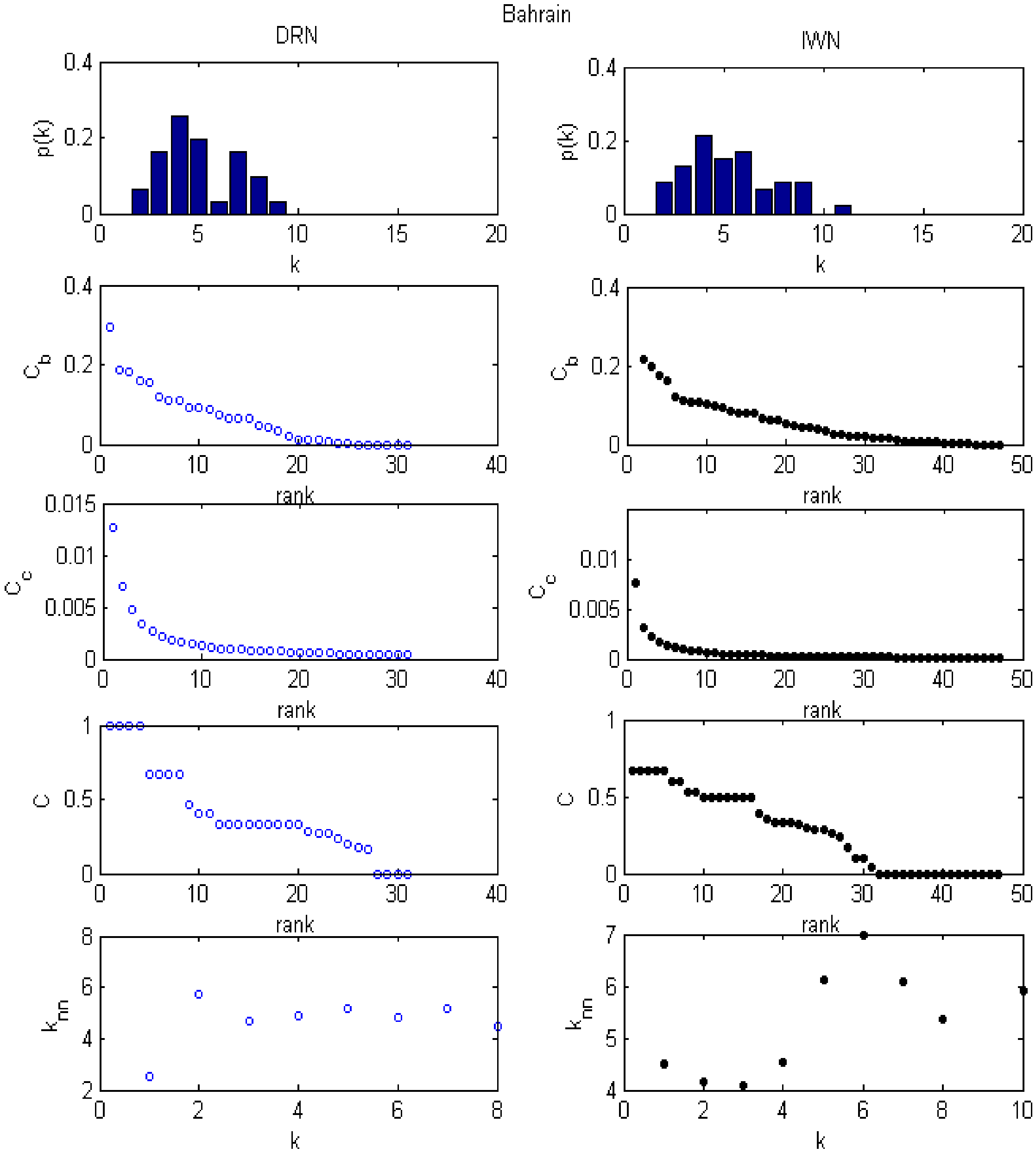

FIGURE 9.1: A one-to-one comparison of topological properties of Barhains DRN and IWN

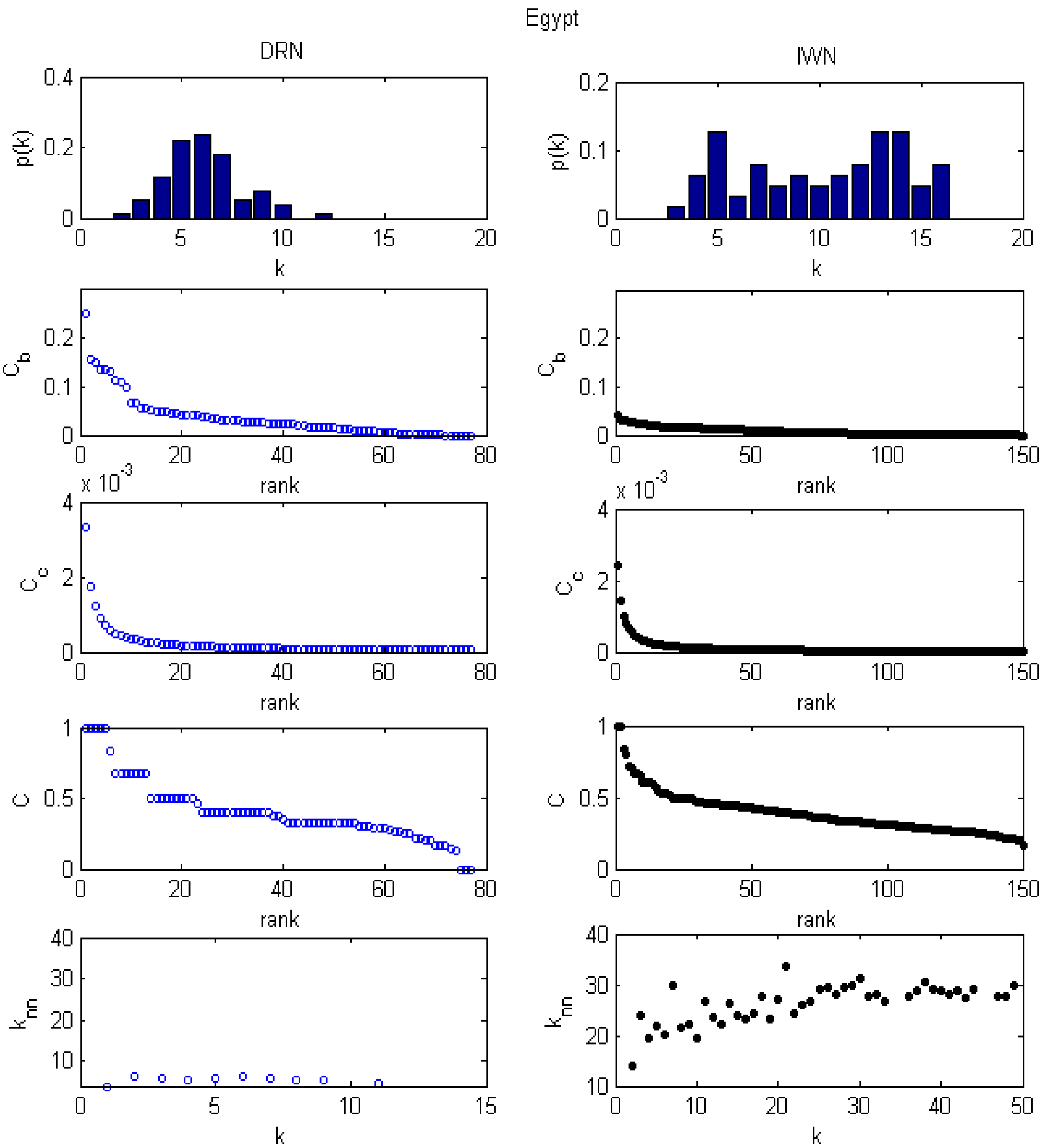

FIGURE 9.2: A one-to-one comparison of topological properties of Egypts DRN and IWN

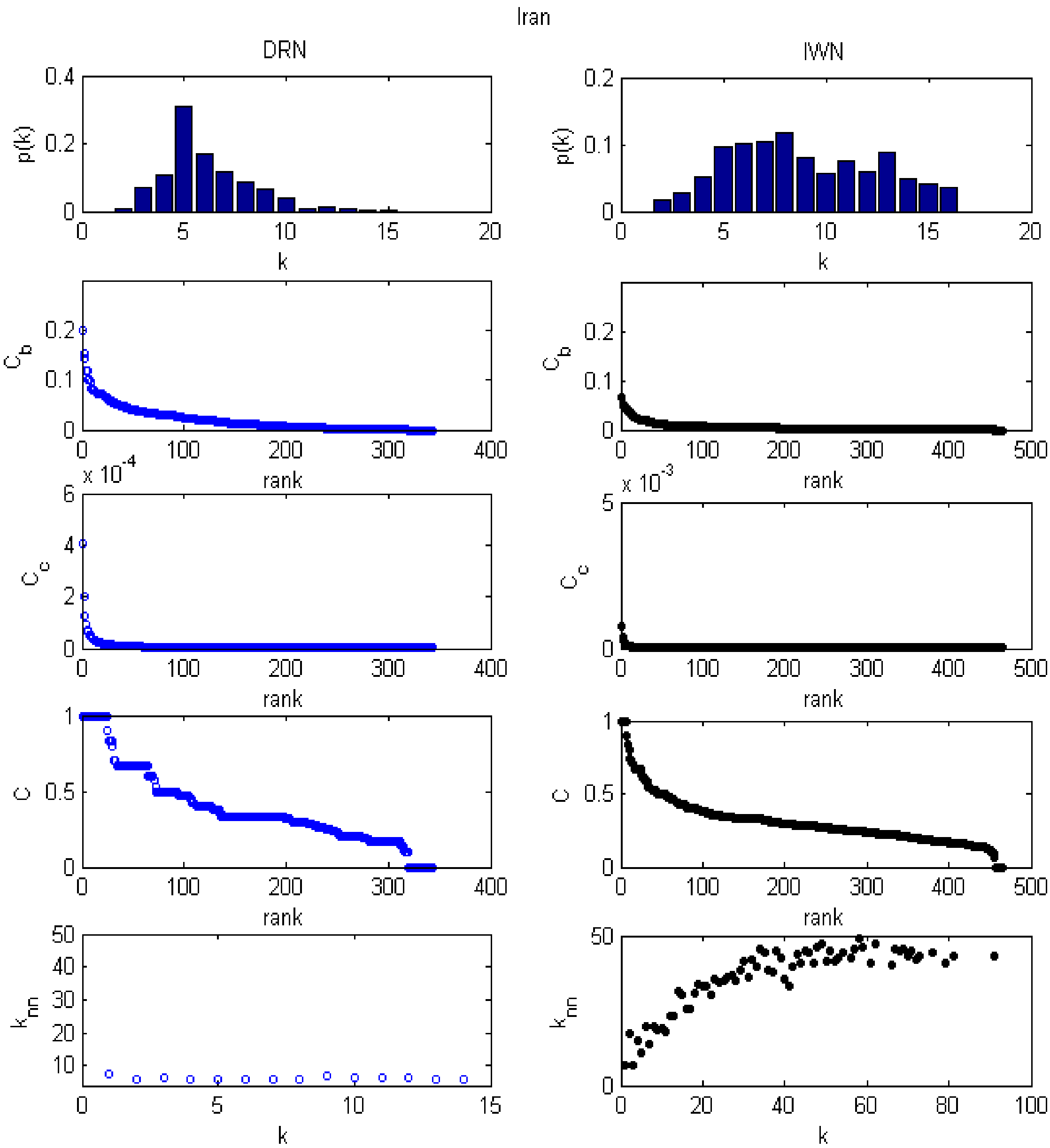

FIGURE 9.3: A one-to-one comparison of topological properties of Irans DRN and IWN

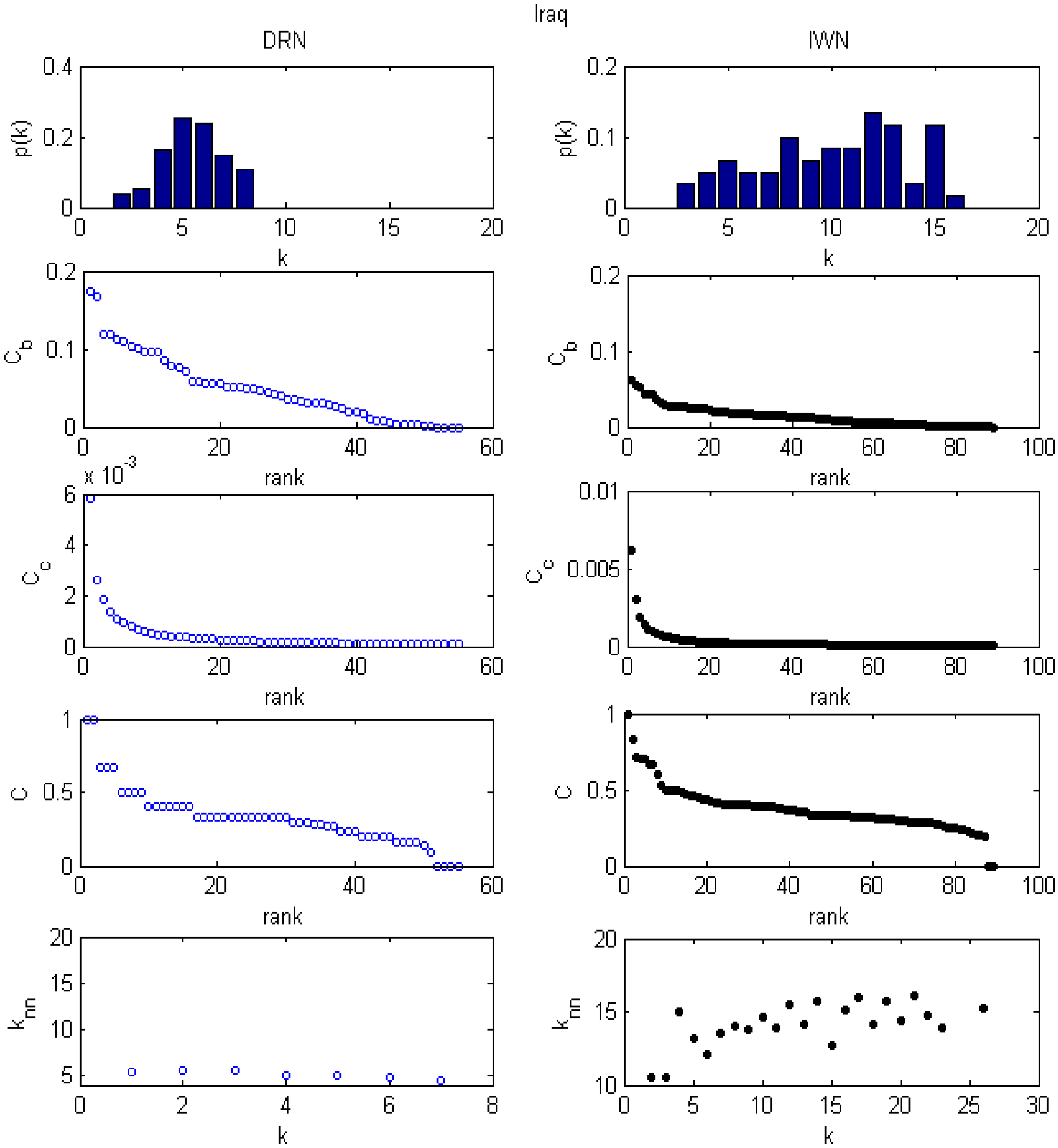

FIGURE 9.4: A one-to-one comparison of topological properties of Iraqs DRN and IWN

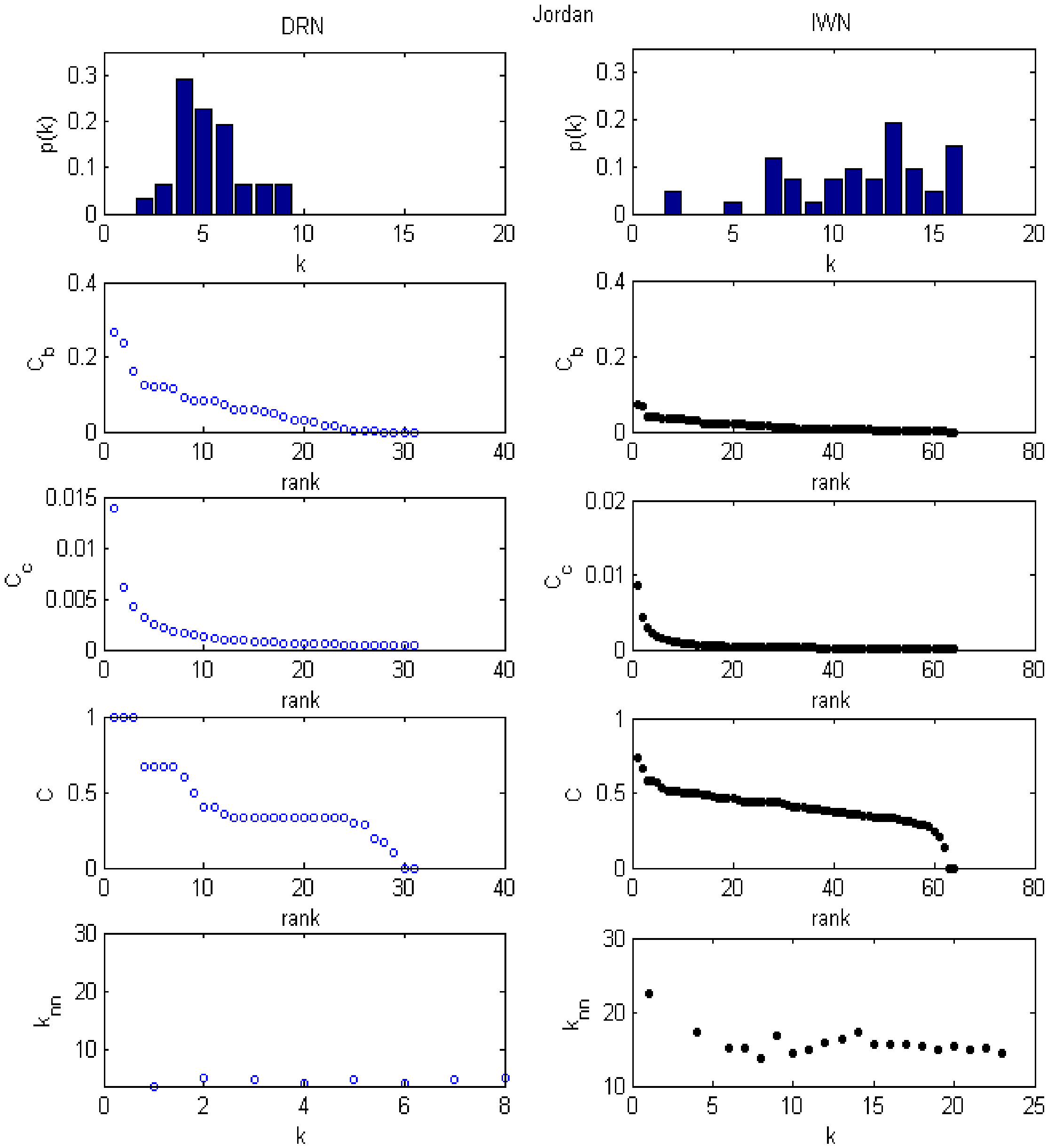

FIGURE 9.5: A one-to-one comparison of topological properties of Jordans DRN and IWN

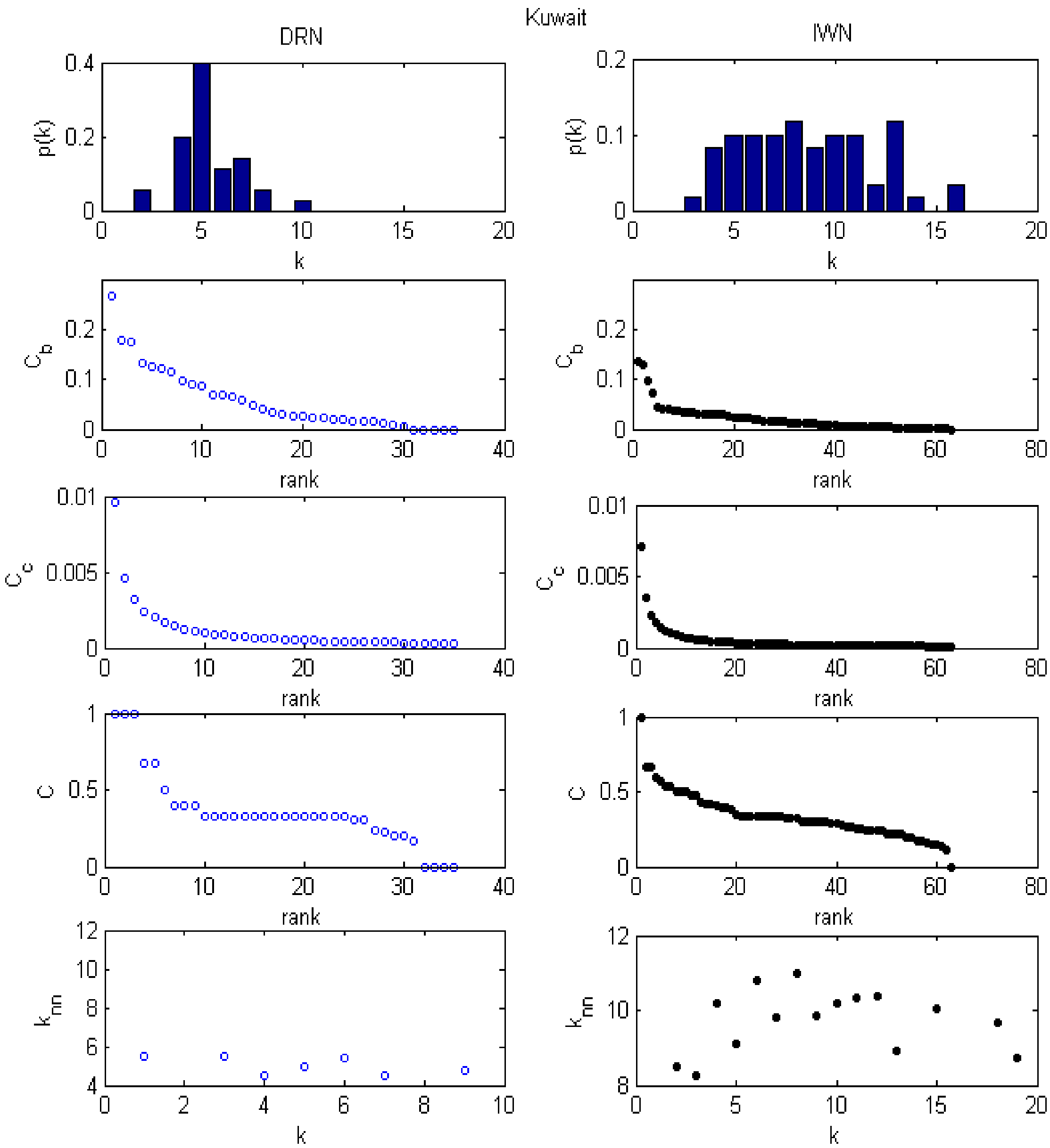

FIGURE 9.6: A one-to-one comparison of topological properties of Kuwaits DRN and IWN

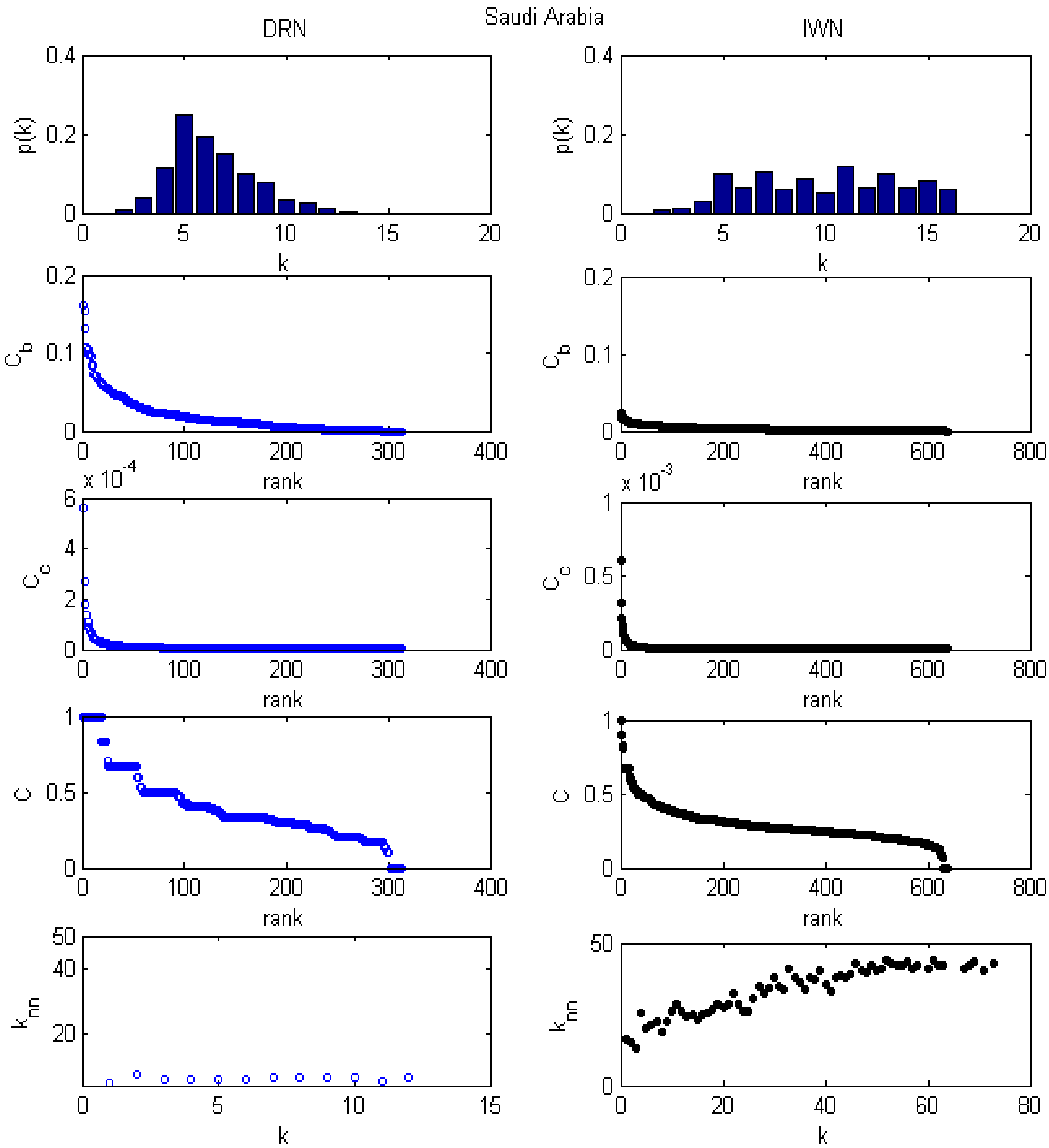

FIGURE 9.7: A one-to-one comparison of topological properties of Saudis DRN and IWN

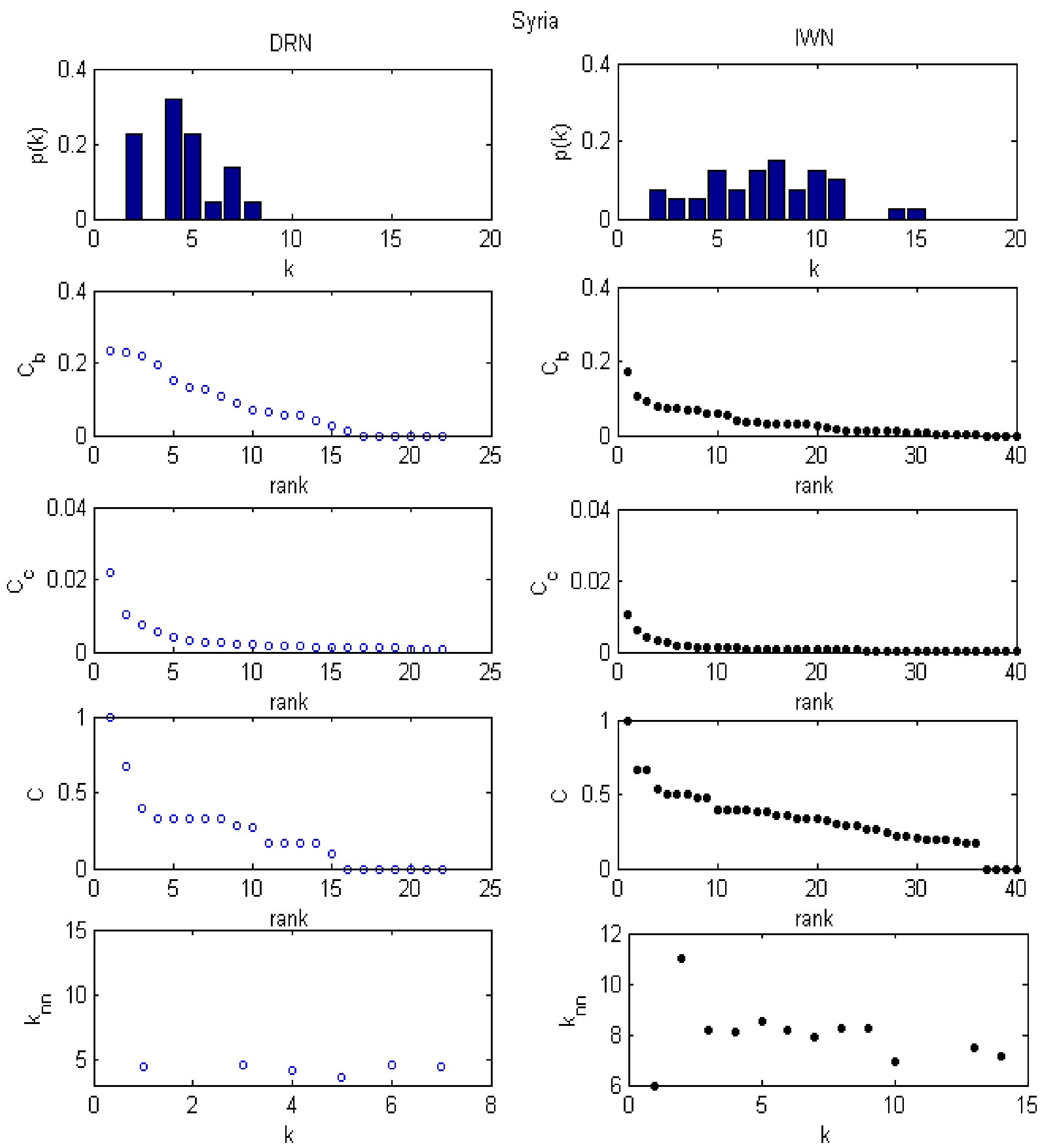

FIGURE 9.8: A one-to-one comparison of topological properties of Syrias DRN and IWN

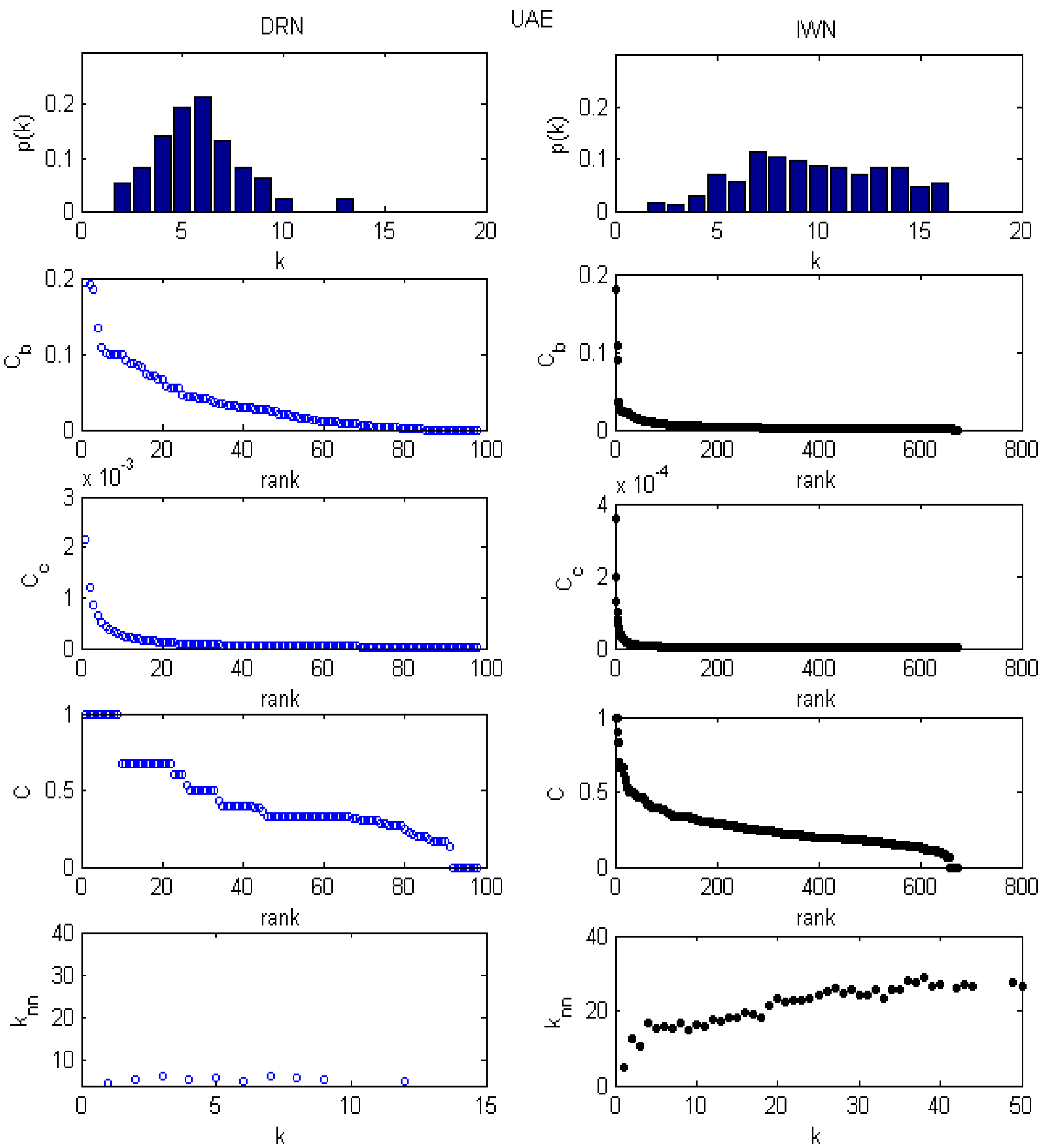

FIGURE 9.9: A one-to-one comparison of topological properties of UAEs DRN and IWN

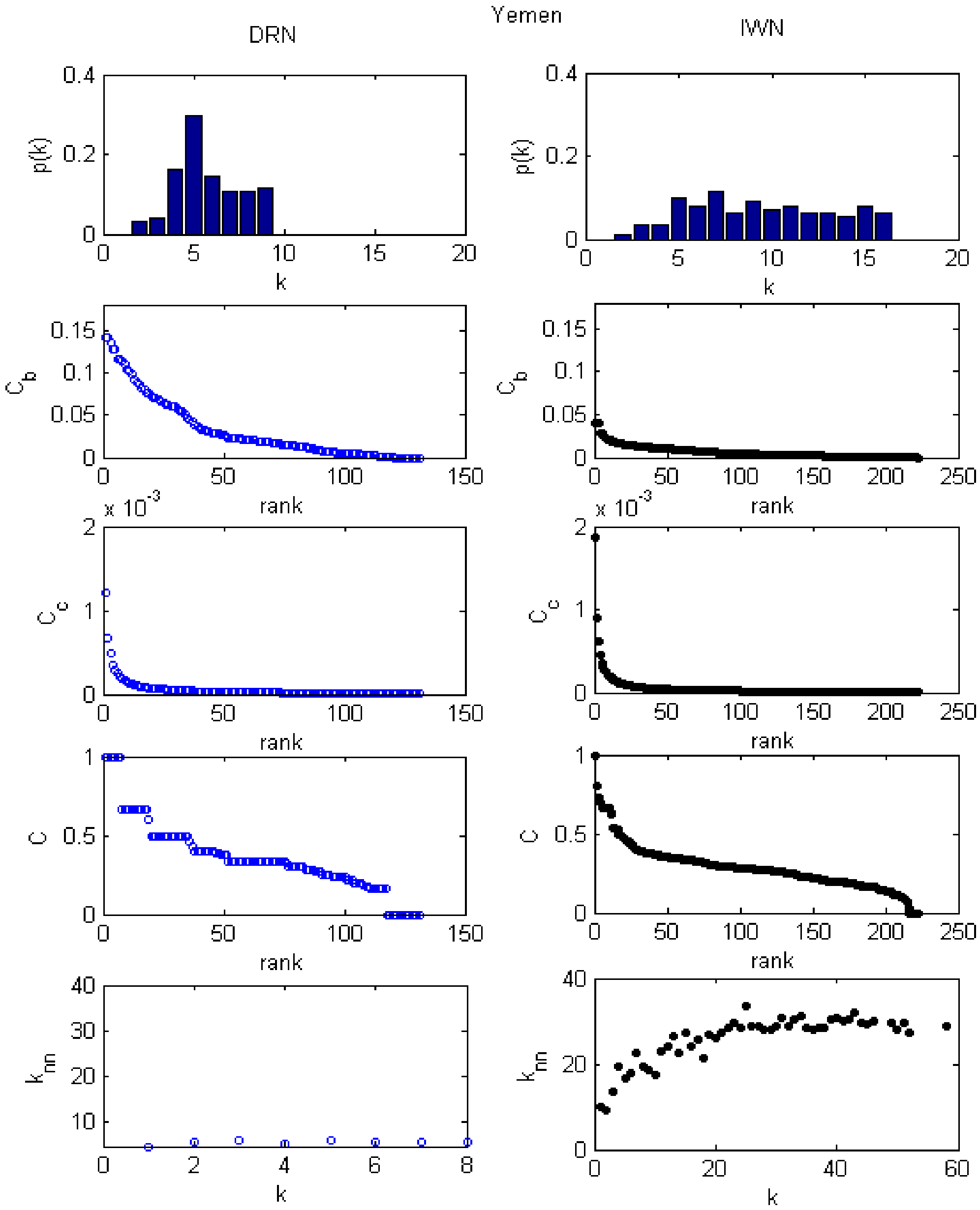

FIGURE 9.10: A one-to-one comparison of topological properties of Yemens DRN and IWN

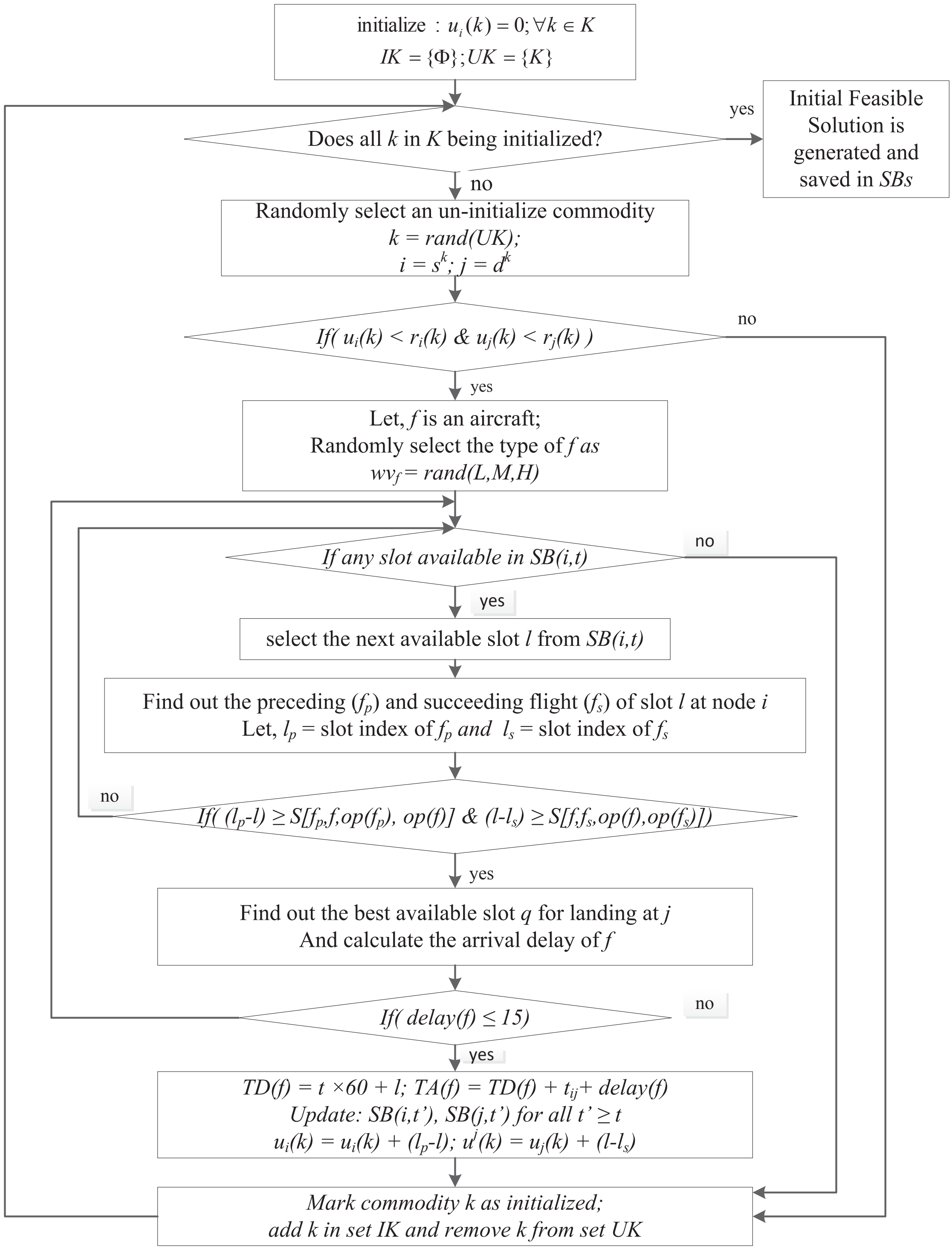

FIGURE 9.11: Initial feasible solution generation process

Bibliography

[1] Doc 4444-rac/501: Procedures for air navigation services. Technical report, ICAO, Montreal, Canada, 1996.

[2] North Atlantic Systems Planning Group. Technical report, ICAO, 2007. NAT SPG Conclusion 43/20 - Publication of NAT safety related material mtg/pirg/natspg/natspg43/followup-07-0237.slg.

[3] Concept of operations for the next generation air transportation system (nextgen), 2007. Joint Planning and Development Office, Washington, D.C.

[4] ATC - SESAR 2020 Concept Mid-Term Validation (MTV),Episode 3, EUROCONTROL , 2008. URL `http://www.eurocontrol.int`.

[5] Ash cloud chaos: Airlines face huge task as ban ends, 21 April 2010. URL `http://news.bbc.co.uk/2/hi/uk/8633892.stm`.

[6] The bureau of infrastructure, transport and regional economics (BITRE), australia, http://www.bitre.gov.au. URL `http://www.bitre.gov.au`.

[7] H. A. Abbass and R. Sarker. The pareto differential evolution algorithm. *International Journal on Artificial Intelligence Tools*, 11(4):531–552, 2002.

[8] Y. Akamastu and O. Miyawaki. Maximum network capacity problem under the transportation equilibrium assignment. *Infrastructure Planning Review*, 12:719–729, 1995. ISSN 0913-4034.

[9] S. Alam, L. T. Bui, H. A. Abbass, and M. Barlow. Pareto meta-heuristics for generating safe flight trajectories under weather hazards. In *Simulated Evolution and Learning*, pages 829–836. Springer, 2006.

[10] S. Alam, K. Shafi, H. A. Abbass, and M. Barlow. Evolving air traffic scenarios for the evaluation of conflict detection models. In *Proc. 6th Eurocontrol Innovative Research Workshop, Eurocontrol Experiment Research Center*, 2007.

[11] S. Alam, H. A. Abbass, and M. Barlow. Atoms: Air traffic operations and management simulator. *IEEE Transactions on Intelligent Transportation Systems*, 9(2):209–225, 2008.

[12] S. Alam, K. Shafi, H. A. Abbass, and M. Barlow. Forming an intelligent ensemble of conflict detection algorithms in free flight by data mining the scenario space. *Transportation Research Part-C: Emerging Technologies*, page 25, 2009.

[13] S. Alam, C. Lokan, G. Aldis, S. Barry, R. Butcher, and H. Abbass. Systemic identification of airspace collision risk tipping points using an evolutionary multi-objective scenario-based methodology. *Transportation research part C: emerging technologies*, 35:57–84, 2013.

[14] R. Albert and A.-L. Barabási. Statistical mechanics of complex networks. *Reviews of Modern Physics*, 74(1):47, 2002.

[15] M. Ali, M. Pant, and A. Abraham. Unconventional initialization methods for differential evolution. *Applied Mathematics and Computation*, 219(9): 4474–4494, 2013.

[16] L. Amaral, A. Scala, M. Barthélémy, and H. Stanley. Classes of small-world networks. *Proceedings of the National Academy of Sciences*, 97(21):11149,

2000.

[17] S. B. Amor. Modeling ATM as a complex system. In *Doctoral Symposium - International Conference On Research In Air Transportation*, pages 1–4, 2006.

[18] J. Anthonisse. The rush in a directed graph. 1971.

[19] Y. Asakura and M. Kashiwadani. Estimation model of maximum road network capacity with parking constraints and its application. *Infrastructure Planning Review*, 11:129–136, 1993.

[20] T. Back, D. B. Fogel, and Z. Michalewicz. *Handbook of evolutionary computation*. IOP Publishing Ltd., 1997.

[21] G. Bagler. Analysis of the airport network of india as a complex weighted network. *Physica A: Statistical Mechanics and its Applications*, 387(12): 2972–2980, 2008.

[22] G. Bagler. Complex network view of performance and risks on airport networks. *arXiv preprint arXiv:0805.0924*, 2008.

[23] G. Bakker, H. Kremer, and H. Blom. Geometric and probabilistic approaches towards conflict prediction. In *Proceedings of 3rd USA/Europe Air Traffic Management R&D Seminar, Italy*, 2000.

[24] M. Ball, C. Barnhart, G. Nemhauser, and A. Odoni. Air transportation: Irregular operations and control. *Handbooks in operations research and management science*, 14:1–67, 2007.

[25] A. Barabási and R. Albert. Emergence of scaling in random networks. *Science*, 286(5439):509, 1999.

[26] A. Barabási and R. Crandall. Linked: The new science of networks. *American Journal of Physics*, 71:409, 2003.

[27] C. Barnhart, D. Fearing, A. Odoni, and V. Vaze. Demand and capacity management in air transportation. *EURO Journal on Transportation and Logistics*, 1(1-2):135–155, 2012.

[28] A. Barrat, M. Barthelemy, R. Pastor-Satorras, and A. Vespignani. The architecture of complex weighted networks. *Proceedings of the National Academy of Sciences of the United States of America*, 101(11):3747, 2004.

[29] A. Barrat, M. Barthélemy, and A. Vespignani. Weighted evolving networks: coupling topology and weight dynamics. *Physical Review Letters*, 92(22): 228701, 2004.

[30] M. Barthélemy. Spatial networks. *Physics Reports*, 499(1):1–101, 2011.

[31] M. Barthélemy and A. Flammini. Optimal traffic networks. *Journal of Statistical Mechanics: Theory and Experiment*, 2006(07):L07002, 2006.

[32] A. Basu, J. S. Mitchell, and G. K. Sabhnani. Geometric algorithms for optimal airspace design and air traffic controller workload balancing. *Journal of Experimental Algorithmics (JEA)*, 14:3, 2009.

[33] H. Blom, G. Bakker, P. Blanker, J. Daams, M. Everdij, and M. Klompstra. Accident risk assessment for advanced air traffic management. *Progress in Astronautics and Aeronautics*, 193:463–480, 2001.

[34] H. Blom, G. Bakker, M. Everdij, and M. Van der Park. Collision risk modeling of air traffic. In *Proceedings of European Control Conference*, 2003.

[35] A. Blumstein. An analytical investigation of airport capacity. Technical report, DTIC Document, 1960.

[36] S. Boccaletti, V. Latora, Y. Moreno, M. Chavez, and D. Hwang. Complex networks: Structure and dynamics. *Physics Reports*, 424(4-5):175–308, 2006.

[37] P. Bonnefoy. *Scalability of the air transportation system and development of multi-airport systems: a worldwide perspective*. PhD thesis, Massachusetts Institute of Technology Cambridge, MA 02139 USA, 2008.

[38] P. A. Bonnefoy and R. J. Hansman. Scalability and evolutionary dynamics of air transportation networks in the united states. In *7th AIAA Aviation Technology, Integration and Operations Conference (ATIO), Belfast, Northern Ireland*, 2007.

[39] P. Bourke. Efficient triangulation algorithm suitable for terrain modelling. In *Pan Pacific Computer Conference, Beijing, China*, 1989.

[40] C. R. Brinton, K. Leiden, and J. Hinkey. Airspace sectorization by dynamic density. In *Proceedings of the 9th AIAA Aviation Technology, Integration and Operations (ATIO) Forum. American Institute of Aeronautics and Astronautics*, 2009.

[41] P. Brooker. Aircraft separation assurance: Systems design. *Journal of Navigation*, 36(01):28–36, 1983.

[42] P. Brooker. Controller workload, airspace capacity and future systems. 2003.

[43] P. Brooker and T. Ingham. *Target levels of safety for controlled airspace*. Civil Aviation Authority, 1977.

[44] C. Cai-long and D. Wen-bo. A multi-objective crossing waypoints location optimization in air route network. In *3rd International Workshop on Intelligent Systems and Applications (ISA),*, pages 1–4. IEEE, 2011.

[45] A. Chen and P. Kasikitwiwat. Modeling capacity flexibility of transportation

networks. *Transportation Research Part A: Policy and Practice*, 45(2):105–117, 2011.

[46] A. Chen, H. Yang, H. K. Lo, and W. H. Tang. A capacity related reliability for transportation networks. *Journal of Advanced Transportation*, 33(2): 183–200, 1999.

[47] A. Chen, M. Tatineni, D.-H. Lee, and H. Yang. Effect of route choice models on estimating network capacity reliability. *Transportation Research Record: Journal of the Transportation Research Board*, 1733(1):63–70, 2000.

[48] A. Chen, H. Yang, H. K. Lo, and W. H. Tang. Capacity reliability of a road network: an assessment methodology and numerical results. *Transportation Research Part B: Methodological*, 36(3):225–252, 2002.

[49] L. Cheng, M. Du, X. Jiang, and H. Rakha. Modeling and estimating the capacity of urban transportation network with rapid transit. *Transport*, 29 (2):165–174, 2014.

[50] B. Chèze, P. Gastineau, and J. Chevallier. Forecasting world and regional aviation jet fuel demands to the mid-term (2025). *Energy Policy*, 39(9): 5147–5158, 2011.

[51] G. Chretien, W. Konig, and J. Rech. The sita network. *Computer Communication Networks, RL Grimsdale, FF Kuo, Eds. Noordhoff: NATO Advanced Study Institute Series*, pages 373–396, 1975.

[52] ComplexWorld. ComplexWorld Position Paper. SESAR WP-E ComplexWorld Research Network. Deliverable 23.2, 2012. URL `www.complexworld.eu/sesar-and-wp-e/`.

[53] U. Congress. Office of technology assessment. safe skies for tomorrow: Aviation safety in a competitive environment. Technical report, OTA-SET-381

(Government Printing Office, Washington, DC, 1988), 1988.

[54] R. Coppenbarger, G. Kanning, and R. Salcido. Real-time data link of aircraft parameters to the Center-TRACON Automation System (CTAS). In *4th USA/Europe ATM R& D Seminar, Sante Fe, NM*, 2001.

[55] L. Costa, F. Rodrigues, G. Travieso, and P. Boas. Characterization of complex networks: A survey of measurements. *Advances in Physics*, 56(1): 167–242, 2007.

[56] L. da Rocha. Structural evolution of the brazilian airport network. *Journal of Statistical Mechanics: Theory and Experiment*, 2009:P04020, 2009.

[57] L. DallAsta, A. Barrat, M. Barthélemy, and A. Vespignani. Vulnerability of weighted networks. *Journal of Statistical Mechanics: Theory and Experiment*, 2006(04):P04006, 2006.

[58] B. Danila, Y. Yu, J. A. Marsh, and K. E. Bassler. Transport optimization on complex networks. *Chaos: An Interdisciplinary Journal of Nonlinear Science*, 17(2):026102, 2007.

[59] L. Davis. Handbook of genetic algorithms. 1991.

[60] R. De Neufville and A. Odoni. *Airport Systems. Planning, Design and Management*. 2003.

[61] D. Delahaye and S. Puechmorel. 3D airspace sectoring by evolutionary computation: Real-world applications. In *Proceedings of the 8th annual conference on genetic and evolutionary computation*, pages 1637–1644. ACM, 2006.

[62] D. Delahaye, J.-M. Alliot, M. Schoenauer, and J.-L. Farges. Genetic algorithms for partitioning air space. In *Proceedings of 10th Conference on*

Artificiel Intelligence for Applications, pages pp–291, 1994.

[63] D. Delahaye, M. Schoenauer, and J.-M. Alliot. Airspace sectoring by evolutionary computation. *Spatial evolutionary modelling*, pages 203–233, 2001.

[64] DOC9574-ICAO. Manual on implementation of a 300 m (1000 ft) vertical separation minimum between fl 290 and fl 410 inclusive, 2008.

[65] G. Donohue. *Air Traffic Control Systems. In: Handbook of Transport Systems and Traffic Control*. 2001.

[66] G. L. Donohue. A simplified air transportation system capacity model. *Journal of Air Traffic Control*, 1999.

[67] G. L. Donohue. A macroscopic air transportation capacity model: Metrics and delay correlation. In *New Concepts and Methods in Air Traffic Management*, pages 45–62. Springer, 2001.

[68] V. Duong, G. Gawinowski, J.-P. Nicolaon, and D. Smith. Sector-less air traffic management. In *Proceedings of the fourth USA/Europe Air Traffic Management R&D Seminar*, pages 8–13, 2001.

[69] N. Durand, J.-M. Alliot, and F. Médioni. Neural nets trained by genetic algorithms for collision avoidance. *Applied Intelligence*, 13(3):205–213, 2000.

[70] J. P. Dwyer and S. Landry. Separation assurance and collision avoidance concepts for the next generation air transportation system. In *Symposium on Human Interface*, pages 748–757. Springer, 2009.

[71] A. A. El Ela, M. Abido, and S. R. Spea. Differential evolution algorithm for emission constrained economic power dispatch problem. *Electric Power Systems Research*, 80(10):1286–1292, 2010.

[72] P. Erdős and A. Rényi. *On the Evolution of Random Graphs*. 1960.

[73] EUROCONTROL. A consistent vertical collision risk model for crossing and parallel tracks, 1997. URL `http://www.eurocontrol.int`. Technical Report MDG/5-DP/11.

[74] EUROCONTROL. Eurocontrol Safety Regulatory Requirement - ESARR 4 Risk Assessment and Mitigation in ATM, Edition 1, Eurocontrol, Brussels, 2001. URL `http://www.eurocontrol.int`.

[75] EUROCONTROL. European ATC Harmonization and Integration Programme (EATCHIP)Report Phase 1, 2010. Eurocontrol, Bretigny-sur-Orge.

[76] EUROCONTROL. Indicators and analysis of the atm network operations performance, 2010. Cenrtal Flow Management Unit, Brussels, Network Operations Report.

[77] EUROCONTROL. European route network improvement plan, part 1: European airspace design methodology guidelines, June 2015. Edition 1.5.

[78] A. EUROCONTROL. White paper on resilience engineering for atm. *Report of the Project Resilience Engineering for ATM*, 2009.

[79] L. EUROCONTROL. Fast time simulation to assess the impact of data link on sector capacity, brussels, november 19, 1999, 2000.

[80] A. Evans and A. W. Schäfer. Simulating airline operational responses to airport capacity constraints. *Transport Policy*, 34:5–13, 2014.

[81] M. H. Everdij, H. A. Blom, and B. G. Bakker. Modelling lateral spacing and separation for airborne separation assurance using petri nets. *Simulation*, 83(5):401–414, 2007.

[82] E. Farmer and A. Brownson. Review of workload measurement, analysis and interpretation methods. *European Organisation for the Safety of Air*

Navigation, 33:1–33, 2003.

[83] K. M. Feigh, A. R. Pritchett, A. Shah, S. Kalaver, A. Jadhav, D. Holl, R. Bea, and A. Gilgur. Analyzing air traffic management systems using agent-based modeling and simulation. In *6th USA/Europe Air Traffic Management Research and Development (ATM R&D) Seminar, Baltimore*, pages 27–30, 2005.

[84] G. Flynn, A. Benkouar, and R. Christien. Pessimistic sector capacity estimation. *EEC Note*, 21(03), 2003.

[85] L. R. Ford and D. R. Fulkerson. Maximal flow through a network. *Canadian journal of Mathematics*, 8(3):399–404, 1956.

[86] L. R. Ford Jr and D. R. Fulkerson. *Flows in networks*. Princeton University Press, 2015.

[87] L. Freeman. A set of measures of centrality based on betweenness. *Sociometry*, pages 35–41, 1977.

[88] A. Ghoneim and H. Abbass. A multiobjective distance separation methodology to determine sector-level minimum separation for safe air traffic scenarios. *European Journal of Operational Research*, 2016.

[89] D. Gianazza. Forecasting workload and airspace configuration with neural networks and tree search methods. *Artificial intelligence*, 174(7):530–549, 2010.

[90] D. Gianazza and N. Durand. Separating air traffic flows by allocating 3d-trajectories. In *IEEE 23rd Digital Avionics Systems Conference, 2004. DASC 04*, volume 1, pages 2–D, 2004.

[91] E. P. Gilbo. Airport capacity: Representation, estimation, optimization. *IEEE Transactions on Control Systems Technology*, 1(3):144–154, 1993.

[92] E. P. Gilbo. Optimizing airport capacity utilization in air traffic flow management subject to constraints at arrival and departure fixes. *IEEE Transactions on Control Systems Technology*, 5(5):490–503, 1997.

[93] E. P. Gilbo and M. D. West. Enhanced model for joint optimization of arrival and departure strategies and arrival/departure capacity utilization at congested airports. In *AIAA Modeling and Simulation Technologies (MST) Conference*, 2013.

[94] M. Girvan and M. Newman. Community structure in social and biological networks. *Proceedings of the National Academy of Sciences*, 99(12):7821, 2002.

[95] P. J. Goillau and C. J. Kelly. Malern Capacity Estimate (MACE): A Proposed Cognitive Measure for Complex Systems. *Engineering Psychology and Cognitive Ergonomics. Volume 1, Transportation Systems*, 1, 1997.

[96] D. E. Golberg. Genetic algorithms in search, optimization, and machine learning. *Addion wesley*, 1989, 1989.

[97] J.-B. Gotteland and N. Durand. Genetic algorithms applied to airport ground traffic optimization. In *The Congress on Evolutionary Computation, 2003. CEC'03.*, volume 1, pages 544–551. IEEE, 2003.

[98] R. Graham and D. Young. Preparing an initial assessment of the sesar concept of operations, ep3: Single european sky implementation support through validation. Technical report, Technical report, Eurocontrol Experimental Centre, France, 2006.

[99] R. Graham, N. Pilon, L. Tabernier, H. Koelman, and P. Ravenhill. Performance framework and influence model in atm. In *IEEE/AIAA 28th Digital Avionics Systems Conference, DASC'09*, pages 2–A. IEEE, 2009.

[100] M. Guida and F. Maria. Topology of the italian airport network: A scale-free small-world network with a fractal structure. *Chaos, Solitons & Fractals*, 31 (3):527–536, 2007.

[101] R. Guimera and L. Amaral. Modeling the world-wide airport network. *The European Physical Journal B-Condensed Matter and Complex Systems*, 38 (2):381–385, 2004.

[102] R. Guimera, S. Mossa, A. Turtschi, and L. Amaral. The worldwide air transportation network: Anomalous centrality, community structure, and cities' global roles. *Proceedings of the National Academy of Sciences of the United States of America*, 102(22):7794, 2005.

[103] R. C. Haynie. *An investigation of capacity and safety in near-terminal airspace for guiding information technology adoption*. 2002.

[104] D. He, F. Wang, and Z. Mao. A hybrid genetic algorithm approach based on differential evolution for economic dispatch with valve-point effect. *International Journal of Electrical Power & Energy Systems*, 30(1):31–38, 2008.

[105] B. Hegerty, C.-C. Hung, and K. Kasprak. A comparative study on differential evolution and genetic algorithms for some combinatorial problems. In *Proceedings of 8th Mexican International Conference on Artificial Intelligence*, pages 9–13, 2009.

[106] S. L. Hockaday and A. K. Kanafani. Developments in airport capacity analysis. *Transportation Research*, 8(3):171–180, 1974.

[107] E. Hollnagel, D. D. Woods, and N. Leveson. *Resilience Engineering (Ebk) Concepts and Precepts*. Ashgate Publishing, 2007.

[108] M. Hossain, S. Alam, T. Rees, and H. Abbass. Australian airport network robustness analysis: A complex network approach. In *36th Australian Transport Research Forum (ATRF)*, 2013.

[109] M. M. Hossain, H. A. Abbass, C. Lokan, and S. Alam. Adversarial evolution: Phase transition in non-uniform hard satisfiability problems. In *Proceedings of 2010 IEEE Congress on Evolutionary Computation (CEC)*, pages 1–8, 2010.

[110] D. Hsu. The evaluation of aircraft collision probabilities at intersecting air routes. *Journal of Navigation*, 34(01):78–102, 1981.

[111] Y. Hu, D. Zhu, and N. Zhu. A weighted network evolution model based on passenger behavior. *arXiv preprint arXiv:0709.4143*, 2007.

[112] ICAO. Review of the general concept of separation panel. Technical report, 1995. Working Group A Meeting: Summary of Discussion and Conclusions.

[113] ICAO. Manual on airspace planning methodology for the determination of separation minima, doc 9689, 2001. ICAO, Montreal, Canada.

[114] ICAO. Safety management manual (smm), 2001. Third Edition.

[115] ICAO. Manual on implementation of a 300 m (1000 ft) vertical separation minimum between fl 290 and fl 410 inclusive, 2002. doc 9574 an/934, 2nd edition, Canada.

[116] ICAO. Report on the 2nd AFI RVSM Stakeholder Coordination Meeting, International Civil Aviation Organization (ICAO), Senegal, 2006.

[117] ICAO. Manual of Performance Based Navigation (PBN), DOC 9613. Technical report, ICAO, Montreal, Canada, 2007.

[118] ICAO. Air traffic management doc. 4444 (PANS-ATM), 2007.

[119] ICAO. A unified framework for collision risk modelling in support of the manual on airspace planning methodology with further applications, 2008. circ 319-an/181, Canada.

[120] ICAO. Implementation of strategic lateral offset procedures in the afi region, 2010. AFI Planning and Implementatin Regional Group, APIRG/17 WP/44.

[121] ICAO. Review of the general concept of separation panel. Technical report, ICAO, Montreal, Canada, 28 Nov - 15 Dec, 1988. 6th Meeting ICAO doc. 9536. RGCSP/6, Vol. 1 &2.

[122] M. Ignaccolo. A simulation model for airport capacity and delay analysis. *Transportation Planning and Technology*, 26(2):135–170, 2003.

[123] Y. Iida. Methodology for maximum capacity of road network. *Transaction of Japan Society of Civil Engineers*, 205:147–150, 1972.

[124] R. Irvine. A geometrical approach to conflict probability estimation. *Air Traffic Control Quarterly*, 10(2):85–113, 2002.

[125] A. Jacquillat and A. R. Odoni. Endogenous control of service rates in stochastic and dynamic queuing models of airport congestion. *Transportation Research Part E: Logistics and Transportation Review*, 73:133–151, 2015.

[126] M. Janic. *Air Transport System Analysis and Modelling*, volume 16. CRC Press, 2000.

[127] M. Janić and V. Tošić. Terminal airspace capacity model. *Transportation Research Part A: General*, 16(4):253–260, 1982.

[128] M. Janić and V. Tošić. En route sector capacity model. *Transportation Science*, 25(4):299–307, 1991.

[129] C. Kai-Quan, Z. Jun, D. Wen-Bo, and C. Xian-Bin. Analysis of the chinese air route network as a complex network. *Chinese Physics B*, 21(2):028903, 2012.

[130] K. A. Kane and D. E. Hayes. Tectonic corridors in the south atlantic: Evidence for long-lived mid-ocean ridge segmentation. *Journal of Geophysical Research: Solid Earth (1978–2012)*, 97(B12):17317–17330, 1992.

[131] R.-G. Kang and C.-Y. Jung. The improved initialization method of genetic algorithm for solving the optimization problem. In *Neural Information Processing*, pages 789–796. Springer, 2006.

[132] E. Khaji and A. S. Mohammadi. A heuristic method to generate better initial population for evolutionary methods. *arXiv preprint arXiv:1406.4518*, 2014.

[133] A. Klein, M. Rodgers, and H. Kaing. Dynamic fpas: A new method for dynamic airspace configuration. In *Integrated Communications, Navigation and Surveillance Conference, 2008. ICNS 2008*, pages 1–11, 2008.

[134] A. Klein, M. D. Rodgers, and K. Leiden. Simplified dynamic density: a metric for dynamic airspace configuration and nextgen analysis. In *Proceedings of 28th AIAA Digital Avionics Systems Conference, DASC'09*, pages 2–D, 2009.

[135] M. J. Kochenderfer, M. W. M. Edwards, L. P. Espindle, J. K. Kuchar, and J. D. Griffith. Airspace encounter models for estimating collision risk. *Journal of Guidance, Control, and Dynamics*, 33(2):487–499, 2010.

[136] R. Koenker. Quantreg: quantile regression. *R package version*, 5, 2013.

[137] P. Kopardekar, K. D. Bilimoria, and B. Sridhar. Airspace configuration concepts for the next generation air transportation system. *Air Traffic Control Quarterly*, 16(4), 2008.

[138] P. Kopardekar, J. Rhodes, A. Schwartz, S. Magyarits, and B. Willems. Relationship of maximum manageable air traffic control complexity and sector capacity. In *26th International Congress of the Aeronautical Sciences (ICAS 2008), and AIAA-ATIO-2008-8885, Anchorage, Alaska, Sept*, pages 15–19, 2008.

[139] P. H. Kopardekar, A. Schwartz, S. Magyarits, and J. Rhodes. Airspace complexity measurement: An air traffic control simulation analysis. *International Journal of Industrial Engineering: Theory, Applications and Practice*, 16(1):61–70, 2009.

[140] J. K. Kuchar and L. C. Yang. A review of conflict detection and resolution modeling methods. *IEEE Transactions on Intelligent Transportation Systems*, 1(4):179–189, 2000.

[141] C. F. Lai and S. Zelinski. Simplified dynamic density based capacity estimation. In *Proceeding of 28th AIAA Digital Avionics Systems Conference (DASC'09)*, pages 2–E, 2009.

[142] T. Lauderdale and H. Erzberger. Automated separation assurance with weather and uncertainty. In *Air Traffic Management and Systems*, pages 35–47. Springer, 2014.

[143] D. A. Lee, C. Nelson, and G. Shapiro. *The aviation system analysis capability airport capacity and delay models.* 1998.

[144] X. Lin, N. Fulton, and M. Westcott. Target level of safety measures in air

transportation–review, validation and recommendations. In *Proceedings of the IASTED International Conference*, volume 662, page 222, 2009.

[145] W. Liu and I. Hwang. Probabilistic trajectory prediction and conflict detection for air traffic control. *Journal of Guidance, Control, and Dynamics*, 34 (6):1779–1789, 2011.

[146] O. Lordan, J. Florido, J. M. Sallan, V. Fernandez, P. Simo, and D. Gonzalez-Prieto. Study of the robustness of the european air routes network. In *Proceedings of 4th International Conference on Logistics, Informatics and Service Science (LISS)*, page 195, 2015.

[147] Z. Luo, Y. Liu, and J. Yu. Estimation of urban transportation network capacity considering traveler road preferences. *Journal of Urban Planning and Development*, 138(2):133–142, 2011.

[148] R. Machol. An aircraft collision model. *Management Science*, pages 1089–1101, 1975.

[149] T. L. Magnanti and R. T. Wong. Network design and transportation planning: Models and algorithms. *Transportation Science*, 18(1):1–55, 1984.

[150] A. Majumdar, W. Y. Ochieng, J. Bentham, and M. Richards. En-route sector capacity estimation methodologies: An international survey. *Journal of Air Transport Management*, 11(6):375–387, 2005.

[151] J. McDonnell, R. Reynolds, and D. Fogel. Genetic algorithms for automatic regrouping of air traffic control sectors. In *Evolutionary Programming IV:Proceedings of the Fourth Annual Conference on Evolutionary Programming*. MIT Press, 1995.

[152] D. McNally and D. Thipphavong. Automated separation assurance in the

presence of uncertainty. In *Proc 26th International Congress of the Aeronautical Sciences*, 2008.

[153] K. Mehadhebi. A methodology for the design of a route network. In *Proceedings of the Third Air Traffic Management R & D Seminar ATM-2000*, pages 8–69, 2000.

[154] K. Mehadhebi and P. Lazaud. A synthesis of current collision risk models. In *ICAO Separation and Airspace Safety Panel, 5th Meeting of the Working Group of the Whole (SASP-WG/WHL)*, 2004.

[155] M. Mesgarpour, C. N. Potts, and J. A. Bennell. Models for aircraft landing optimization. In *Proceedings of the 4th international conference on research in air transportation (ICRAT)*, 2010.

[156] C. A. Miller and J. A. Scardina. Air traffic management. *Avionics Navigation Systems, Second Edition*, pages 642–690, 1997.

[157] R. Milo, S. Shen-Orr, S. Itzkovitz, N. Kashtan, D. Chklovskii, and U. Alon. Network motifs: simple building blocks of complex networks. *Science*, 298 (5594):824–827, 2002.

[158] B. Mirkovic and V. Tosic. Airport apron capacity: estimation, representation, and flexibility. *Journal of Advanced Transportation*, 48(2):97–118, 2014.

[159] G. Moek and J. Smeltink. Revised p revised pre-implementation collision risk implementation collision risk assessment for rvsm in the africa indian ocean region ocean region. 2007.

[160] S. Mondoloni and S. Conway. An airborne conflict resolution approach using a genetic algorithm. In *Proceedings of AIAA Guidance, Navigation, and Control Conference*, 2001.

[161] S. Nagaoka. Effects of measurement errors in estimating the probability of vertical overlap. *Journal of Navigation*, 38(02):234–243, 1985.

[162] National Civil Aviation Review Commission (US). *Avoiding aviation gridlock & reducing the accident rate: A consensus for change.* National Civil Aviation Review Commission, 1997.

[163] NATS. Time based separation at heathrow a world first, 28 February 2014. URL `http://www.nats.aero/newsbrief/time-based-separation-heathrow-world-first/`

[164] r. P. . NATS Ltd, UK Aeronautical Information Service. Differences training in single pilot piston engined aeroplanes with single lever power control (slpc aeroplanes) and single pilot aeroplanes with electronic flight instrumentation systems (efis), 07 October 2010. URL `http://www.nats-uk.ead-it.com/`.

[165] F. Netjasov. Conflict risk assessment model for airspace strategic planning. *system*, 2008.

[166] F. Netjasov and M. Janic. A review of research on risk and safety modelling in civil aviation. *Journal of Air Transport Management*, 14(4):213–220, 2008.

[167] G. F. Newell. Airport capacity and delays. *Transportation Science*, 13(3): 201–241, 1979.

[168] M. Newman. The structure and function of complex networks. *SIAM review*, pages 167–256, 2003.

[169] M. Nolan. *Fundamentals of air traffic control*. Cengage Learning, 2010.

[170] J. Nosedal, M. A. Piera, A. O. Solis, and C. Ferrer. An optimization model to fit airspace demand considering a spatio-temporal analysis of airspace

capacity. *Transportation Research Part C: Emerging Technologies*, 61:11–28, 2015.

[171] OAG. Official airline guide (OAG) the global leader in aviation intelligence, http://http://www.oag.com/. URL `http://http://www.oag.com/`.

[172] A. R. Odoni and R. Simpson. Review and evaluation of national airspace system models. Technical report, Cambridge, MA: Flight Transportation Laboratory, Dept. of Aeronautics and Astronautics, Massachusetts Institute of Technology; 1979, 1979.

[173] A. R. Odoni, J. Bowman, D. Delahaye, J. J. Deyst, E. Feron, R. J. Hansman, K. Khan, J. K. Kuchar, N. Pujet, and R. W. Simpson. *Existing and required modeling capabilities for evaluating ATM systems and concepts*. Massachusetts Institute of Technology, International Center for Air Transportation, 1997.

[174] T. Opsahl and P. Panzarasa. Clustering in weighted networks. *Social Networks*, 31(2):155–163, 2009.

[175] S. Oussedik and D. Delahaye. Reduction of air traffic congestion by genetic algorithms. In *Parallel Problem Solving from NaturePPSN V*, pages 855–864. Springer, 1998.

[176] M. M. Paglione, R. D. Oaks, and K. D. Bilimoria. Methodology for generating conflict scenarios by time shifting recorded traffic data. In *American Institute of Aeronautics and Astronautics Technology, Integration, and Operations (ATIO) Technical Forum*, 2003.

[177] R. A. Paielli and H. Erzberger. Conflict probability for free flight. *Journal of Guidance, Control, and Dynamics*, 20(3):588–596, 1997.

[178] R. A. Paielli and H. Erzberger. Conflict probability estimation generalized to non-level flight. *Air Traffic Control Quarterly*, 7(3):195–222, 1999.

[179] H. M. Pandey, A. Shukla, A. Chaudhary, and D. Mehrotra. Evaluation of genetic algorithms selection methods. In *Information Systems Design and Intelligent Applications*, pages 731–738. Springer, 2016.

[180] R. Pastor-Satorras, A. Vázquez, and A. Vespignani. Dynamical and correlation properties of the internet. *Physical Review Letters*, 87(25):258701, 2001.

[181] B. Pesic, N. Durand, and J.-M. Alliot. Aircraft ground traffic optimisation using a genetic algorithm. In *GECCO 2001, Genetic and Evolutionary Computation Conference*, 2001.

[182] D. M. Pfeil and H. Balakrishnan. Identification of robust terminal-area routes in convective weather. *Transportation Science*, 46(1):56–73, 2012.

[183] S. D. Phase. Task 2.3. 1/d3,compute and map operational concepts & airspace kpis based on identified available tools and methodologies. Technical report, DLT-0612-231-00-02, SESAR Consortium, Toulouse, 2007.

[184] J. Planning. Development office: Concept of operations for the next generation air transportation system. *Draft Version 0.2 (July 24, 2006)*, 2007.

[185] J. Planning. Development office: Concept of operations for the next generation air transportation system. *Draft Version 0.2 (July 24, 2006)*, 2007.

[186] F. Poldy. *Airport runway capacity and delay: some models for planners and managers.* Bureau of Transport Economics, 1982.

[187] K. Price, R. M. Storn, and J. A. Lampinen. *Differential evolution: a practical approach to global optimization.* Springer Science & Business Media, 2006.

[188] N. Pyrgiotis, K. M. Malone, and A. Odoni. Modelling delay propagation within an airport network. *Transportation Research Part C: Emerging Technologies*, 27:60–75, 2013.

[189] V. Ramanujam. *Estimation and tactical allocation of airport capacity in the presence of uncertainty*. PhD thesis, Massachusetts Institute of Technology, 2011.

[190] K. A. Ravindra, T. L. Magnanti, and J. B. Orlin. *Network flows: Theory, algorithms, and applications*. Prentice Hall Englewood Cliffs, 1993.

[191] R. Rawlings. The application of offset tracks in europen airsapce, 2008. HindSight (6), EUROCONTROL.

[192] A. Reggiani, S. Signoretti, P. Nijkamp, and A. Cento. Network measures in civil air transport: A case study of lufthansa. *Networks, Topology and Dynamics*, pages 257–282, 2009.

[193] P. Reich. Analysis of long-range air traffic systems: separation standards -III. *Journal of Navigation*, 19(03):331–347, 1966.

[194] P. Reich. Separation standards-I. *Journal of the Institute of Navigation*, 19: 88–98, 1966.

[195] P. Reich. Separation standards-II. *Journal of Navigation*, 19(02):169–186, 1966.

[196] T. Reynolds and R. J. Hansman. Analysis of separation minima using a surveillance state vector approach. In *3rd USA/Europe Air Traffic Management Research and Development Seminar, Naples*, 2000.

[197] A. Roli. Links between complex networks and combinatorial optimization.

In *Proc. of Workshop on Experimental Analysis of Algorithms for Artificial Intelligence - AI*IA Working Group on Knowledge Representation and Reasoning, (2005)*. Università di Ferrara, Italy, 2005.

[198] A. Roli. On the impact of small-world on local search. *AI* IA 2005: Advances in Artificial Intelligence*, pages 13–24, 2005.

[199] G. Sabidussi. The centrality index of a graph. *Psychometrika*, 31(4):581–603, 1966.

[200] M. Sales-Pardo, R. Guimera, A. A. Moreira, and L. A. N. Amaral. Extracting the hierarchical organization of complex systems. *Proceedings of the National Academy of Sciences*, 104(39):15224–15229, 2007.

[201] J. Saramäki, M. Kivelä, J.-P. Onnela, K. Kaski, and J. Kertesz. Generalizations of the clustering coefficient to weighted complex networks. *Physical Review E*, 75(2):027105, 2007.

[202] C. Schinwald, K. O. Plötner, and M. Hornung. Using airport fast-time simulation models to increase the quality of airport capacity utilization studies. In *AIAA Modeling and Simulation Technologies Conference*, page 0421, 2016.

[203] M. Sergeeva, D. Delahaye, L. Zerrouki, and N. Schede. Dynamic airspace configurations generated by evolutionary algorithms. In *Proceeding of 34th AIAA Digital Avionics Systems Conference (DASC)*, pages 1F2–1, 2015.

[204] W. Shang, K. Han, K.-C. Pien, A. Majumdar, and W. Ochieng. Robustness and topology analysis of european air traffic network using complex network theory. In *Proceeding of the 94th Transportation Research Board Annual Meeting*, number 15-4846, 2015.

[205] H. D. Sherali, J. Cole Smith, and A. A. Trani. An airspace planning model for selecting flight-plans under workload, safety, and equity considerations.

Transportation Science, 36(4):378–397, 2002.

[206] K. L. Shiu and K. Y. Szeto. Self-adaptive mutation only genetic algorithm: An application on the optimization of airport capacity utilization. In *Intelligent Data Engineering and Automated Learning–IDEAL 2008*, pages 428–435. Springer, 2008.

[207] J. Shortle, R. Xie, C. Chen, and G. Donohue. Estimating collision probabilities of landing airplanes at non-towered aiports. *Transportation Research Board - Annual Meeting*, 2003.

[208] W. Siddiqee. A mathematical model for predicting the number of potential conflict situations at intersecting air routes. *Transportation Science*, 7(2): 158–167, 1973.

[209] M. Siddiquee. Mathematical aids in air route network design. In *1973 IEEE Conference on Decision and Control including the 12th Symposium on Adaptive Processes*, number 12, pages 651–654, 1973.

[210] R. Storn and K. Price. Differential evolution-a simple and efficient adaptive scheme for global optimization over continuous spaces. *International Computer Science Institute-Publication-Tr*, 1995.

[211] R. Storn and K. Price. Differential evolution–a simple and efficient heuristic for global optimization over continuous spaces. *Journal of global optimization*, 11(4):341–359, 1997.

[212] S. H. Stroeve, H. A. Blom, and G. B. Bakker. Systemic accident risk assessment in air traffic by monte carlo simulation. *Safety Science*, 47(2):238–249, 2009.

[213] S. Strogatz. Exploring complex networks. *Nature*, 410(6825):268–276, 2001.

[214] F. Symon, S. Alam, M. M. Hossain, and H. Blom. Airspace network characterization for effect of intermediate waypoints on collision risk assesmnet. In *Proceedings of the 6th International Conference on Research in Air Transportation (ICRAT)*, pages 1–8, 2014.

[215] J. Tang, S. Alam, C. Lokan, and H. Abbass. A multi-objective approach for dynamic airspace sectorization using agent based and geometric models. *Transportation Research Part C: Emerging Technologies*, 21(1):89–121, 2012.

[216] R. Vivona, D. Karr, and D. Roscoe. Pattern-based genetic algorithm for airborne conflict resolution. In *AIAA Guidance, Navigation and Control Conference and Exhibit, Keystone, Colorado*, 2006.

[217] J. Wang, H. Mo, F. Wang, and F. Jin. Exploring the network structure and nodal centrality of china's air transport network: A complex network approach. *Journal of Transport Geography*, 2010.

[218] D. Watts and S. Strogatz. Collective dynamics of small-world networks. *Nature*, 393(6684):440–442, 1998.

[219] Z. Wenjing, C. Richard, and H. Abbass. Dynamic capacity-demand balance in air transport systems using co-evolutionary computational red teaming. In *Proceeding of the 5th International Air Transport and Operations Symposium*, 2015.

[220] L. Werfelman. Stepping Aside, Flight Safety Foundation, 2010. `http://flightsafety.org/aerosafety-world-magazine/may-2010/stepping-aside` .

[221] D. J. Wing and W. B. Cotton. Autonomous flight rules-a concept for self-separation in us domestic airspace. 2011.

[222] Z. Xu and R. Harriss. Exploring the structure of the us intercity passenger air

transportation network: a weighted complex network approach. *GeoJournal*, 73(2):87–102, 2008.

[223] M. Xue. Airspace sector redesign based on voronoi diagrams. *Journal of Aerospace Computing, Information, and Communication*, 6(12):624–634, 2009.

[224] X. Yao. *Evolutionary computation: theory and applications*. World Scientific, 1999.

[225] B. Ye, M. Hu, and J. F. Shortle. Collision risk-capacity tradeoff analysis of an en-route corridor model. *Chinese Journal of Aeronautics*, 27(1):124–135, 2014.

[226] W. Yingxun and C. Zongji. Genetic algorithms (GA) based flight path planning with constraints. *J. Beijing Univ. Aeronaut. Astronaut.(China)*, 25(3):355–358, 1999.

[227] S.-H. Yook, H. Jeong, A.-L. Barabási, and Y. Tu. Weighted evolving networks. *Physical Review Letters*, 86(25):5835–5838, 2001.

[228] A. Yousefi and G. L. Donohue. Temporal and spatial distribution of airspace complexity for air traffic controller workload-based sectorization. In *Aiaa 4th Aviation Technology, Integration and Operations (ATIO) Forum, Chicago, Illinois*, 2004.

[229] A. Yousefi and R. Xie. Safety-capacity trade-off and phase transition analysis of automated separation assurance concepts. In *Proceedings of 30th AIAA Digital Avionics Systems Conference (DASC)*, pages 1B5–1, 2011.

[230] H. Zhou. Distance, dissimilarity index, and network community structure. *Physical Review E*, 67(6):061901, 2003.

[231] B. Zou and M. Hansen. Flight delays, capacity investment and social welfare under air transport supply-demand equilibrium. *Transportation Research Part A: Policy and Practice*, 46(6):965–980, 2012.

[232] C. Zuniga, M. M. Mota, and A. H. García. Analyzing airport capacity by simulation: A mexican case study. *Handbook of Research on Military, Aeronautical, and Maritime Logistics and Operations*, page 115, 2016.